



# Saurashtra University

Re – Accredited Grade 'B' by NAAC  
(CGPA 2.93)

Patel, Jignesh V., 2011, “*Studies on some speciality Cardio Polymers*”, thesis  
PhD, Saurashtra University

<http://etheses.saurashtrauniversity.edu/id/eprint/440>

Copyright and moral rights for this thesis are retained by the author

A copy can be downloaded for personal non-commercial research or study,  
without prior permission or charge.

This thesis cannot be reproduced or quoted extensively from without first  
obtaining permission in writing from the Author.

The content must not be changed in any way or sold commercially in any  
format or medium without the formal permission of the Author

When referring to this work, full bibliographic details including the author, title,  
awarding institution and date of the thesis must be given.

Saurashtra University Theses Service  
<http://etheses.saurashtrauniversity.edu>  
repository@sauuni.ernet.in

*STUDIES ON SOME SPECIALTY  
CARBO POLYMERS*

A

THESIS

SUBMITTED TO THE SAURASHTRA UNIVERSITY

FOR

THE DEGREE OF

*DOCTOR OF PHILOSOPHY*

IN

THE FACULTY OF SCIENCE (CHEMISTRY)

BY

*JIGNESH V. PATEL*

UNDER THE GUIDANCE

OF

Dr. P. H. PARSANIA

DEPARTMENT OF CHEMISTRY  
SAURASHTRA UNIVERSITY  
RAJKOT- 360 005  
INDIA

January-2011

Gram: UNIVERSITY  
Fax: 0281-2577633

Phone: (R) 2581097  
(O) 2578512

## SAURASHTRA UNIVERSITY

**Dr. P. H. PARSANIA**  
M.Sc., Ph.D.  
Professor & Head  
Department of Chemistry



**Residence**  
“Maulik”  
20-A/1, University  
Karmachari Co. Hsg. Society  
University Road,  
Rajkot – 360 005  
Gujarat – (INDIA)

### Statement under O. Ph. D. 7 of Saurashtra University

The work included in the thesis is my own work under the supervision of **Dr. P. H. Parsania** and leads to some contribution in Chemistry subsidized by a number of references.

Date: -1-2011  
Place: Rajkot.

**(Mr. Jignesh V. Patel)**

This is to certify that the present work submitted for the Ph. D. Degree of Saurashtra University by **Mr. Jignesh V. Patel** is his own work and leads to advancement in the knowledge of Chemistry. The thesis has been prepared under my supervision.

Date : -1-2011  
Place : Rajkot

**Dr. P. H. PARSANIA**  
Professor & Head  
Department of Chemistry,  
Saurashtra University  
Rajkot - 360 005

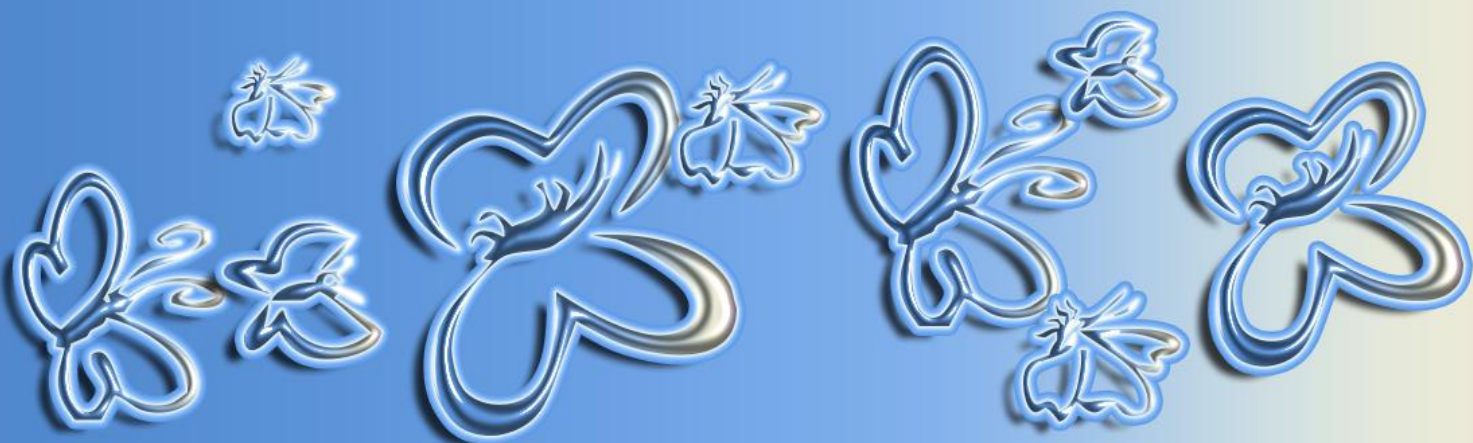


*Dedicated*

*To*

*My Family*

*& Guide*



## ACKNOWLEDGEMENTS

*First and foremost, I would like to pay my homage to THE ALMIGHTY GOD for making me capable of completing my Ph.D. thesis; with his blessings only I have accomplished this huge task.*

*I express deep sense of gratitude to real mentor and philosopher Dr. P. H. Parsania - Professor and Head, Department of Chemistry, Saurashtra University, Rajkot. It is my immense pleasure and privilege to express my profound gratitudes to him for his never ending guidance and perseverance. His keen interest, patience and constant encouragement during my research work have enabled me to put my work in the form of the thesis. Association with him has been a life time achievement for me.*

*I am also thankful to all faculty members: Dr. A. K. Shah, Dr. V. H. Shah, Dr. H. S. Joshi, Dr. S. Baluja, Dr. M. K. Shah, Dr. Y. T. Naliapara, Dr. U. C. Bhoya, Dr. R. C. Khunt, Dr. F. D. Karia and administrative staff for their encouragement during my research work.*

*I would like to extend my sincere thanks to my seniors as well as juniors - Dr. Ragin, Dr. Bhavesh, Dr. Niraj, Dr. Sunil, Dr. Paresh, Dr. Vrajesh, Dr. Viren, Dr. Bharat, Dr. Pankaj, Dr. Sandip, Urvishbhai, Punit, Suresh, Pooja, Lina, Ritesh, Rizwan for their help and cooperation.*

*I also thankful to my colleagues Deepak, Vaibhav, Renish, Dinesh, Bhavesh, Dr.Kapil, Dr.Ram Vijay, Dr.Rahul, Dr.Ravi, Ashish, Mehu, Dr Atul, Dr.Rupesh, Ravi, Bhavin, Bharat, Manisha, Amit, Vipul, Rakesh, Naimish, Minaxi, Anil, and Piyush for continuous encouragement during my research work.*

*The never ending process of unsurpassable dedication on the name of friendship of the best friends: Darshana, Shrina, Jeni-Deepika, Jayesh-Ridhi, Deep, Ajay, Ojas and Ketan for their appreciation, inspiration and motivation during the tenure of my research work.*

*A special appreciation is extended to Mr. M. J. Meghpara for his enthusiasm, devotion to task assigned and patience, while tracing figures.*

*I am also indebted to The Directors, RSIC-Chandigarh and SICART- V. V. Nagar for instrumental facilities.*

*I would like to extend my sincere thanks to Puvesh Vyas as well as Purvesh Dobariya for their analytical help during my research work.*

*I express my deepest thanks to Mrs. Vijyaben, Jignesh and Maulik Parsania for the hospitality extended to me during prolonged research discussion at their home during this work.*

*The never ending process of unsurpassable devotion, love and affection, which was showered upon me by my father **Dr. Vallabhbhai** (Res. Sci., Entomology, JAU), mother **Geetaben**, brother **Hiren**, my Grandfather and Grandmother, Uncle and Aunt, Cousins (Tirth & Disha), who have enlightened my path and always boosted me to go ahead to reach the goal.*

*Jignesh V. Patel*

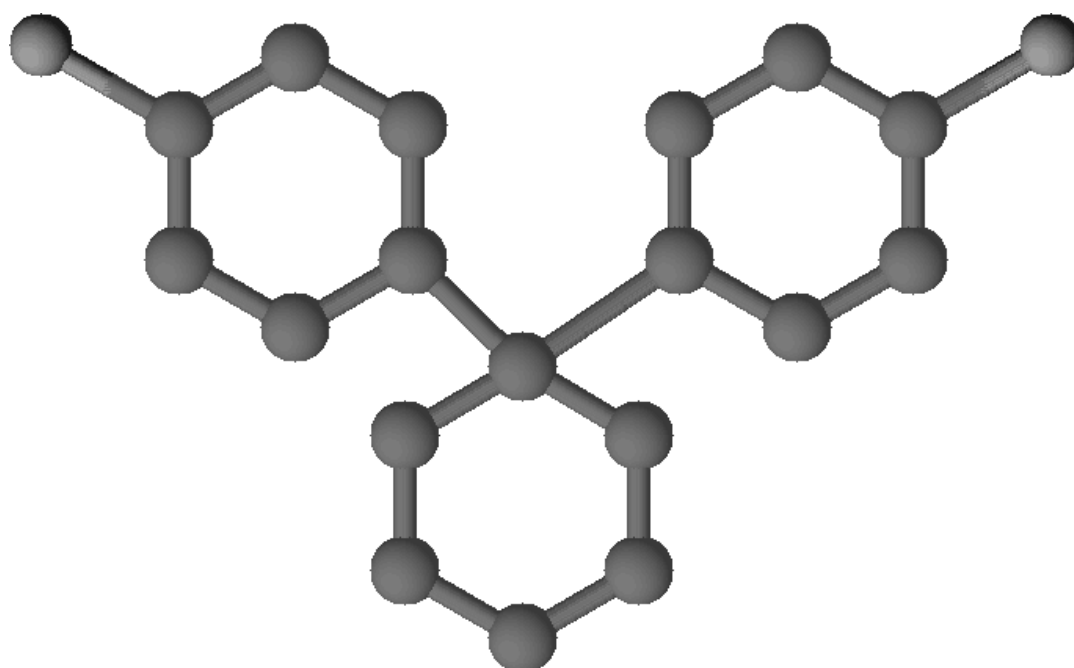
## CONTENTS

<b>Sr. No.</b>	<b>TITLE</b>	<b>Page No.</b>
1	synopsis	1-8
2	<b>Chapter-1: INTRODUCTION</b>	<b>9-48</b>
3	<b>Chapter-2: SYNTHESIS OF DIAMINES, SCHIFF BASES AND THEIR POLYMERS</b> Section-I: Synthesis of 1-1' bis(4-aminophenyl)cyclohexane Section-II: Synthesis of symmetric double Schiff bases Section-III: Syntheses of polymers	<b>49-58</b> <b>49</b> <b>51</b> <b>53</b>
4	<b>Chapter-3: CHARACTERIZATION OF POLYMERS</b> Section-I: Solubility of polymers Section-II: Spectral characterization of polymers Section-III: Thermal analysis of polyschiff bases	<b>59-150</b> <b>59</b> <b>66</b> <b>112</b>
5	<b>Chapter-4: ULTRASONIC STUDY OF EPOXY AND BISBENZOXAZINES</b>	<b>151-219</b>
6	<b>Chapter-5: SUMMARY</b>	<b>220-221</b>



# *SYNOPSIS*

## STUDIES ON SOME SPECIALTY CARDO POLYMERS



*Mr. Jignesh V. Patel*

*Department of Chemistry,  
Saurashtra University, Rajkot-360005*

**SYNOPSIS OF THE THESIS TO BE SUBMITTED TO  
SAURASHTRA UNIVERSITY FOR THE DEGREE OF  
PHILOSOPHY IN THE FACULTY OF SCIENCE -  
CHEMISTRY**

FACULTY : **SCIENCE**  
SUBJECT : **CHEMISTRY**  
TITLE OF THE THESIS : **STUDIES ON SOME SPECIALTY CARDO  
POLYMERS**  
NAME OF THE CANDIDATE : **JIGNESH V. PATEL**  
REGISTRATION NO. : **3714**  
DATE OF REGISTRATION : **31<sup>st</sup> JULY - 2007**  
NAME OF THE GUIDE : **Dr. P. H. PARSANIA**  
**PROFESSOR & HEAD**  
**DEPARTMENT OF CHEMISTRY,**  
**SAURASHTRA UNIVERSITY,**  
**RAJKOT – 360 005**  
SUBMITTED TO : **SAURASHTRA UNIVERSITY**

**PLACE OF THE WORK**

**DEPARTMENT OF CHEMISTRY,  
SAURASHTRA UNIVERSITY,  
RAJKOT-360 005  
GUJARAT-INDIA**

A summary of the work to be incorporated in the thesis entitled, "Studies on some specialty cardo polymers".

### GENERAL INTRODUCTION

Among nitrogen containing compounds, amino compounds are more useful. They find their usefulness as intermediates for synthetic fibers and medicines. Aromatic diamines are the important constituents for the syntheses of dyes, agrochemicals, varnishes, adhesive, and coating materials, pesticides, fertilizers and in other applications. They are widely used in manufacturing thermally stable polyamides, amino and epoxy resins. They are also used as curing agents for epoxy resins and in the synthesis of variety of Schiff bases for various purposes. [1-4]. Schiff bases are most widely used as fine chemicals [5] medical substrates and ligands for metal complexes [6].

They are also useful as starting materials for the synthesis of important drugs like antibiotics, antiallergic, antiphlogistics and antitumor [7-9] and components of rubber compounds [10]. Schiff bases based on salicylaldehyde and other hydroxy aldehydes possess unique characteristic properties of improving both antiwear and corrosion inhibition of synthetic lubricating oils and greases. [10]

- 
1. Y.T. Chern and H.C. Shiue. "Low dielectric constants of soluble polyimides derived from the novel 4, 9-bis [4-(4-aminophenoxy) phenyl] diamantane". *Macromolecules*, 30, 5766-5772, 1997.
  2. Saraii, Mahnaz, Entezami, Ali Akbar "Synthesis and characterization of poly Schiff bases derived from 5a, 10b dihydrobenzofuro [2, 3-b] benzofuran- 2, 9 dicarbaldehyde with various diamines" *Iranian Polym. J.*, 12, 43 ,2003
  3. S. Samal, R. R. Das, S. Acharya, P. Mohopatra and R. K. Dey "A comparative study on metal ion uptake behavior of chelating resins derived from the formaddelehyde condensed phenolic Schiff bases of 4,4' diaminodiphenyl sulfone and hydroxy benzaldehyde" *Polym. Plast. Technol. Eng.* 41, 229-246, 2002
  4. M. H. Yi, W. Huang, B. J. Lee and K. Y. Choi "Synthesis and characterization of soluble polyimides from 2, 2 bis (4-aminophenyl) cycloalkanes derivatives". *J. Appl. Polym. Sci.- Part – A* , 37, 3449-3454, 2000
  5. S. Patai "The Chemistry of the carbon-nitrogen double bond" John-Wiley and Sons. Ltd., London, 1970.

The work to be incorporated in the thesis is divided into five Chapters:

**CHAPTER 1: INTRODUCTION**

**CHAPTER 2: SYNTHESIS OF DIAMINES, SCHIFF BASES AND THEIR POLYMERS**

**CHAPTER 3: CHARACTERIZATION OF POLYMERS**

**CHAPTER 4: ULTRASONIC STUDY OF EPOXY AND BISBENZOXAZINES**

**CHAPTER 5: SUMMARY**

**CHAPTER 1: INTRODUCTION**

This chapter of the thesis describes the up to date literature survey on syntheses, applications and characterization of diamines, Schiff bases, epoxy and bisbenzoxazines.

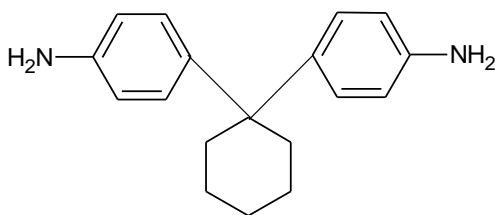
- 
6. S. D. Ittel, L. K. Johnson, M. Brookhant, Chem. Rev., 100, 1169-1203, 2000
  7. D. Barton and W. D. Ollis "Comprehensive Organic Chemistry" Eds. Oxford, Pergamon, Vol. 2, 1979
  8. C. K. Ingold "Structure and Mechanism in Organic Chemistry." Cornell Univ. Press., 2nd Ed. 1969
  9. A. P. Mishra, M. Khare and S. K. Gautam "Synthesis, physico-chemical characterization and antibacterial studies of some bioactive Schiff bases and their metal chelates". Synthesis and Reactivity in Inorganic and Metal Organic Chemistry, 32, 1485-1500, 2002.
  10. V. S. Agarwala, A. R. Krishnaswamy and P. K. Sen "Synthetic lubricating oil greases containing metal chelates of Schiff bases". US Pat. 5, 147, 567, Sept.-1992

## CHAPTER 2: SYNTHESIS OF DIAMINES, SCHIFF BASES AND THEIR POLYMERS

This chapter is further subdivided into three sections:

### SECTION-I: Synthesis of 1-1' bis(4-aminophenyl)cyclohexane

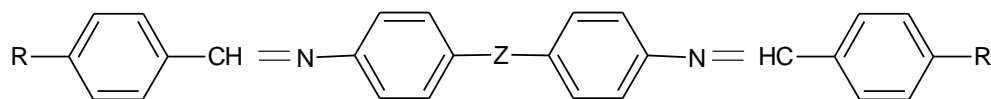
Aromatic diamines can be synthesized by acid catalyzed condensation of hydrochloride salt of aromatic amines and cyclic ketones. Thus, appropriate amount of aniline and cyclohexanone were condensed at 150°C in presence of hydrochloric acid for 24h. The resultant solution was cooled and made alkaline by using 10% NaOH solution, separated diamine was filtered, washed well with distilled water and crystallized repeatedly from chloroform–n-hexane system. The yield was 39 % and mp 162°C. Purity was checked by TLC in ethyl acetate-n-hexane (50:50 v/v) solvent system.



I

### SECTION-II : Synthesis of symmetric double Schiff bases

Schiff bases of general structure (Scheme-2) were synthesized by condensing diamine and substituted aldehydes in ethanol by using glacial acetic acid as a catalyst at reflux temperature. Schiff bases were isolated from excess of chilled water, filtered, washed well with sodium bisulphite, distilled water and dried at 50°C in an oven. Schiff bases are soluble in common solvents and were crystallized at least three times from appropriate solvent system. Their purity was checked by TLC in appropriate solvent system.



Where, Z = -CH<sub>2</sub>-, -O-, -SO<sub>2</sub>-,

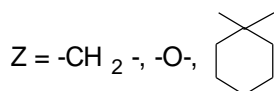
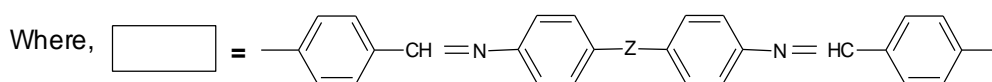
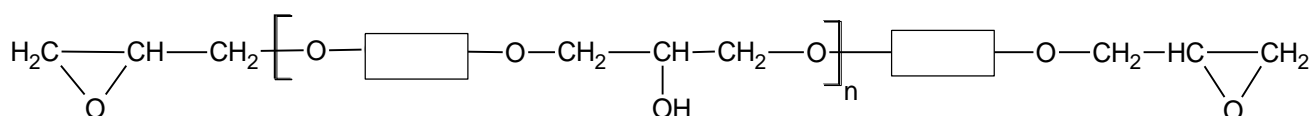
R = 4-OH, 4-Cl, 4-F

II

### SECTION-III: SYNTHESSES OF POLYMERS

#### (A) Synthesis of epoxy resins and their curing study

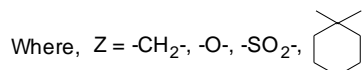
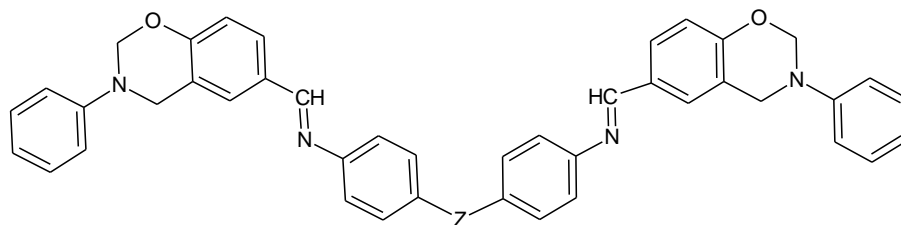
Epoxydation was carried out by using 4-hydroxy symmetric double Schiff bases with epichlorohydrine by using isopropanol as a solvent and alkali as a catalyst at reflux temperature for 2 h. Epoxy resins were isolated from excess water, filtered, washed well with distilled water and purified using DMF-Water system. The epoxy equivalent of the resins was determined by pyridinium method. The resins were cured by phthalic anhydride as a hardener.



#### III (Epoxy resins of symmetric double Schiff bases)

#### (B) Synthesis of bisbenzoxazines and their ring opening polymerization

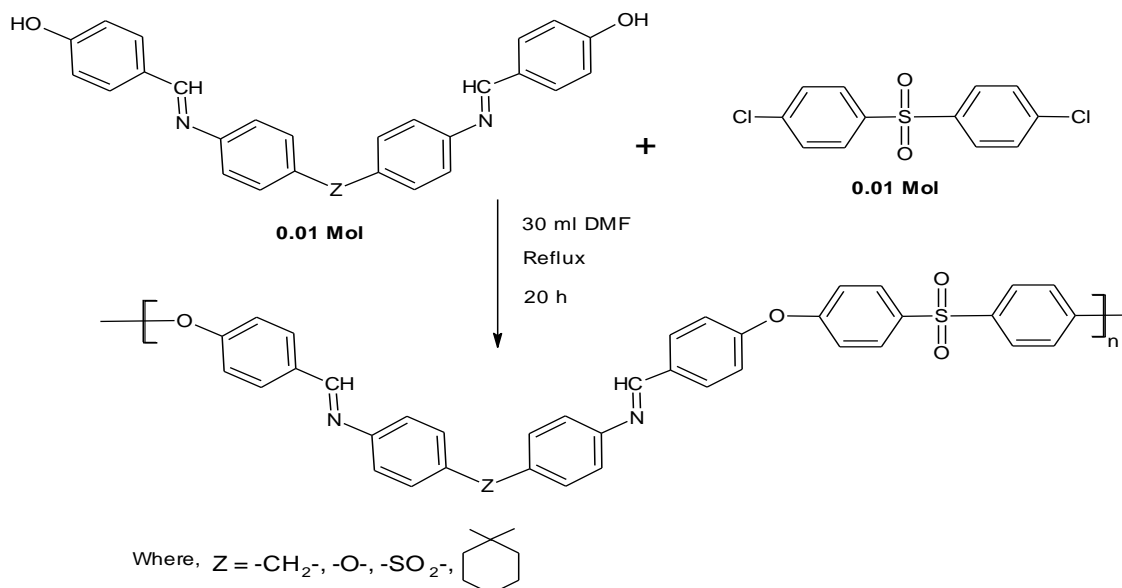
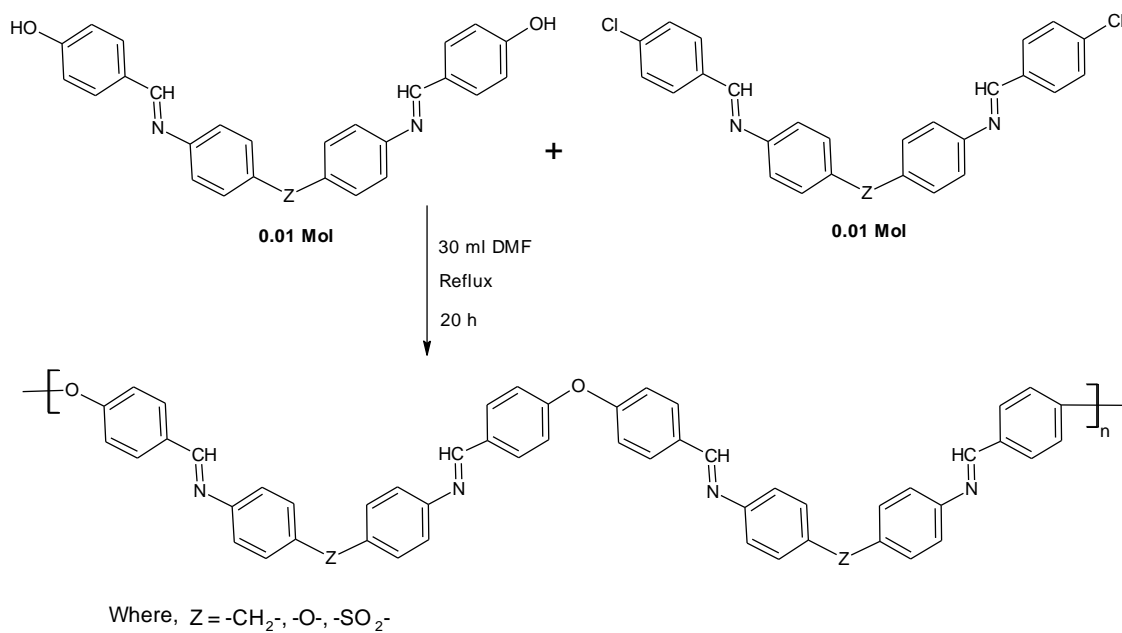
Bisbenzoxazines were synthesized by condensing aniline, formaldehyde and a Schiff bases using dioxane as a solvent, at reflux temperature for 15 h and isolated from chilled water filtered, washed well with water and dried at room temperature. Bisbenzoxazines were crystallized four times from dioxane-water system. It is proposed to polymerize bisbenzoxazines via ring opening polymerization.

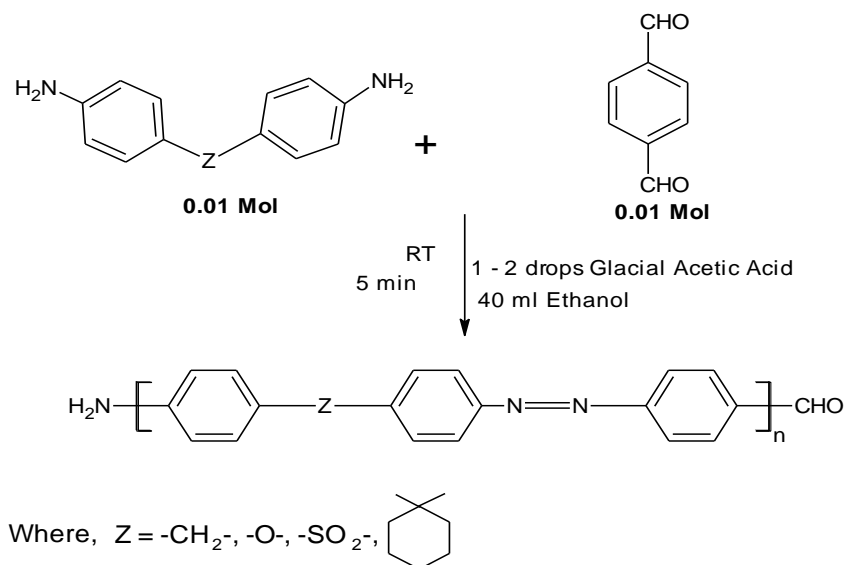


#### IV(Bisbenzoxazines)

**(C) Synthesis of polySchiff bases**

PolySchiff bases were synthesized according to following polymerization Schemes V-VII. Resultant polySchiff bases were isolated from water, filtered washed well with water and dried at room temperature. The yields were 90- 96 %.

**Scheme-V****Scheme-VI**



Scheme-VII

### CHAPTER 3: CHARACTERIZATION OF POLYMERS

This chapter is further subdivided into four sections:

#### SECTION-I: SOLUBILITY OF POLYMERS

Solubility of polymers was tested in various organic solvents at room temperature and thermodynamic goodness of the solvents is reported.

#### SECTION-II: SPECTRAL CHARACTERIZATION OF POLYMERS

Formation of different linkages in the monomers and polymers are supported by IR and NMR spectral data.

#### SECTION-III: THERMAL ANALYSIS OF POLYSCHIFF BASES

Thermogravimetry can precisely describe the degradation of polymers under varying temperature range and atmosphere. Various kinetic parameters provide usefulness of the potentially unstable nature of materials under investigation. Polymers are characterized by DSC and TGA techniques at  $10^\circ\text{C}/\text{min}$  heating rate under nitrogen atmosphere. Thermal stability and various kinetic parameters are determined and discussed in this chapter.



**CHAPTER-4: ULTRASONIC STUDY OF EPOXY AND BISBENZOXAZINES**

Recently ultrasonic has become the subject of extensive research because it finds applications in numerous fields of science like consumer industries, medical fields, engineering, process industries, etc. Knowledge of acoustical properties of solutions furnishes a wealth of information on molecular interactions occurring in the solutions, the nature and the strength of interactions. The density, viscosity and ultrasonic speed measurements of epoxy resins and bisbenzoxazines solutions in different solvents were carried out at 30°, 35° and 40°C. Various acoustical parameters such as isentropic compressibility ( $\kappa_s$ ), specific acoustical impedance (Z), Rao's molar sound function (R), Van der wals constant (b), internal pressure ( $\pi$ ), classical absorption coefficient  $(\alpha/f^2)_{cl}$ , viscous relaxation time ( $\tau$ ), solvation number ( $S_n$ ), free volume ( $V_f$ ) and intermolecular free length ( $L_f$ ) are determined and discussed in light of effect of solvent, temperature, concentration, etc.

**CHAPTER 5: SUMMARY**

This chapter describes a brief summary of the work investigated during the tenure of the research programme.

**Signature of the guide****Signature of the candidate****(Dr. P. H. Parsania)****(Mr. Jignesh V. Patel)**

Professor and Head,  
Department of Chemistry,  
Saurashtra University,  
Rajkot – 360 005

**Date:**



# CHAPTER – 1

## INTRODUCTION

## CHAPTER-1 INTRODUCTION

### GENERAL INTRODUCTION

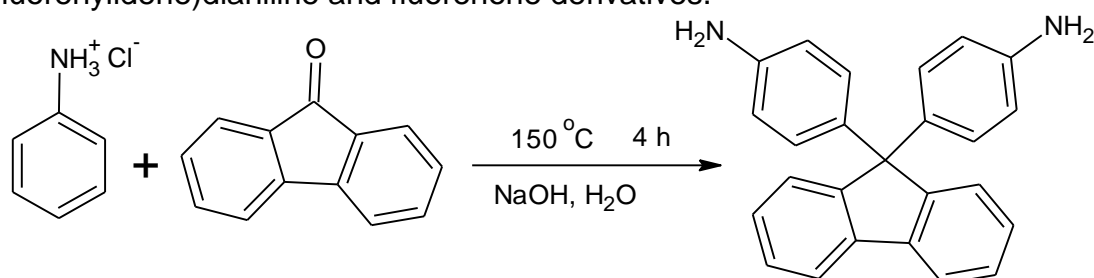
Functional groups containing nitrogen are responsible for their unique chemical reactivity patterns. These are the key molecules in syntheses of drugs, dyes, agrochemicals, polymers, etc. There are many functional groups, which contain one or more nitrogen atoms. Some categories of compounds based on these functional groups include nitrocompounds, amines, cyanides, isocyanides and diazo compounds. The chief commercial use of amine compounds are found as intermediates in the synthesis of dyes, synthetic fibers, medicines, etc.

Commercially amines are prepared from a variety of compounds. Generally they are synthesized by reduction of nitro compounds by catalytic hydrogenation or by using a metal and acid. Aniline is one of the most important of all amines. It is manufactured by the reduction of nitro benzene.

#### Section I: Literature survey on aromatic diamines

Diamines are the important constituents or intermediates in dyes, agrochemicals, varnish, coating, pesticides, fertilizers, etc. They are useful in manufacturing thermally stable polyimides, epoxy resins, formaldehyde resins, Schiff bases and as hardeners.

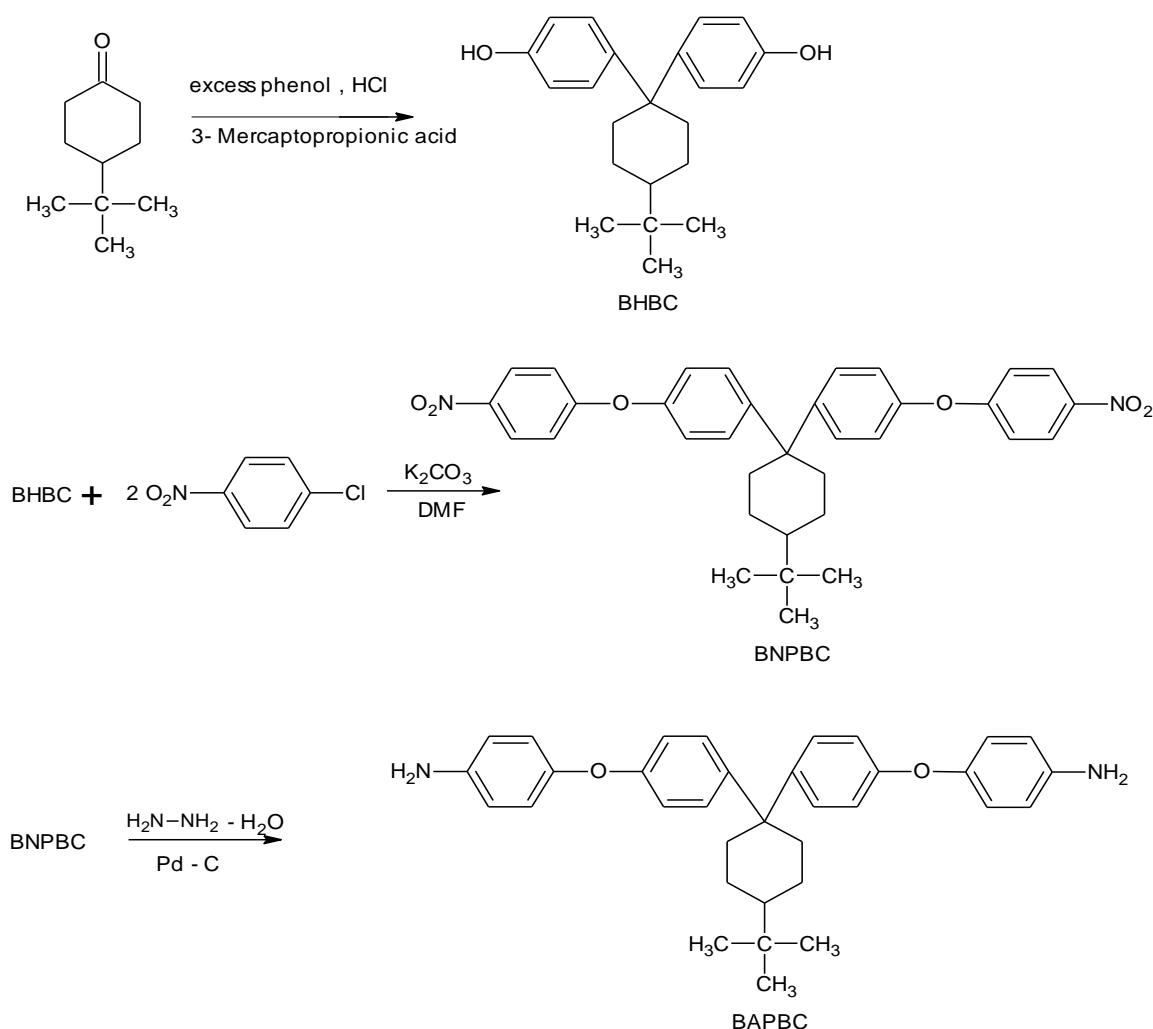
Xie Linghai et. al [1] have reported synthesis of 4,4'-(9-fluorenylidene)dianiline and fluorenone derivatives.



1. Xie Linghai, Huang Wei, Zhao Jianfeng, Chang Yongzheng, Lin Zongqiong and Qian Yan, "A process for preparing fluorenone derivatives" Assignee Nanjing University of Posts and Telecommunications, CN 101643381, 2010

0.22 mol aniline hydrochloride and 0.1 mol 9-fluorenone mixture was heated at 150°C. At this temperature the reaction mixture was stirred for 4h. The resultant 4,4'-(9-fluorenylidene)dianiline hydrochloride was poured in distilled water and precipitated by adding NaOH solution and put it at room temperature for 4h, then filtered, washed repeatedly with water and dried.

Liaw et. al [2] have reported synthesis of new cardo diamine monomer 1,1'-bis [4-(4-aminophenoxy)phenyl]4-tertbutyl cyclohexane. This cardo diamine was prepared in three steps from 4-tert butyl cyclohexanone as under.



2. D. J. Liaw, B. Y. Liaw, C. Y. Chung, "Synthesis and characterization of new cardo polyamides and polyimides containing tert-butylcyclohexylidene units", *Macromol. Chem. Phys.*, 201, 1887-1893, 2000.

**1,1'-Bis(4-hydroxyphenyl)-4-tert-butylcyclohexane (BHBC)**

A flask was charged with a mixture of 0.067 mol 4-*tert*-butylcyclohexanone, 0.2 mol phenol and 1 mol 3-mercaptopropionic acid. Heat was applied and when the reaction mixture became liquid at 58°C, hydrochloric acid (gas) was passed through it until the solution became saturated. Stirring was continued at 60°C for 2 h, during which period white solid began to separate out from the reddish-orange reaction mixture. The solid mass was dispersed in 1 lit. of water and the mixture was steam distilled to remove the excess phenol and 3-mercaptopropionic acid leaving an aqueous suspension. The solid residue was collected from the mixture by filtration and crystallization from toluene twice gave 1,1'-bis(4-hydroxyphenyl)-4-*tert*-butylcyclohexane (BHBC). The yield was 74% and m. p. 181-182°C.

**1,1'-Bis[4-(4-nitrophenoxy)phenyl]-4-tert-butyl cyclohexane (BNPBC)**

A mixture of 0.028 mol BHBC, 0.06 mol p-chloro nitrobenzene, 0.07mol anhydrous potassium carbonate and 50 ml anhydrous DMF was refluxed for 8 h. The mixture was then cooled and poured into methanol. The crude product, 1,1'-bis[4-(4-nitrophenoxy)phenyl]-4-tert-butylcyclohexane(BNPBC) was recrystallized from glacial acetic acid to give yellow needle shape crystals (m.p. 190-191°C) with 94% yield. The characteristic IR absorption peaks of BNPBC are 1578 and 1334 cm<sup>-1</sup> (NO<sub>2</sub>) 1243 cm<sup>-1</sup> (C-O-C).

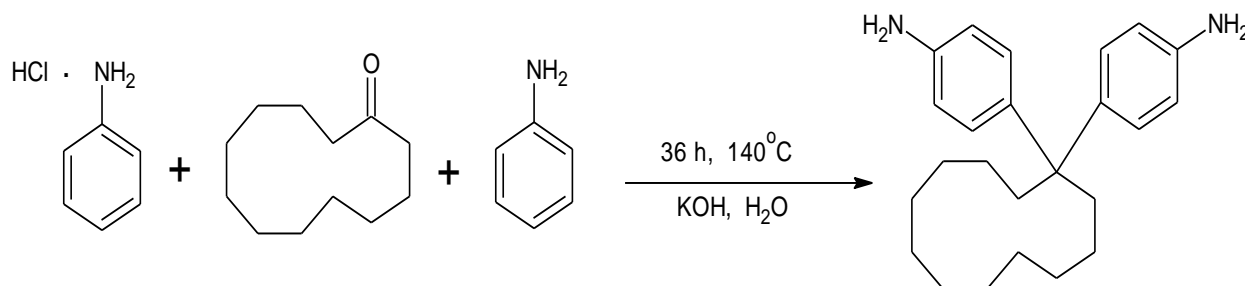
**1,1'-Bis[4-(4-aminophenoxy)phenyl]4-tert-butylcyclohexane (BAPBC)**

A 20 ml hydrazine monohydrate was added dropwise to a mixture of 0.014 mol (7.98g) BNPBC, 160 ml ethanol, and a catalytic amount of 10% palladium on activated carbon (Pd/C, 0.06 g) at the boiling temperature. The mixture became homogeneous after 1 h and the reaction was refluxed for 24h. The mixture was then filtered to remove Pd/C. After cooling, the precipitated white crystals of 1, 1'-bis [4-(4-aminophenoxy) phenyl]-4-tert-butylcyclohexane (BAPBC), were isolated by filtration and recrystallized from ethanol to give 83% yield (m.p. 171-172 °C). The IR spectrum (KBr) of BAPBC exhibited characteristic absorptions at 3418, 3350 and 1613 cm<sup>-1</sup> (N-H), and 1237 cm<sup>-1</sup> (C-O-C). BAPBC was reacted with various aromatic dicarboxylic acids and tetra dicarboxylic dianhydrides to produce polyamides

and polyimides, respectively. Polyamides and polyimides imparted greater solubility, enhance rigidity as well as better thermo-mechanical properties.

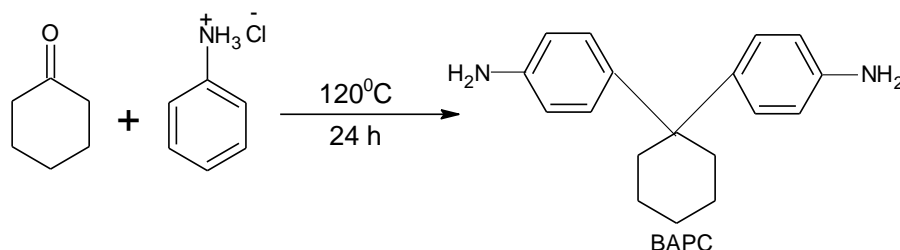
Aromatic diamines are widely used for the synthesis of polyimides, which have been noted for their excellent characteristic properties. But their processability is poor, which limits their application area [3] and therefore various efforts have been made to synthesize soluble polyimides without sacrifice of their excellent properties. By using diamines having cyclic ring between two benzene rings, the obtained polymer showed good thermal stability as well as solubility [4].

Huang Wei and Yin Jie [5] have reported the synthesis of alicyclic bis(2-aminobenzothiazole) derivatives. They prepared 4, 4'-bis(benzenamine)cyclododecylidene by using 0.1 mol aniline hydrochloride, 0.1 mol alicyclic ketone and 0.1 mol aniline, the mixture was heated at 140°C for 36 h, cooled to room temperature. Then added KOH, water and refluxed for 10 min. The resultant 4, 4'-bis(benzenamine) cyclododecylidene hydrochloride was poured in distilled water and precipitated by adding KOH solution till 10 pH, filtered, washed repeatedly with water and dried.



3. Kai Wang, Lin Fan, Jin-Gang Liu, Mao-Sheng Zhan and Shi-Yong Yang, "Preparation and properties of melt-processable polyimides based on fluorinated aromatic diamines and aromatic dianhydrides", *J. Appl. Polym. Sci.*, 107(4), 2126–2135, 2008
4. M. H. Yi, M. Y. Jin, K. Y. Choi. "Synthesis and characterization of poly(amide imides) containing aliphatic diamine moieties", *Macromol. Chem.*, 223, 89-101, 1995.
5. Huang Wei and Yin Jie, "Process for preparation of alicyclic bis(2-aminobenzothiazole) derivatives", Assignee Shanghai Jiao Tong University, CN 1683348, 2005.

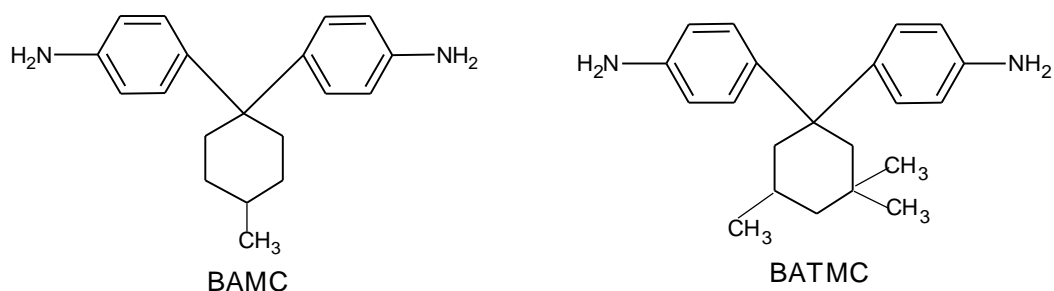
Yi et. al [6] have reported the synthesis of series of novel aromatic diamines containing cyclohexane moieties. They have also synthesized and characterized soluble polyimides from 1,1'-bis(4-aminophenyl)cyclohexane derivatives.



### 1,1'-Bis (4-aminophenyl)cyclohexane (BAPC)

BAPC was prepared by the condensation of cyclohexanone and excess aniline [7, 8]. To a solution of 0.41 mol (40.0 g) cyclohexanone in 35% HCl aqueous solution in a 1 Lit autoclave equipped with a mechanical stirrer was added 1.68 mol (156.3 g) aniline and the mixture was stirred at  $120^\circ\text{C}$  for 20 h. After cooling, the solution was made basic with aqueous NaOH solution to pH 10, and the oily layer was separated and steam distilled to remove the unreacted excess aniline. The residual crude product was recrystallized from benzene to give 86.4 g (79.4% yields) of light-yellow crystal; (m. p.  $112^\circ\text{C}$ ). 1,1'-Bis(4-aminophenyl)-4-methylcyclohexane (BAMC) and 1,1'-bis(4-amino phenyl)-3,3,5- trimethyl cyclohexane (BATMC) were prepared in a similar manner to that of BAPC by reacting 4-methylcyclohexanone and 3,3,5-trimethyl cyclohexanone with aniline.

6. M. H. Yi, W. Huang, M. Y. Tin and K. Y. Choi, "Synthesis and characterization of soluble polyimides from 1,1'-bis (4-aminophenyl)cyclohexane derivatives", *Macromolecules*, 30, 5606-5611, 1997.
7. H. Waldmann, U. Leyrer, H. P. Mueller, K. J. Idel, C. Casser, G. Fengler, U. Westeppe, *Ger. Offen D. E. 847, 4,014*, 1991.
8. J. Myska, "Note on preparation of 1, 1'-bis(4-amino phenyl)cyclohexane", *Chem. Abstra.*, 61, 14558, 1964.

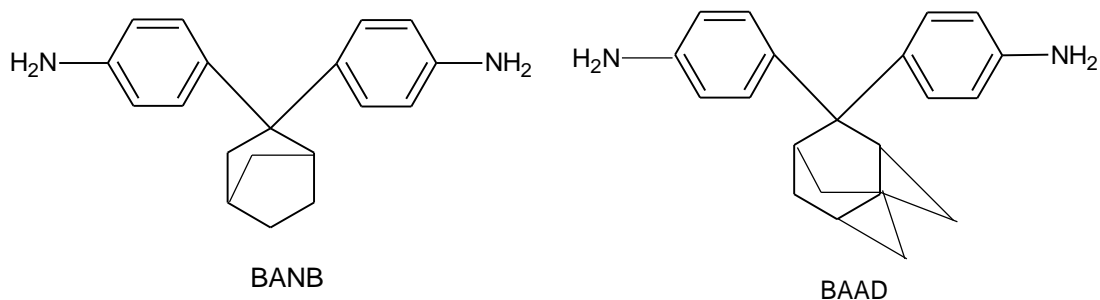


BAMC was recrystallized from isopropyl alcohol to give 70% light yellow crystals (m. p. 158.8<sup>o</sup>C). BATMC was recrystallized from isopropyl alcohol to give 40% pale yellow powder (m. p. 46<sup>o</sup>C). The structures of BAPC, BAMC and BATMC were supported by elemental, IR, Mass and NMR spectral data. They have also proposed the mechanism of diamines formation and was confirmed by the structural identification of a major by product by <sup>1</sup>H NMR. The dehydration reaction was faster than the substitution reaction of aniline and therefore diamine yield is low.

Yi et. al [9] have reported the synthesis and characterization of soluble polyimides from aromatic diamines containing polycycloalkane structure between two benzene rings. 2,2'-Bis(4-aminophenyl)norbornane (BANB) and 2,2'-Bis(4-amino phenyl)adamantane (BAAD) were synthesized by HCl catalyzed condensation reaction of corresponding polycycloalkanone with aniline hydrochloride at 140-160 <sup>o</sup>C for 20 h. The yields of diamines were 32-35% and the structures of diamines were supported by FTIR, <sup>1</sup>H NMR, <sup>13</sup>C NMR spectroscopy and elemental analysis. The detail process and spectral data of diamine are given.

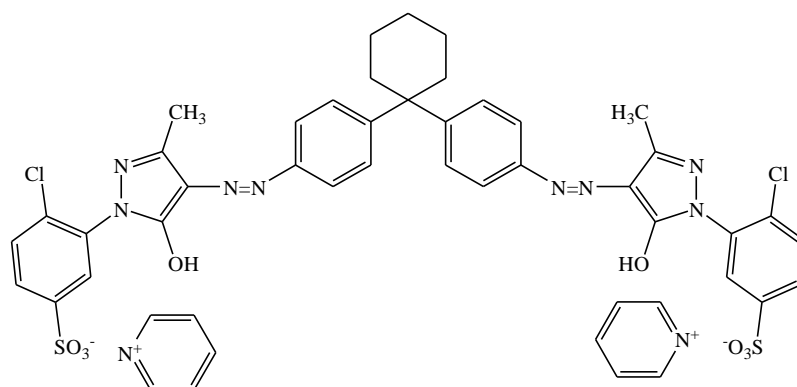
- 
9. M. H. Yi, W. Huang, B. J. Lee and K. Y. Choi, "Synthesis and characterization of soluble polyimides from 2,2'-bis(4-aminophenyl)cycloalkane derivatives", J. Polym. Sci. Part-A Polym. Chem., 37, 3449-3454, 1999.





To a 500-ml four-neck flask equipped with a mechanical stirrer was placed 0.16 mol of 2-norbornanone, 0.48 mol aniline and 0.32 mol aniline hydrochloride and the mixture was stirred at 140-160 °C for 20 h. After cooling, the solution was made basic with aqueous NaOH solution to pH 10, and the purple oily layer was separated and steam distilled to remove the unreacted aniline. The residual crude product was treated with active carbon to remove the dark color, and then recrystallized from ethyl acetate to give 15.0 g (35.2%) off white crystals of BANB (m. p. 202 °C). The structure of BANB was supported by MS [ $m/z$  197 and 278 ( $M^+$ )], FTIR [3444 and 3359 (NH str.), 1615 (NH def)] spectral and elemental analysis.

Fuji Photo Film Co. Ltd. [10] has reported synthesis of yellow disazo dye using 1,1'-bis(4-aminophenyl)cyclohexane. It was synthesized by coupling between 1, 1'-bis(4-aminophenyl)cyclohexane and 1-(2-chloro-5-sulfophenyl)-3-methyl-5-pyrazolone Na salt in the presence of NaOH and NaOAc in water, and the diazo coupling product (Na salt) was treated with  $\text{POCl}_3$  in  $\text{AcNMe}_2$  to give the sulfonyl chloride derivative. This was treated with pyridine in  $\text{AcNMe}_2$  to give yellow disazo dye. It is very useful in color filters.



10. Fuji Photo Film Co. Ltd., Japan, "Yellow disazo dye", JP 210642, 1982.

## Section II: Literature survey on Schiff bases

The chemistry of carbon-nitrogen double bond has played a vital role in the progress of chemical sciences. Due to presence of a lone pair of electrons on the nitrogen atom and general electron donating character of the double bond, these compounds have found very large applications in the field of chemistry. The compounds containing  $>C=N$  group are known as imines or azomethines or anils or ligands, but generally they are known as a "Schiff bases" in honors of Schiff, who have synthesized such compounds very first time [11, 12].

The literature survey revealed that Schiff bases are useful as starting material in the synthesis of important drugs, such as antibiotic, antiallergic, anticancer, antiphlogistics and antitumor, etc [13-15].

Schiff base compounds are widely used as fine chemicals, analytical reagents, corrosion inhibitors as well as ligands [16, 17]. Metal complexes synthesized from Schiff bases have been widely studied because of their industrial, antifungal and biological applications [18].

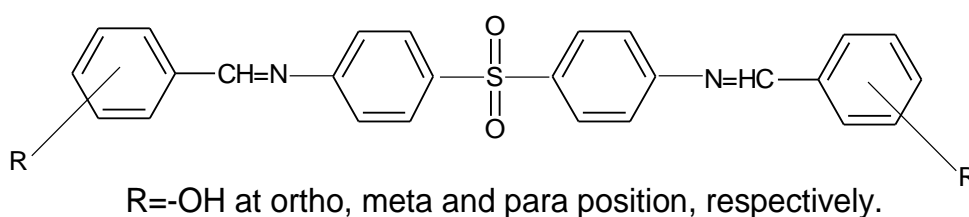
Schiff bases possess characteristic properties like manifest of thermal stabilities, abnormal magnetic properties, relevant biological properties, high synthetic flexibility, co-ordinating ability and medicinal utility. A wide range of Schiff bases have been synthesized and extensively studied [19, 20].

- 
11. H. Schiff, *Ann. Chem.*, 131, 118-119, 1864.
  12. S Patai, "The chemistry of the carbon nitrogen double bond", John Wiley and Sons Ltd., London 1970.
  13. V. E. Kyzmin, A. G. Artemenko, R. N. Lozytska, A. S. Fedtchouk, V. P. Lozitsky, E. N. Muratov and A. K. Mescheriakov, "Investigation of anticancer activity of macro cyclic Schiff bases by means of 4-D QSAR based on simplex representation of molecular structure" SAR and QSAR in *Enviro. Res.*, 16, 219-230, 2005.
  14. C. K. Ingold, "Structure and mechanism in organic chemistry", Ithaca Cornell Univ. 2<sup>nd</sup> ed. 1969.

The Schiff bases are the condensation products of aromatic or aliphatic aldehydes (e.g. benzaldehyde, cinamaldehyde, crotonaldehyde, etc.), with aliphatic or aromatic mono or diamines (e.g. aniline, aminophenols, 1,2-ethanediamine, benzidine, diamino diphenyl methane, diamino diphenyl sulphone, etc.) [21, 22].

15. A. P. Mishra, M. Khare and S. K. Gautam, "Synthesis, physico-chemical characterization and antibacterial studies of some bioactive Schiff bases and their metal chelates", *Synth. React. Inorg. Metal Org. Chem.*, 32, 1485-1500, 2002.
16. S. Bilgic and N. Caliskan, "An investigation of some Schiff bases as a corrosion inhibitors for austenitic chromium-nickel steel in H<sub>2</sub>SO<sub>4</sub>", *J. Appl. Electroche.*, 31, 79-83, 2001.
17. D. Y. Sabry, T. A. Youssef, S. M. El-Medani and R. M. Ramadan, "Reaction of chromium and molybdenum carbonyls with bis (salicylaldehyde) ethylene diimine Schiff base ligand", *J. Coord. Chem.* 56, 1375-1381, 2003.
18. M. E. Hossain, M. N. Alam, J. Begum, M. A. Ali, F. E. Smith and R. C. Hynes, "The preparation, characterization, crystal structure and biological activities of some copper (II) complexes of the 2-benzoyl pyridine Schiff bases of 5-methyl and 5-benzylidithiocarbamate", *Inorg. Chim. Acta*, 249, 207-213, 1996.
19. Ismet Kaya and Ali Bilici, "Synthesis, characterization and thermal degradation of oligo-2-[(4-hydroxyphenyl) imino methyl]-1-naphthol and oligomer-metal complexes", *J. Macromol. Sci., Part A*, 43, 719-733, 2006
20. Akbar Mobinikhaledi, Peter. J. Steel and Matthew Polson, "Rapid and efficient synthesis of Schiff bases catalyzed by copper nitrate", *Syn. React. Inorg., Metal-Org., and Nano-Metal Chem.*, 39, 189-192, 2009
21. Saraii, Mahnaz, Entezami, Ali Akbar, "Synthesis and characterization of polySchiff bases derived from 5a, 10b-dihydrobenzofuro 2,9-dicarbaldehyde with various diamines", *Iranian Polym. J.*, 12, 43-50, 2003.

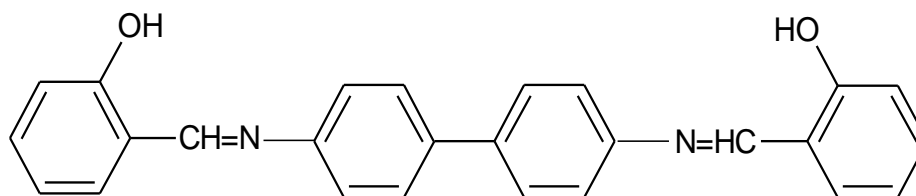
Das et. al [23] have reported metal ion uptake behavior of chelating resins derived from formaldehyde and phenolic Schiff bases. The phenolic Schiff base was synthesized by the condensation of 4-4' diamino diphenyl sulfone with ortho, meta and para, hydroxy benzaldehyde, respectively. The metal ion uptake behavior of these resins towards  $\text{Cu}^{+2}$ ,  $\text{Ni}^{+2}$ ,  $\text{Co}^{+2}$  and  $\text{UO}^{+2}$  ions in dilute aqueous media was studied. The optimum conditions for efficient uptake of metal ions were determined by varying the various parameters like contact time, size of sorbents, concentration of metal ion in the solution and pH of the reaction medium. It was observed that the structural features of the resins have profound effect on the uptake characteristics.



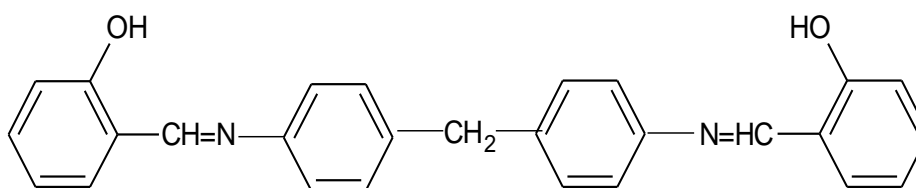
They have reported that out of three resins, resin containing -OH groups at meta position has a significant influence on the extent of metal ion uptake tendency. They have also reported that all these resins could be employed successfully to separate  $\text{Cu}^{2+}$  efficiently from binary mixture of  $\text{Cu}^{2+}$ - $\text{Ni}^{2+}$  and  $\text{Cu}^{2+}$ - $\text{UO}_2^{2+}$  at different pH values.

- 
22. A. Mishra, P. Panwar, M. Chopra, R. Sharma and Jean-Francois Chatal, "Synthesis of novel bifunctional Schiff bases ligands derived from condensation of 1-(p-nitro benzyl) ethylene diamine and 2-(p-nitro benzyl) 3-monooxo, 1,4,7-triazaheptane with salicylaldehyde", *New J. of Chem.*, 27, 1054-1058, 2003.
  23. R. R. Das, S. Samal, S. Acharya, P. Mohapatra and R. K. Dey, "A comparative study on metal ion uptake behavior of chelating resins derived from the formaldehyde condensed phenolic Schiff bases of 4,4'-diamino-diphenyl sulfone and hydroxy benzaldehydes", *Polym.- Plast. Technol. Eng.*, 41, 229-246, 2002

Ray et. al [24] have reported metal ion uptake behavior of formaldehyde condensed resins of phenolic Schiff bases derived from the reaction of 4,4'-diamino diphenyl and 4,4'-diamino diphenyl methane with o-hydroxy benzaldehyde.



**o-HB DDM**

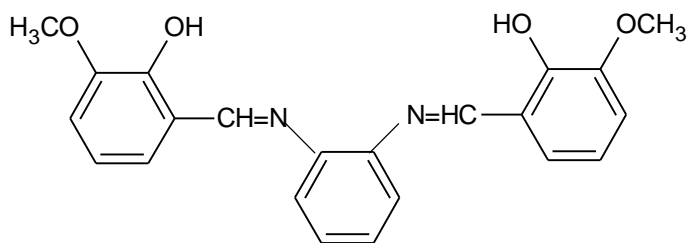


**o-HB-DD**

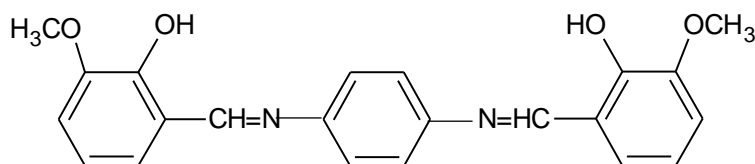
They have examined metal ion uptake characteristic of o-HB-DDM-HCHO and o-HB-DD-HCHO towards transition metal ions like  $\text{Cu}^{+2}$ ,  $\text{Ni}^{+2}$  and  $\text{UO}_2^{+2}$  under both competitive and non-competitive conditions. The resin o-HB-DDM-HCHO is more effective in removing metal ions in comparison of o-HB-DD-HCHO. Preferential adsorption of  $\text{Cu}^{+2}$  by both the resins was observed from the salt solution.

Ma et. al [25] have reported that Schiff bases synthesized from 3-methoxy salicylaldehyde with aromatic diamines exhibited strong inhibition of copper corrosion in chloride solution at different pH. In addition these molecules are environmentally friendly. The chemical structures of two Schiff bases are

- 
24. A. R. Ray, S. Samal, S. Acharya and R. K. Dey, "Studies of metal ion uptake behavior of formaldehyde condensed resins of phenolic Schiff bases derived from the reaction of 4,4'-diamino diphenyl and 4,4'-diamino diphenyl methane with o-hydroxy benzaldehyde", Ind. J. Chem. Technol., 11, 695-703, 2004.

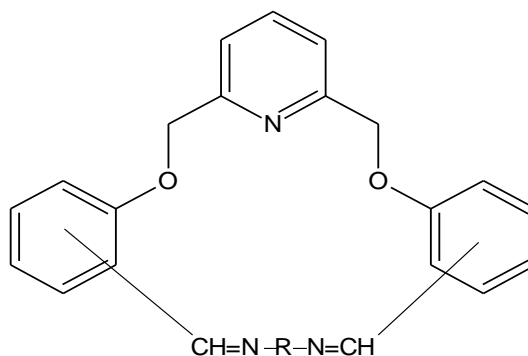


N,N'- o-phenylene – bis(3-methoxy salicylideneimine)



N,N'- p-phenylene – bis(3-methoxy salicylideneimine)

Kuzmin et.al [26] have reported anticancer activity of a set of macrocyclic Schiff bases based on 2,6- bis (2 and 4 formylaryl -oxy methyl) pyridines. They have derived correlation equation between the anticancer activity and structural parameters of the molecules studied.



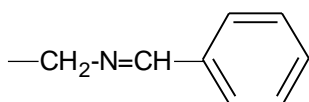
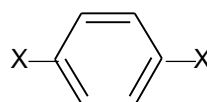
Where R= Various aromatic and aliphatic diamines

- 
25. H. Ma, S. Chen, L. Niu, S. Zhao, S. Li and D. Li "Inhibition of copper corrosion by several Schiff bases in aerated halide solutions", J. Appl. Electrochem., 32, 65-72, 2002.
  26. V. E. Kuzmin, V. P. Lozitsky, G. L. Kamalov R. N. Lozitskaya, A. I. Zheltvay, A. S. Fedtchouk and D. N. Kryzhanovsky, "Analysis of the structure-anticancer activity relationship in a set of Schiff bases of macrocyclic 2,6-bis (2 and 4-formylaryl oxymethyl) pyridines", Acta Biochimica Polonica, 47, 867-875, 2000.

They have proved that the increase in activity of the investigated Schiff bases towards leukemia and prostate cancer is caused by the presence of  $F_1$  fragments and the increased in number of  $F_2$  fragments lowered the activity both towards the CNS cancer and melanoma and so average activity towards nine tumors.

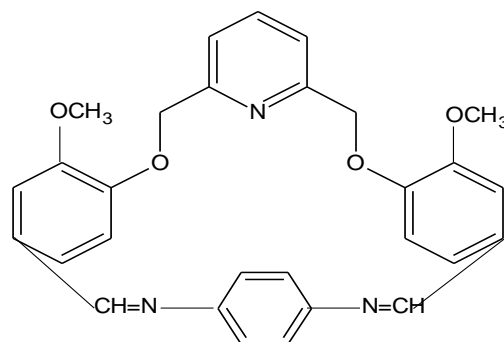
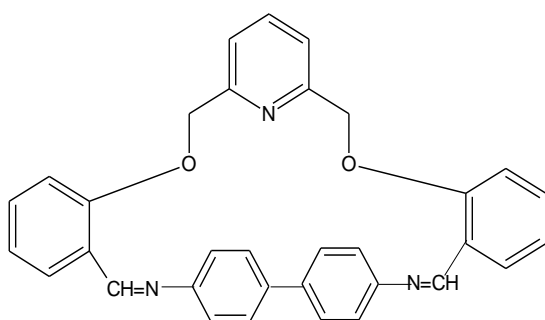
Ortho-dialdehydes and aliphatic diamines macrocyclic Schiff bases containing two  $F_1$  fragments are the most effective, while the appropriate 4,4' derivatives and 1,4-phenylene diamine Schiff bases containing two  $F_2$  fragments give lower anticancer activity.

$nF_1$  = number of structural fragments  $f_1$ ,  $nF_2$  = number of structural fragments  $f_2$

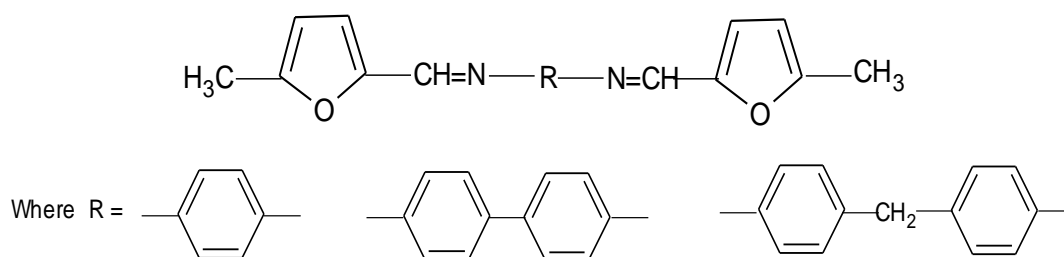
F<sub>1</sub>F<sub>2</sub>

Where x = non aromatic carbon atom

Lozitsky et. al [27] have reported 4D-QSAR study and anticancer activity of macrocyclic Schiff bases. The Schiff bases were synthesized by the condensation of various aliphatic and aromatic diamines with 2,6 - bis ( 2 and 4-formyl aryloxy methyl) pyridine derivatives. The results of biological activities showed that Schiff bases are active towards cell growth of the nine cell culture of human malignant tumors like leukemia, CNS cancer, prostate cancer, breast cancer, melanoma, small cell lung cancer, colon cancer, ovarian cancer and renal cancer. They claimed that pyridine ring has a negative influence on anticancer activity, while the presence of the  $>C=N$  group with different substituents promotes anticancer activity. Para substituted phenyl with non-aromatic substituents prevent the activity.



Kraicheva et. al [28] have reported synthesis and NMR spectroscopic study of three novel 5-methylfuryl containing Schiff bases. These three Schiff bases were synthesized by condensation of 5-methyl furfuraldehyde with appropriate mole ratio of 4,4'-diaminodiphenyl methane, 1,4-phenylene diamine and benzidine, respectively in diethyl ether with stirring at room temperature in nitrogen atmosphere for 4 h. Schiff bases were crystallized from cyclohexane and characterized by elemental analysis, TLC, IR,  $^1\text{H}$  NMR and  $\text{C}^{13}$  NMR spectral analysis. They have also synthesized bis (amino phosphonates) of these three Schiff bases, which have biological properties and various applications in agrochemistry.



Salman et. al [29] have studied keto-enol tautomerism and mass spectra of series of Schiff bases derived from the condensation of salicylaldehyde with aniline and naphthaldehyde.

- 
27. V. P. Lozitsky, V. E. Kuzmin, A. G. Artemenko, R. N. Lozytska, A. S. Fedtchouk, E. N. Muratov and A. K. Mescheriakov, "Investigation of anticancer activity of macrocyclic Schiff bases by means of 4D-QSAR based on simplex representation of molecular structure", SAR and QSAR in Environmental Research, 16, 219-230, 2005.
  28. I. Kraicheva, P. Finocchiaro, and S. Failla, "Synthesis and NMR spectroscopic study of new 5-methylfuryl containing Schiff bases and related bis (amino phosphonates)", Phosphorus, Sulfur, and Silicon, 179, 2345-2354, 2004.
  29. S. R. Salman and F. S. Kamounah, "Mass spectral study of tautomerism in some 1-hydroxy-2-naphthaldehyde Schiff bases", Spectroscopy Letters, 35, 327-335, 2002.

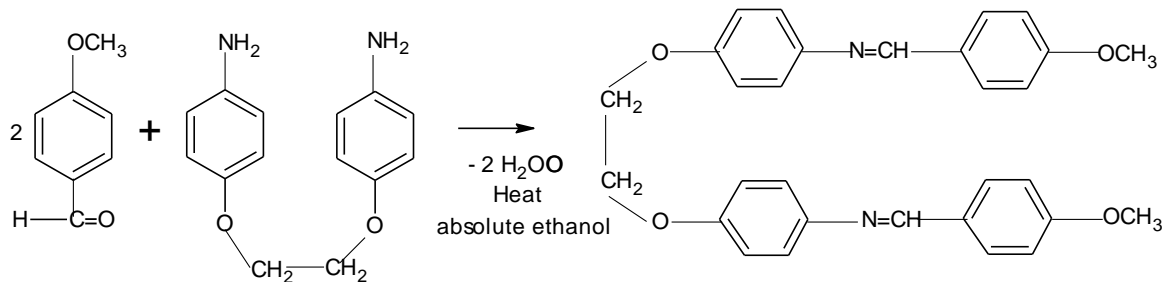


Schiff bases play an important role in Inorganic Chemistry as they easily form stable complexes with the most metal cations [30, 31]. Transition metal complexes of tetradentate Schiff base ligands find applications as model of certain metal enzymes, in catalysis and material chemistry [32].

In the field of co-ordination chemistry ortho-hydroxylated Schiff bases have received considerable attention [33]. The introduction of lateral polar hydroxy groups enhances the molecular polarizability as well as stabilizing the liquid crystalline compounds [34].

Cakir et. al [35] have synthesized Cu(II), Ni(II), Zn(II) and Co(II) complexes of Schiff base derived from 4-methoxy benzaldehyde and 1,2 bis(4-aminophenoxy) ethane. Schiff base and its complexes were characterized by magnetic susceptibility, conductance measurements, elemental analysis, UV-Vis, <sup>1</sup>H NMR and IR spectral studies. Based on the physical and chemical data of spectral studies they have proposed structure of Schiff base and its complexes.

- 
30. H. Temel and Sekerci, "Novel complexes of manganese (II), Cobalt (II), Copper (II), and Zinc (II) with Schiff base derived from 1,2 bis (p-amino phenoxy) ethane and salicylaldehyde", *Synth. React. Inorg. Met.-Org. Chem.*, 31, 849-857, 2001.
  31. Adeola A. Nejoa, Gabriel A. Kolawolea, Andy R. Opokub, Christo Mullerc and Joanna Wolowskad, "Synthesis, characterization, and insulin-enhancing studies of unsymmetrical tetradentate Schiff-base complexes of oxovanadium(IV)", *J. Coordination Chem.*, 62(21), 3411–3424, 2009.
  32. H. Temel, S. Ilhan and M. Sekerci, "Synthesis and characterization of a new bidentate Schiff base and its transition metal complexes", *Synth. React. Inorg. Met. Org. Chem.* 32, 1625-1634, 2002.
  33. H. Temel, U. Cakir, H. I. Urgas and M. Sekerci, "The synthesis, characterization and conductance studies of new Cu(II), Ni(II) and Zn(II) complexes with Schiff base derived from 1,2- bis(o-amino phenoxy) ethane and salicylaldehyde", *J. Coord. Chem.* 56, 943-951, 2003.



Gangani and Parsania [36] synthesized a series of new symmetric double Schiff bases of 1, 10-bis(4-aminophenyl)-cyclohexane and substituted aromatic benzaldehyde via classical and microwave-irradiated techniques. The synthesis time is much shorter and yields of the Schiff bases are found to be better with the microwave-irradiation technique than classical technique. The purity of Schiff bases is checked by TLC. The structures of Schiff bases are supported by FTIR,  $^1\text{H}$  NMR, and MS techniques. The biological activity of Schiff bases is checked against Gram-positive and Gram-negative microbes. Schiff bases showed moderate antibacterial activity but showed moderate to excellent antifungal activity in comparison with chosen standard drugs.

- 
34. G. Y. Yeap, S. T. Ha, P. L. Lim, P. L. Boey and W. A. K. Mahmood, "Synthesis and mesomorphic properties of Schiff base esters ortho-hydroxy, para-alkoxy benzylidene-para substituted anilines", *Mol. Crystal, Liq. Cryst.*, 423, 73-84, 2004.
  35. U. Cakir, H. Temel, S. Ilhan, and H. I. Urgas, "Spectroscopic and conductance studies of new transition metal complexes with a Schiff base derived from 4-methoxybenzaldehyde and 1,2 bis- (4-aminophenoxy) ethane", *Spectroscopy Lett.*, 36, 429-440, 2003.
  36. B. J. Gangani and P. H. Parsania, "Microwave irradiated and classical syntheses of symmetric double Schiff bases of 1,1'-bis(4-amino phenyl)cyclohexane and their physico-chemical characterization", *Spectroscopy Letters*, 40(1), 97-112, 2007.

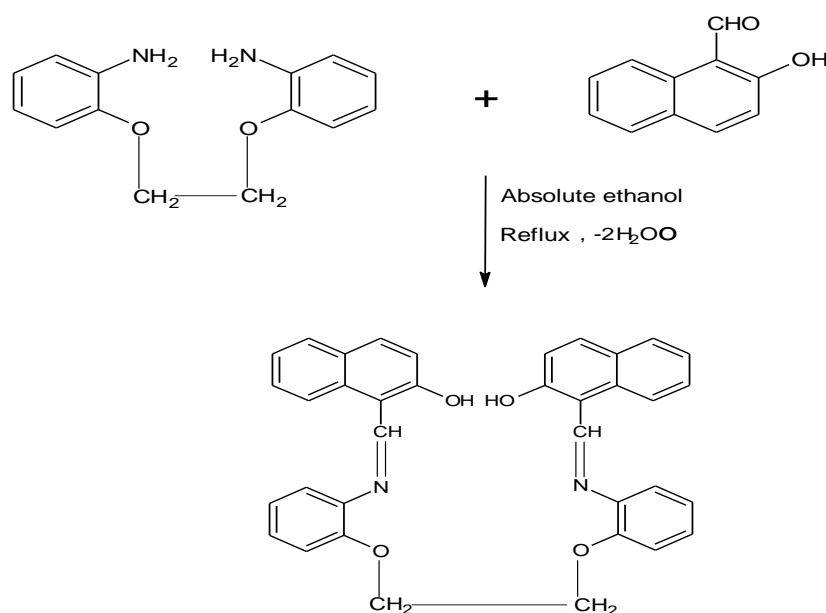
Aghera et. al [37] synthesized novel symmetric double quinoline derivatives using the Vilsmeier–Haack reagent and symmetric double acetamides of 1,1'-bis(R,4-aminophenyl)cyclohexane/methane. The structure of the intermediates (SDA-1 to SDA-3) and final products (SDQ-1 to SDQ-3) were supported by UV, FTIR,  $^1\text{H}$  NMR,  $^{13}\text{C}$  NMR and Mass spectroscopic measurements. SDA-1 to SDA-3 and SDQ-1 to SDQ-3 possess moderate to good antibacterial and antifungal activities. They had also studied thermal behavior with TGA and DSC technique. Schiff bases are thermally stable up to 173-272 °C and followed single step or two step degradation. Different magnitudes of  $\eta$ , E and A suggested different degradation mechanisms [38].

Gangani and Parsania [39, 40] reported the density ( $\rho$ ), viscosity ( $\eta$ ) and ultrasonic speeds (U) [2MHz] of pure solvents: chloroform (CF), DMF, and symmetric double Schiff bases solutions have been investigated to understand the effect of substituents on intermolecular interactions at 303, 308 and 313K. Various acoustical parameters such as acoustical impedance (Z), isentropic compressibility( $K_s$ ), Rao's molar sound function (R), Van der Waals constant (b), internal pressure( $\pi$ ), free volume ( $V_f$ ), intermolecular free path length ( $L_f$ ), classical absorption coefficient ( $\alpha/f^2$ )<sub>Cl</sub>, and viscous relaxation time ( $\tau$ ) were determined and correlated with concentration(C). A good to excellent correlation between a given parameter and concentration is observed at all temperatures and solvent systems studied. Linear or non-

- 
37. V. K. Aghera, J. P. Patel and P. H. Parsania, "Synthesis, spectral and microbial studies of some novel quinoline derivatives via Vilsmeier-Haack reagent", ARKIVOC XII, 195-204, 2008.
  38. V. K. Aghera and P. H. Parsania, "Effect of substituents on thermal behavior of some symmetric double Schiff's bases containing a cardo group", J. Sci. and Ind. Res., 67, 1083-1087, 2008.
  39. B. J. Gangani and P. H. Parsania, "Ultrasonic speeds and acoustical parameters of symmetric double Schiff's bases solutions at 303, 308 and 313 K", J. Appld. and Pure Ultras., 30, 90-96, 2008.
  40. B. J. Gangani and P. H. Parsania, "Density, viscosity and ultrasonic velocity studies of cardo group containing symmetric double Schiff bases solutions at 303, 308 and 313 K", J. Ind. Chem. Soc., 86, 942-949, 2009.

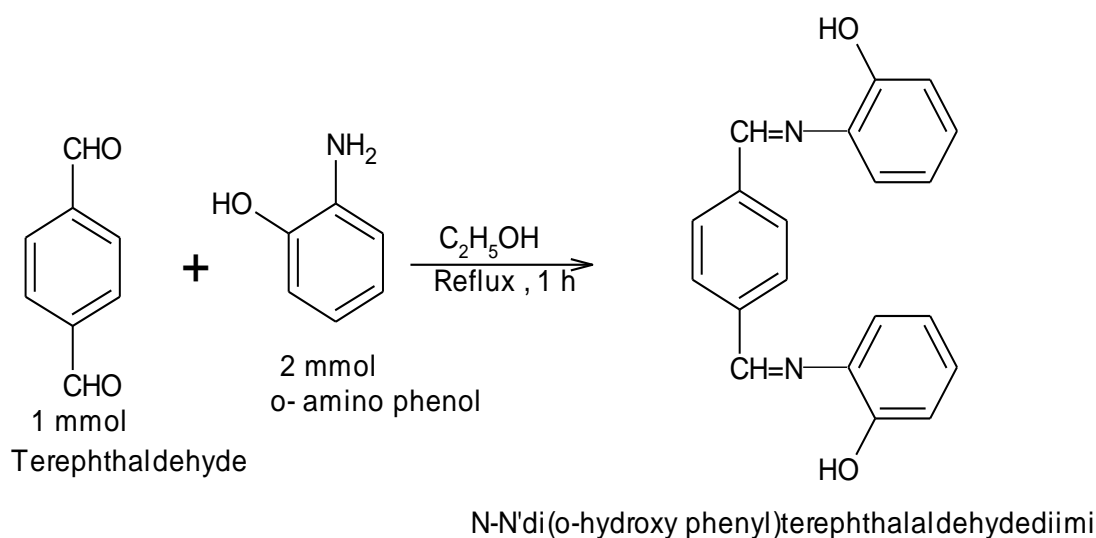
linear increase or decrease of acoustical parameters with concentration and temperature (T) indicated the existence of strong intermolecular interactions. The linear or non-linear increase of solvation number ( $S_n$ ) with C and decrease with T; and non linear decrease (CF system) and non linear increase (DMF system) of apparent molar volume ( $\phi_v$ ) with C and T also supported the existence of molecular interactions.

Temel [41] has reported Cu(II), Ni(II), and Zn(II) complexes with the Schiff base derived from 1,2-bis (o-amino phenoxy) ethane and 2-hydroxynaphthaline 1-carbaldehyde and are characterized by elemental analysis, magnetic measurement,  $^1\text{H}$  NMR, UV – Visible and IR spectra, as well as conductance studies. Magnetic properties showed that Cu(II) Schiff base complex is paramagnetic and its magnetic moment is 1.61 BM. Since Cu(II) complex is a paramagnetic and as a result its  $^1\text{HNMR}$  spectrum could not be obtained, while Ni(II) and Zn(II) Schiff base complexes are diamagnetic and  $^1\text{HNMR}$  spectra were obtained. Conductivity studies showed that the complexes are non-electrolyte as shown by their molar conductivity measurements in DMF. Synthesis of the ligand N,N'-bis(2-hydroxy naphthalin-1-carbaldehyde)-1,2- bis (o- amino phenoxy) ethane.



41.H. Temel, "Synthesis and spectroscopic studies of new Cu(II), Ni(II), VO(IV), and Zn(II) complexes with N-N' bis (2-hydroxy naphthalin-1-carbaldehyde)1,2-bis(o-amino phenoxy) ethane", J. Coord. Chem., 57, 723-729, 2004.

Patel et. al [42, 43] have reported synthesis of symmetric Schiff base known as N,N'- di (o-hydroxy phenyl) terephthalaldehyde diimine. They have also reported synthesis of Mn(II), Ni(II), Cu(II), Zn(II) and Cd(II) complexes of Schiff base ligand and characterized by elemental analysis, IR and electronic spectra, magnetic measurements and thermo gravimetric analysis. The Schiff base was derived from terephthalaldehyde and o-aminophenol. They have noticed that when ethanolic solutions of terephthalaldehyde and o-aminophenol were mixed, a yellow crystalline solid was obtained immediately. The mixture was heated on a water bath for 1 h and the ligand was filtered, washed successively with water and ethanol and dried in air. The ligand is insoluble in organic solvents like benzene, chloroform and acetone but soluble in DMF.



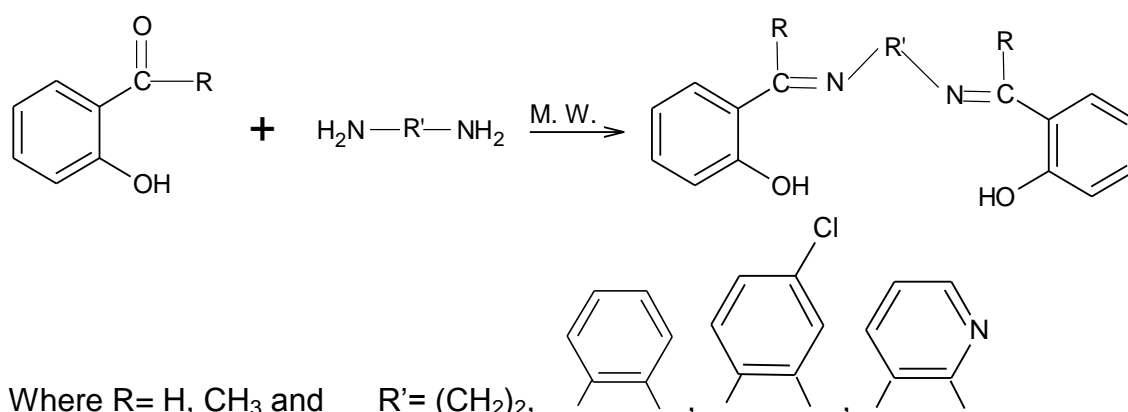
- 
42. N. H. Patel, K. M. Patel, K. N. Patel and M. N. Patel, "Co-ordination chain polymers of transition metals with Schiff base", *Synth. React. Inorg. Met-Org. Chem.* 31, 1031-1039, 2001.
43. N. H. Patel, P. K. Panchal and M. N. Patel, "Synthesis and characterization and co-ordination polymers of trivalent lanthanides with a Schiff base", *Synth. React. InOrg. Met. Org. and Nonmetal Chem.*, 35, 107-110, 2005.

Ismet Kaya et. al [44] have synthesized a new conjugated aromatic oligo(azomethine) derivative using oxidative polycondensation of 1,4-bis[(2-hydroxyphenyl)methylene] phenylenediamine (HPMPDA) by air, H<sub>2</sub>O<sub>2</sub> and NaOCl oxidants in an aqueous alkaline medium. The structures of 1,4-bis[(2-hydroxyphenyl) methylene] phenylenediamine and oligo-1,4-bis[(2-hydroxyphenyl)methylene] phenylenediamine (OHPMPDA) were confirmed by FTIR, <sup>1</sup>H NMR, <sup>13</sup>C NMR and elemental analysis. The characterization was made by TGA–DTA, size exclusion chromatography (SEC), magnetic moment and solubility tests. Metal complex compounds of OHPMPDA were synthesized with metal salts of Fe, Co, Ni, Cu, Zn, Cd, Mn, Cr, Pb and Hg. Elemental analyses of oligomer–metal complexes suggested that the ratio of metal to oligomer is 1:1. The results of this study showed that aromatic oligo azomethine and its metal complexes were an interesting class of conjugated compounds of which electronic structure and the other properties can be regulated over a wide range by using different oxidation reagents.

Yang et. al [45] have reported microwave assisted condensation of salicylaldehyde and aryl amines without solvent with high yields, which were confirmed by IR, <sup>1</sup>H NMR, <sup>13</sup>C NMR and elemental analyses. They have reported that solvent free organic synthesis mediated by microwave irradiation (M.W.) offers significant advantages such as economy, environmental friendly, simple work up procedure and high yields along with fairly mild conditions, while on the contrary in classical organic synthesis it is common to meet the problem of removing solvents especially in the case of aprotic dipolar solvents with high boiling points or the isolation of reaction products through liquid – liquid extraction. The absence of solvent reduces the risk of hazardous explosion when the reaction takes place in a closed vessel in a microwave oven.

- 
44. Ismet Kayaa, Ali Bilici and Mehmet Sacak, “New conjugated azomethine oligomers obtained from bis (hydroxyphenyl)methylenediamine via oxidative polycondensation and their complexes with metals”, *Synthetic Metals*, 159, 1414–1421, 2009.

Aghayan et. al [46] have synthesized tetradentate Schiff bases using microwave activation under solvent free condition with and without support. They have proved microwave (M.W.) enhanced chemical reaction in general and on organic supports. Microwave assisted reactions have gained popularity over the usual homogeneous and heterogeneous reactions. They can be conducted rapidly and provide pure products in quantitative yields without using solvent.



They have synthesized tetradentate Schiff bases by the reaction of salicylaldehyde or 2-hydroxy acetophenone with the corresponding diamines such as ethylene diamine, phenylene diamine, 2-3-diaminopyridine and 4-chlorophenylenediamine supported on silica gel. In short they have developed simple and rapid procedure for the synthesis of tetradentate Schiff bases.

- 
45. H. Yang, W.H. Sun, Z. Li and L. Wang, "Solvent free synthesis of salicylaldimines assisted by microwave irradiation", *Synthetic Communications*, 32, 2395-2402, 2002.
46. M. M. Aghayan, M. Ghassemzadeh, M. Hoseini and M. Bolourtchian, "Microwave assisted synthesis of the tetradentate Schiff bases under solvent free-and catalyst free condition", *Synthetic Communication*, 33, 521-525, 2003.

### Section-III: Literature survey on epoxy resins

Epoxy and phenolic resins are the most versatile class of contemporary plastics. Due to tendency of undergoing variety of chemical reactions, both resins became material of choice for researchers for several years. By the help of reactions like co-polymerization, chain extension by reactive diluents, side chain modification, incorporation of variety of fillers and structure modifiers, the resin structure can be modified. The capabilities of undergoing vast chemical reactions of the resins the desire properties can be achieved.

Epoxy resins are widely used as a matrix in composites in different applications where chemical, mechanical, thermal, and dielectric properties are necessary. In addition, epoxy resins are versatile cross-linked thermosetting polymers with an excellent chemical resistance and good adhesion properties to different substrates. Due to these properties, they are used as adhesives and coatings [47]. Epoxy is best for laminates in combination with glass fiber to achieve excellent electrical insulators, while phenolics are best with wood based cheap composites due to excellent adhesion with cellulosic materials. Excellent chemical and corrosion resistance, thermal and dimensional stability, superior mechanical and electrical properties, together with the ease of handling and processability, have made epoxy resins highly useful as surface coatings, and structural adhesive [48-51].

Shah et. al [52] reported the curing reactions of epoxy resin of 1,1'-bis(4-hydroxy phenyl) cyclohexane with phthalic anhydride by differential scanning calorimetry. The overall kinetics of curing have been found to follow a simple Arrhenius-type rate-temperature dependence, with an average overall activation energy of  $75.4 \pm 8.0 \text{ kJ mol}^{-1}$  and natural log of Arrhenius frequency factor of about  $18 \text{ min}^{-1}$  up to at least 90% conversion. The curing reaction is found to follow overall first-order kinetics.

---

47. I. Hackman, and L. Hollaway, "Epoxy-layered silicate nanocomposites in civil engineering", *Composites Part A*, 37(8), 1161–1170, 2006.



Use of epoxy resins in composite matrix in high technology areas is limited, as these areas require material with inherent low thermal expansion coefficients and high toughness [53, 54] and better heat and moisture stability. Recently, a lot of research work has been done to improve the required parameters of epoxy resins through modifications in both the backbone and pendant groups. Urea-formaldehyde and silicon resins have been reported to have excellent properties as modifiers for the epoxy resins. The first commercial attempts to prepare resins from epichlorohydrin were made in 1927 in the United States. Credit for the first synthesis of bisphenol-A-based epoxy resins is shared by Dr. Pierre Castan of Switzerland and Dr. S. O. Greenlee of the United States in 1936. Dr. Castan's work was licensed by Ciba, Ltd. of Switzerland, which went on to become one of the three major epoxy resin producers worldwide. Ciba's epoxy business was spun off and later sold in the late 1990s and is now the advanced materials business unit of

- 
48. Hua Ren, Jian Zhong Sun, A Binjie Wu and Qiyun Zhou, "Synthesis and properties of a phosphorus-containing flame retardant epoxy resin based on bis-phenoxy(3-hydroxy)phenyl phosphine oxide", *Polym. Degr. and Stab.*, 92(6), 956–961, 2007.
  49. Guoyuan Pana, Zhongjie Dua, Chen Zhanga, Congju Lib, Xiaopin Yanga and Hang Quan Li, "Synthesis characterization, and properties of novel novolac epoxy resin containing naphthalene moiety", *Polymer* 48(13), 3686–3693, 2007.
  50. Gue Yanga, B., Shao-Yun Fu and Jiao-Ping Yang, "Preparation and mechanical properties of modified epoxy resins with flexible amines", *Polymer*, 48(1), 302–310, 2007.
  51. L. A. Marcad, A. M. Galia and J. A. Rina, "Silicon-containing flame retardant epoxy resins synthesis, characterization and properties", *Polym. Degr. and Stab.*, 91(11), 2588–2594, 2006.
  52. P. P. Shah, P. H. Parsania and S. R. Patel, "Curing of epoxy resin of 1,1'-bis (4-hydroxyphenyl)cyclohexane with phthalic anhydride-A Differential scanning calorimetric investigation", *British Polym. J.*, 17 (4), 354, 1985.

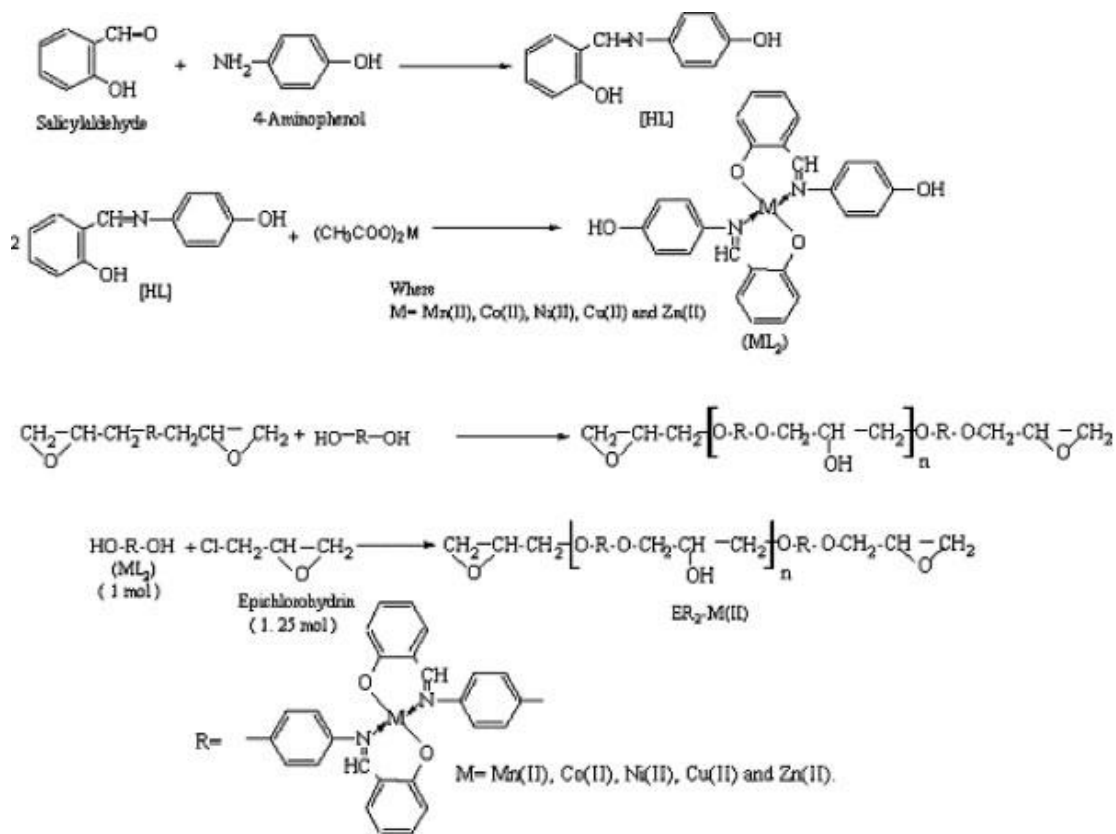
Huntsman Corporation of the United States. Dr. Greenlee's work was for the firm of Devoe-Reynolds of the United States. Devoe-Reynolds, which was active in the early days of the epoxy resin industry, was sold to Shell Chemical (now Hexion, formerly Resolution Polymers and others). Phenol formaldehyde condensation polymers often referred as phenolic resins, were the first true synthetic polymers to gain commercial acceptance. They have maintained a prominent position in the polymer market to the present time. About 70% of all the thermosetting polymers produced are made up of phenol, urea and melamine-formaldehyde polymers, with phenolics enjoying the lion's share. The ability of formaldehyde to form resinous substance had been observed by chemists in the second half of the 19th century. In 1859 Butlerov described formaldehyde polymers, while in 1872 Adolf Bayer reported that phenol and aldehyde react to give resinous substances.

Tansir Ahamad and Nishant [55] reported a new epoxy resins, bearing Schiff-base metal complexes were prepared by the condensation of epichlorohydrin with Schiff-base metal complexes (L2M, azomethine metal complexes) in 2 : 1 and 1.25 : 1 molar ratios, respectively, in an alkaline medium. The synthesized epoxy resins were characterized by various instrumental techniques, such as analytical, spectral, and thermal analysis. The epoxide equivalent weight (g/equiv) and epoxy value (equiv/100 g) of the synthesized epoxy resins were measured by standard procedures. The glass-transition temperatures of all of the synthesized polymers were in the range 153–230°C. The antimicrobial activities of these resins were screened against some bacteria and against some yeast with an agar well diffusion method. All of the synthesized resins showed promising antimicrobial activities.

---

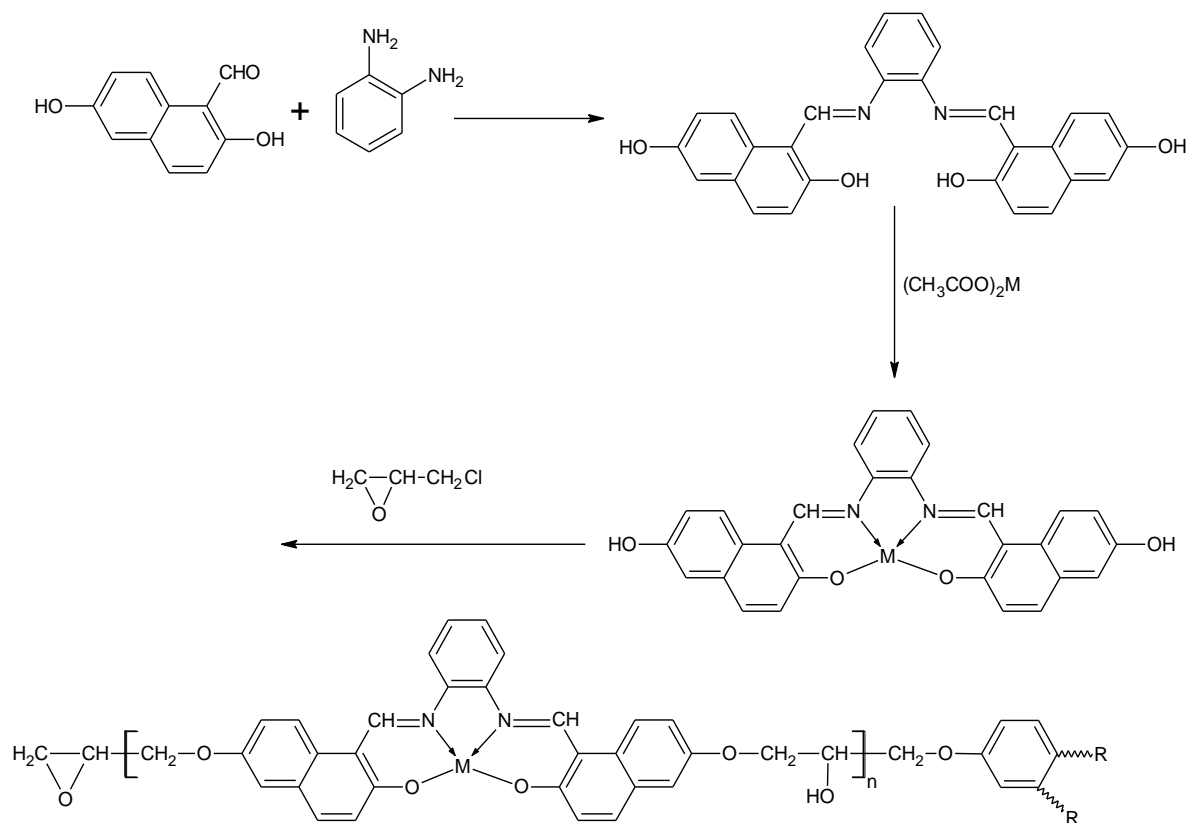
53. D. Puglia, L. B. Manfredi, A. Vazquez and J. M. Kenny, "Thermal degradation and fire resistance of epoxy-amine phenolic blends", *Polym. Degr. and Stab.*, 73(3), 521–527, 2001.

54. K. E. L. Gersifi, N. Destais-Orvoe<sup>n</sup>, and G. Tersac, "Glycolysis of epoxid-amine hardened networks. 1. diglycidylether/aliphatic amines model networks", *Polymer*, 44(14), 3795–3801, 2003.



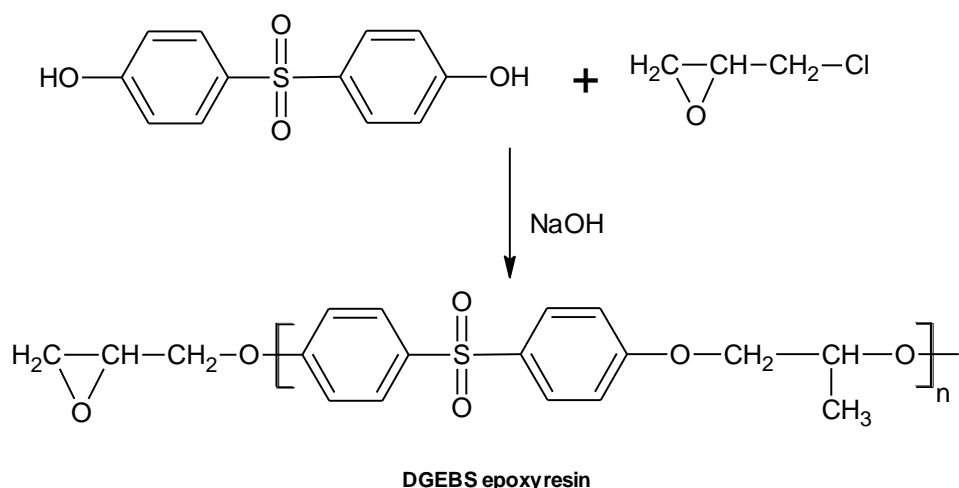
Tansir Ahamad and Alshehri [56] reported a series of metal-containing epoxy polymers have been synthesized by the condensation of epichlorohydrin with Schiff base metal complexes in alkaline medium. Schiff base was initially prepared by the reaction of 2,6 dihydroxy-1-naphthaldehyde and o-phenylenediamine in 1 : 2 molar ratio and then with metal acetate. All the synthesized compounds were characterized by elemental, spectral, and thermal analysis. The physicochemical properties, viz., epoxy value, hydroxyl content, and chlorine content were measured by standard procedures. The antimicrobial activities of these metal-containing epoxy polymers were carried out by using minimum inhibitory concentration (MIC) and minimum bactericidal concentration (MBC) methods.

55. Tansir Ahamad and N. Nishat, "New antimicrobial epoxy-resin-bearing Schiff-base metal complexes", *J. Appl. Polym. Sci.*, 107, 2280–2288, 2008.
56. Tansir Ahamad and Saad M. Alshehri, "New thermal and microbial resistant metal-containing epoxy polymers", *Bioinorganic Chemistry and Applications*, April 2010, accepted, doi:10.1155/2010/976901.



Soo-Jin Park and Fan-Long Jin [57] reported sulfone-containing epoxy resin, the diglycidylether of bisphenol-S (DGEBS) and its structure was confirmed by FT-IR and NMR spectra, and elemental analysis. Curing behaviours, thermal stabilities, and dynamic mechanical properties of the DGEBS resin cured with phthalic anhydride (PA) and tetrahydrophthalic anhydride (THPA) as curing agents were studied using dynamic differential scanning calorimetry (DSC), thermogravimetric analysis (TGA) and dynamic mechanical analysis (DMA). The DGEBS/THPA/DMBA system showed higher glass transition temperature, initial decomposition temperature, and activation energy for decomposition than those of the DGEBS/PA/DMBA system, which was attributed to the higher cross-linking density of the DGEBS/THPA/DMBA system.

57. Soo-Jin Park and Fan-Long Jin, "Thermal stabilities and dynamic mechanical properties of sulfone-containing epoxy resin cured with anhydride", *Polymer Degradation and Stability*, 86, 515-520, 2004.



Atta et al. [58] reported epoxy binders prepared from Schiff base monomers through two steps. The first step is based on condensation of hydroxy benzaldehyde derivatives with *o*- and *p*-phenylenediamine. The second step includes the reaction between Schiff base monomers with epichlorohydrin to produce epoxy binder. The synthesized epoxy binders were characterized by determination of epoxy contents and epoxy functionalities. The chemical structures and epoxy functionalities were determined by  $^1\text{H}$  NMR analysis. The thermal stability and characteristics of the prepared Schiff base monomers and polymers as well as their epoxy resins were measured by DSC and TGA analysis. The prepared epoxy resins were cured with polyamine like pentaethylene hexamine (PEHA) and *p*-phenylenediamine (PDA). The cured epoxy polyamine systems were evaluated in coating applications of steel by measuring the mechanical properties and chemical resistance of the cured films.

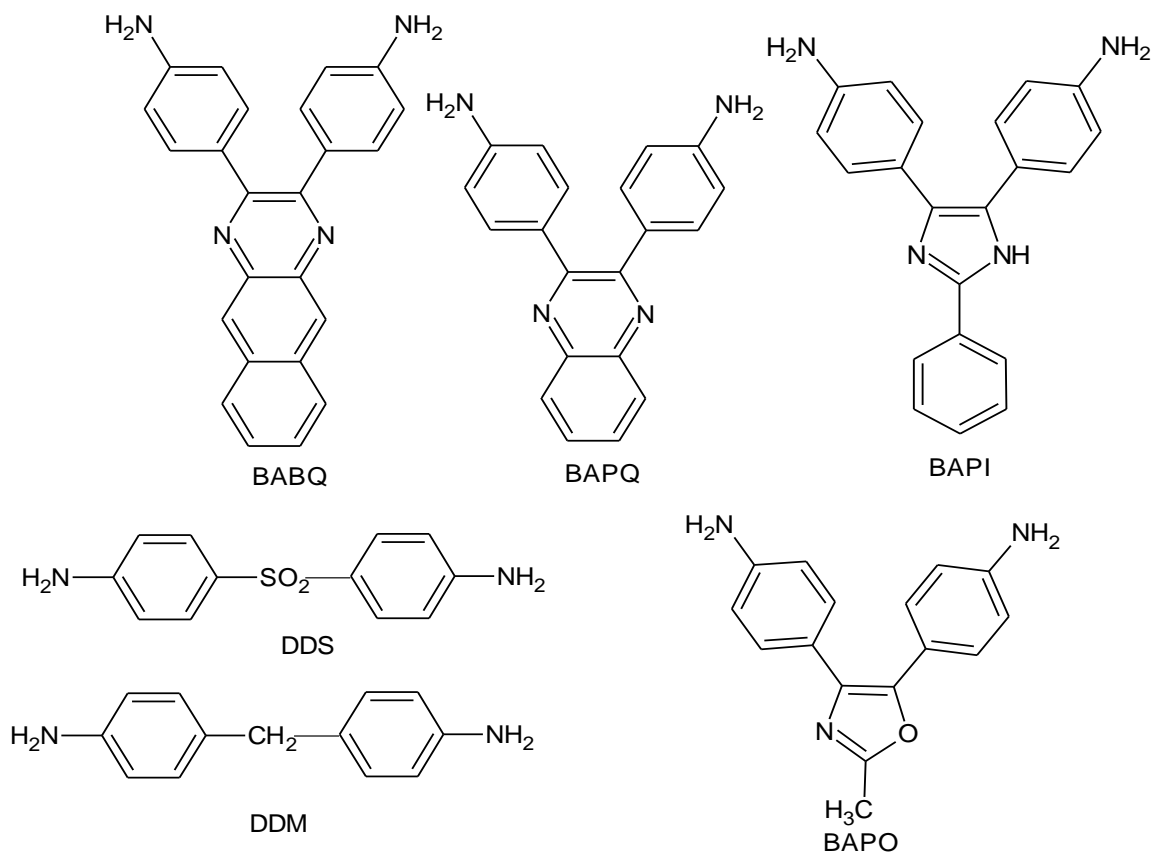
- 
58. A. M. Atta, N. O. Shaker and N.E. Maysour, "Influence of the molecular structure on the chemical resistivity and thermal stability of cured Schiff base epoxy resins", *Progress in Organic Coatings*, 56, 100–110, 2006.
59. Fengfeng Liua, Hao Weib, Xiaobin Huang, Jiawei Zhanga, Yubo Zhoua and Xiaozhen Tang, "Preparation and properties of novel inherent flame-retardant cyclotriphosphazene-containing epoxy resins", *J. Macromol. Sci., Part B*, 49(5), 1002 – 1011, 2010.

Fengfeng Liu et. al [59] synthesized a novel flame-retardant cyclotriphosphazene-based epoxy resin (CPEP) by epoxidation of bis-(4-hydroxyphenylsulfonylphenoxy) tetraphenoxycyclotriphosphazene with epichlorohydrin, and was characterized by  $^1\text{H}$  NMR, FTIR, and gel permeation chromatography (GPC). Then the blends of CPEP and diglycidyl ether of bisphenol A (E51) with different mass ratios were cured using 4, 4'-diaminodiphenylmethane as a curing agent. The curing behavior and the glass transition temperatures of the resulting thermosets were studied by differential scanning calorimetry. The thermal stabilities and flame-retardant properties of the cured resins were studied by TGA and UL94 tests, respectively. In addition, mechanical, hydrophobic, and electrical properties were also characterized. Compared to the corresponding E51-based thermosets, the cured resins with a mixture of CPEP and E51 showed better thermal stabilities, higher char yields, and greatly improved flame-retardant properties. Furthermore, relatively good mechanical properties, hydrophobicity, and electric resistance were maintained. The cured resins of CPEP/E51 (mass ratio 1:1) achieved UL94 V-0 rating, indicating that the epoxy resin prepared in this study could be used as a flame-retardant coating material.

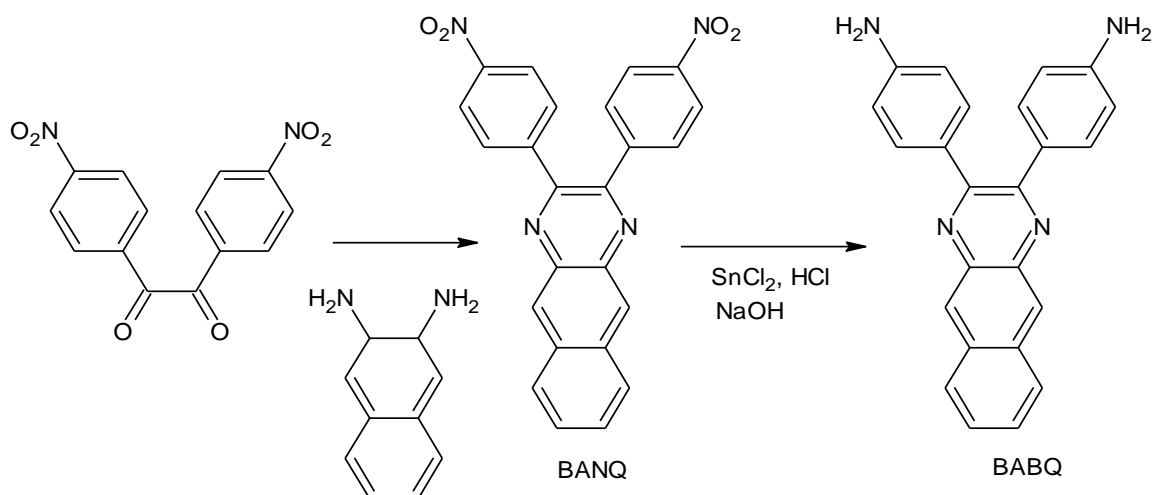
Inoki et. al [60] have studied curing behavior and properties of epoxy resins cured with the diamines having heterocyclic ring. The diamines 2-3'-bis(4-amino phenyl) benzoquinoxaline (BAPQ), 4,5-bis(4-aminophenyl)2-phenyl imidazole (BAPI), and 4,5-bis(4-amino phenyl)2-methyl oxazole (BAPO) were prepared and used as curing agents. They have reported that DGEBA cured with aromatic diamines having heterocyclic ring, especially 2, 3-bis(4-aminophenyl)quinoxaline (BAPQ) displayed both excellent bonding strength and thermal stability.

- 
60. M. Inoki, S. Kimura, N. Daicho, Y. Kasashima, F. Akutsu and K. Marushima, "Curing behavior and properties of epoxy resins cured with diamine having heterocyclic ring", *J. Macromol. Sci- Pure & App. Chem.*, 4, 321-331, 2002.

Commercially available diamines such as, 4, 4'-diamino diphenyl sulfone (DDS), 4, 4'-diamino diphenyl methane (DDM) or m-phenylene diamine possess high bonding strength at lower temperature, but fall at elevated temperature, while the epoxy resin cured with BAPQ has high bonding strength even at 180 °C.



The reaction route of BABQ is as under



Union Carbide Co. [61] has reported curing of polyepoxides with liquid glycol diamines ( $\text{H}_2\text{N}(\text{CH}_2)_3\text{O}(\text{C}_n\text{H}_{2n}\text{O})_x(\text{CH}_2)_3\text{NH}_2$ ) (I), where  $n$  is 2-5 and  $x$  is 1-11. The cured compounds have excellent impact strength and flexibility and are stable as protective coatings. Thus, 100g of diglycidyl ether was mixed with 29.4 g stoichiometric amount of  $\text{H}_2\text{N}(\text{CH}_2)_3\text{O}(\text{CH}_2\text{CH}_2\text{O})_2(\text{CH}_2)_3\text{NH}_2$  for 5 min. The mixture was applied on cold-rolled steel and was cured by storing 7 days at room temperature.

Joshi et. al [62] have studied curing behavior and properties of epoxy resins of 1,1'-bis(4-hydroxy-phenyl)cyclohexane cured by using 50% pyromellitic dianhydride (PMDA), tetrachloro phthalicanhydride (TCP), bisphenol-C-formaldehyde resin (BCF), diamino diphenyl methane (DDM) and 1,1'-bis(4-amino phenyl)cyclohexane (DDC) as curing agents at  $230^\circ\text{C}/150^\circ\text{C}$ .

PMDA, TCP and BCF cured resins are insoluble in all common solvents, while DDM and DDC cured resins are soluble in common solvents. BCF, PMDA, TCP and DDC cured samples are thermally stable up to about  $350\text{-}365^\circ\text{C}$  except DDM cured sample ( $275^\circ\text{C}$ ).

#### **Section-IV: Literature survey on bisbenzoxazines**

Heterocyclic compounds are used for various purposes because they possess a specific chemical reactivity. Introduction of heterocyclic group into drugs may affect their physical properties, for example the dissociation constants of sulpha drugs or modify their pattern of absorption, metabolism or toxicity, etc.

- 
61. Union Carbide Co. (by Norman H. Reinking.), "Liquid glycol diamine curing agent for polyepoxides", Brit. 904, 403, 1962. Chem. Abstr. 58, 1643, 1963.
  62. J. K. Joshi, S. T. Gadhia, P. H. Parsania, "Thermal properties of cured bisphenol-C-epoxy resins", J. Polym. Mater., 22, 133-144, 2005.



In recent years, processing of thermosetting resins has received strong attention from the automotive, aerospace and construction industries because of the great potential of these materials. The processing of these materials is complicated because of the involvement of chemical reactions. In addition, reinforcements, fillers, pigments and other additives are commonly added. Thus, the understanding of curing is fundamental in the analysis, control and design of any processing operation.

Kinetic study deals with a new type of phenolic resin obtained via ring-opening polymerization. These new materials are supposed to solve the problems related to traditional phenolic resins, such as brittleness, release of water and ammonia during the condensation curing reactions, toxicity of raw materials (especially phenol), high viscosity of the precursors, strong acid compounds as catalyst, and a narrow processability window.

These novel phenolic resins are based on benzoxazine structure, which were first synthesized by Holly and Cope [63]. These structures were not recognized as phenolic resins precursors until Schreiber [64] reported in 1973 that a hard and brittle phenolic materials was formed from benzoxazines precursors. No further details about structures and properties were included.

Tarek Agag et al. [65] prepared amino-functional benzoxazine. Several routes have been applied to incorporate amino group into benzoxazine structure. These approaches include reduction of the corresponding nitro-functional benzoxazines and deprotection of protected aminofunctional benzoxazine monomers. Various approaches that allow primary amine groups to be prepared without damaging the existing benzoxazine groups have been evaluated. FTIR and  $^1\text{H}$  and  $^{13}\text{C}$  NMR are used to characterize the structure of the monomers. The polymerization behavior of amino-functional monomers and model compound are studied by differential scanning calorimetry (DSC).

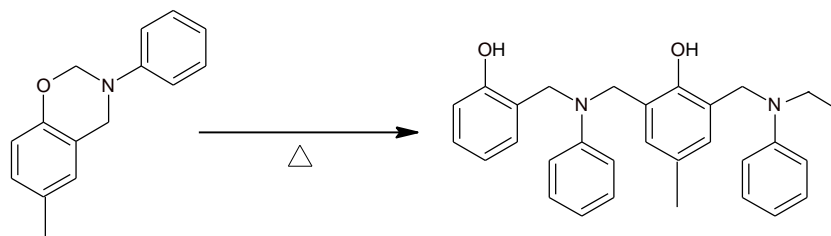
---

63. F.W. Holly and A. C. Cope, "Condensation products of aldehydes and ketones with o-aminobenzyl alcohol and o-hydroxybenzylamine", J. Am. Chem. Soc., 66, 1875-1879, 1944.

64. H. Schreiber, Ger. Offen. 2225504, 1973; Ger. Offen. 2323936, 1973.

Benzoxazine based resin has such unique characteristic as dimensional stability, near-zero shrinkage, in addition to good heat resistance, water resistance, electrical insulation properties, mechanical properties, and flame resistance [66, 67].

It is well known that the benzoxazine ring is stable at low temperature,



The ring-opening reaction of a benzoxazine ring

but the ring-opening reaction occurs at high temperature and a novolac type oligomer with a phenolic hydroxyl group and tertiary amine group is produced [68]. Using this benzoxazine compound as a phenolic resin, a new type of phenolic resin that releases no volatile during the curing reaction and need no catalysts can be developed.

- 
65. Tarek Agag, Carlos R. Arza, Frans H. J. Maurer and Hatsuo Ishida, "Primary amine-functional benzoxazine monomers and their use for amide-containing monomeric benzoxazines", *Macromolecules*, 43, 2748–2758, 2010.
  66. H. Ardhyanta, M. H. Wahid, M. Sasaki, T. Agag, T. Kawauchi, H. Ismail and T. Takeichi, "Performance enhancement of polybenzoxazine by hybridization with polysiloxane", *Polymer*, 49, 4585-4591, 2008.
  67. Y. Liu and S. Zheng, "Inorganic–organic nanocomposites of polybenzoxazine with octa(propylglycidyl ether) polyhedral oligomeric silsesquioxane", *J Polym Sci Part A: Polym Chem*, 44, 1168-1181, 2006.
  68. G. Riess, J. M. Schwob, G. Guth, M. Roche, B. Lande, In *Advances in Polymer Synthesis*; Culbertson, B. M., Mcgrath, J. E., Eds.; Plenum: New York, 1985.

The physical, mechanical and thermal properties of polybenzoxazines are primarily decided by the nature of the diphenol and the amine. Similar to benzoxazines, naphthoxazines were obtained from hydroxy naphthalene with aniline and formaldehyde [69]. The polynaphthoxazine also showed a  $T_g$  higher than the cure temperature. Thermal properties in terms of the weight loss after isothermal ageing in static air, the decomposition temperature from thermogravimetric analysis, and the change of dynamic storage moduli at high temperatures also confirmed their superior thermal characteristics. The dependence of thermal stability and mechanical properties on the nature of the amine was also examined. Thus, the thermal and mechanical properties of polybenzoxazine thermoset networks containing varying amounts of phenolic Mannich bridges were investigated [70].

In materials based on m-toluidine and 3, 5-xylidine, the onset of thermal degradation is delayed until around 350<sup>0</sup> C with no significant effect on the final char-yield. Materials with additional amounts of arylamine Mannich bridges and methylene bridges show improved mechanical properties, including higher cross link densities and rubbery plateau moduli. Regulation of the viscosity a difunctional benzoxazine resin is achieved by addition of a monofunctional benzoxazines monomer or a difunctional epoxy monomer as reactive diluents to further improve processibility [71]. The glassy state properties, such as stiffness at room temperature, are unaffected by the incorporation of the monofunctional benzoxazines. The thermal stability of the monofunctional modified polybenzoxazine is not significantly affected below 200 °C. Properties sensitive to network structure, however, are affected. The

- 
69. S.B. Shen and H. Ishida, "Synthesis and characterization of polyfunctional naphthoxazines and related polymers", *J. Appl. Polym. Sci.*, 61(9), 1595-1605, 1996.
  70. H. Ishida and D. P. Sanders, "Improved thermal and mechanical properties of polybenzoxazines based on alkyl-substituted aromatic-amines", *J. Polym. Sci.-B*, 38(24), 3289-3301, 2000.
  71. M.T. Huang and H. Ishida, "Dynamic-mechanical analysis of reactive diluent modified benzoxazine-based phenolic resin", *Polym. and Polym. Comp.*, 7(4), 233-247, 1999.

incorporation of the monofunctional benzoxazine reduces cross link density and produces a looser network structure, while the difunctional epoxy increases cross link density and leads to a more connected network structure.

Another strategy to improve T<sub>g</sub> and thermal stability is by fluorination of benzoxazine. Thus, a fluorinated polybenzoxazine was synthesized by the ring-opening polymerization of hexafluoroisopropylidene containing benzoxazine monomer. Substantial development of T<sub>g</sub> occurred at low degrees of conversion. The thermal stability also improved upon fluorination [72].

Fluorinated polybenzoxazine with fluorine groups on the amine (3,4-dihydro-3-pentafluorophenyl-2H-1,3-benzoxazine) was obtained in high yield from penta-fluoroaniline [73]. This monomer, synthesized by a non-conventional route is a potential precursor for a polybenzoxazine in electronic applications in view of its, low flammability, low refractive index, low coefficient of friction and high glass transition temperature.

Wenjie Du et. al [74] have reported the benzoxazine/incomplete trisilanol POSS mixtures were prepared by solvent method [75], and the corresponding composites were obtained after curing. The structures, curing behavior and thermal properties were characterized by FTIR, X-ray diffraction, DSC, DMA and TGA. The results showed that chemical bonds have been formed between trisilanolphenyl POSS and PBZ, and trisilanolphenyl POSS possessed better compatibility with the matrix than trisilanolisobutyl POSS; the dynamic viscoelastic properties and thermal stability of the composites have been greatly enhanced by the incorporation of trisilanolphenyl POSS. However, the improvements on the dynamic viscoelastic properties of PBZ/trisilanolisobutyl POSS were not so markedly.

---

72. M. Kanchanasopa, N. Yanumet, K. Hemvichian and H. Ishida, "The effect of polymerization conditions on the density and T<sub>g</sub> of bisphenol-A and hexafluoroisopropylidene containing polybenzoxazines", *Polym. and Polym. Comp.*, 9(6), 367–375, 2001.

73. J. P. Liu and H. Ishida., "High-yield synthesis of fluorinated benzoxazine monomers and their molecular characterization", *Polym. Polym. Comp*, 10(3), 191–203, 2002.

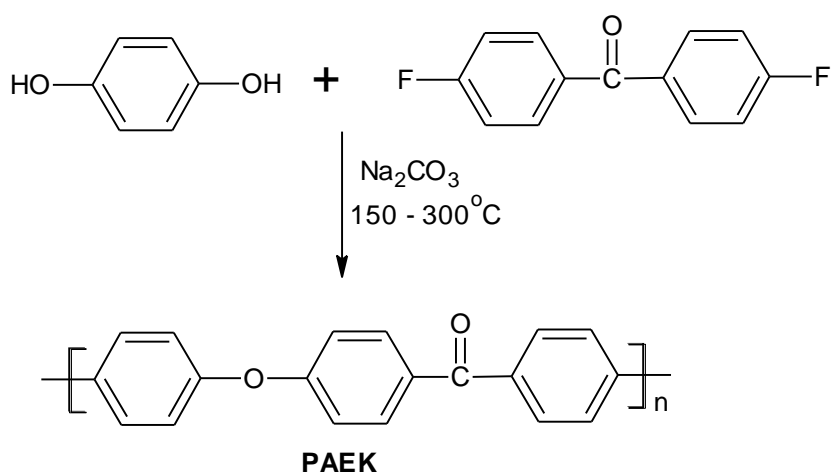
Ghetiya et. al [76, 77] synthesized bisbenzoxazines of bisphenol-C (BCO) and phenolphthalein (PHO) by condensing 0.05 mol bisphenol-C/phenolphthalein, 0.2 mol formaldehyde, and 0.1 mol aniline. Both BCO and PHO were thermally polymerized via ring-opening polymerization. The resultant cross-linked polymers (PBCO and PPHO) were characterized by solubility, Infrared (IR), Nuclear Magnetic Resonance (NMR), Differential Scanning Calorimetry (DSC), and Thermogravimetric Analysis (TGA). The bisoxazines and their polymers followed two-step degradation. Both BCO and PHO undergo selective ring-opening polymerization over the temperature range 100-150°C and are thermally stable up to about 250°C. The % residue at 550°C is substantially higher for PHO samples (56-67%) than BCO samples (20-25%), indicating the highly thermally stable nature of PHO. A ring transformation reaction is also supported by DSC. New thermosetting materials may be useful for specific applications to be exploited.

- 
74. Wenjie Du, Jiajia Shan, Yixian Wu, Riwei Xu and Dingsheng Yu, "Preparation and characterization of polybenzoxazine/ trisilanol polyhedral oligomeric silsesquioxanes composites", *Materials and Design*, 31, 1720–1725, 2010
  75. Qiao Chen, Riwei Xu, Jun Zhang and Dingsheng Yu, "Polyhedral oligomeric silsesquioxane (POSS) nanoscale reinforcement of thermosetting resin from benzoxazine and bisoxazoline", *Macromol. Rapid Commun.*, 26, 1878–1882, 2005.
  76. R. M. Ghetiya, D. S. Kundariya and P. H. Parsania, "Synthesis and characterization of cardo bisbenzoxazines and their thermal polymerization", *Polym. Plast. Techno. Engg.*, 47 (8), 836-841, 2008.
  77. D. S. Kundariya, R. M. Ghetiya and P. H. Parsania, "Synthesis and physico-chemical characterization of thermosetting material via ring opening polymerization of bisoxazine", *J. Polym. Mater.*, 25(1), 119-126, 2008.

## Section-V: Literature survey on polySchiff bases

Johnson et al. [78] reported the first attempt to synthesize PEEK by polycondensation of bisphenolate with activated dihalides using DMSO as a solvent and NaOH as a base. High molecular weight polymers were difficult to obtain due to the crystallinity and the resulting insolubility of polymers in DMSO.

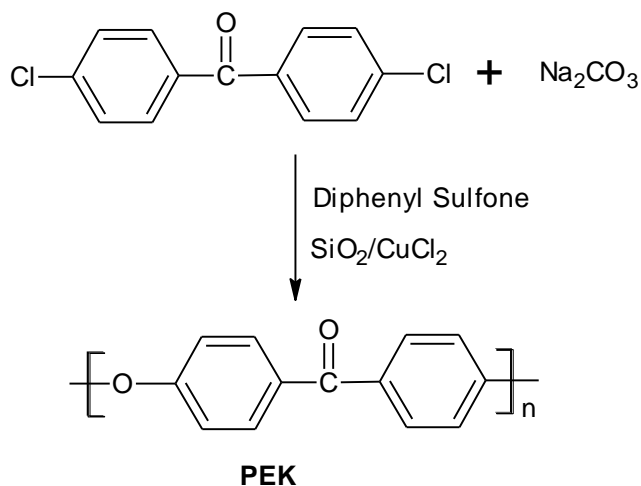
One of the major drawbacks for this synthetic route is the expense of fluoro monomers. For dihalides activated with carbonyl groups, less reactive chloro monomers fail to produce high molecular weight polymers. Side reactions such as single electron transfer reaction were observed during polymerization of dichlorides [79, 80].



To develop a low cost route to PAEKs, expensive fluoro monomers are being replaced with activated chloro monomers.

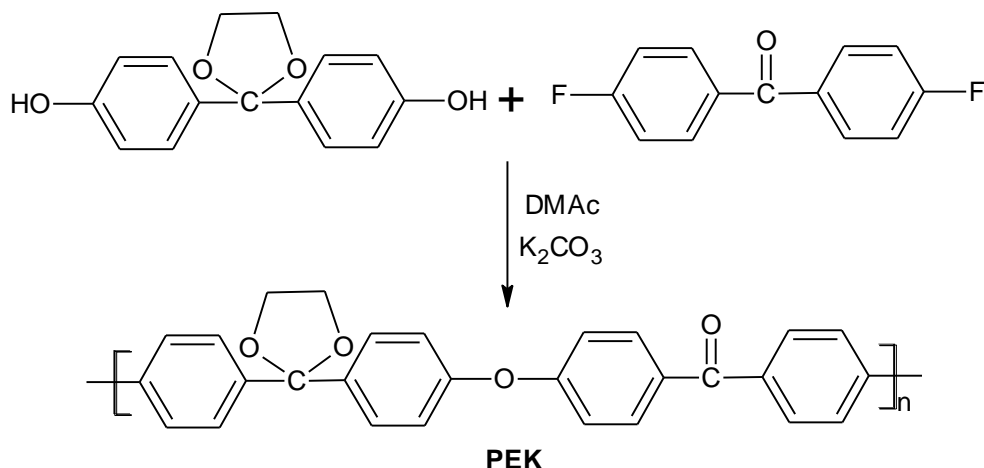
78. R. N. Johnson, A. G. Farnham, R. A. Clendinning, W. F. Hale and C. N. Merriam, "Poly(aryl ethers) by nucleophilic aromatic substitution. I. Synthesis and properties", *J. Polym. Sci. Part A-1*, 5, 2375-2398, 1967.
79. V. Percec and R. S. Clough, "Reductive dehalogenation vs substitution in the polyetherification of bis(aryl chloride)s activated by carbonyl groups with hydroquinones: a potential competition between SET and polar pathways", *Macromolecules*, 27, 1535-1547, 1994.
80. V. Percec, R. S. Clough, M. Grigors, P. L. Rinaldi and V. E. Litman, "Reductive dehalogenation versus substitution in the polyetherification of 4,4'-dihalodiphenyl sulfones with bisphenolates", *Macromolecules*, 26, 3650-3662, 1993.

Fukawa [81] successfully prepared high molecular weight PEK with 1.15 dL/g inherent viscosity using 4,4'-dichlorobenzophenone. The polymerization was carried out in diphenyl sulfone at high temperature (2 hours at 280°C, 1 hour at 300 °C, and then 1 hour at 320°C) using 4,4'-dichlorobenzophenone to react with sodium carbonate in the presence of SiO<sub>2</sub>/CuCl<sub>2</sub> catalyst. SiO<sub>2</sub> was removed by washing with 4% aqueous NaOH solution at 60 °C.

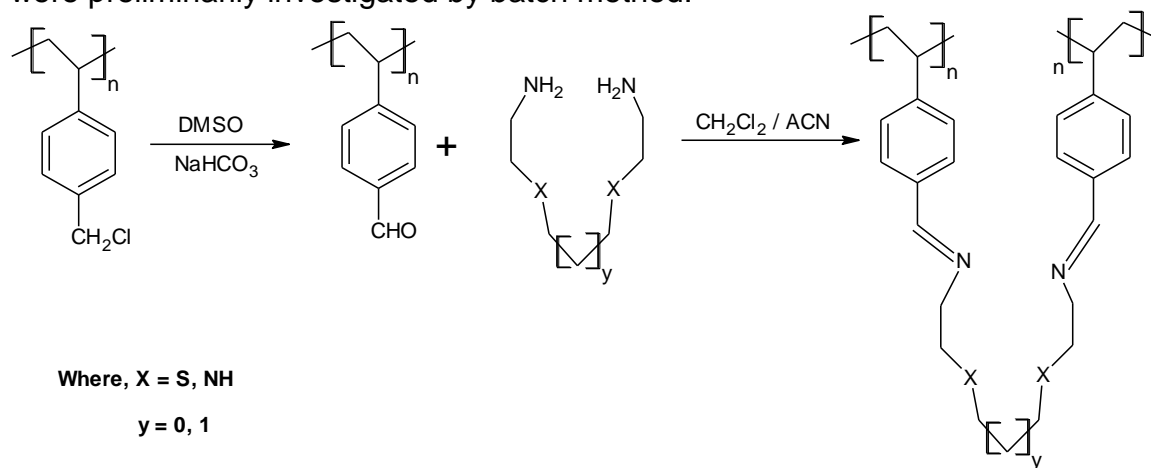


Kelsey et al. [82] used the cyclic ketal of 4,4'-dihydroxybenzophenone to polymerize with 4,4'-difluorobenzophenone in DMAc at 150 °C. The polymerization produced soluble amorphous polyketal, which was quantitatively converted to PEK by acid catalyzed hydrolysis. Since the polymerization is carried out at lower temperatures, PEK with minimal defect structures can be obtained by this process. Compared to PEEK prepared under the usual high temperature conditions (diphenyl sulfone as solvent), PEK produced by this approach displayed excellent physical properties, especially the high degree of crystallinity and higher T<sub>g</sub>, which indicate a uniform linear backbone structure.

- 
81. I. Fukawa, T. Tanabe and T. Dozono, "Preparation of aromatic poly(ether ketones) from an aromatic dihalide and sodium carbonate", *Macromolecules*, 24, 3838-3844, 1991.
82. D. R. Kelsey, L. M. Robeson and R. A. Clendinning, "Defect-free, crystalline aromatic poly(etherketones): a synthetic strategy based on acetal monomers", *Macromolecules*, 20, 1204-1212, 1987.



Nutthanara et al. [83] synthesized and characterized three new types of functionalized polystyrene-divinylbenzene resins containing two sulfur and two nitrogen atoms and four nitrogen atoms in cyclic form were prepared by using two lab- synthesized ligands. Chloromethylated polystyrene-divinylbenzene copolymer was initially oxidized to aldehydic polystyrene-divinylbenzene (CHO-PS-DVB) then it subsequently reacted with the ligands through dual Schiff base linkage. The appropriate amount of the three ligands was 2.65 mmol/g CHO-PS-DVB corresponding to the mole ratio between the chelating ligand and aldehyde group of 1:2. All derivative resins were characterized by elemental analysis, thermogravimetry, FT-IR and FTRaman spectroscopy and ninhydrin test. The adsorption properties of the synthesized resins towards Pb(II), Cu(II), Cd(II), Zn(II), Ni(II), Co(II) and Cr(III) ions in aqueous solution were preliminarily investigated by batch method.



83. Pradit Nutthanara, Wittaya Ngeontae, Apichat Imyim and Thanapong Kreethadumrongdat, "Cyclic dithia/diaza with dual Schiff base linkage functionalized polymers for heavy metal adsorption", J. Appl. Polym. Sci., 116, 801–809, 2010.



Georg Schwab et al. [84] reported novel highly cross-linked microporous polymers based on Schiff base chemistry. Polymers were synthesized by condensing melamine and different aldehydes using DMSO as a solvent at 180 °C. Several unique characteristics make the materials promising candidates for potential applications in material science. The proposed condensation approach leads to materials with high surface areas and a tailorable microporosity which has only been observed in few cases. The use of melamine as amine component leads to materials with a nitrogen content of up to 40 wt %, which has never been obtained for a microporous material and may be beneficial for the storage of gases or the stabilization of metal species. Finally, the nitrogen-rich polymer scaffold of the networks may also be helpful for the development of novel proton conducting materials.

A new synthesis of polymers containing ferrocenyl Schiff base and terephthaloyl chloride monomers by the Friedel–Crafts method [85]. The model compound and copolymers of three novel poly (ferrocenyl-Schiff bases) and their charge transfer complexes with iodine were successfully obtained and their structures were characterized by <sup>1</sup>H-NMR, infrared, and ultraviolet spectra. The effect of degree of iodine doping on their structures was studied. It appears that poly-p-bis(ferrocenyl-Schiff base) can be doped to a higher iodine level than the other two prepared materials. Electrical measurement results showed that the conductivity can be increased several orders of magnitude after doping with iodine. The maximum conductivity at room temperature is  $3.17 \times 10^{-4} \text{ Scm}^{-1}$  indicating that the conducting polymer has potential as a semiconductor material.

- 
84. Matthias Georg Schwab, Birgit Fassbender, Hans Wolfgang Spiess, Arne Thomas, Xinliang Feng and Klaus Mullen, "Catalyst-free preparation of melamine-based microporous polymer networks through Schiff base chemistry", *J. Am. Chem. Soc.*, 131, 7216–7217, 2009.
  85. Wei-Jun Liu, Guo-Xuan Xiong and Dong-Hai Zeng, "Synthesis and electrical properties of three novel poly(ferrocenyl-Schiff bases) and their charge transfer complexes with iodine", *J. Inorg. Organomet. Polym.*, 20, 97–103, 2010.

## **Aim and Objectives**

1. To collect literature on synthesis, characterization of diamines, symmetric double Schiff bases and their epoxy resins, bisbenzoxazines and polyschiff bases.
2. To synthesize 1,1'-bis (4-aminophenyl)cyclohexane.
3. To synthesize symmetric double Schiff bases and their epoxy resins, bisbenzo-xazines and polyschiff bases.
4. To characterize synthesized compounds by IR and NMR spectral techniques, solubility, epoxy equivalent.
5. To cure epoxy resins and bisbenzoxazines.
6. To assess thermal behavior of the synthesized compounds by DSC and TGA techniques.
7. To evaluate acoustical parameters of epoxy resins and bisbenzoxazines.



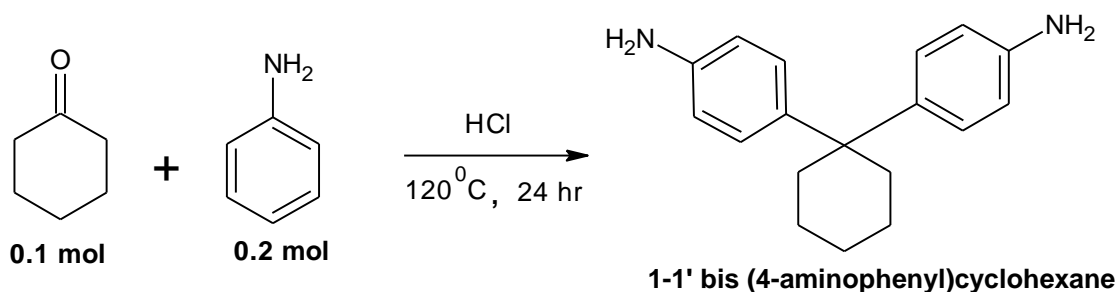
## **CHAPTER – 2**

# **SYNTHESIS OF DIAMINES, SCHIFF BASES AND THEIR POLYMERS**

## CHAPTER-2 SYNTHESIS OF DIAMINES, SCHIFF BASES AND THEIR POLYMERS

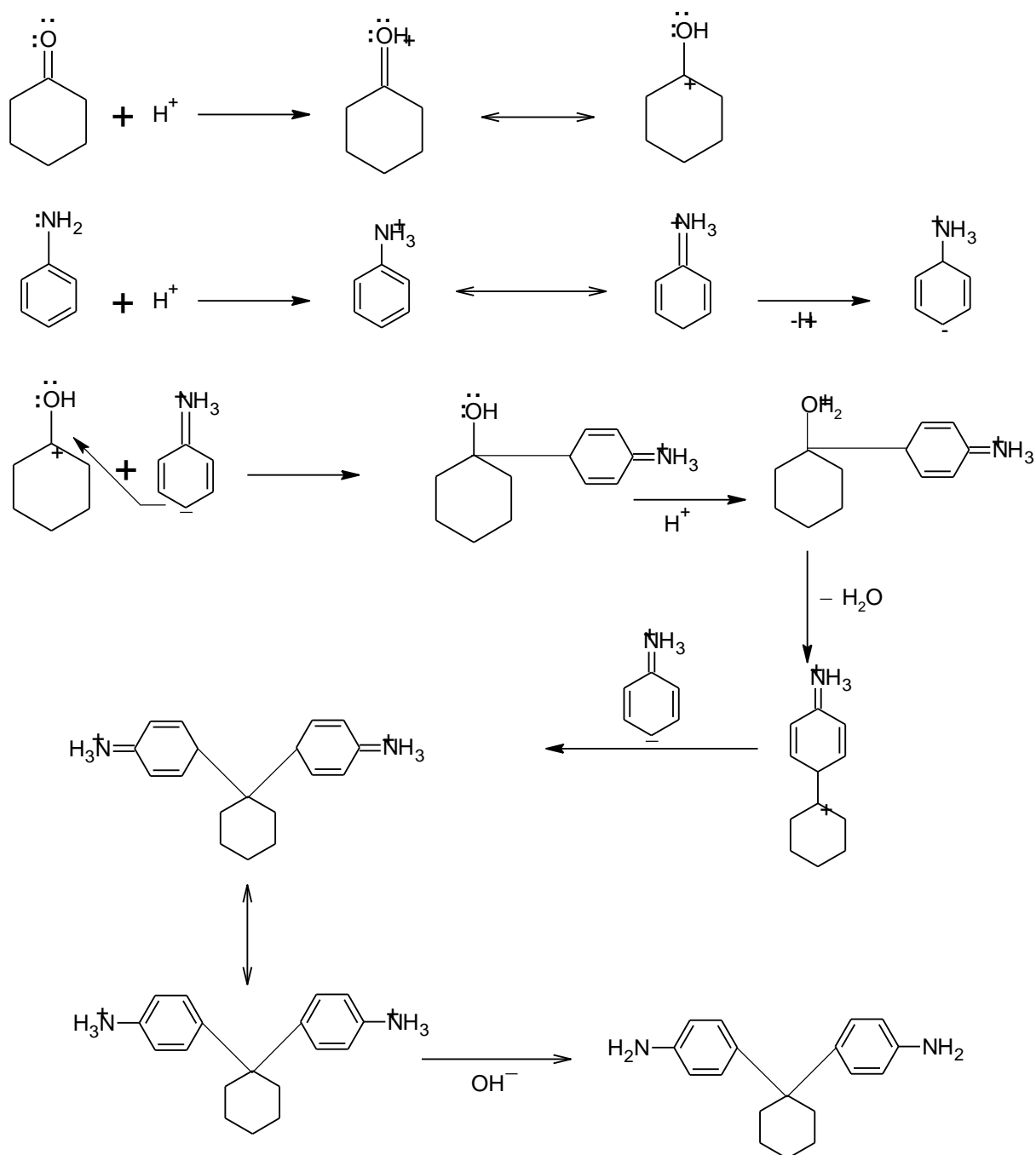
### Section-I: Synthesis of 1-1' bis (4-aminophenyl)cyclohexane [DADPCy]

Aromatic diamines can be synthesized by acid catalyzed condensation of aniline hydrochloride and cyclic ketones [1-3]. Thus, 0.23 mol (29.79 g) aniline hydrochloride and 0.10 mol (9.8 g) cyclohexanone were condensed with stirring at 120 °C for 2h and then at 140-150 °C for 9h. The resultant solution of 1,1' bis (4-aminophenyl) cyclohexane hydrochloride was cooled to 120 °C and 50 ml boiling water was added to get deep red solution. The solution was refluxed with activated charcoal for 15 min and filtered off charcoal and resinous mass. The clear blood red solution was made alkaline by using 10% NaOH solution. DADPCy was filtered, washed well with distilled water and dried in an oven at 50 °C. DADPCy was recrystallized repeatedly from chloroform-n hexane system to harvest light brown needle shaped crystals. The yield was 42% and m. p. 114 °C. The purity of DADPCy was checked by TLC in Ethyl acetate-n-Hexane (80:20 V/V) solvent system.



Scheme-I

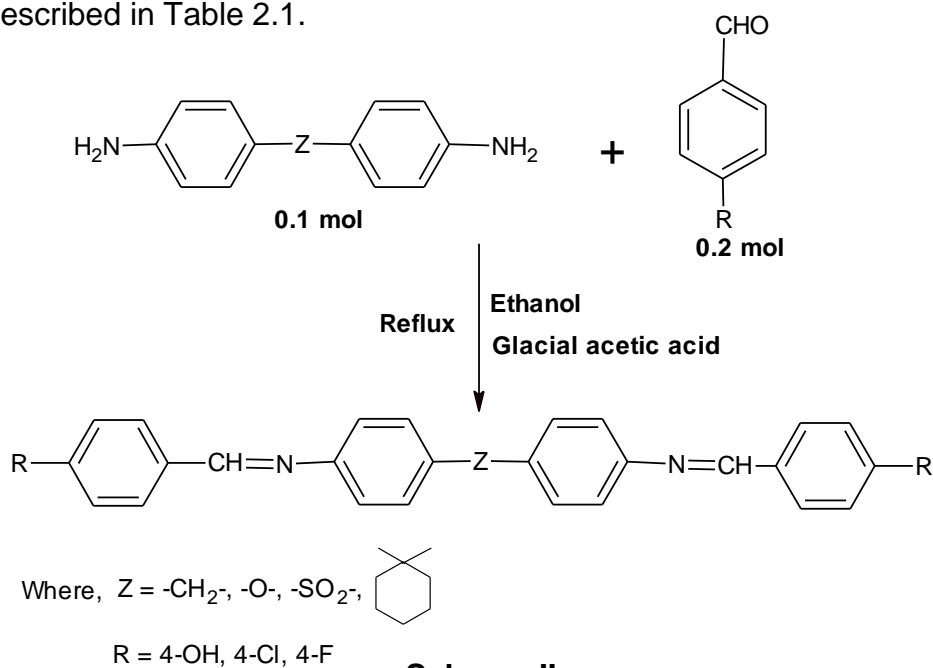
1. Y. S. Vygodskii, N. A. Churochkina, T. A. Panova and Y. A. Fedotov "Novel condensation functional polymers having highly basic groups", *Reactive & Functional Polymers*, 30, 241-250, 1996.
2. M. H. Yi, W. Huang, M. Y. Jin and K. Y. Choi "Synthesis and characterization of soluble polyamides from 1,1' bis (4-aminophenyl) cyclohexane derivatives", *Macromolecules*, 30, 5606-5611, 1997.



3. M. H. Yi, W. Huang, B. J. Lee and K. Y. Choi. "Synthesis and characterization of soluble polyimides from 2,2' bis ( 4-aminophenyl) cycloalkane derivatives", J. Polym. Sci. - Part A Polym. Chem., 37, 3449-3454, 1999.

## Section-II: Synthesis of symmetric double Schiff bases

A series of new symmetric double Schiff bases of 1,1'-bis(4-aminophenyl)cyclohexane and substituted aromatic benzaldehyde are synthesized by classical and microwave-irradiated techniques[4]. Schiff bases of general Scheme II were synthesized by condensation of related diamines and substituted aromatic aldehydes in ethanol using glacial acetic acid as a catalyst at reflux temperature. Thus, into a 100 ml RBF, 0.01 mol diamine was dissolved in 15ml ethanol containing 2ml glacial acetic acid. To this solution 0.021 mol aldehyde was dissolved in 10 ml ethanol and added drop wise at room temperature and then refluxed for 1-8 h. The product was isolated from chilled water, filtered, washed well with sodium bisulfite to remove excess aldehyde, water and finally with ethanol and dried at 50 °C in an oven. The Schiff bases are soluble in common solvents like  $\text{CHCl}_3$ , benzene, THF, DMF, DMSO, 1,4-dioxane, etc. The Schiff bases were crystallized 3-4 times from appropriate solvent systems and purity was checked by TLC using Ethyl acetate- Hexane (3:2 v/v) solvent systems. Analytical and experimental details are described in Table 2.1.



- B. J. Gangani and P. H. Parsania. "Microwave-irradiated and classical syntheses of symmetric double Schiff bases of 1,1'-Bis(4-aminophenyl)cyclohexane and their physico-chemical characterization", Spectroscopy Letters, 40(1), 97-112, 2007.

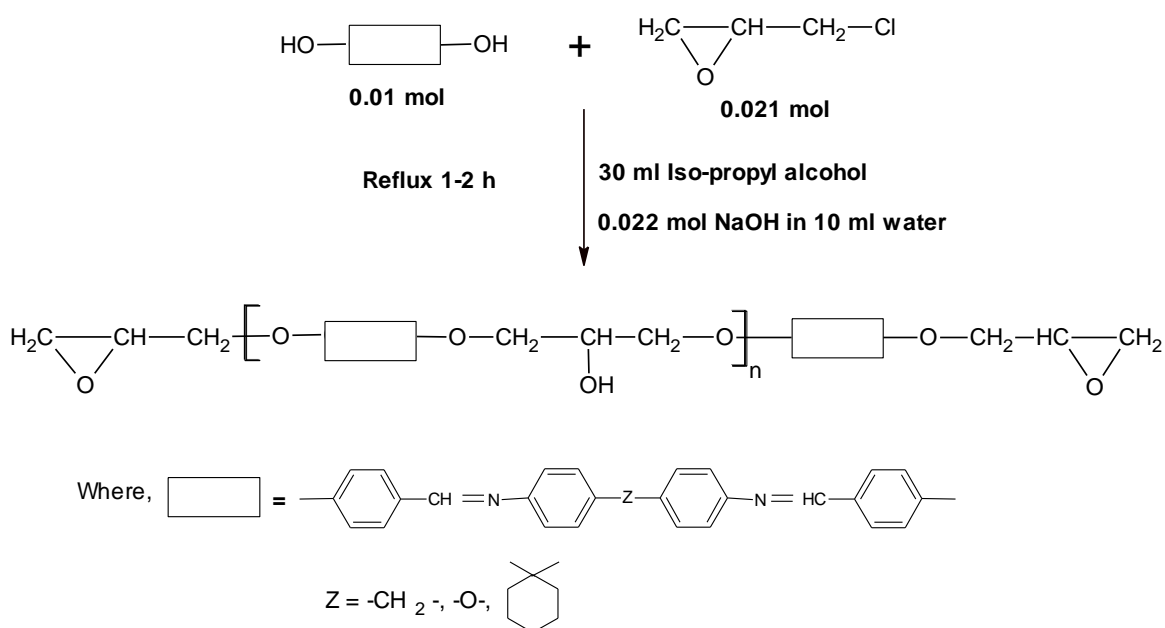
**Table 2.1 Analytical data of Schiff bases**

<b>Sample</b>	<b>Z</b>	<b>R</b>	<b>M.F.</b>	<b>M.W.</b>	<b>M.P.</b> <b>°C</b>	<b>R<sub>f</sub></b> <b>Value</b>
SB4HCy	Cyclohexyl	4-OH	C <sub>32</sub> H <sub>30</sub> N <sub>2</sub> O <sub>2</sub>	474.6	240	0.82
SB4ClCy	Cyclohexyl	4-Cl	C <sub>32</sub> H <sub>28</sub> Cl <sub>2</sub> N <sub>2</sub>	511.5	134	0.81
SB4FCy	Cyclohexyl	4-F	C <sub>32</sub> H <sub>28</sub> F <sub>2</sub> N <sub>2</sub>	478.6	136	0.82
SB4HM	-CH <sub>2</sub> -	4-OH	C <sub>27</sub> H <sub>22</sub> N <sub>2</sub> O <sub>2</sub>	406.5	215	0.85
SB4ClM	-CH <sub>2</sub> -	4-Cl	C <sub>27</sub> H <sub>20</sub> Cl <sub>2</sub> N <sub>2</sub>	443.4	156	0.84
SB4FM	-CH <sub>2</sub> -	4-F	C <sub>27</sub> H <sub>20</sub> F <sub>2</sub> N <sub>2</sub>	410.5	133	0.85
SB4HE	-O-	4-OH	C <sub>26</sub> H <sub>20</sub> N <sub>2</sub> O <sub>3</sub>	408.5	240	0.83
SB4ClE	-O-	4-Cl	C <sub>26</sub> H <sub>18</sub> Cl <sub>2</sub> N <sub>2</sub> O	445.3	232	0.86
SB4FE	-O-	4-F	C <sub>26</sub> H <sub>18</sub> F <sub>2</sub> N <sub>2</sub> O	412.4	182	0.85
SB4HS	-SO <sub>2</sub> -	4-OH	C <sub>26</sub> H <sub>20</sub> N <sub>2</sub> O <sub>4</sub> S	456.5	145	0.86
SB4ClS	-SO <sub>2</sub> -	4-Cl	C <sub>26</sub> H <sub>18</sub> Cl <sub>2</sub> N <sub>2</sub> O <sub>2</sub> S	493.4	72	0.87
SB4FS	-SO <sub>2</sub> -	4-F	C <sub>26</sub> H <sub>18</sub> F <sub>2</sub> N <sub>2</sub> O <sub>2</sub> S	460.5	95	0.85

### Section-III: Syntheses of polymers

#### A. Synthesis of epoxy resins and their curing study

Epoxy resins of symmetric double Schiff bases were synthesized according to following method [5]. Thus, Schiff base (0.01 mol), epichlorohydrin (0.021 mol) and isopropanol (30 ml) were placed in a 250 ml round bottomed flask equipped with a condenser. The mixture was brought to reflux with stirring and 0.022 mol NaOH in 10 ml water was slowly added to the solution and refluxed for 1-2 h. The separated solid resin was isolated by filtration. The solid resin was washed well with water and repeatedly purified five times using chloroform-hexane system. Off-white resins are soluble in  $\text{CHCl}_3$ , DMF, DMSO and DMAc.



**Scheme-II**

- M. R. Sanariya, D. R. Godhani, S. Baluja and P. H. Parsania, "Synthesis and characterization of epoxy resins based on 1,1'-bis(4-hydroxy phenyl).cyclohexane and 1,1'-bis(3-methyl-4-hydroxyphenyl) cyclohexane", J. Polym. Mater., 15, 45-49, 1998.



## Curing of epoxy resins

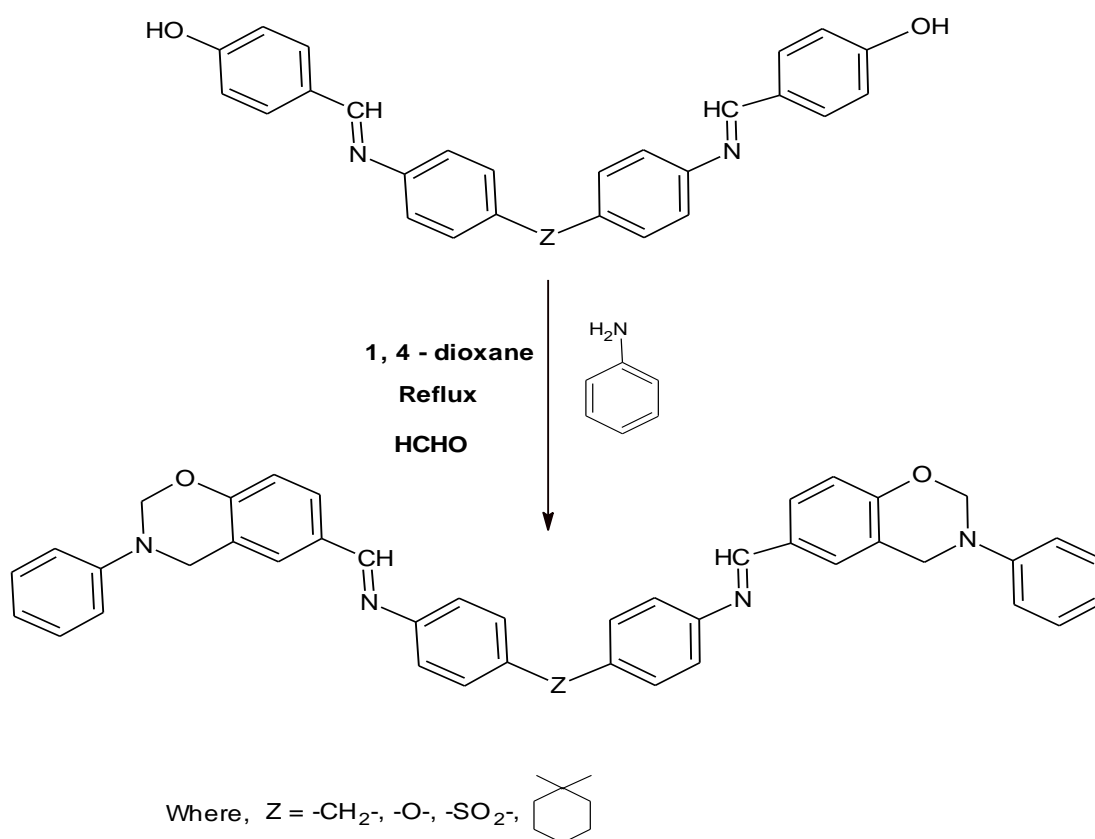
Epoxy resins were cured by using varying amounts of phthalic anhydride (5-15 wt% of resin) as a curing agent. Thus, in an oil bath 2g epoxy resin, 5-15 wt% phthalic anhydride and 5ml DMF were placed into a wide mouth corning test tube. DMF was allowed to evaporate at 155°C and then gel time was monitored (Table 2.2) and post cured further 30 min at 160°C. The cured resins are insoluble in common solvents. Here after cured samples are designated as ECyP-5 to ECyP-15, EMP-5 to EMP-15 and EEP-5 to EEP-15. Numerical figures indicate phthalic anhydride content in the cured samples. From Table 2.2, it is observed that gel time decreased with increasing concentration of phthalic anhydride.

**Table 2.2: Phthalic anhydride composition and gel time for epoxy resins**

<b>CODE</b>	<b>Phthalic anhydride, %</b>	<b>Gel time, min.</b>
ECyP-5	5	220
ECyP-10	10	205
ECyP-15	15	195
EMP-5	5	180
EMP-10	10	175
EMP-15	15	170
EEP-5	5	180
EEP-10	10	165
EEP-15	15	155

### B. Synthesis of bisbenzoxazines and their ring opening polymerization

Into a 100 ml round bottomed flask containing 0.04 mol (3.6 ml) formaldehyde was added 0.02 mol (1.8 ml) aniline in 20 ml 1, 4-dioxane dropwise below 10°C [6]. To this solution 0.01 mol Schiff base in 80 ml 1,4-dioxane was added and refluxed for 15 h, cooled to room temperature, poured in the crushed ice, separated yellowish solid product was filtered, washed well with water and dried at room temperature. Bisbenzoxazines were crystallized four times from dioxane-water system.



Scheme-III

6. R. M. Ghetiya, D. S. Kundariya, P. H. Parsania, V. A. Patel. "Synthesis and characterization of cardo bisbenzoxazines and their thermal polymerization", Polym. Plas. Technol. and Eng., 47(8), 836 – 841, 2008.

**Table 2.3 Analytical data of bisbenzoxazines**

Sample	Z	M.F.	M.W.	M.P. °C	R <sub>f</sub> Value
BSB4HCy	Cyclohexyl	C <sub>48</sub> H <sub>44</sub> N <sub>4</sub> O <sub>2</sub>	708.9	81.7	0.82
BSB4HM	-CH <sub>2</sub> -	C <sub>43</sub> H <sub>36</sub> N <sub>4</sub> O <sub>2</sub>	640.8	79.6	0.84
BSB4HE	-O-	C <sub>42</sub> H <sub>34</sub> N <sub>4</sub> O <sub>3</sub>	642.7	80.6	0.82
BSB4HS	-SO <sub>2</sub> -	C <sub>42</sub> H <sub>34</sub> N <sub>4</sub> O <sub>4</sub> S	690.8	95.7	0.85

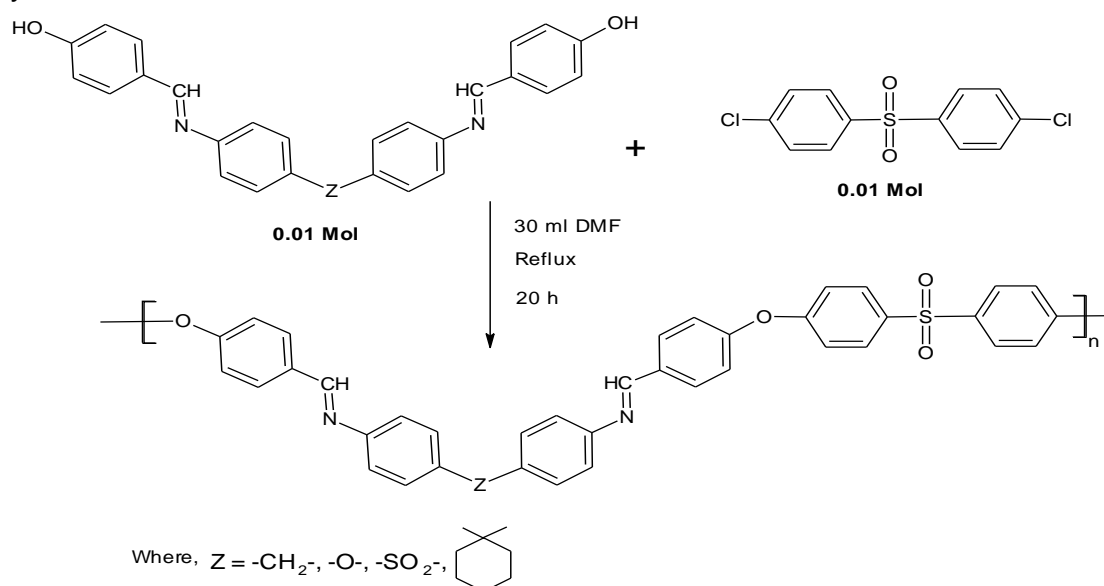
Ring opening polymerization of bisbenzoxazines undergoes self curing. Thus, into a wide mouth corning test tube 2g bisbenzoxazine was placed and heated to 160-220 °C (Table-2.3) for 30 min and post cured for 15 min. Here after cured samples are designated as BCCy, BCM, BCE and BCS. The cured samples are insoluble in most of the common solvents.

**Table 2.3: Bisbenzoxazine curing time**

Code	Temperature, °C	Curing time, min.
BCCy	160	30
BCM	220	30
BCE	160	30
BCS	160	30

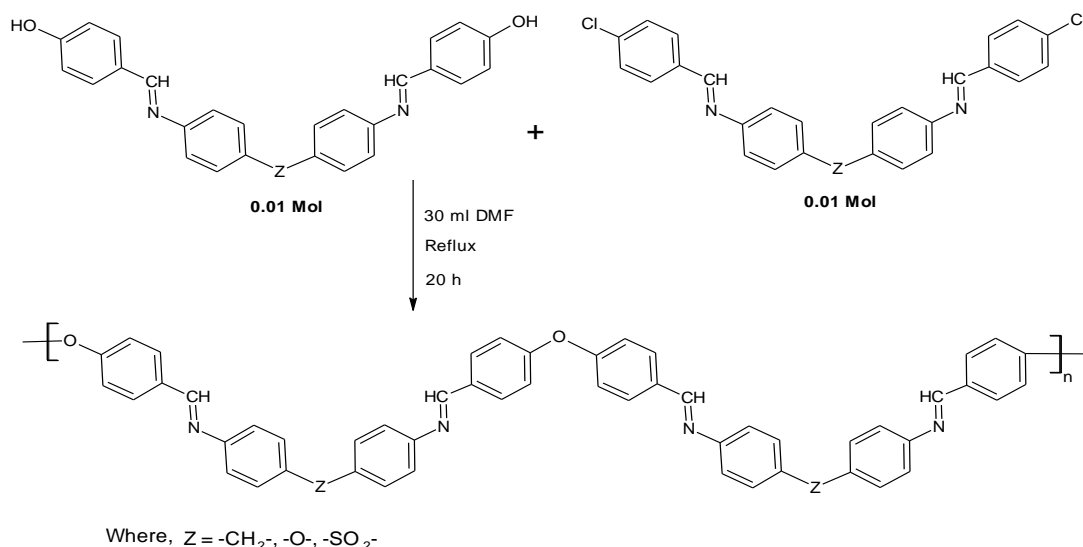
### C. Synthesis of polySchiff bases

To a 250 ml round bottomed flask equipped with a Dean and stark condenser and thermometer in an oil bath, were placed 0.01 mol Schiff base in 30 ml DMF and 0.015 mol potassium carbonate and the resultant mixture was heated to 120 °C for 15 min and then 0.01 mol 4, 4'-dichloro diphenyl sulfone and 15 ml toluene were added and azeotrope was distilled off and further 15ml toluene was added distilled off and further heated at reflux temperature for 20 h. The reaction mass was cooled to room temperature and polymer was isolated from cold water, filtered, washed well with water and dried at 50°C. The polymers were purified four times from DMF-Water. The yield was 97%.



**Scheme-V**

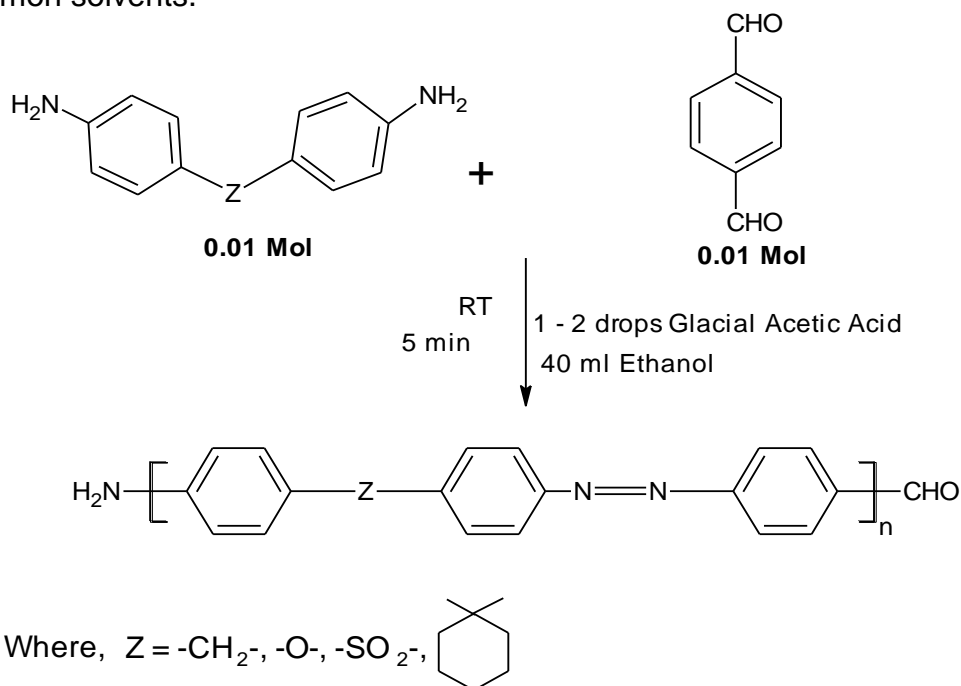
0.01mol related free hydroxyl group Schiff bases and 0.01mol of related free halogen group Schiff bases in 30 ml DMF, and then add 0.015 mol potassium carbonate and 15 ml toluene as a azeotropic solvent. Mixture was heated to remove water part, for 2 h at azeotropic temperature. After the removal of water part collect all the toluene solvent from denenstark. Then temperature of the mixture was raised and refluxed for 20h, cooled, poured in the crushed ice, separated yellowish solid filtered, washed well with water and dried at room temperature. PolySchiff bases were purified repeatedly from DMF-water solvent system.



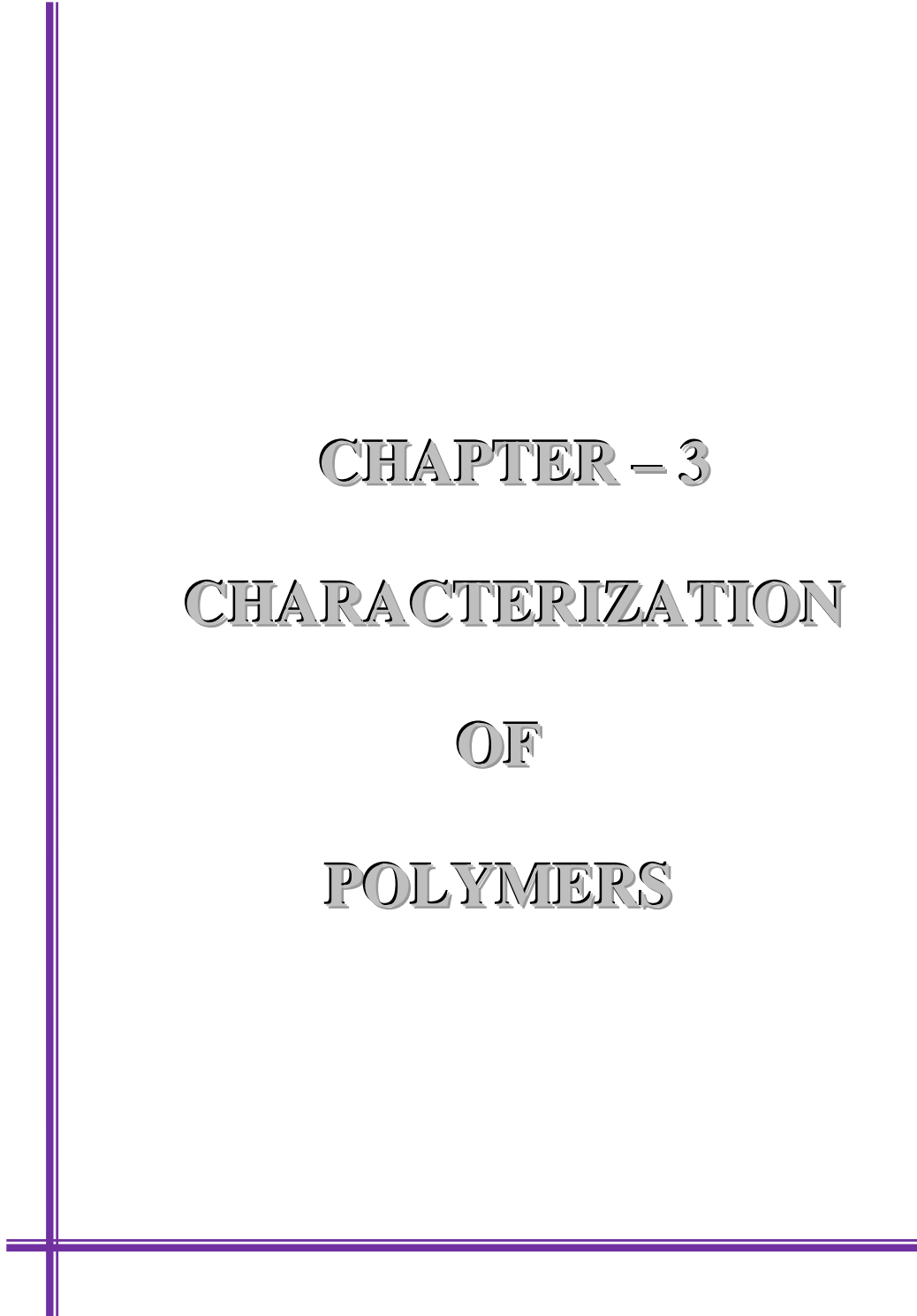
Scheme-VI

#### D. Synthesis of PolySchiff bases

Into a 100 ml round bottomed flask equipped with a mechanical stirrer were placed 0.01 mol Schiff base in 15 ml ethanol and 2 ml glacial acetic acid at room temperature and was added 0.01 mol terephthalaldehyde in 15 ml ethanol dropwise over 10-15 min. The reaction mixture was stirred at room temperature for 30 min. The separated solid poly Schiff bases was filtered, washed well with sodium bisulfate solution, water and finally with ethanol and dried at  $50^{\circ}\text{C}$ . The yield was 97 %. The polySchiff bases are insoluble in common solvents.



Scheme-VII



**CHAPTER – 3**

**CHARACTERIZATION**

**OF**

**POLYMERS**

## CHAPTER-3 CHARACTERIZATION OF POLYMERS

### Section-I: Solubility of polymers

The solubility consideration is of prime importance [1-3] in solution processing during the casting of films, manufacturing of fibers and adhesives materials and also during the use of polymers under conditions, which expose them to attack by potential solvents either in industry or in the household applications.

The solubility of liquids and gases in polymer strongly depends on crystallinity. Crystallinity decreases the solubility of polymers markedly, since the process of solution involves overcoming the heat and entropy factors associated with crystallization as well as those of the intermolecular interactions in the amorphous regions. Properties related to solubility, such as the cloud point of the dilute solutions are often functions of crystallinity and relatively independent of molecular weight.

When we introduce the polar groups among the polymer chain, solubility of that polymer decreases, since strong polymer-polymer bonds usually develop. The situation is complicated however, by factors such as the arrangement and bulkiness of the groups, which in turn influence crystallinity. The solubility of a polymer may improve or grow worse with increasing temperature. In this same temperature range some polymers will dissolve better when heated, while others when cooled, in the same solvent. Solubility relation in polymer systems are more complex than those among low molecular weight compounds because of the size, molecular weight difference, viscosity difference between the polymer, and solvent molecules and the possible presence of a crystalline phase.

- 
1. J. H. Hildebrand, R. L. Scott, "The Solubility of Non-electrolytes" 3<sup>rd</sup> Ed. Reinhold, New York, 1950.
  2. F. W. Billmeyer, "Textbook of Polymer Science" 4<sup>th</sup> Ed., John Willey and Sons., New York, 1994.
  3. P. J. Flory. "Principles of Polymer Chemistry" Cornell University Press, Ithaca, New York, 1962.

Dissolution of a polymer is a slow process and occurring in two stages. First, solvent is slowly imbibed into the polymer to produce a swollen gel. In the second stage, the gels gradually disintegrate into a true solution. Only the second stage is materially speed up by agitation. If the polymer is cross linked by primary valence bonds or strong hydrogen bonds or is highly crystalline, only swelling may take place.

### **Solubility test**

In order to test the solubility of a given polymer, approximately 50 mg of polymer sample was placed in a series of test tubes containing about 5ml of solvents and kept them aside for sometime. Gradual disintegration of swollen gel indicated the formation of true solution. The solubility data for polymers are reported in Tables-3.1 to 3.5.



**Table-3.1: The solubility of epoxy resins in different solvents at room temperature**

Solvent	Epoxy Resin		
	ESB4HCy	ESB4HM	ESB4HE
Methanol	IS	IS	IS
Ethanol	IS	IS	IS
Isopropyl alcohol	IS	IS	IS
Acetone	IS	IS	IS
Chloroform	IS	IS	IS
Dichloromethane	IS	IS	IS
1,2 - Dichloroethane	IS	IS	IS
Carbon tetrachloride	IS	IS	IS
1,4 – Dioxane	IS	IS	IS
Diethyl ether	IS	IS	IS
Methyl ethylketone	IS	IS	IS
Ethyl acetate	IS	IS	IS
n-Hexane	IS	IS	IS
Tetrahydrofuran	S	S	IS
Toluene	IS	IS	IS
Benzene	IS	IS	IS
N,N-Dimethylformamide	S	S	PS
Dimethyl acetamide	S	S	IS
Dimethylsulfoxide	S	S	IS

S=Soluble, IS=Insoluble, PS=Partial Soluble

**Table-3.2: The solubility of bisbenzoxazines in different solvents at room temperature**

Solvent	Bisbenzoxazine			
	BSB4HCy	BSB4HM	BSB4HE	BSB4HS
Methanol	IS	IS	IS	IS
Ethanol	IS	IS	IS	IS
Isopropyl alcohol	IS	IS	IS	IS
Acetone	IS	IS	IS	IS
Chloroform	IS	IS	IS	IS
Dichloromethane	IS	IS	IS	IS
1,2 - Dichloroethane	IS	IS	IS	IS
Carbon tetrachloride	IS	IS	IS	IS
1,4 – Dioxane	S	S	S	S
Diethyl ether	IS	IS	IS	IS
Methyl ethylketone	IS	IS	IS	IS
Ethyl acetate	IS	IS	IS	IS
n-Hexane	IS	IS	IS	IS
Tetrahydrofuran	IS	IS	IS	IS
Toluene	IS	IS	IS	IS
Benzene	IS	IS	IS	IS
N,N-Dimethylformamide	S	S	S	S
Dimethyl acetamide	S	S	S	S
Dimethylsulfoxide	S	S	S	S

**Table-3.3: The solubility of polySchiff bases in different solvents at room temperature.**

Solvent	PolySchiff bases			
	SB4HCy-DCDPS	SB4HM-DCDPS	SB4HE-DCDPS	SB4HS-DCDPS
Methanol	IS	IS	IS	IS
Ethanol	IS	IS	IS	IS
Isopropyl alcohol	IS	IS	IS	IS
Acetone	S	IS	IS	IS
Chloroform	PS	PS	IS	PS
Dichloromethane	IS	IS	IS	IS
1,2 - Dichloroethane	PS	IS	PS	IS
Carbon tetrachloride	IS	IS	IS	IS
1,4 – Dioxane	S	IS	S	PS
Diethyl ether	IS	IS	IS	IS
Methyl ethylketone	S	IS	IS	PS
Ethyl acetate	IS	IS	IS	IS
n-Hexane	IS	IS	IS	IS
Tetrahydrofuran	S	PS	S	S
Toluene	IS	IS	IS	IS
Benzene	IS	IS	IS	IS
N,N-Dimethylformamide	S	S	PS	S
Dimethyl acetamide	S	S	S	S
Dimethylsulfoxide	S	PS	IS	S

**Table-3.4: The solubility of polySchiff Bases in different solvents at room temperature**

Solvent	PolySchiff bases			
	SB4HCy - SB4CICy	SB4HM - SB4CIM	SB4HE - SB4CIE	SB4HS - SB4CIS
Methanol	IS	IS	IS	IS
Ethanol	IS	IS	IS	IS
Isopropyl alcohol	IS	IS	IS	IS
Acetone	IS	IS	IS	IS
Chloroform	IS	IS	IS	IS
Dichloromethane	IS	IS	IS	IS
1,2 - Dichloroethane	IS	IS	IS	IS
Carbon tetrachloride	IS	IS	IS	IS
1,4 – Dioxane	IS	IS	IS	IS
Diethyl ether	IS	IS	IS	IS
Methyl ethylketone	IS	IS	IS	S
Ethyl acetate	IS	IS	IS	IS
n-Hexane	IS	IS	IS	IS
Tetrahydrofuran	IS	PS	IS	IS
Toluene	IS	IS	IS	IS
Benzene	IS	IS	IS	IS
N,N-Dimethylformamide	IS	IS	IS	PS
Dimethyl acetamide	IS	IS	IS	PS
Dimethylsulfoxide	IS	IS	IS	PS

**Table-3.5: The solubility of polySchiff bases in different solvents at room temperature**

Solvent	PolySchiff bases			
	TDADPCy	TDADPM	TDADPE	TDADPS
Methanol	IS	IS	IS	IS
Ethanol	IS	IS	IS	IS
Isopropyl alcohol	IS	IS	IS	IS
Acetone	IS	IS	IS	IS
Chloroform	IS	IS	IS	IS
Dichloromethane	IS	IS	IS	IS
1,2 - Dichloroethane	IS	IS	IS	IS
Carbon tetrachloride	IS	IS	IS	IS
1,4 – Dioxane	IS	IS	IS	IS
Diethyl ether	IS	IS	IS	IS
Methyl ethylketone	IS	IS	IS	IS
Ethyl acetate	IS	IS	IS	IS
n-Hexane	IS	IS	IS	IS
Tetrahydrofuran	IS	IS	IS	IS
Toluene	IS	IS	IS	IS
Benzene	IS	IS	IS	IS
N,N-Dimethylformamide	IS	IS	IS	IS
Dimethyl acetamide	IS	IS	IS	IS
Dimethylsulfoxide	IS	IS	IS	IS

## Section-II: Spectral characterization of polymers

This section of the thesis includes the IR and NMR spectral characterization of the monomers, epoxy resins, bisbenzoxazines and polySchiff bases.

### [A] IR spectral characterization

IR spectroscopy is an excellent technique for the qualitative analysis because except for optical isomers, the spectrum of compound is unique. Information about the structure of a molecule could frequently be obtained from its absorption spectrum. An infrared spectrum is obtained by passing infrared radiation through a sample. A detector generates a plot of % transmission of radiation versus the wave number or wavelength of the radiation transmitted. At 100% transmission, all the energy of radiation passes through the molecule. At lower values of % transmission, some of the energy is being absorbed by the compound. Each spike in the infrared (IR) spectrum represents absorption of energy. These spikes are called absorption bands. Electromagnetic radiation with wave numbers from 4000 to 400  $\text{cm}^{-1}$  has just the right energy to correspond to stretching and bending vibrations in molecules. Electromagnetic radiation with this energy is known as infrared radiation because it is just below the “red region” of visible light. (Infra is Latin word meaning “below”).

The intensity of an absorption band depends on the size of dipole moment change associated with the vibration. In other words, depends on polarity of the vibrating bond. Intensity of the absorption band also depends on number of bonds responsible for the absorption. The concentration of the sample used to obtain an IR spectrum also affects the intensity of absorption bands. Concentrated samples have greater wave numbers and therefore more intense absorption bands.

The IR spectra of diamine, symmetric double Schiff bases, epoxy resins, bisbenzoxazines, and polySchiff bases were scanned on a Nicolet-IR200 FTIR spectrometer over the frequency range from 4000-400  $\text{cm}^{-1}$ .

### IR spectral analysis of diamine and Schiff bases

IR spectra of 1,1'-bis(4-aminophenyl)cyclohexane (DCDPCy), symmetric double Schiff bases (SB4HCy and SB4CICy) are presented in Figs. 3.1 to 3.3, respectively. IR absorption frequencies ( $\text{cm}^{-1}$ ) are summarized in Table 3.5. Characteristic absorption peaks for DADPCy are  $3423.2$  ( $\text{NH } \nu_{\text{as}}$ ),  $3360.5$  ( $\text{NH } \nu_{\text{s}}$ ) and  $1628.6$  ( $\text{N-H def.}$ )  $\text{cm}^{-1}$  besides normal modes of alicyclic and aromatic groups. Characteristic absorption peaks of SB4HCy and SB4CICy are  $1608.4$  ( $\text{N=CH str.}$ ) and  $1631.9$  ( $\text{N=CH str.}$ )  $\text{cm}^{-1}$ , respectively.

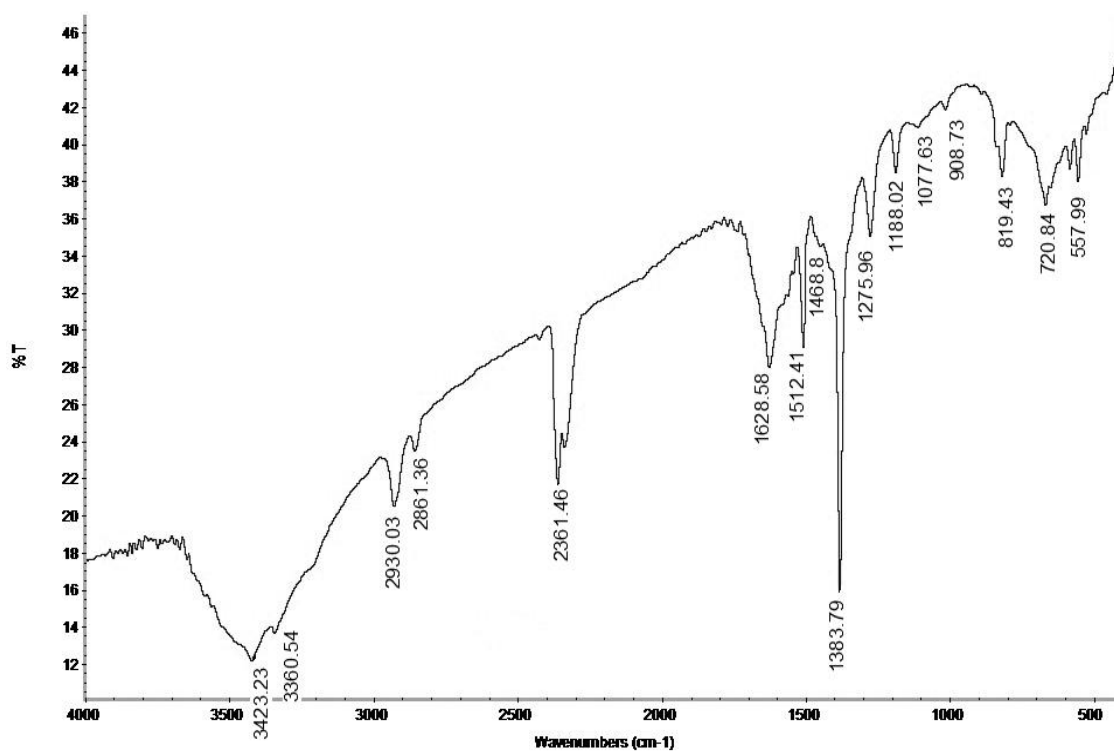


Fig. 3.1: IR (KBr) spectrum of 1,1'-bis (4-aminophenyl)cyclohexane (DADPCy)

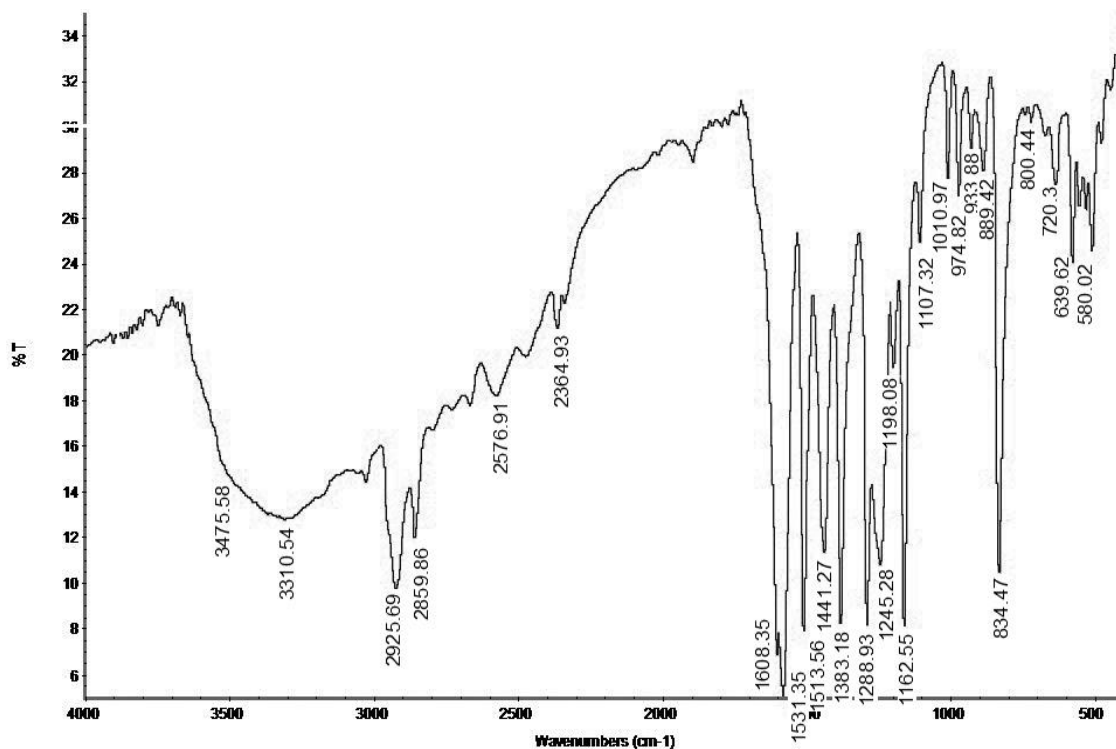


Fig. 3.2: IR (KBr) spectrum of Schiff base (SB4HCy)

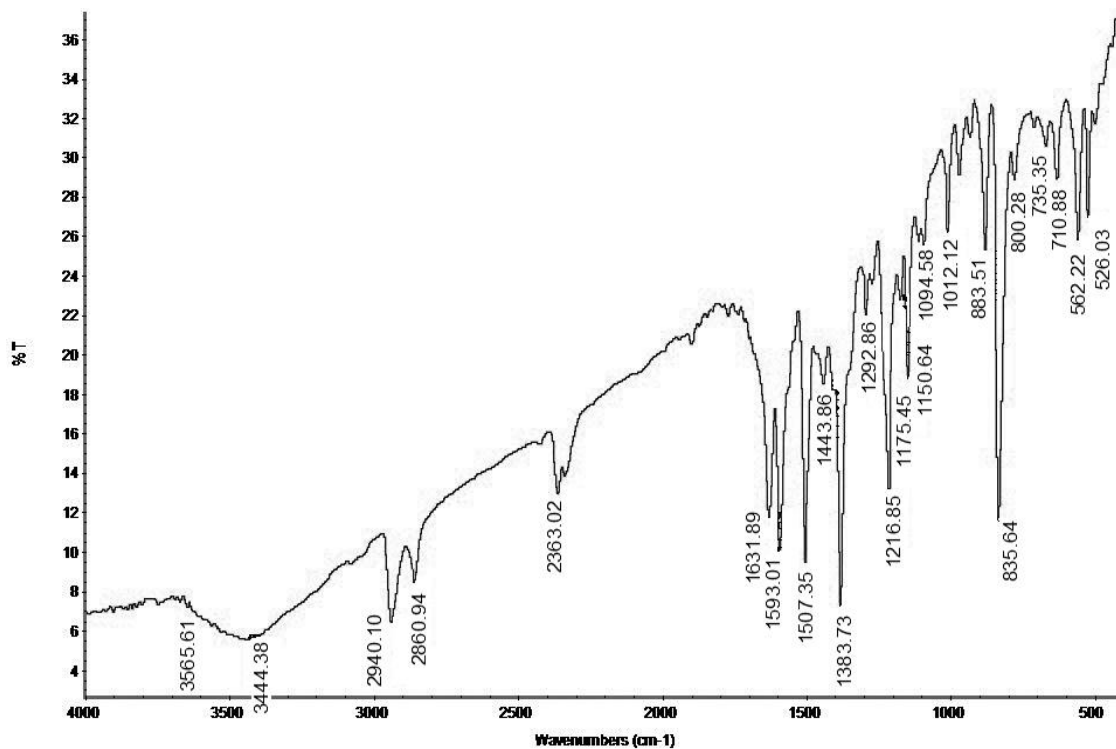


Fig. 3.3: IR (KBr) spectrum of Schiff base (SB4ClCy)



**Table-3.6: The characteristic IR absorption frequencies of DADPCy, SB4HCy, SB4ClCy.**

Types	Group vibration mode	Observed IR frequencies, (cm <sup>-1</sup> )			Expected frequencies, (cm <sup>-1</sup> )
		DADPCy	SB4HCy	SB4ClCy	
Alkane -CH <sub>2</sub> -	C-H (v <sub>as</sub> )	2930.0	2925.7	2940.1	2975-2950
	C-H (v <sub>s</sub> )	2861.4	2859.9	2860.9	2880-2860
	C-H def.	1468.8	1441.3	1443.9	1470-1435
	Twisting & Wagging	1276.0	1245.3	1216.9	~1250
	Skeletal CH <sub>2</sub>	-	720.3	710.9	750-720
Aromatic	C=C str.	1512.4 1468.8	1531.4 1513.6 1441.3	1593.0 1507.4 1443.9	1600-1400
	C-H (i.p.d.)	1276.0 1188.0	1245.3 1162.6 1107.3 1011.0	1175.5 1094.6 1012.1	1258±11, 1175±6, 1117±7, 1013±5 (1,4 sub.)
	C-H (o.p.d.)	819.4	834.5	835.6	830-750 (1,4 sub.)
Primary amine -NH <sub>2</sub>	N-H (v <sub>as</sub> )	3423.2	-	-	3550-3350
	N-H (v <sub>s</sub> )	3360.5	-	-	3450-3250
	N-H def.	1628.6	-	-	1650-1580
	C-N str.	1276.0	1288.9	1292.9	1340-1250
	N-H wagg.	819.4	-	-	850-750
Schiff base	N = CH str.	-	1608.4	1631.9	1690 – 1635
	C – N vib.	-	1288.9	1292.9	1360 – 1310
-OH	O-H str.	-	3310.5	-	3400-3200
	O-H def.	-	1288.9	-	1350-1260
	C-O-H def.	-	1107.3	-	1120-1030
Halogen	C-Cl str.	-	-	710.9	800-600

### IR spectral analysis of uncured and cured epoxy resins

IR spectra of epoxy resins (ESB4HCy, ESB4HM and ESB4HE) are presented in Figs. 3.4 to 3.6 and IR absorption peaks in Table 3.7. Observed characteristic absorption peaks are 3423-3386 (OH str.), 1678-1654 (N=CH str.), 1254-1248 (C-O-C str.), 1384-1308 (O-H def.) and 1166-1109 (C-OH def.) besides alicyclic and aromatic groups, confirming formation of epoxy resins.

IR spectra of epoxy resins cured using phthalic anhydride (ECyP-5, ECyP-10, ECyP-15, EMP-5, EMP-10, EMP-15, EEP-5, EEP-10 and EEP-15) are presented in Figs. 3.7 to 3.15 and absorption peaks in Tables 3.8 to 3.10. Observed characteristic IR absorption peaks for ECyP-5 to ECyP-15 are 3425-3422 (O-H str.), 1717-1715 (C=O str.), 1246-1245 (C-O-C str.), 1320-1319 (O-H def.) and 1096-1080 (C-OH def.) For EMP-5 to EMP-15: 3448-3422 (O-H str.), 1711-1706 (C=O str.), 1662-1661 (N=CH str.), 1269-1234 (C-O-C str.), 1317-1269 (O-H def.) and 1118-1105 (C-OH def.); and for EEP-5 to EEP-15: 3408-3360 (O-H str.), 1712-1711 (C=O str.), 1239-1236 (C-O-C str.) 1308-1307 (O-H def.) and 1102-1036 (C-OH def.).

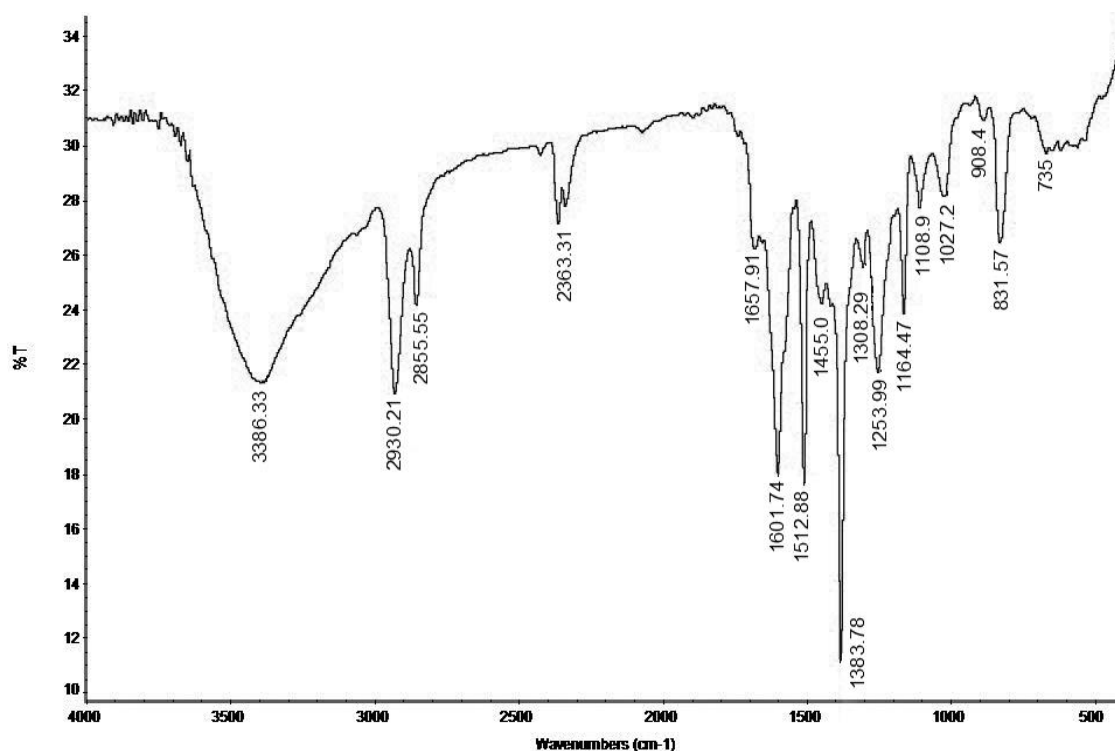


Fig. 3.4: IR (KBr) spectrum of epoxy resin (ESB4HCy)

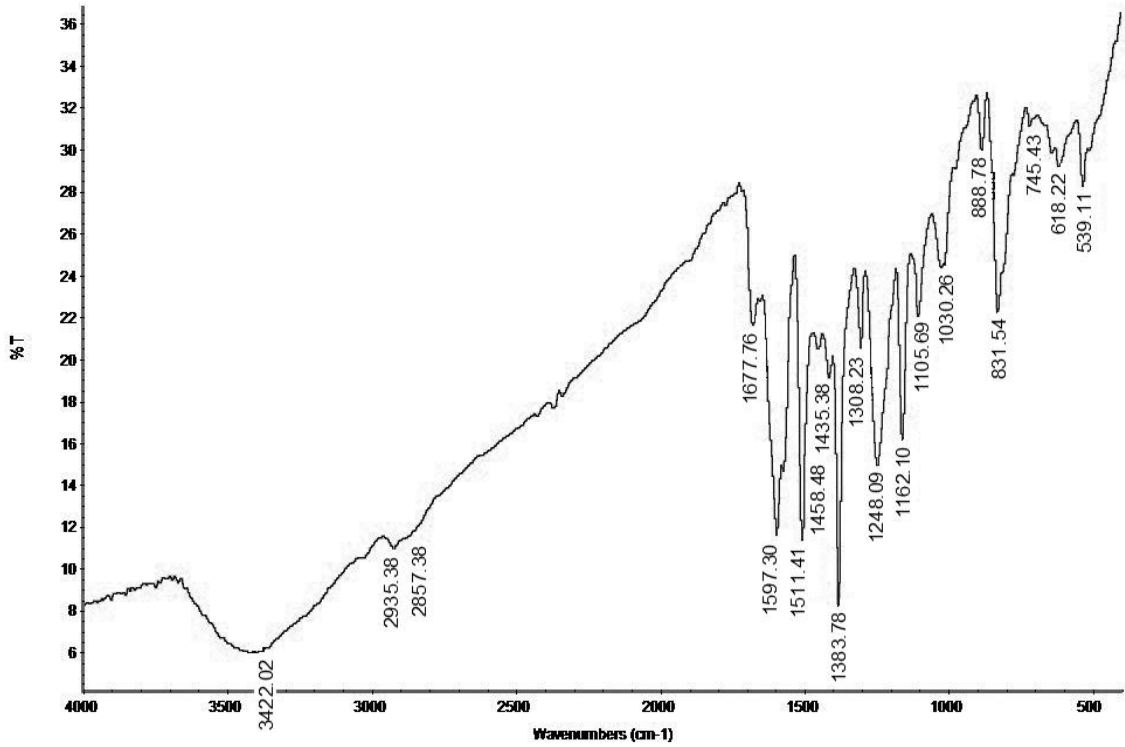


Fig. 3.5: IR (KBr) spectrum of epoxy resin (ESB4HM)

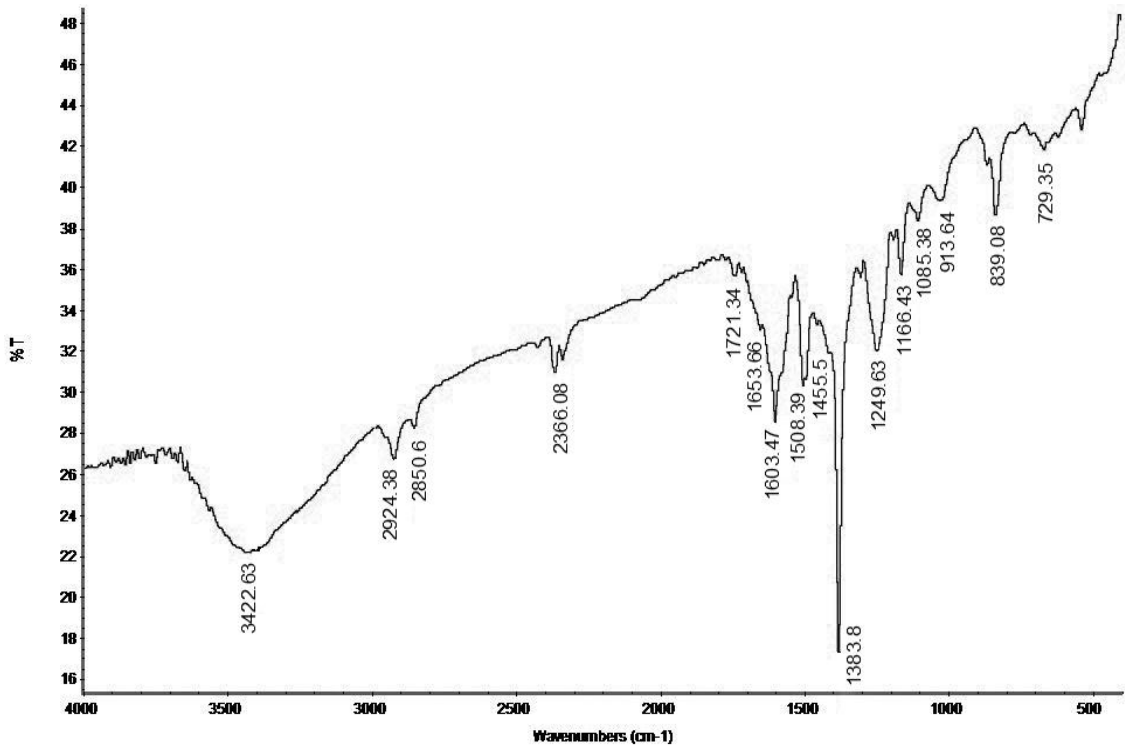


Fig. 3.6: IR (KBr) spectrum of epoxy resin (ESB4HE)

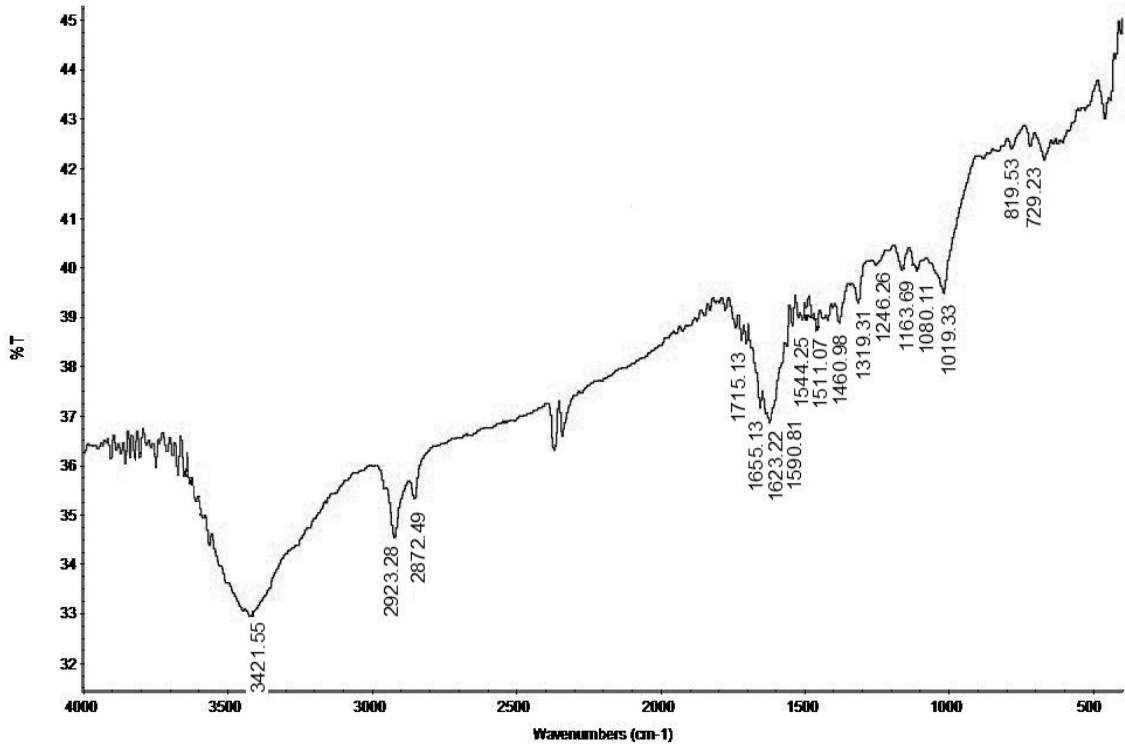


Fig. 3.7: IR (KBr) spectrum of cured epoxy resin (ECyP-5)

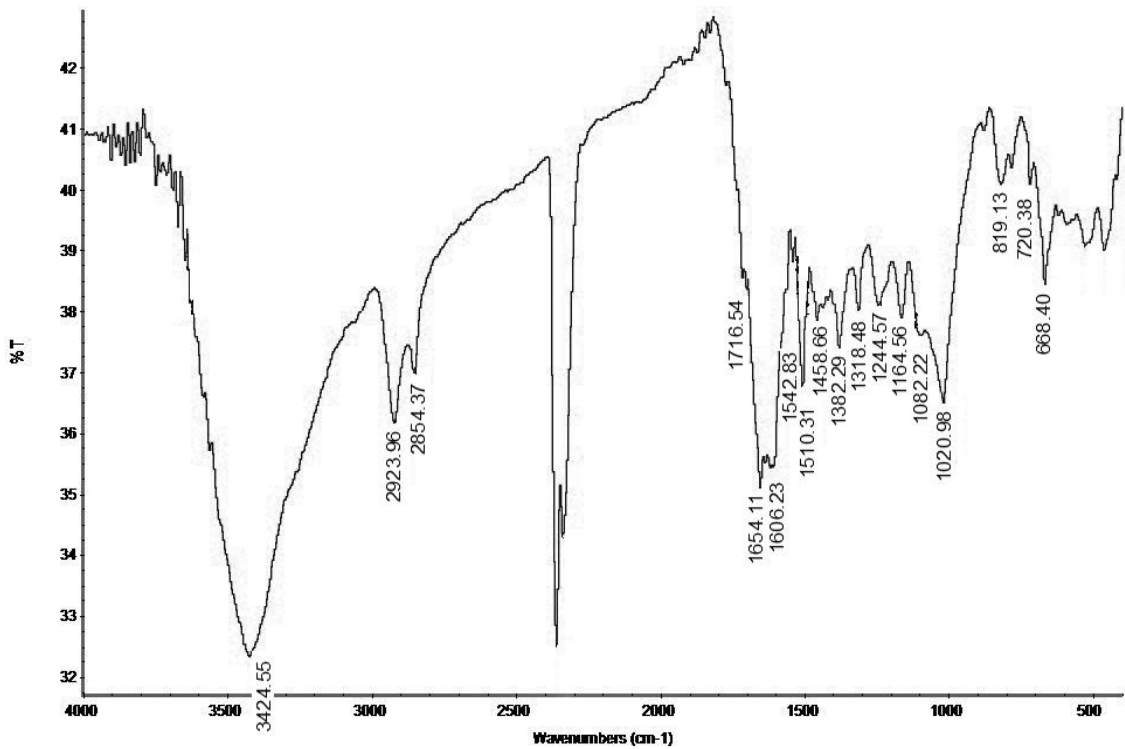


Fig. 3.8: IR (KBr) spectrum of cured epoxy resin (ECyP-10)

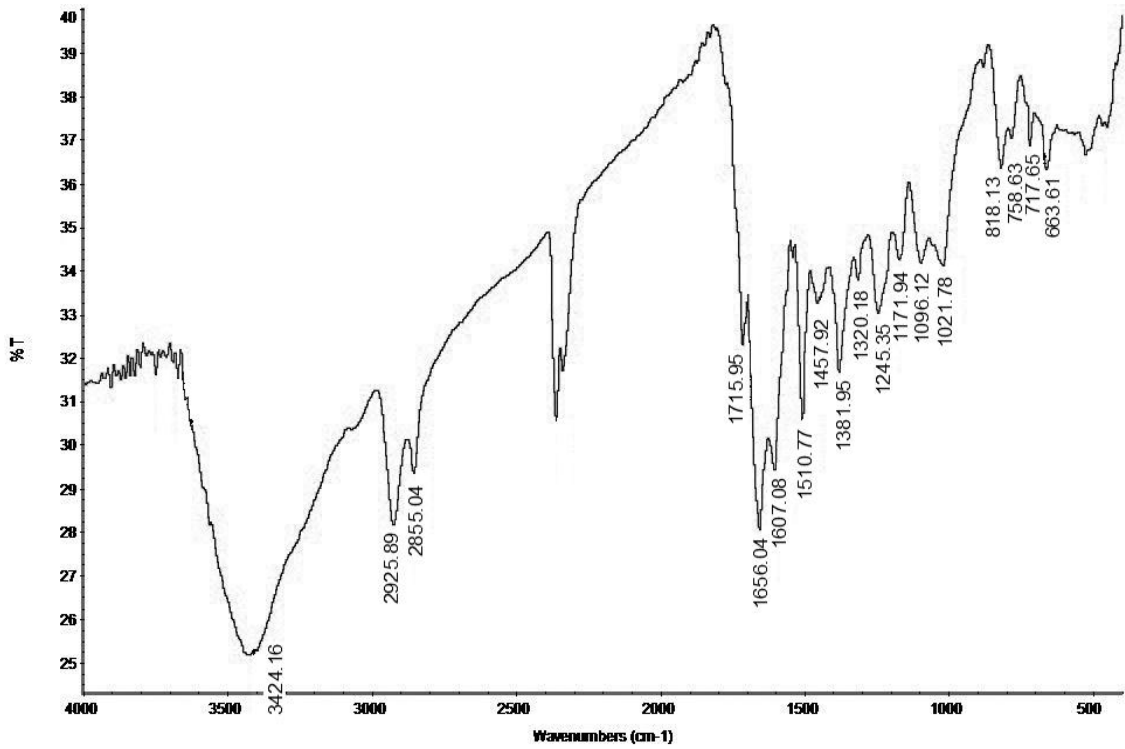


Fig. 3.9: IR (KBr) spectrum of cured epoxy resin (ECyP-15)

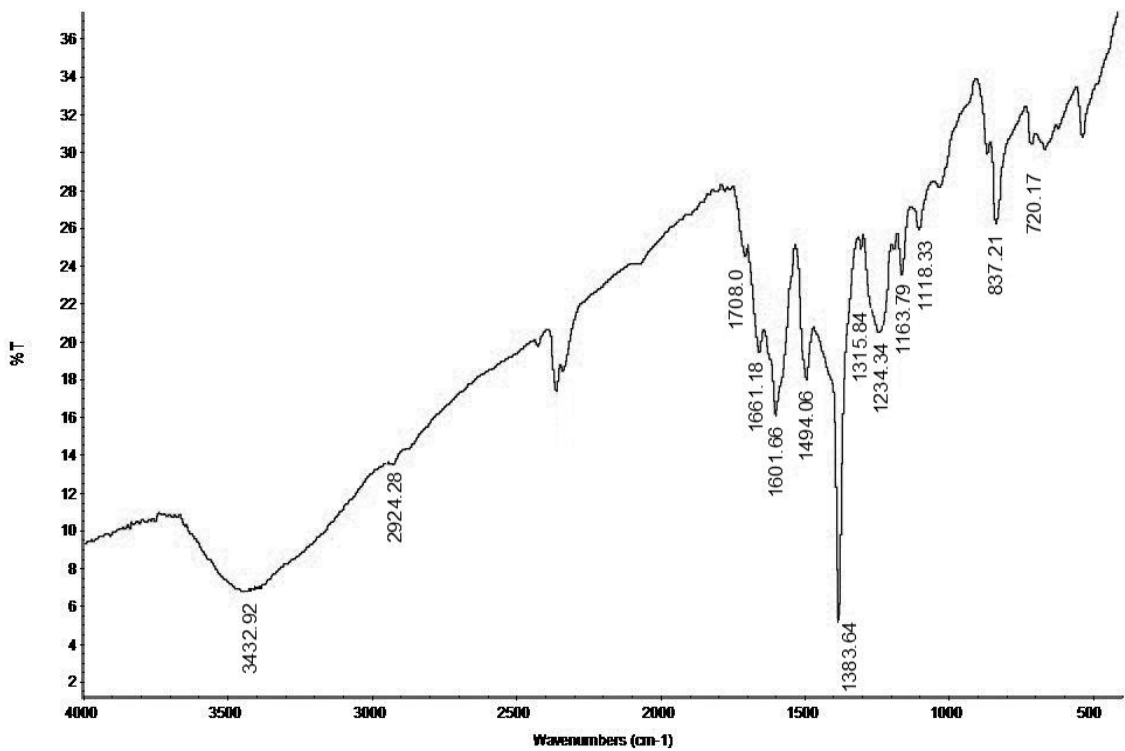


Fig. 3.10: IR (KBr) spectrum of cured epoxy resin (EMP-5)

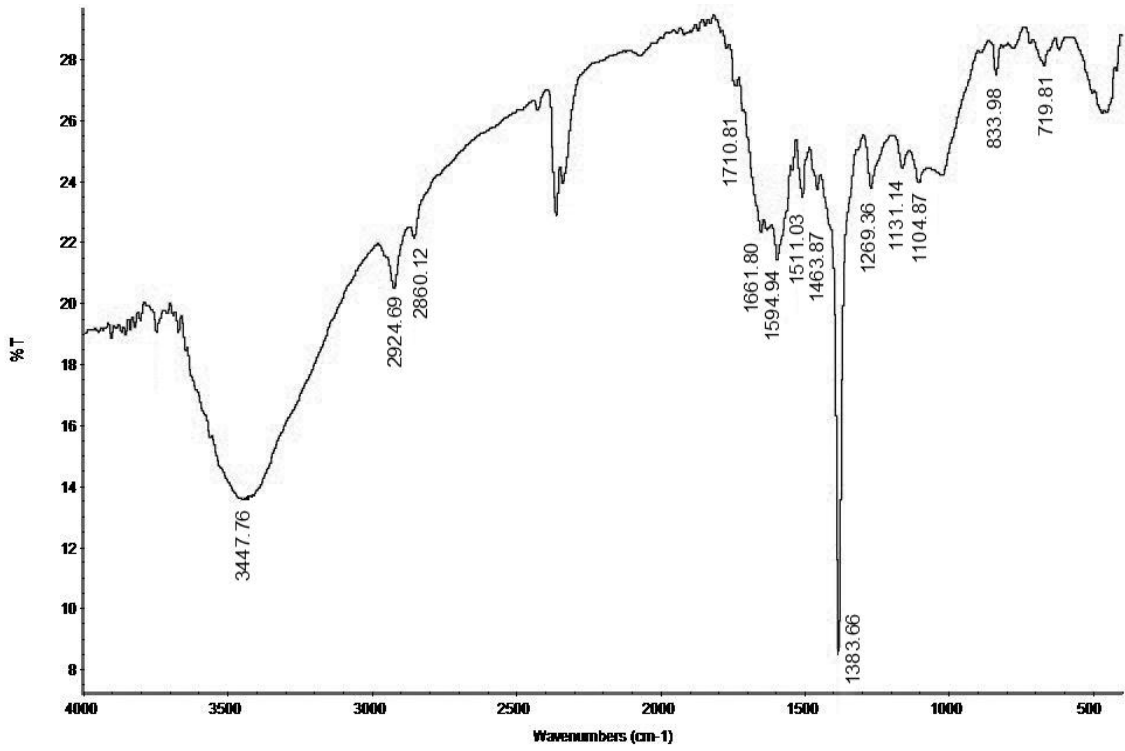


Fig. 3.11: IR (KBr) spectrum of cured epoxy resin (EMP-10)

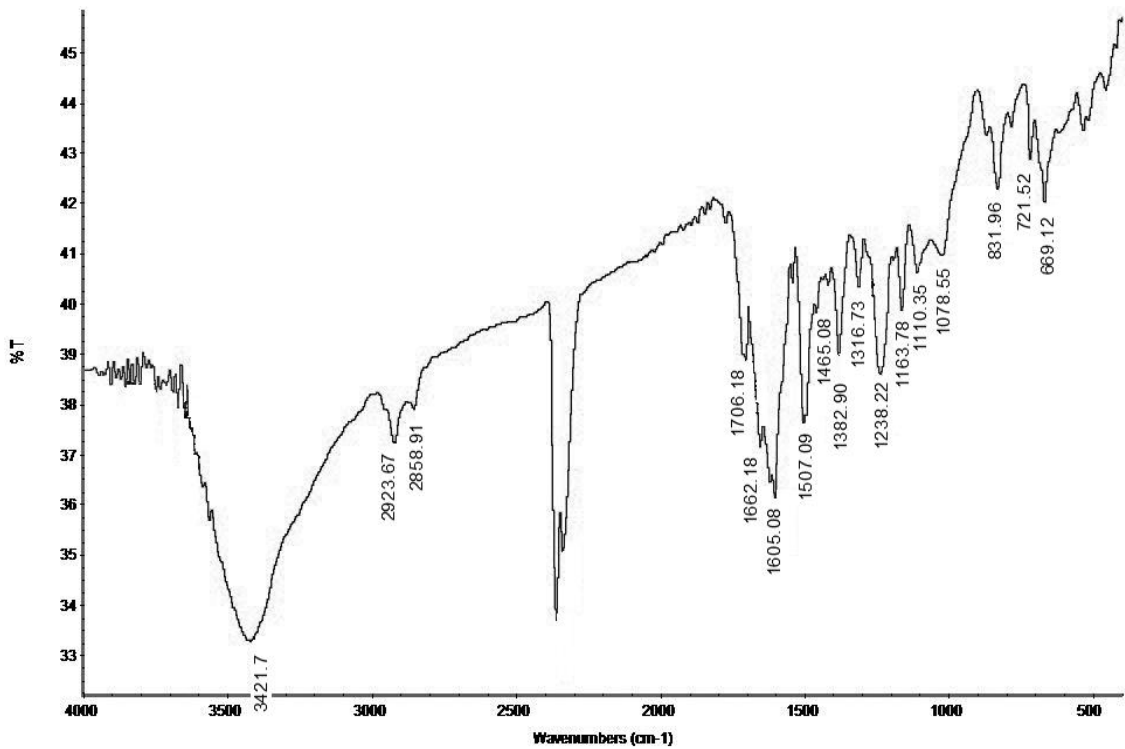


Fig. 3.12: IR (KBr) spectrum of cured epoxy resin (EMP-15)

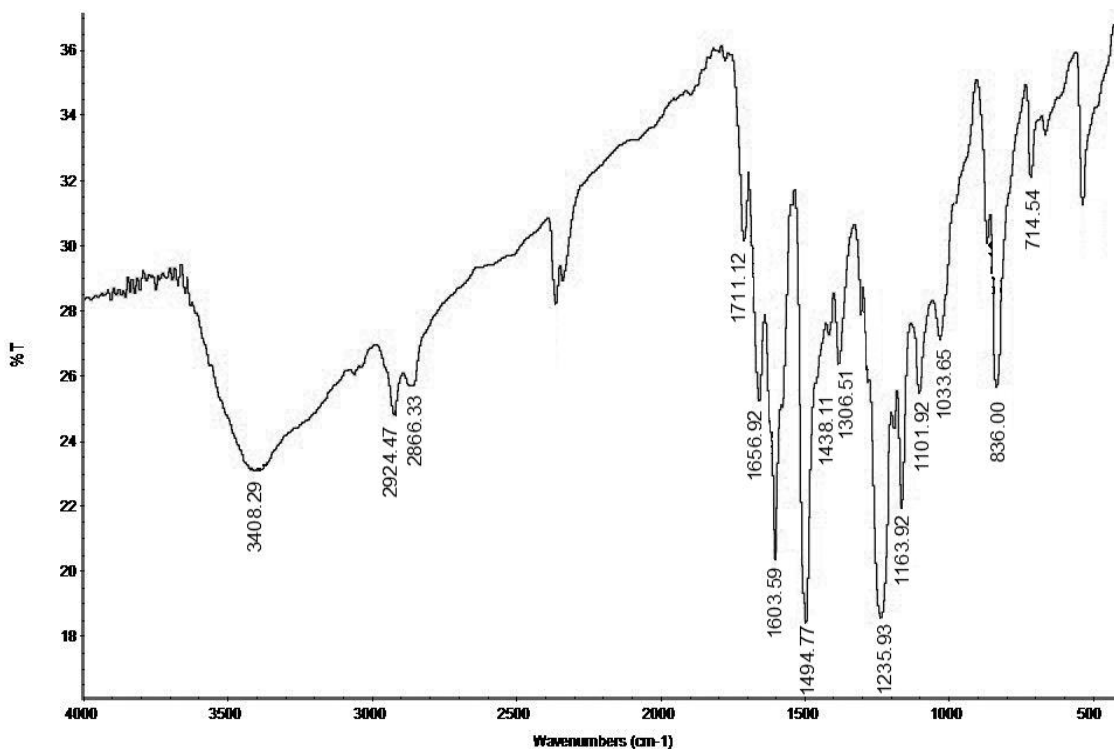


Fig. 3.13: IR (KBr) spectrum of cured epoxy resin (EEP-5)

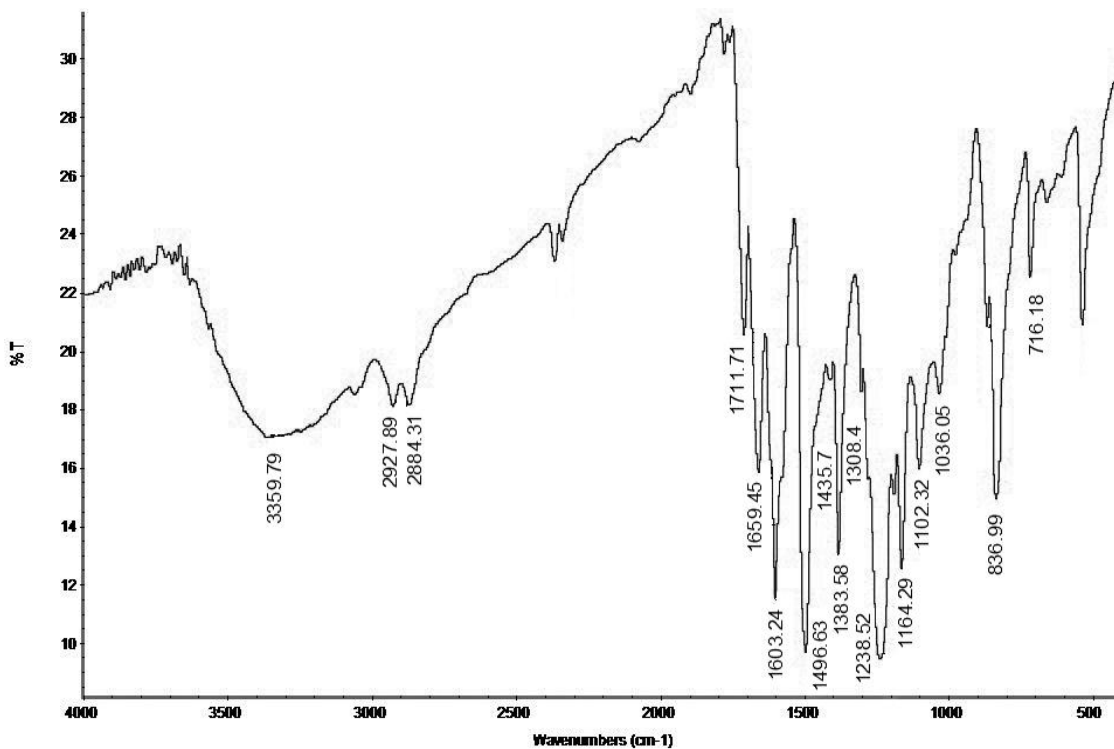


Fig. 3.14: IR (KBr) spectrum of cured epoxy resin (EEP-10)

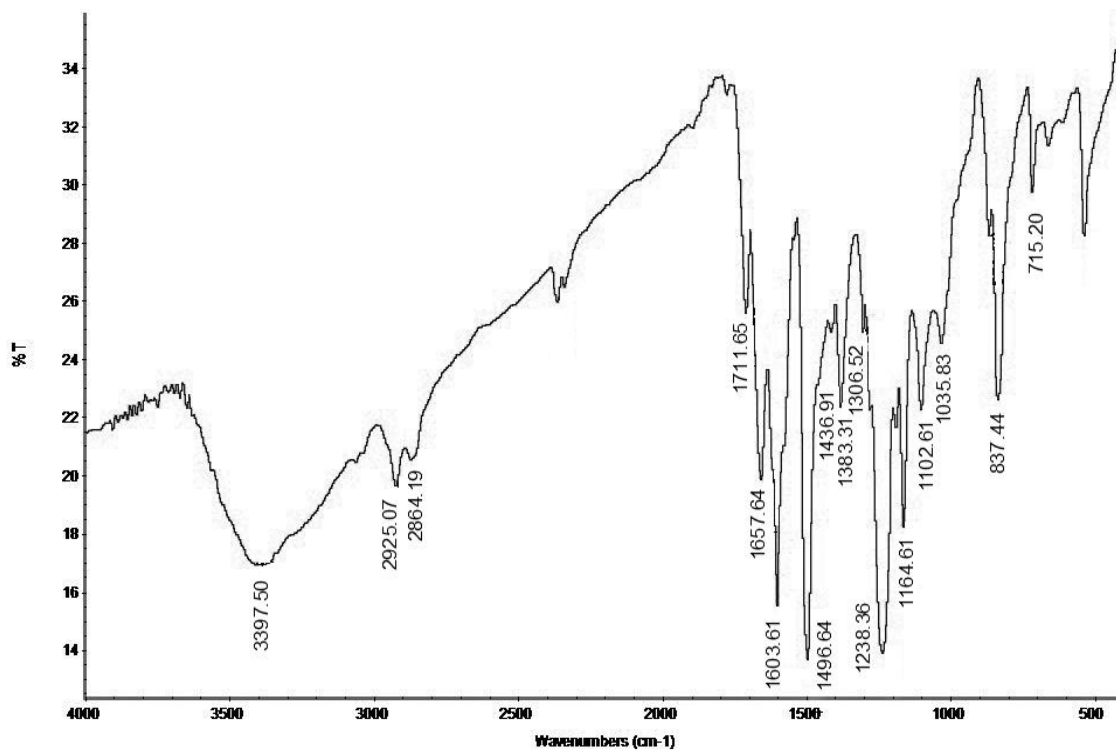


Fig. 3.15: IR (KBr) spectrum of cured epoxy resin (EEP-15)



**Table-3.7: The characteristic IR absorption frequencies of ESB4HCy, ESB4HM and ESB4HE.**

Types	Group vibration mode	Observed IR frequencies, (cm <sup>-1</sup> )			Expected frequencies, (cm <sup>-1</sup> )
		ESB4HCy	ESB4HM	ESB4HE	
Alkane -CH <sub>2</sub> -	C-H (v <sub>as</sub> )	2930.2	2935.4	2924.4	2975-2950
	C-H (v <sub>s</sub> )	2855.6	2857.4	2850.6	2880-2860
	C-H def	1455.0	1458.5	1456	1470-1435
	Twisting & Wagging	1254.0	1248.1	1249.6	~1250
	Skeletal CH <sub>2</sub>	735.0	745.4	729.4	750-720
Arom- atic	C=C str.	1601.7	1597.3 1511.4	1603.5	1600-1400
		1512.9			
		1455.0			
	C-H (i.p.d.)	1254.0	1248.1	1249.6	1258±11, 1175±6, 1117±7, 1013±5 (1,4 sub.)
1164.5		1162.1	1166.4		
1108.9		1105.7	1108.1		
1027.2		1030.3	1085.4		
C-H (o.p.d.)	831.6	831.5	839.1	817±15 (1,4 sub.)	
Schiff base	N = CH str.	1657.9	1677.8	1653.7	1690-1635
	C – N vib.	1383.8	1308.2	1333.8	1360-1310
Ether	C-O-C	1254.0	1248.1	1249.6	1275-1200
-OH	O-H str.	3386.3	3422.0	3422.6	3400-3200
	O-H def.	1383.8	1308.2	1383.8	1350-1260
	C-O-H def.	1108.9	1105.7	1166.4	1120-1030

**Table-3.8: The characteristic IR absorption frequencies of cured epoxy ESB4HCy.**

Types	Group vibration mode	Observed IR frequencies, (cm <sup>-1</sup> )			Expected frequencies, (cm <sup>-1</sup> )
		ECyP-5	ECyP-10	ECyP-15	
Alkane -CH <sub>2</sub> -	C-H (v <sub>as</sub> )	2923.3	2924.0	2925.9	2975-2950
	C-H (v <sub>s</sub> )	2872.5	2854.4	2855.0	2880-2860
	C-H def.	1461.0	1458.7	1457.9	1470-1435
	Twisting & Wagging	1246.3	1244.6	1245.4	~1250
	Skeletal CH <sub>2</sub>	729.2	720.4	717.7	750-720
Aromatic	C=C str.	1544.3	1606.2	1607.1	1600-1400
		1511.1	1542.8	1510.8	
		1461.0	1510.3	1457.9	
			1458.7		
	C-H (i.p.d.)	1246.3	1244.6	1245.4	1258±11, 1175±6, 1117±7, 1013±5 (1,4 sub.)
		1163.7	1164.6	1171.9	
C-H (i.p.d.)	1019.3	1021.0	1021.8	1269±17, 1160±4, 1125±14, 1033±11 (1,2 sub.)	
	1163.7	1164.6	1171.9		
	1019.3	1021.0	1021.8		
C-H (o.p.d.)	819.5	819.1	818.1	817±15 (1,4 sub.)	
C-H (o.p.d.)	729.2	720.4	758.6	751±7 (1,2 sub.)	
Schiff base	N = CH str.	1655.1	1654.1	1656.0	1690-1635
	C – N vib.	1319.3	1382.3	1381.9	1360-1310
Ester	C=O str.	1715.1	1716.5	1716.0	1780-1710
	C-O str.	1246.3	1244.6	1245.4	1300-1250
Ether	C-O-C	1246.3	1244.6	1245.4	1275-1200
-OH	O-H str.	3421.6	3424.6	3424.2	3400-3200
	O-H def.	1319.3	1318.5	1320.2	1350-1260
	C-O-H def.	1080.1	1082.2	1096.1	1120-1030

**Table-3.9: The characteristic IR absorption frequencies of cured epoxy ESB4HM.**

Types	Group vibration mode	Observed IR frequencies, (cm <sup>-1</sup> )			Expected frequencies, (cm <sup>-1</sup> )
		EMP-5	EMP-10	EMP-15	
Alkane -CH <sub>2</sub> -	C-H (v <sub>as</sub> )	2924.7	2924.7	2923.7	2975-2950
	C-H (v <sub>s</sub> )	-	2860.1	2858.9	2880-2860
	C-H def.	1494.1	1463.9	1465.1	1470-1435
	Twisting & Wagging	1234.3	1269.4	1238.2	~1250
	Skeletal CH <sub>2</sub>	720.2	719.8	721.5	750-720
Aromatic	C=C str.	1601.7 1494.1	1594.9 1511.0 1463.9	1605.1 1507.1 1465.1	1600-1400
	C-H (i.p.d.)	1234.3 1163.8 1118.3	1269.4 1104.9	1238.2 1163.8 1110.4	1258±11, 1175±6, 1117±7, 1013±5 (1,4 sub.)
	C-H (i.p.d.)	1234.3 1163.8 1118.3	1269.4 1131.1 1104.9	1238.2 1163.8 1110.4	1269±17, 1160±4, 1125±14, 1033±11 (1,2 sub)
	C-H (o.p.d.)	837.2	834.0	832.0	817±15 (1,4 sub.)
	C-H (o.p.d.)	720.2	719.8	721.5	751±7 (1,2 sub.)
	Schiff base	N = CH str.	1661.2	1661.8	1662.2
C – N vib.		1383.6	1383.7	1382.9	1360-1310
Ester	C=O str.	1708.0	1710.8	1706.2	1780-1710
	C-O str.	1234.3	1269.4	1238.2	1300-1250
Ether	C-O-C	1234.3	1269.4	1238.2	1275-1200
-OH	O-H str.	3432.9	3447.8	3421.7	3400-3200
	O-H def.	1315.8	1269.4	1316.7	1350-1260
	C-O-H def.	1118.3	1104.9	1110.4	1120-1030

**Table-3.10: The characteristic IR absorption frequencies of cured epoxy ESB4HE.**

Types	Group vibration mode	Observed IR frequencies, (cm <sup>-1</sup> )			Expected frequencies, (cm <sup>-1</sup> )
		EEP-5	EEP-10	EEP-15	
Alkane -CH <sub>2</sub> -	C-H (v <sub>as</sub> )	2924.5	2927.9	2925.1	2975-2950
	C-H (v <sub>s</sub> )	2866.3	2884.3	2864.2	2880-2860
	C-H def.	1438.1	1435.7	1436.9	1470-1435
	Twisting & Wagging	1236.0	1238.5	1238.4	~1250
	Skeletal CH <sub>2</sub>	714.5	716.2	715.2	750-720
Arom- atic	C=C str.	1603.6 1438.1	1603.2 1496.6	1603.6 1496.6 1436.9	1600-1400
	C-H (i.p.d.)	1236.0 1102.0	1238.5 1102.3	1238.4 1102.6	1258±11, 1175±6, 1117±7, 1013±5 (1,4 sub.)
	C-H (i.p.d.)	1163.9 1033.7	1164.3 1036.1	1164.6 1035.8	1269±17, 1160±4, 1125±14, 1033±11 (1,2 sub)
	C-H (o.p.d.)	836.0	837.0	837.4	817±15 (1,4 sub.)
	C-H (o.p.d.)	714.5	716.2	715.2	751±7 (1,2 sub.)
Schiff base	N = CH str.	1656.9	1659.5	1657.6	1690-1635
	C – N vib.	1306.5	1308.4	1383.3	1360-1310
Ester	C=O str.	1711.1	1711.7	1711.7	1780-1710
	C-O str.	1236.0	1238.5	1238.4	1300-1250
-OH	O-H str.	3408.3	3359.8	3397.5	3400-3200
	O-H def.	1306.5	1308.4	1306.5	1350-1260
	C-O-H def.	1101.9	1102.3	1035.8	1120-1030

### IR spectral analysis of bisbenzoxazines

IR spectra of bisbenzoxazines (BSB4HCy, BSB4HM, BSB4HE and BSB4HS) are presented in Figs. 3.16 to 3.19 and absorption frequencies in Table 3.11. Observed characteristic IR frequencies for BSB4HCy are 1684 (N=CH str.) and 1239.4 (C-O-C str.); for BSB4HM: 1670.6 (N=CH str.) and 1273.4 (C-O-C str.); for BSB4HE: 1680.7 (N=CH str.) and 1234 (C-O-C str.); and for BSB4HS: 1670.1 (N=CH str.) and 1282.3 (C-O-C str.) besides other normal modes of vibrations of alicyclic, aliphatic and aromatic groups.

IR spectra of cured bisbenzoxazines via ring opening polymerization (BCCy, BCM, BCE and BCS) are presented in Figs. 3.20 to 3.23 and absorption frequencies in Table 3.12. Observed characteristic IR frequencies for BCCy are 1658.1 (N=CH str.) and 1271.2 (C-O-C str.); for BCM: 1650.3 (N=CH str.) and 1271.5 (C-O-C str.); for BCE: 1655.4 (N=CH str.) and 1271.4 (C-O-C str.); and for BCS: 1650.1 (N=CH str.) and 1272.1 (C-O-C str.) besides other normal modes of vibrations of alicyclic, aliphatic and aromatic groups.

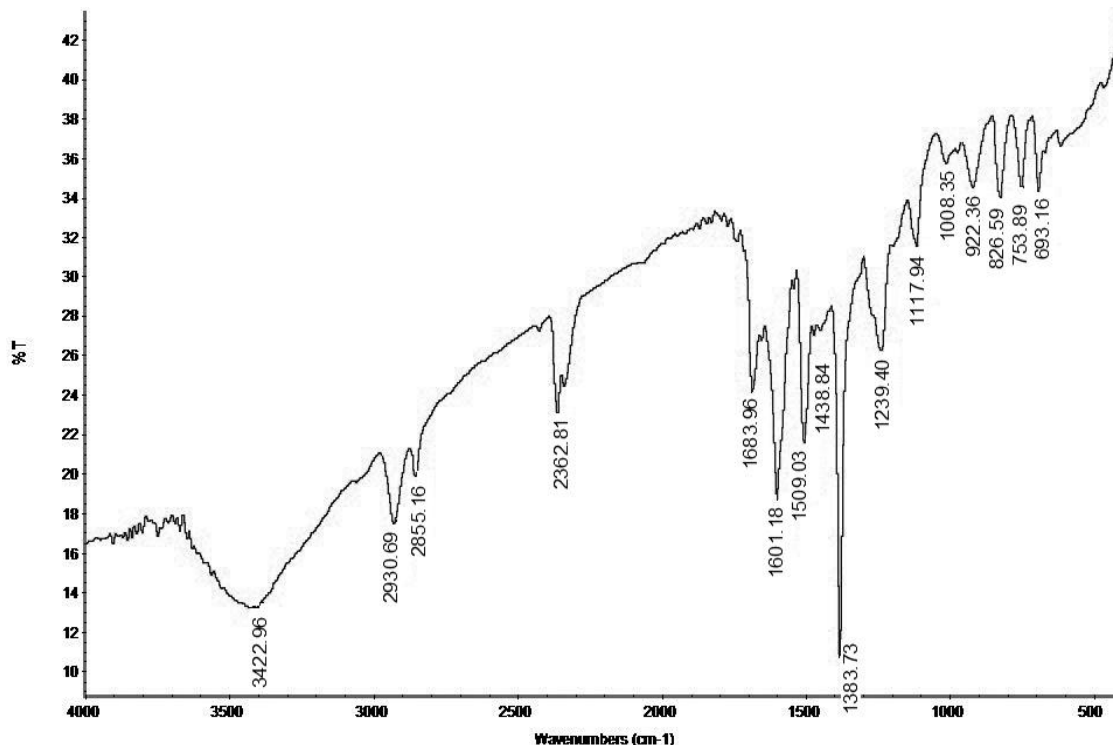


Fig. 3.16: IR (KBr) spectrum of bisbenzoxazine (BSB4HCy)

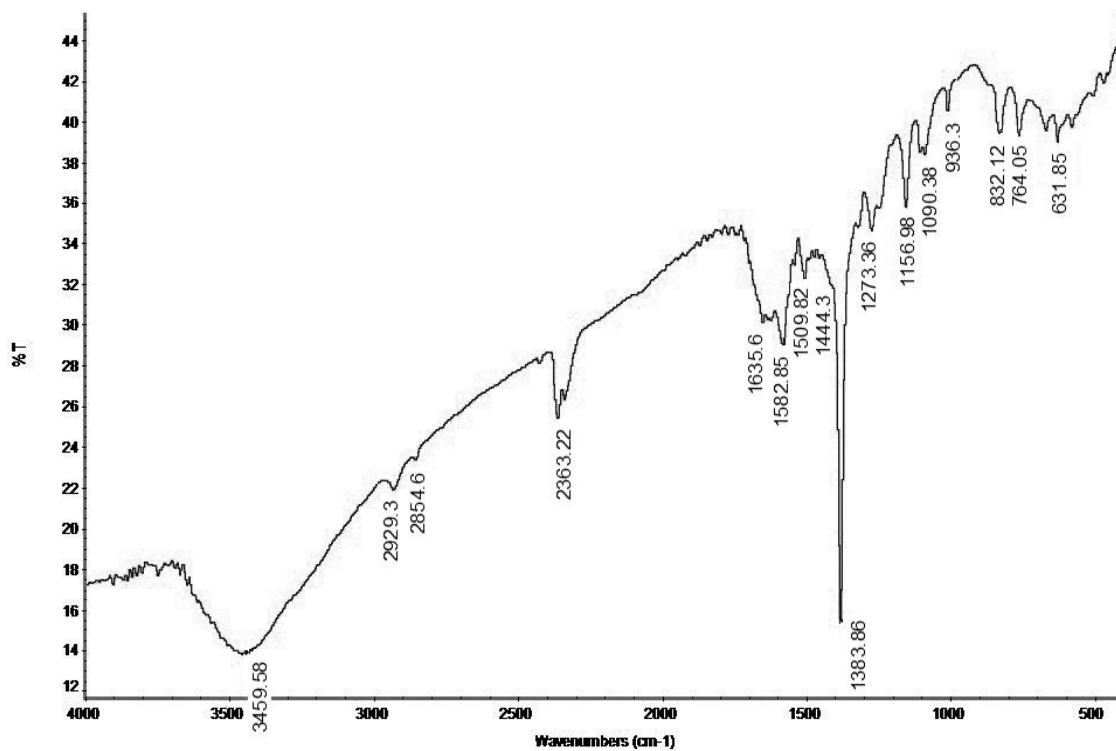


Fig. 3.17: IR (KBr) spectrum of bisbenzoxazine (BSB4HM)

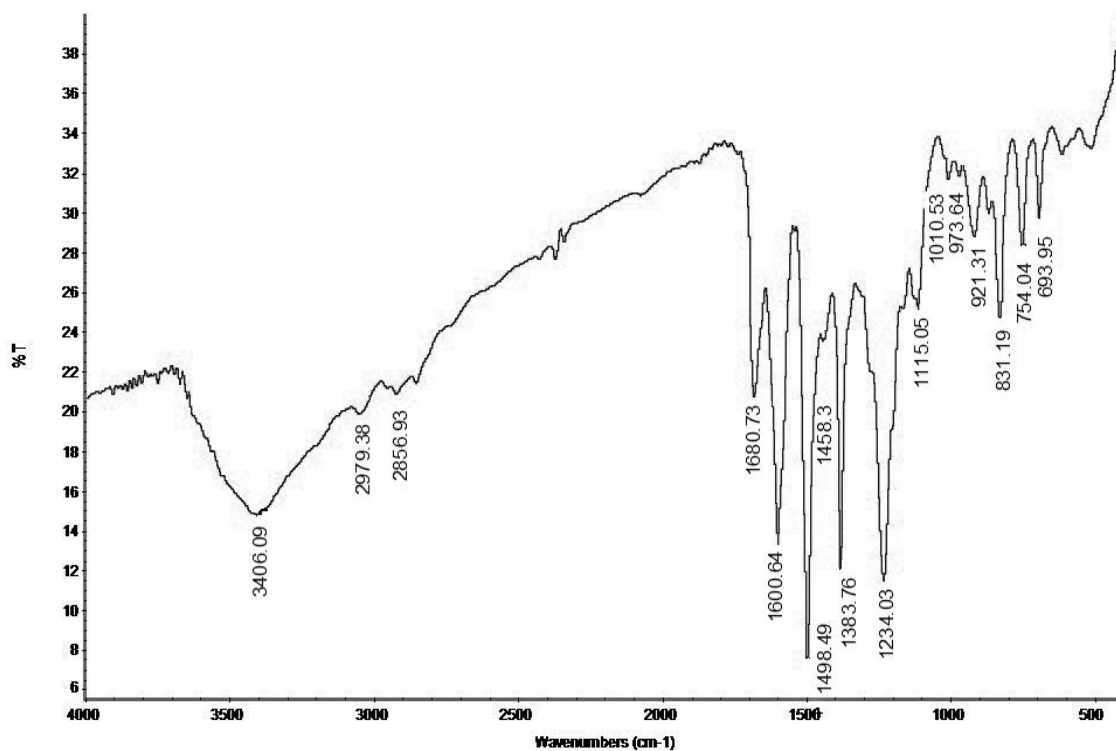


Fig. 3.18: IR (KBr) spectrum of bisbenzoxazine (BSB4HE)

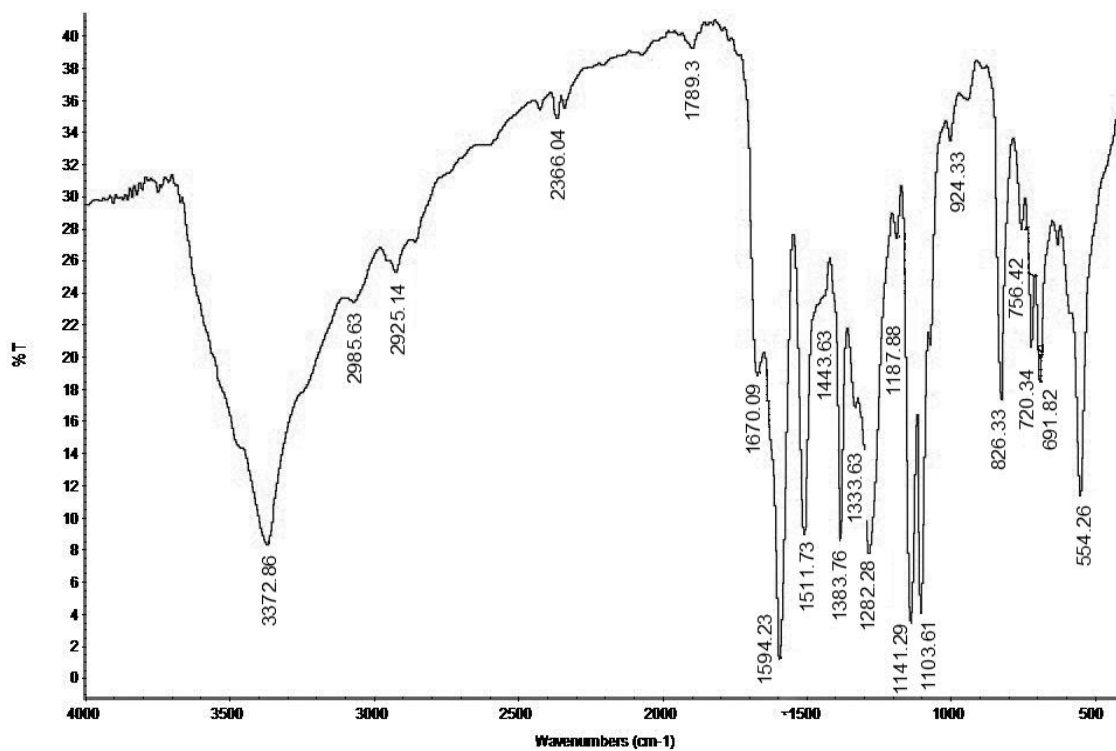


Fig. 3.19: IR (KBr) spectrum of bisbenzoxazine (BSB4HS)

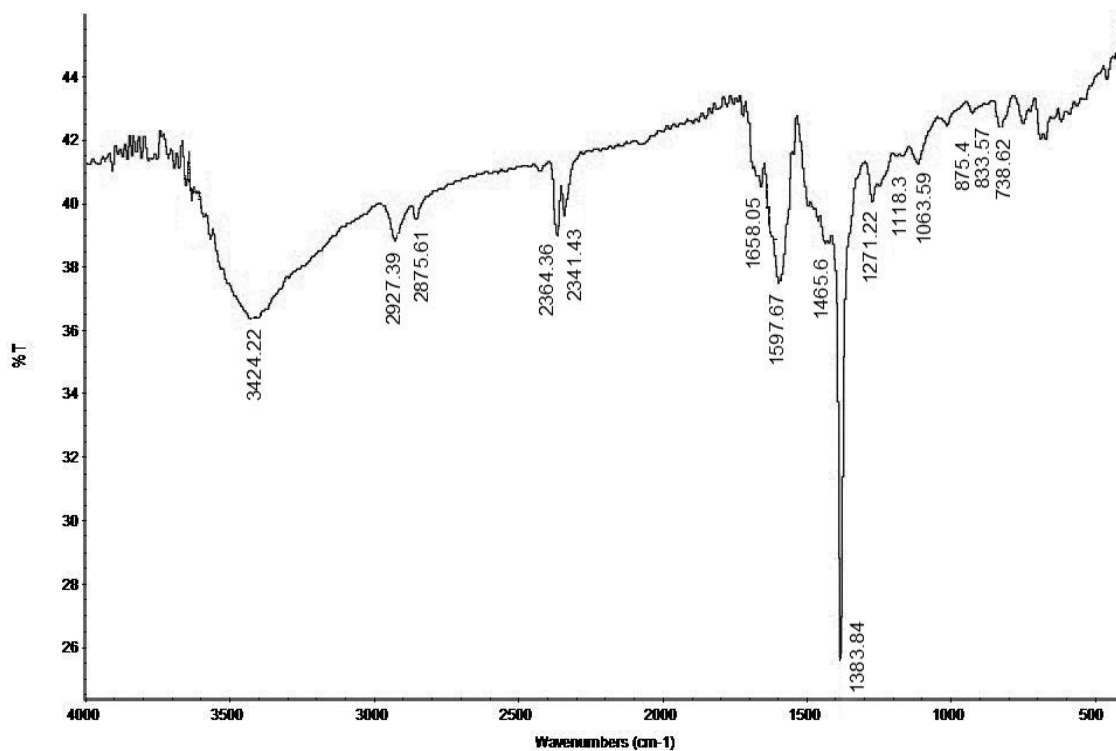


Fig. 3.20: IR (KBr) spectrum of cured bisbenzoxazine (BCCy)

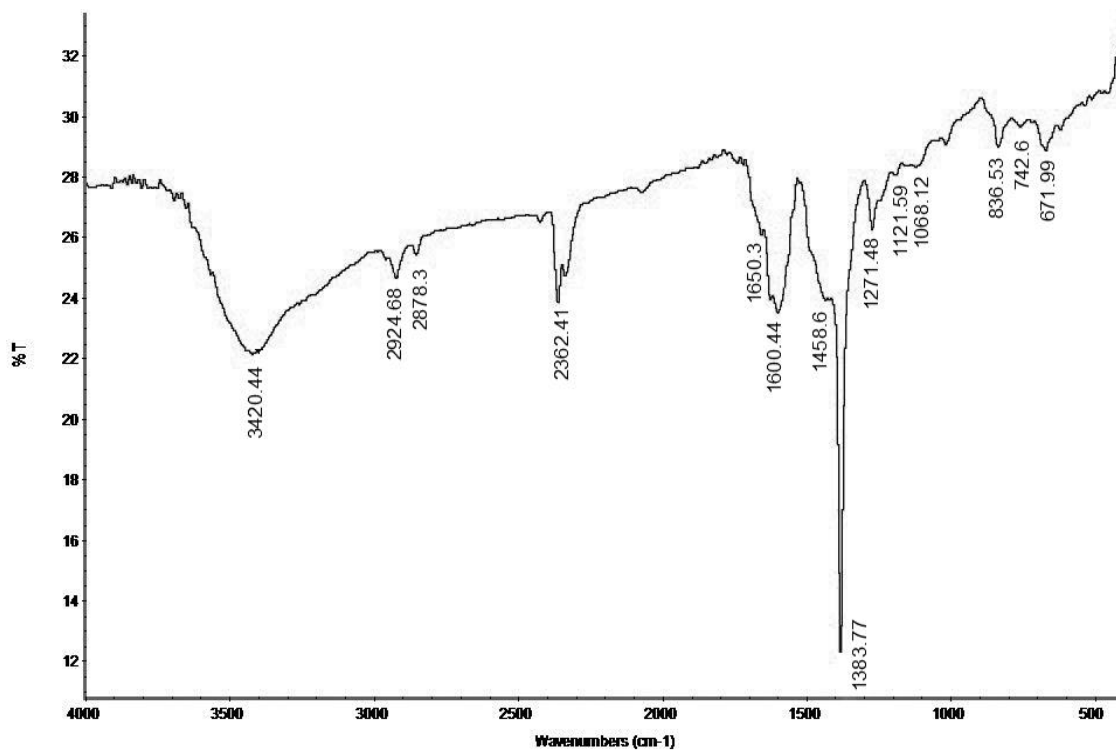


Fig. 3.21: IR (KBr) spectrum of cured bisbenzoxazine (BCM)

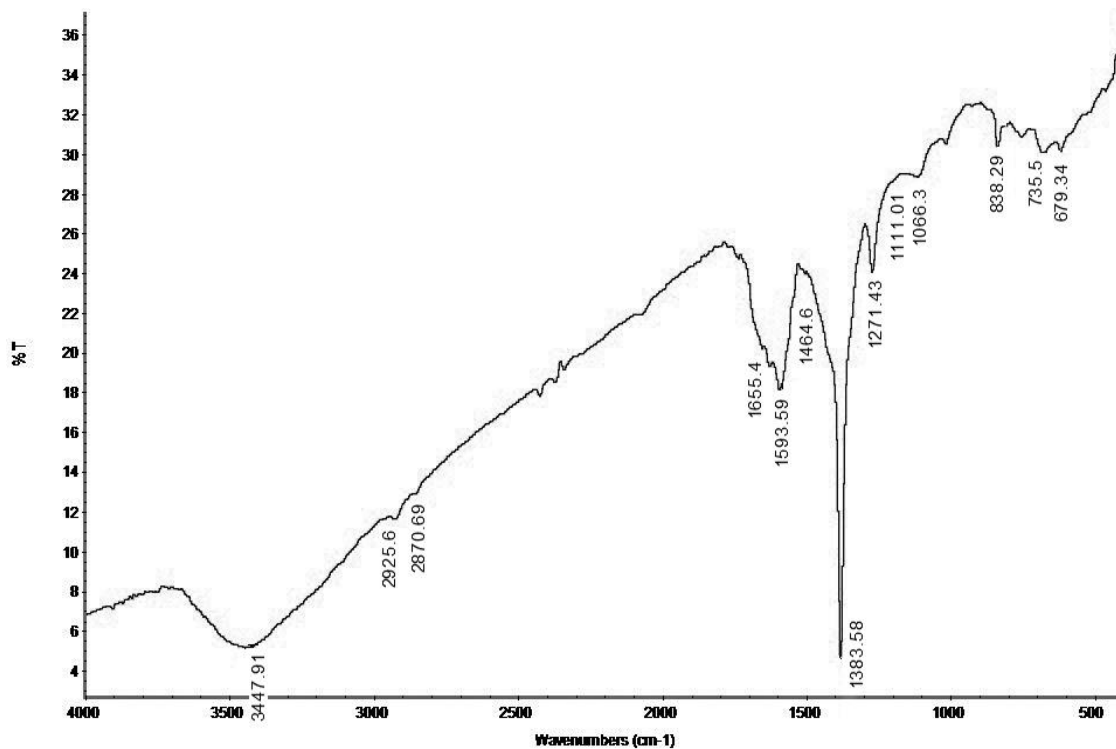


Fig. 3.22: IR (KBr) spectrum of cured bisbenzoxazine (BCE)



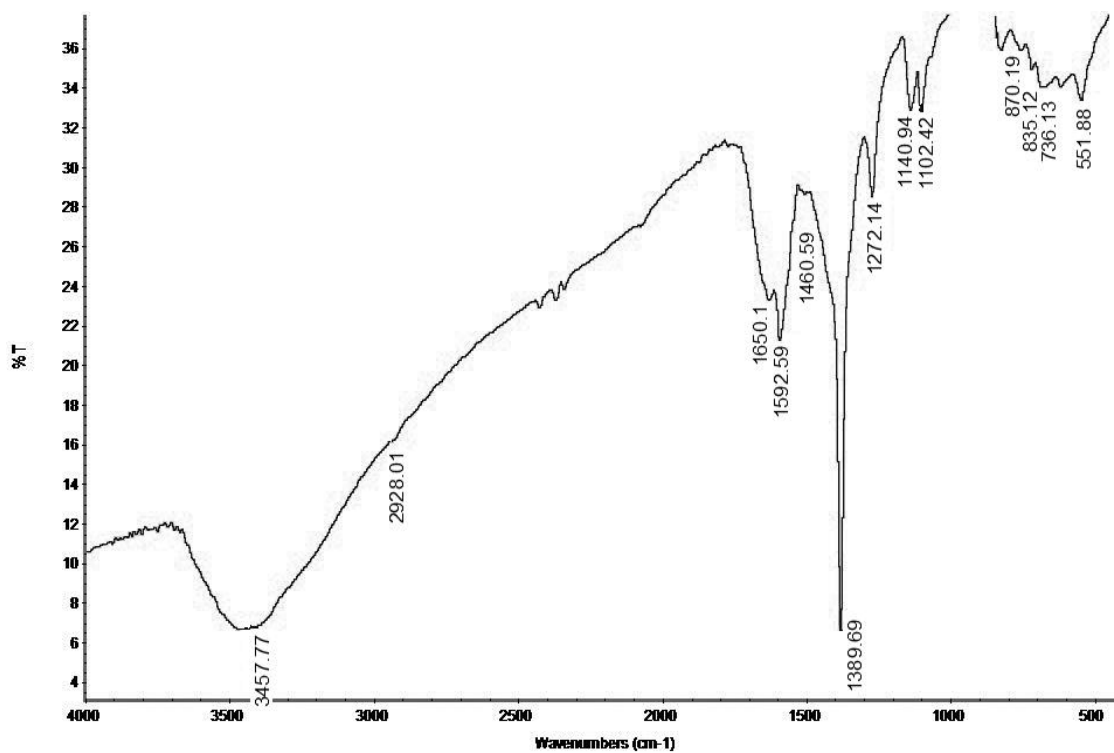


Fig. 3.23: IR (KBr) spectrum of cured bisbenzoxazine (BCS)

**Table-3.11: The characteristic IR absorption frequencies of bisbenzoxazine.**

Types	Group vibration mode	Observed IR frequencies, (cm <sup>-1</sup> )				Expected frequencies, (cm <sup>-1</sup> )
		BSB4HCy	BSB4HM	BSB4HE	BSB4HS	
Alkane -CH <sub>2</sub> -	C-H (ν <sub>as</sub> )	2930.7	2929.3	2979.4	2985.6	2975-2950
	C-H (ν <sub>s</sub> )	2855.2	2854.6	2856.9	2925.1	2880-2860
	C-H def.	-	-	-	-	1470-1435
	Twisting & Wagging	1239.4	1273.4	1234.0	1282.3	~1250
	Skeletal CH <sub>2</sub>	-	-	-	-	750-720
Aromatic	C=C str.	1601.2 1509.0	1582.9	1600.6 1498.5	1594.2 1511.7	1600-1400
	C-H (i.p.d.)	1117.9 1008.4	1157.0 1090.4	1115.1 1010.5	1187.9 1141.3	1177±6, 1156±5, 1073±4, 1027±3 (mono sub.)
	C-H (i.p.d.)	1239.4 1117.9 1008.4	1273.4 1157.0 1090.4	1234.0 1115.1 1010.5	1282.31 187.9 1103.6	1258±11, 1175±6, 1117±7, 1013±5 (1,4 sub.)
	C-H (o.p.d.)	753.9 693.2	764.1 691.9	754.0 694.0	756.4 691.8	751±15, 697±11 (mono sub.)
	C-H (o.p.d.)	826.6	832.1	831.2	826.3	817±15 (1,4 sub.)
Schiff base	N = CH str.	1684	1670.6	1680.7	1670.1	1690-1635
	C – N vib.	1383.4	1383.9	1383.8	1333.6	1360-1310
Ether	C-O-C str.	1239.4	1273.4	1234.0	1282.3	1275-1200
Sulfone	S=O (ν <sub>as</sub> )	-	-	-	1383.6	1350-1300
	S=O (ν <sub>s</sub> )	-	-	-	1141.3	1160-1120

**Table-3.12: The characteristic IR absorption frequencies of cured bisbenzoxazine.**

Types	Group vibration mode	Observed IR frequencies, (cm <sup>-1</sup> )				Expected frequencies, (cm <sup>-1</sup> )
		BCCy	BCM	BCE	BCS	
Alkane -CH <sub>2</sub> -	C-H (v <sub>as</sub> )	2927.4	2924.7	2925.6	2928.0	2975-2950
	C-H (v <sub>s</sub> )	2870.6	2878.3	2870.7	-	2880-2860
	C-H def.	1465.6	1458.6	1464.6	1460.6	1470-1435
	Skeletal CH <sub>2</sub>	738.3	742.6	735.5	736.1	750-720
Aromatic	C=C str.	1597.7 1465.6	1600.4 1458.6	1593.6 1464.6	1592.6 1460.6	1600-1400
	C-H (i.p.d.)	1063.6	1121.6 1068.1	1066.3	1140.9	1177±6, 1156±5, 1073±4, 1027±3 (mono sub.)
	C-H (i.p.d.)	1271.2 1118.3	1271.5 1121.6	1271.4	1272.1 1102.4	1258±11, 1175±6, 1117±7, 1013±5 (1,4 sub.)
	C-H (o.p.d.)	738.6 674.1	742.6 672.0	735.5 679.3	736.1 685.3	751±15, 697±11 (mono sub.)
	C-H (o.p.d.)	-	836.5	838.3	835.1	817±15 (1,4 sub.)
Schiff base	N = CH str.	1658.1	1650.3	1655.4	1650.1	1690-1635
	C – N vib.	1383.8	1383.8	1383.6	1383.7	1360-1310
Ester	C-O str.	1271.2	1271.5	1271.4	1272.1	1300-1250
-OH	O-H str.	3424.2	3420.4	3447.9	3457.8	3400-3200
	O-H def.	1271.2	1271.5	1271.4	1272.1	1350-1260
	C-O-H def.	1063.6	1068.1	1066.3	1102.4	1120-1030
Sulfone	S=O (v <sub>as</sub> )	-	-	-	-	1350-1300
	S=O (v <sub>s</sub> )	-	-	-	1140.9	1160-1120

### IR spectral analysis of polySchiff bases

IR spectra of polySchiff bases derived from SB4HCy, SB4HM, SB4HE and SB4HS with DCDPS are presented in Figs. 3.24 to 3.27 and absorption frequencies in Table 3.13. Observed characteristic frequencies for SB4HCy-DCDPS are 1680.6 (N=CH str.) , 1273.3 (C-O-C str.), 1383.9 (S=O  $v_{as}$ ) and 1157 (S=O  $v_s$ ); for SB4HM-DCDPS: 1689.9 (N=CH str.), 1243.8 (C-O-C str.), 1383.9 (S=O  $v_{as}$ ) and 1152 (S=O  $v_s$ ); for SB4HE-DCDPS: 1610.4 (N=CH str.), 1252.8 (C-O-C str.), 1383.9 (S=O  $v_{as}$ ) and 1157 (S=O  $v_s$ ); and for SB4HS-DCDPS: 1683.4 (N=CH str.), 1243.9 (C-O-C str.), 1386.5 (S=O  $v_{as}$ ) and 1149.1 (S=O  $v_s$ ).

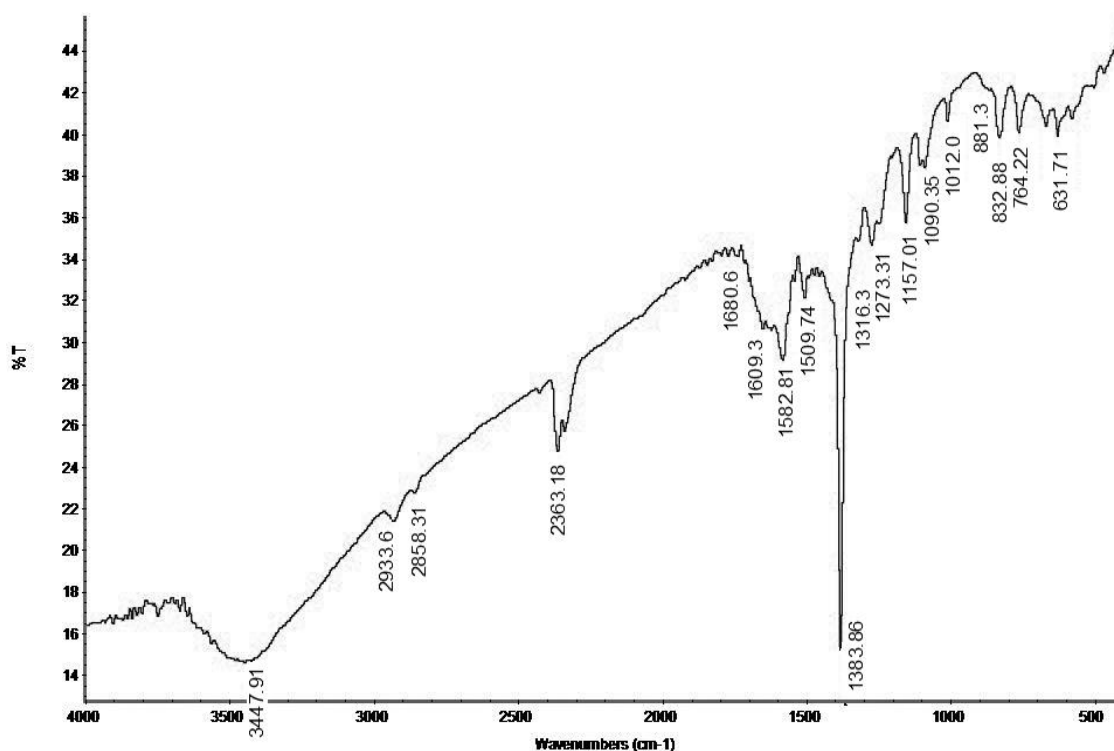


Fig. 3.24: IR (KBr) spectrum of polySchiff base (SB4HCy-DCDPS)

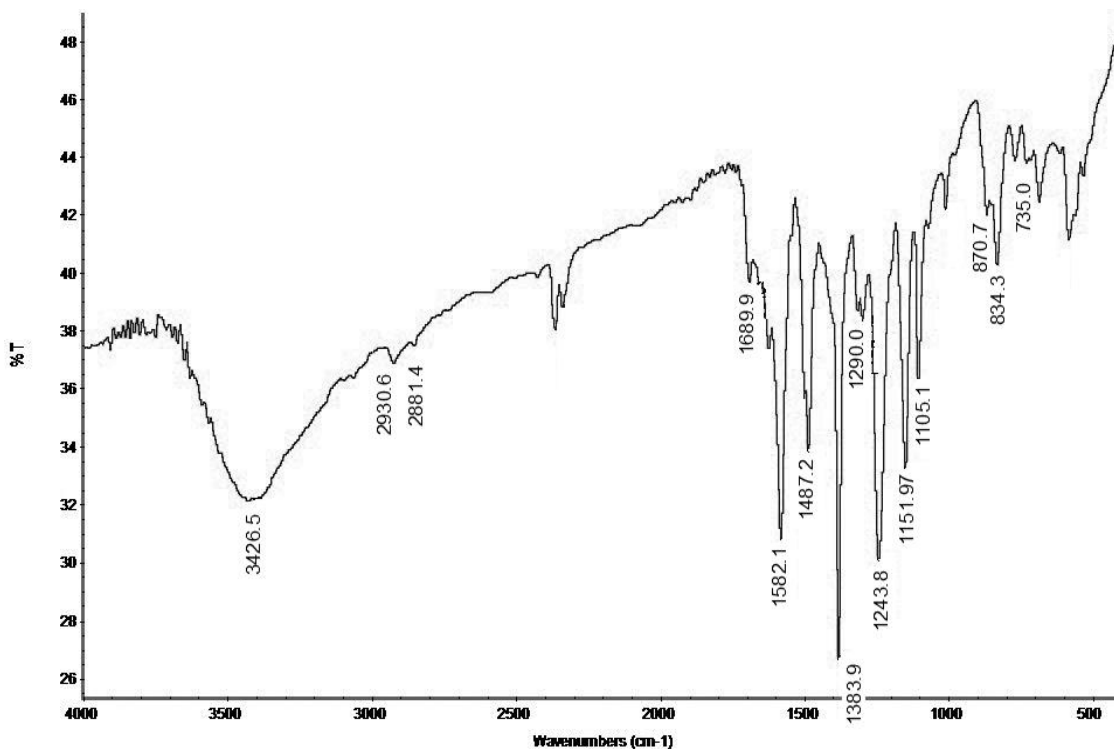


Fig. 3.25: IR (KBr) spectrum of polySchiff base (SB4HM-DCDPS)

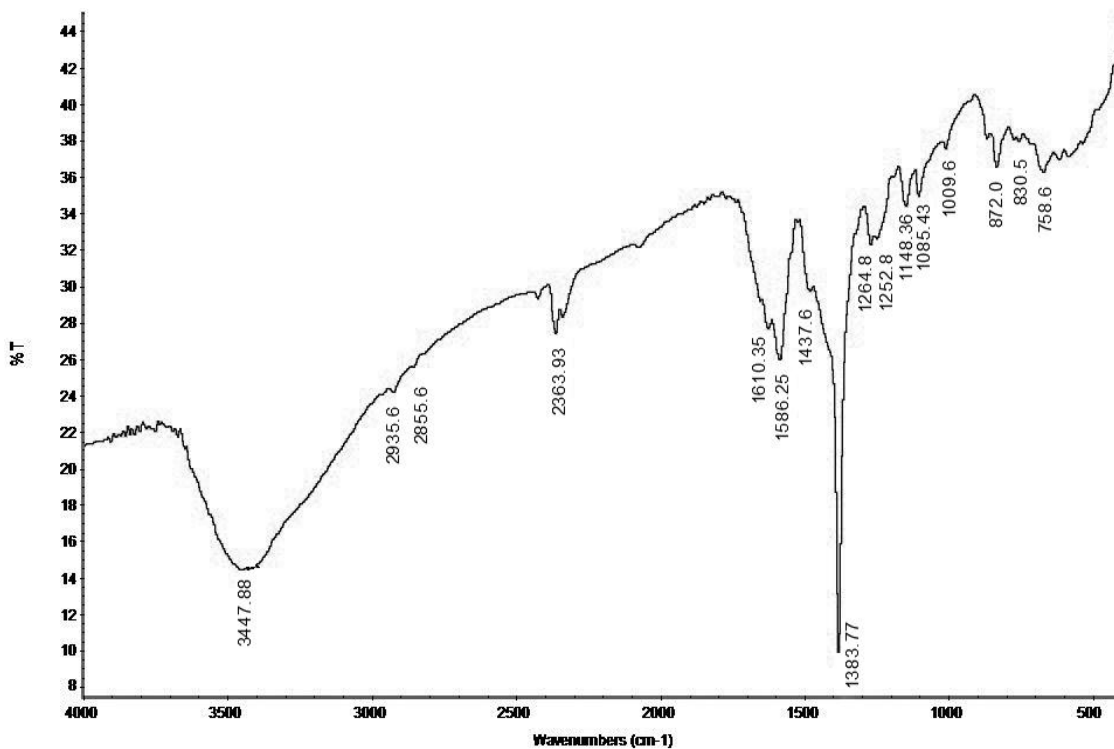


Fig. 3.26: IR (KBr) spectrum of polySchiff base (SB4HE-DCDPS)

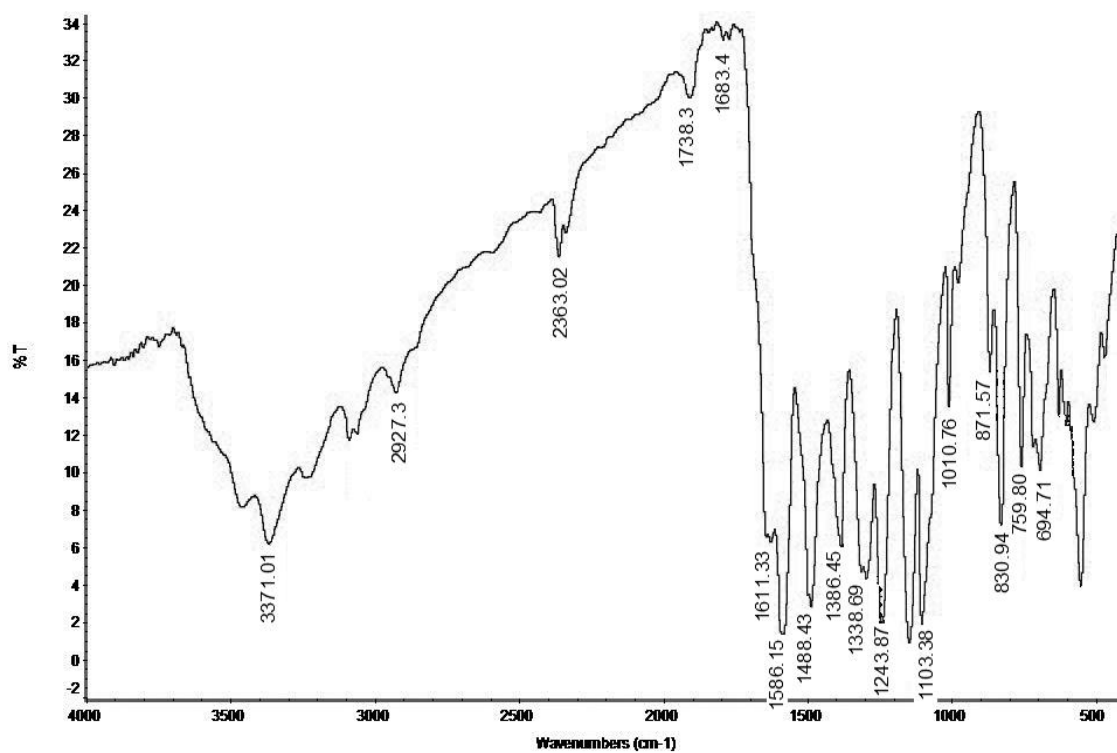


Fig. 3.27: IR (KBr) spectrum of polySchiff base (SB4HS-DCDPS)

**Table-3.13: The characteristic IR absorption frequencies of polySchiff base with DCDPS.**

Types	Group vibration mode	Observed IR frequencies, (cm <sup>-1</sup> )				Expected frequencies, (cm <sup>-1</sup> )
		SB4HCy - DCDPS	SB4HM - DCDPS	SB4HE - DCDPS	SB4HS - DCDPS	
Alkane -CH <sub>2</sub> -	C-H (v <sub>as</sub> )	2933.6	2930.6	2935.6	2927.3	2975-2950
	C-H (v <sub>s</sub> )	2858.3	2881.4	2855.6	2857.9	2880-2860
	C-H def.	1448.0	1487.2	1437.6	1488.4	1470-1435
	Twisting & Wagging	1251.0	1243.8	1252.8	1243.9	~1250
	Skeletal CH <sub>2</sub>	764.2	735	758.6	759.8	750-720
Aromatic	C=C str.	1582.8	1582.1 1487.2	1586.3	1586.2	1600-1400
		1509.7		1437.6	1488.4	
		1448.0				
	C-H (i.p.d.)	1273.3	1243.8	1252.8	1243.9	1258±11, 1175±6, 1117±7, 1013±5 (1,4 sub.)
1157.0		1152.0	1157.0	1149.11		
1090.4		1105.1	1085.4	103.4		
1012.0		1012.1	1009.6	1010.8		
C-H (o.p.d.)	832.9	834.3	830.5	830.9	817±15 (1,4 sub.)	
Schiff base	N = CH str.	1680.6	1689.9	1610.4	1683.4	1690-1635
	C – N vib.	1316.3	1383.9	1383.8	1338.7	1360-1310
Ether	C-O-C	1273.3	1243.8	1252.8	1243.9	1275-1200
-OH	O-H str.	3447.9	3426.5	3447.9	3371.0	3400-3200
	O-H def.	1273.3	1299.0	1290.0	1295.9	1350-1260
	C-O-H def.	1090.4	1105.1	1085.4	1103.4	1120-1030
Sulfone	S=O (v <sub>as</sub> )	1383.9	1383.9	1383.9	1386.5	1350-1300
	S=O (v <sub>s</sub> )	1157.0	1152.0	1157.0	1149.1	1160-1120

IR spectra of polySchiff bases (SB4HCy-SB4ClCy, SB4HM-SB4ClM, SB4HE-SB4ClM and SB4HS-SB4ClS) are presented in Figs. 3.28 to 3.31 and absorption peaks in Table 3.14. Observed characteristic peaks for SB4HCy-SB4ClCy are 1690.8 (N=CH str.) and 1238.4 (C-O-C str.); for SB4HM-SB4ClM: 1658.4 (N=CH str.) and 1250.8 (C-O-C str.); for SB4HE-SB4ClE: 1655.7 (N=CH str.) and 1239.8 (C-O-C str.); and for SB4HS-SB4ClS: 1626.3 (N=CH str.), 1252 (C-O-C str.), 1384.1 (S=O  $v_{as}$ ) and 1143.6 (S=O  $v_s$ ).

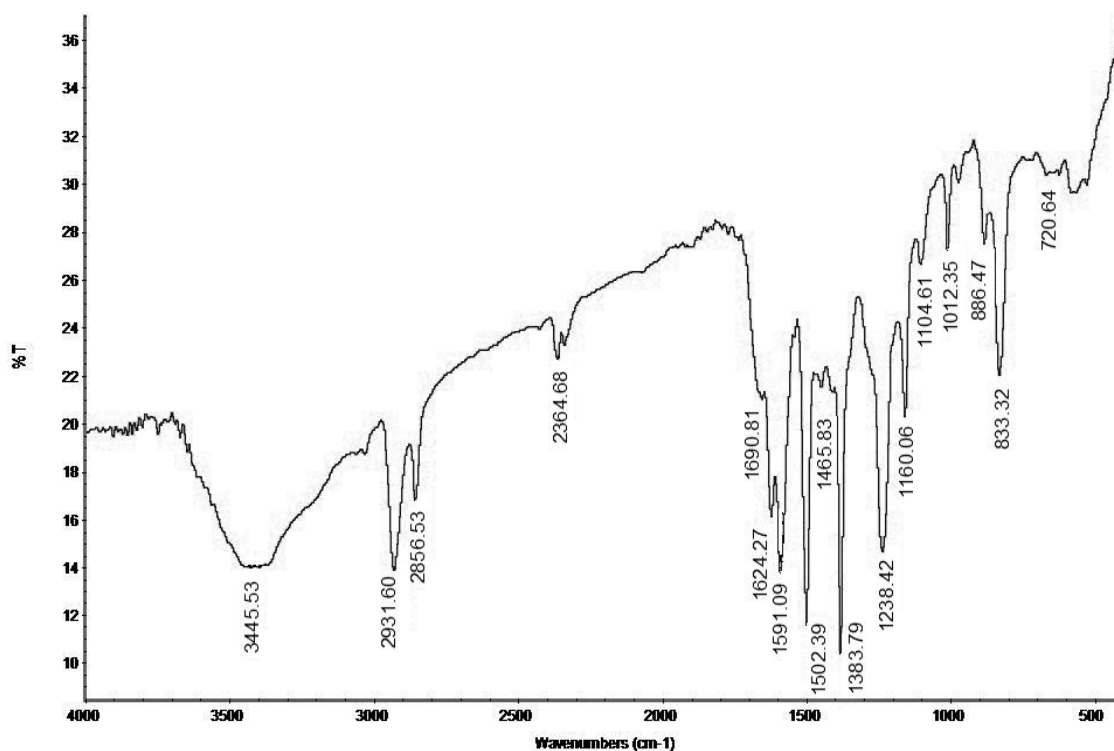


Fig. 3.28: IR (KBr) spectrum of polySchiff base (SB4HCy-SB4ClCy)



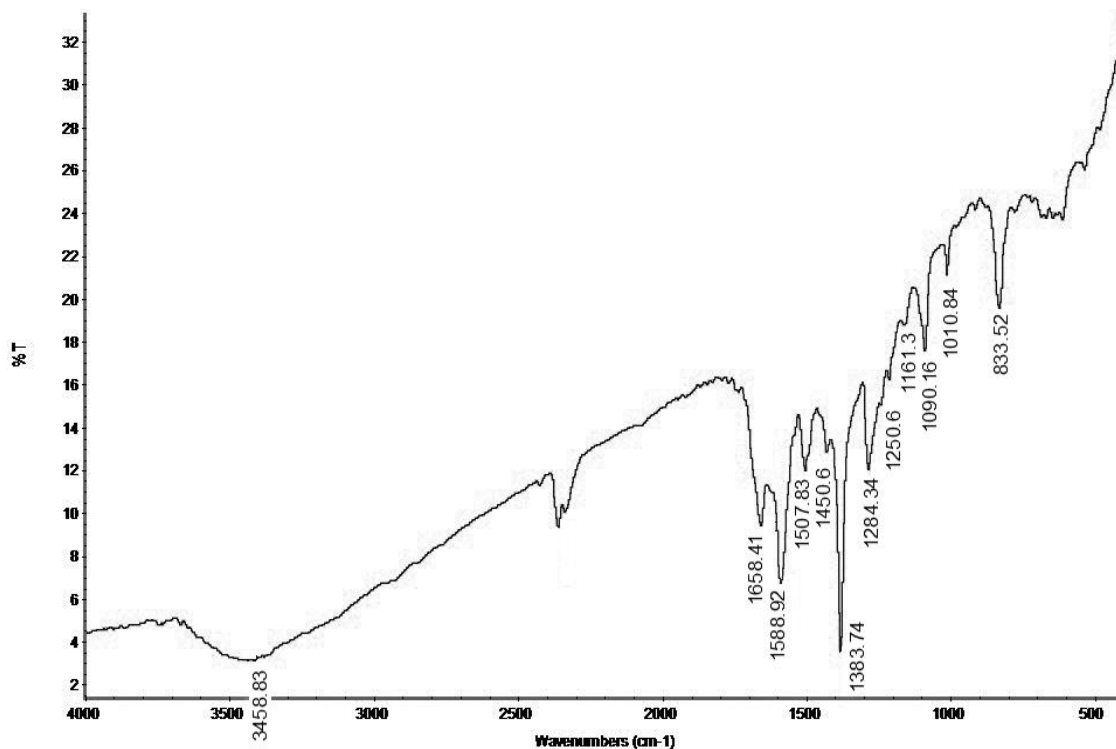


Fig. 3.29: IR (KBr) spectrum of polySchiff base (SB4HM-SB4CIM)

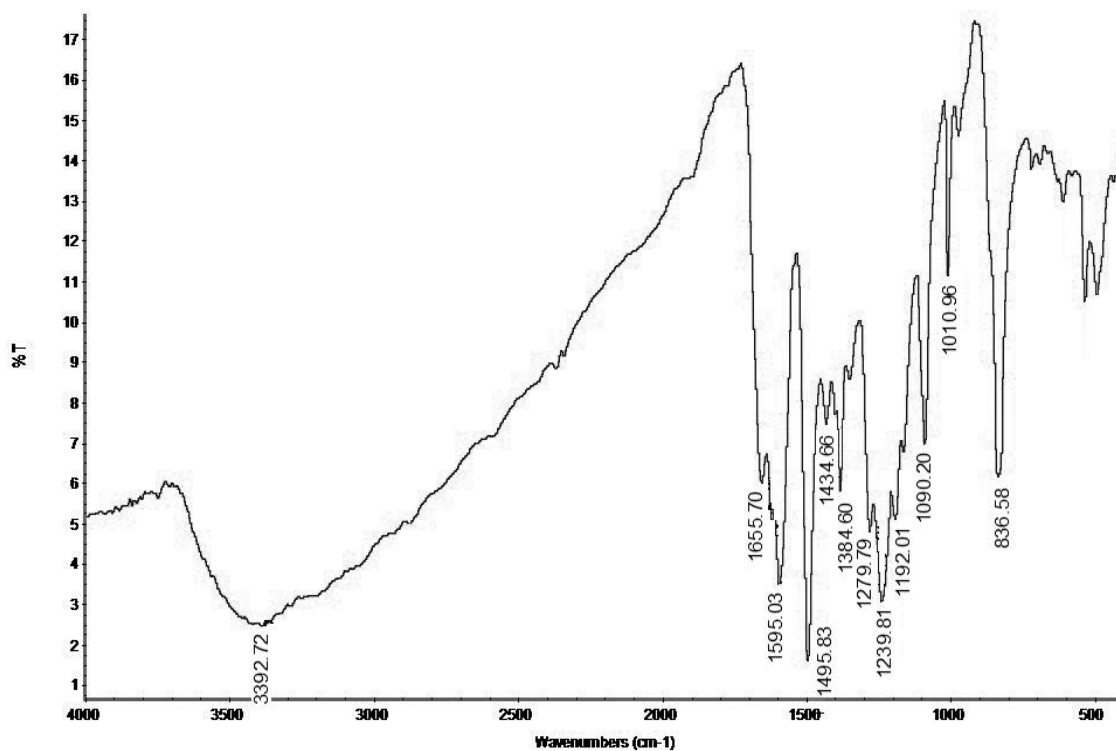


Fig. 3.30: IR (KBr) spectrum of polySchiff base (SB4HE-SB4CIE)

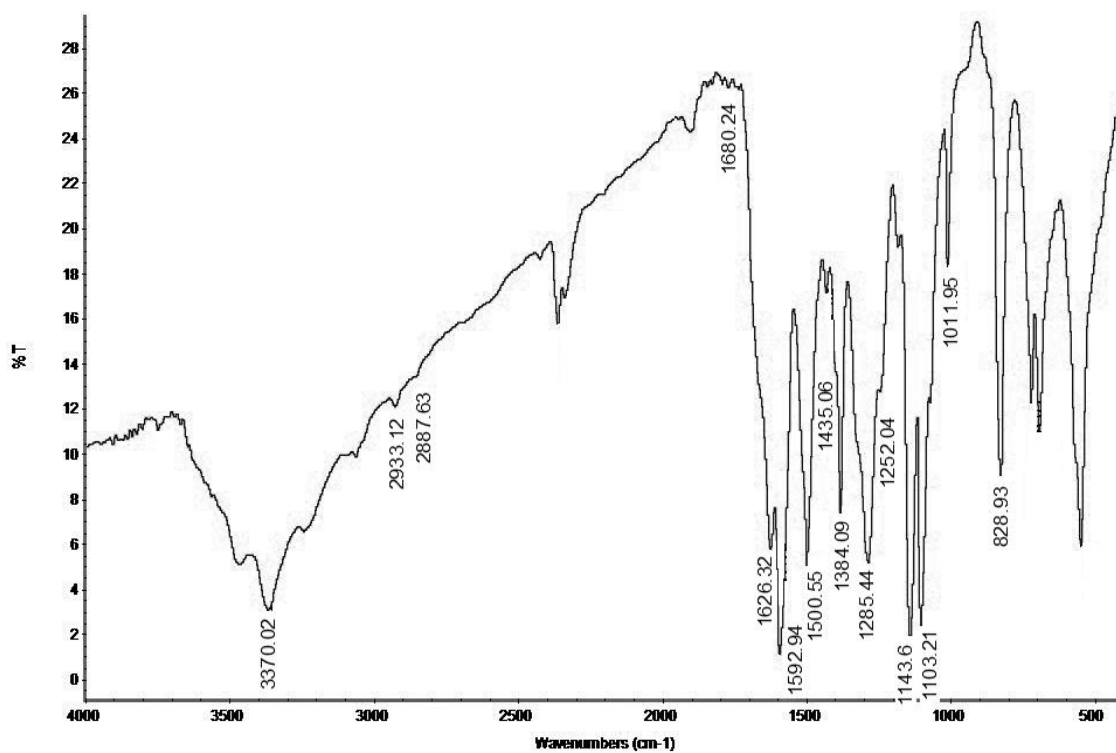


Fig. 3.31: IR (KBr) spectrum of polySchiff base (SB4HS-SB4ClS)

**Table-3.14: The characteristic IR absorption frequencies of PolySchiff base with halide Schiff base.**

Types	Group vibration mode	Observed IR frequencies, (cm <sup>-1</sup> )				Expected frequencies, (cm <sup>-1</sup> )
		SB4HCy - SB4CICy	SB4HM - SB4CIM	SB4HE - SB4CIE	SB4HS - SB4CIS	
Alkane -CH <sub>2</sub> -	C-H (v <sub>as</sub> )	2931.6	-	-	2933.1	2975-2950
	C-H (v <sub>s</sub> )	2856.5	-	-	2887.6	2880-2860
	C-H def.	-	1450.6	1434.7	1435	1470-1435
	Twisting & Wagging	1238.4	1250.6	1239.8	1252	~1250
	Skeletal CH <sub>2</sub>	-	-	-	-	750-720
Aromatic	C=C str.	1624.3	1588.9	1595.0	1592.9	1600-1400
		1591.1	1507.8	1495.8	1500.6	
		1502.4	1450.6		1435.1	
	C-H (i.p.d.)	1238.4		1239.8		1258±11, 1175±6, 1117±7, 1013±5 (1,4 sub.)
1160.1			1192.0	1143.6		
1104.6		1250.6	1090.2	1103.2		
1090.2		1010.8	1011.0	1012.0		
C-H (o.p.d.)	833.3	833.5	836.6	828.9	817±15 (1,4 sub.)	
Schiff base	N = CH str.	1690.8	1658.4	1655.7	1626.3	1690-1635
	C – N vib.	1383.8	1383.7	1384.6	1384.1	1360-1310
Ether	C-O-C	1238.4	1250.6	1239.8	1252.0	1275-1200
-OH	O-H str.	3445.5	3458.8	3392.7	3370.0	3400-3200
	O-H def.	-	1284.3	1279.8	1285.4	1350-1260
	C-O-H def.	1104.6	1090.2	1090.2	1103.2	1120-1030
Halogen	C-Cl	-	-	-	-	800-600
Sulfone	S=O (v <sub>as</sub> )	-	-	-	1384.1	1350-1300
	S=O (v <sub>s</sub> )	-	-	-	1143.6	1160-1120

IR spectra of polySchiff bases (TDADPCy, TDADPM, TDADPE and TDADPS) are presented in Figs. 3.32-3.35 and absorption peaks in Table-3.15. Observed characteristic frequencies for TDADPCy are 1700 and 1624 (N=CH str.); for TDADPM: 1623.1 (N=CH str.); for TDADPE: 1697 and 1619 (N=CH str.); and for TDADPS: 1660 and 1630 (N=CH str.) besides normal modes of vibrations of alicyclic, aliphatic and aromatic groups. Thus, IR spectral study supported the structure of forgoing compounds.

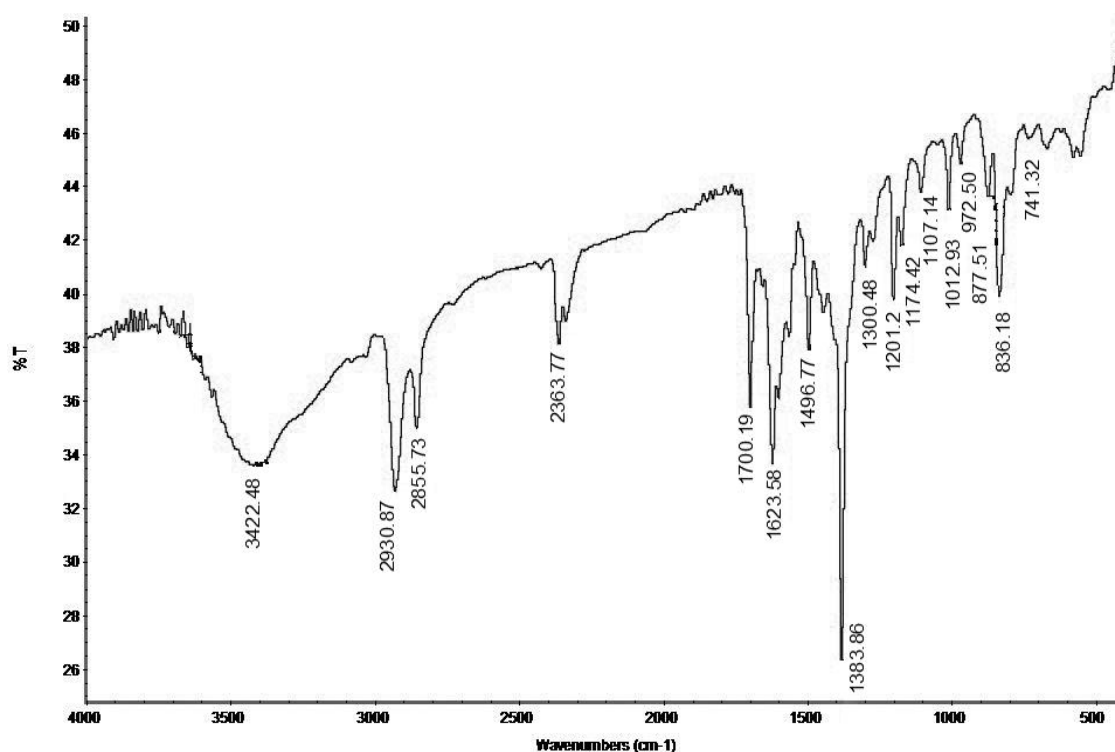


Fig. 3.32: IR (KBr) spectrum of polySchiff base (TDADPCy)

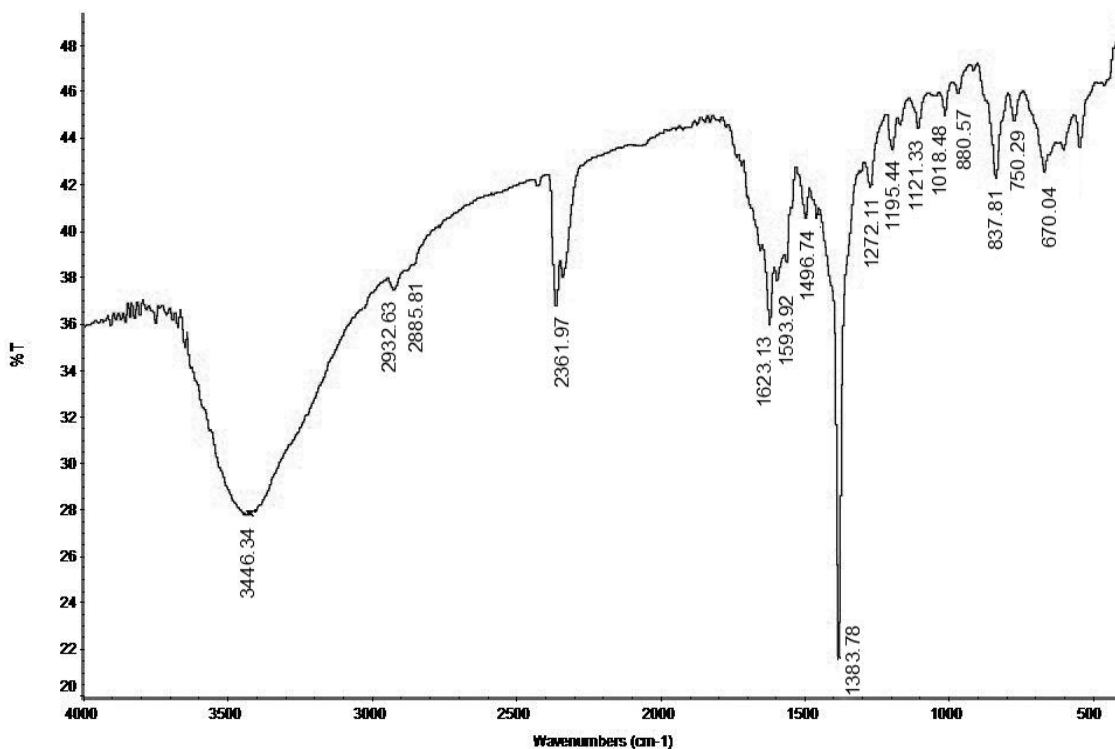


Fig. 3.33: IR (KBr) spectrum of PolySchiff base (TDADPM)

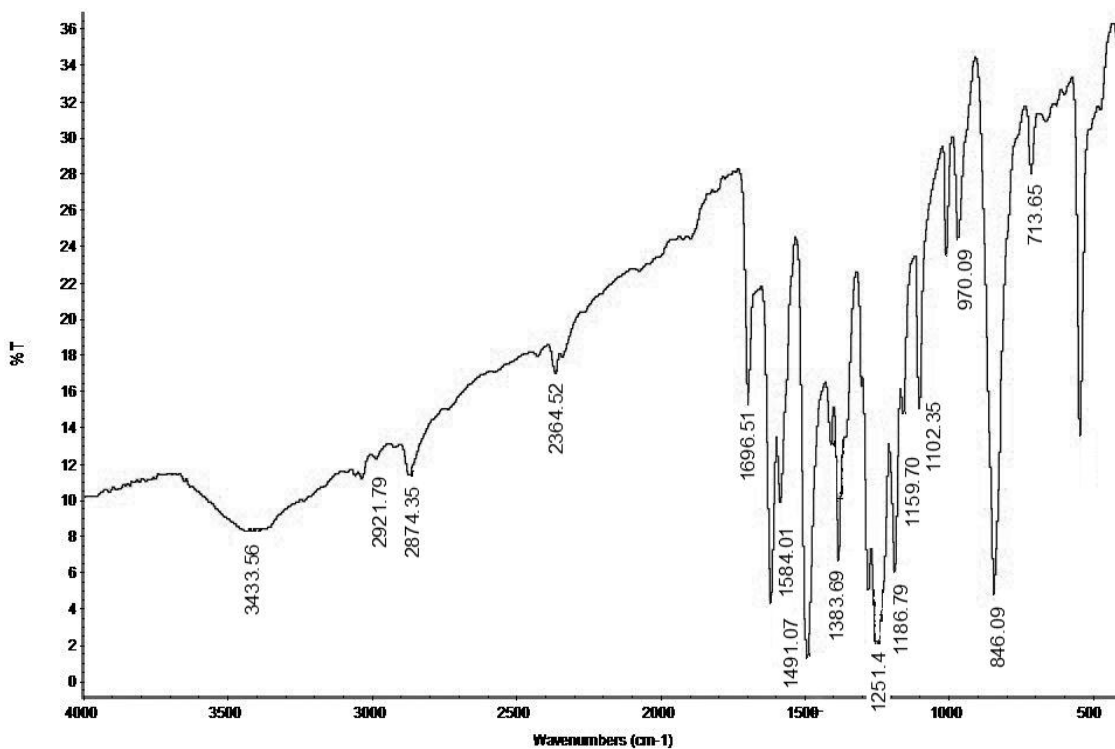


Fig. 3.34: IR (KBr) spectrum of PolySchiff base (TDADPE)

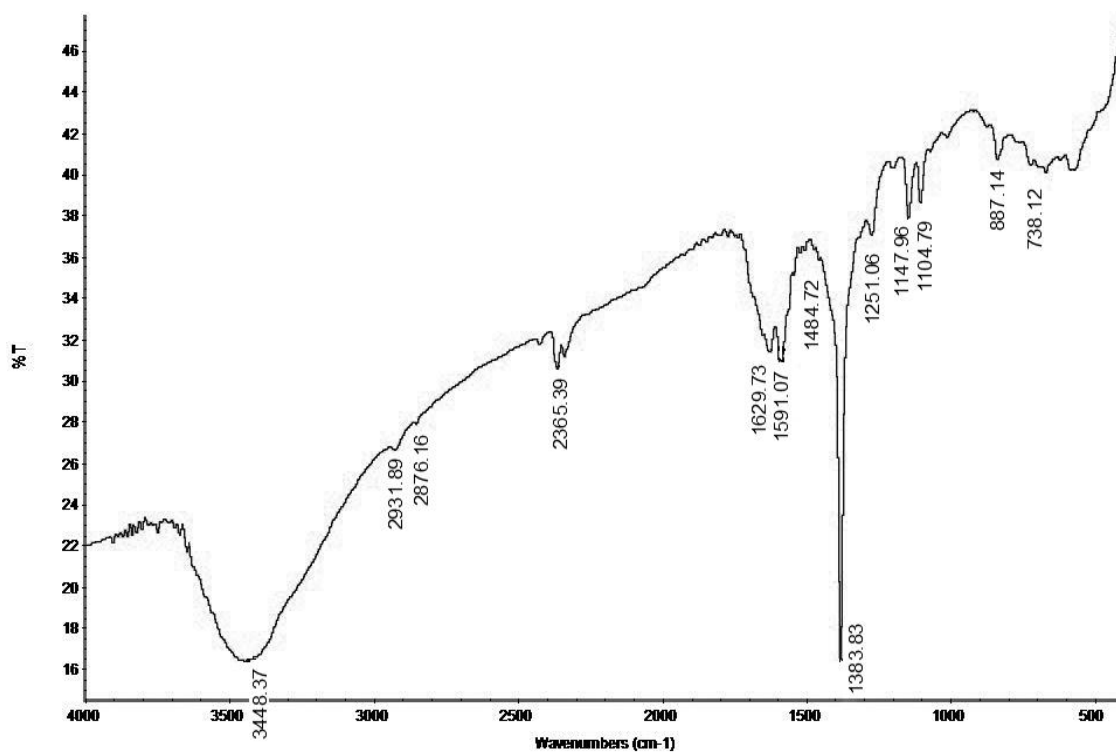


Fig. 3.35: IR (KBr) spectrum of PolySchiff base (TDADPS)

**Table-3.15: The characteristic IR absorption frequencies of PolySchiff base with terephthaldehyde.**

Types	Group vibration mode	Observed IR frequencies, (cm <sup>-1</sup> )				Expected frequencies, (cm <sup>-1</sup> )
		TDADPCy	TDADPM	TDADPE	TDADPS	
Alkane -CH <sub>2</sub> -	C-H (v <sub>as</sub> )	2930.9	2932.6	2921.8	2931.9	2975-2950
	C-H (v <sub>s</sub> )	2855.7	2885.8	2874.4	2876.2	2880-2860
	C-H def.	1496.8	1496.7	1412.6	-	1485-1445
	Twisting & Wagging	1250.4	1272.1	1278.6	1251.1	~1250
Arom- atic	C=C str.	1496.8	1593.9 1496.7	1584.0 1491.1 1412.6	1591.1	1600-1400
	C-H (i.p.d.)	1250.4 1174.4 1107.1 1012.9	1272.1 1195.4 1121.3 1018.5	1278.6 1251.4 1186.8 1102.4 1009.2	1251.1 1148.0 1104.8	1258±11, 1175±6, 1117±7, 1013±5 (1,4 sub.)
	C-H (o.p.d.)	836.2	837.8	846.1	845.3	817±15 (1,4 sub.)
Schiff base	N = CH str.	1700.2 1623.6	1623.1	1696.5 1619.0	1659.7 1629.7	1690-1635
	C – N vib.	1383.9	1383.8	1383.7	1383.8	1360-1310
Sulfone	S=O (v <sub>as</sub> )	-	-	-	-	1350-1300
	S=O (v <sub>s</sub> )	-	-	-	1148.0	1160-1120

**[B] NMR spectral characterization**

Some nuclei spin about their axes in a manner to that electrons spin. In the presence of an externally applied magnetic field, a spinning nucleus can only assume a limited number of stable orientations. Nuclear magnetic resonance occurs, when a spinning nucleus in a lower energetic orientation in a magnetic field absorbs sufficient electromagnetic radiation to be excited to a higher energetic orientation. The excitation energy varies with the type and environment of the nucleus. NMR spectroscopy can be used for the quantitative chemical analysis [1-5].

NMR spectroscopy consists of measuring the energy that is required to change a spinning nucleus from a stable orientation to a less stable orientation in the magnetic field. Different spinning nuclei absorb at different frequencies of radiation to change their orientations. The frequencies at which absorption occur can be used for qualitative analysis. The decrease in intensity of incident radiation owing to absorption during a particular transition is related to the different spinning nuclei at different frequencies in the magnetic field.

The decrease in intensity of incident radiation owing to absorption during a particular transition is related to the number of nuclei in the sample that undergo the transition and can be used for quantitative analysis. NMR spectrometer was invented in 1945 by Felix Bloch (Stanford University) and Edward Purcell. They shared the Nobel Prize (1952) in Physics for their work.

- 
1. V. M. Parikh, "Absorption Spectroscopy of Organic Molecules", Addison Wesley Pub., p. 243-258, (1978).
  2. D. L. Pavia, G. M. Lampman and G. S. Kriz, "Introduction to Spectroscopy", Saunders Publisher, Philadelphia, p. 46, (1979).
  3. R. M. Silverstein, G. C. Bassler and T. C. Morrill, "Spectrometric Identification of Organic Compounds", 6<sup>th</sup> Ed. John Willey and Sons, New York, (1996).
  4. C. N. R. Rao, "Chemical applications of infrared spectroscopy", Academic Press, New York, p. 317-333, (1963).
  5. D. W. Thomson and G. F. L. Ehlers, J Polym. Sci. Part- A-2, 3, 1051-1056, (1964).



### <sup>1</sup>HNMR spectral analysis of epoxy resins

<sup>1</sup>HNMR spectra of ESB4HCy, ESB4HM and ESB4HE were scanned on a Bruker AVANCE II 400 MHz spectrometer by using CDCl<sub>3</sub>/DMSO-d<sub>6</sub> as a solvent and TMS as an internal standard. <sup>1</sup>HNMR spectra of ESB4HCy, ESB4HM and ESB4HE are presented in Figs. 3.36 to 3.38, respectively. Chemical shifts (ppm) and multiplicities of different types of protons of the resins are assigned in corresponding spectrum itself. Residual chloroform is appeared at about 7.25 ppm.

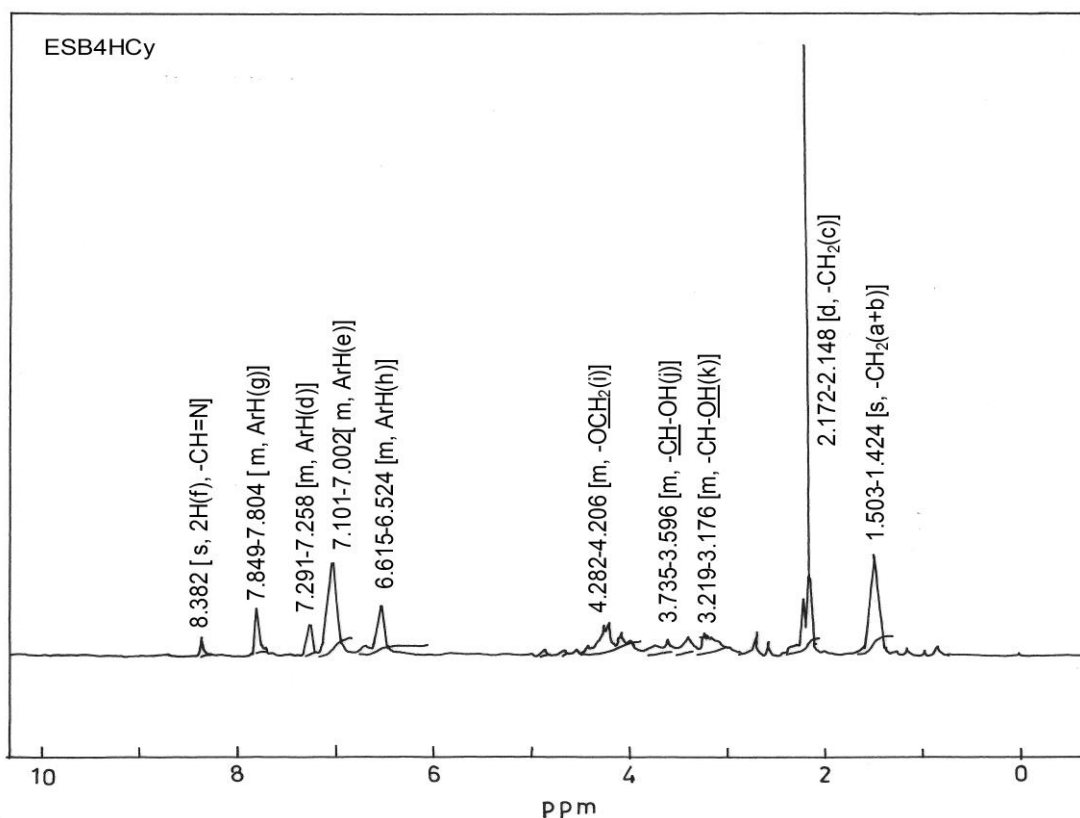
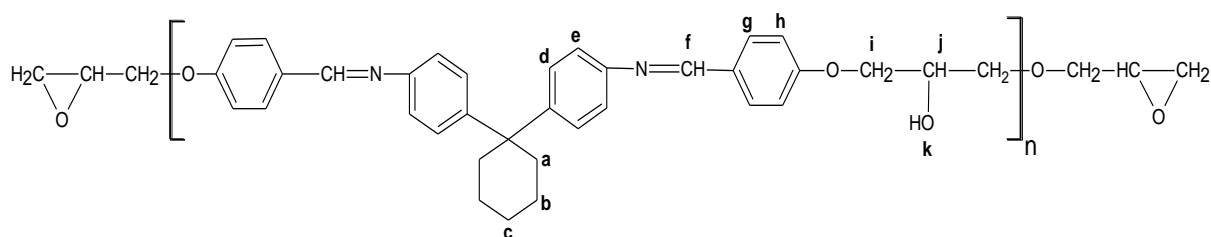


Fig. 3.36: NMR (400MHZ) spectrum of epoxy (ESB4HCy) in CDCl<sub>3</sub>

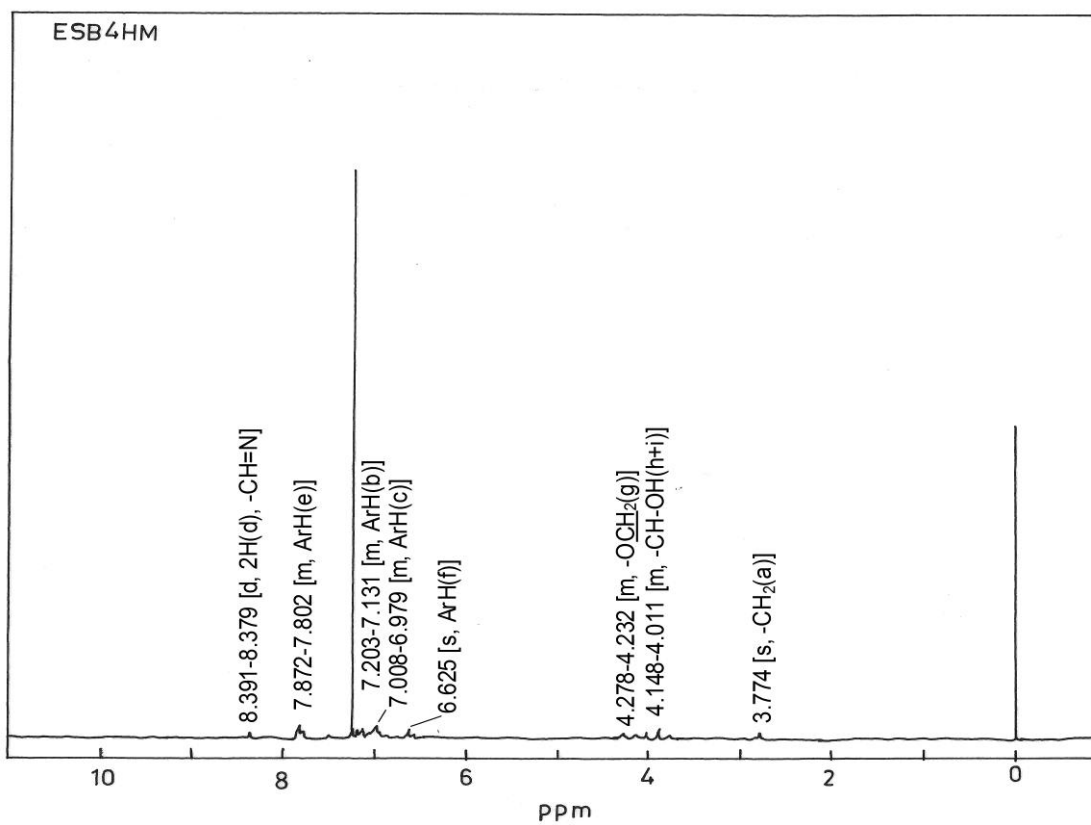
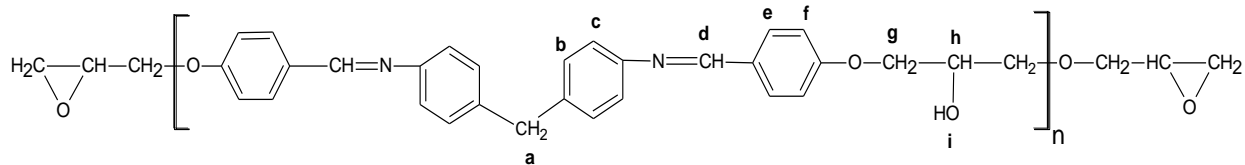


Fig. 3.37: NMR (400MHZ) spectrum of epoxy (ESB4HM) in DMSO-d6

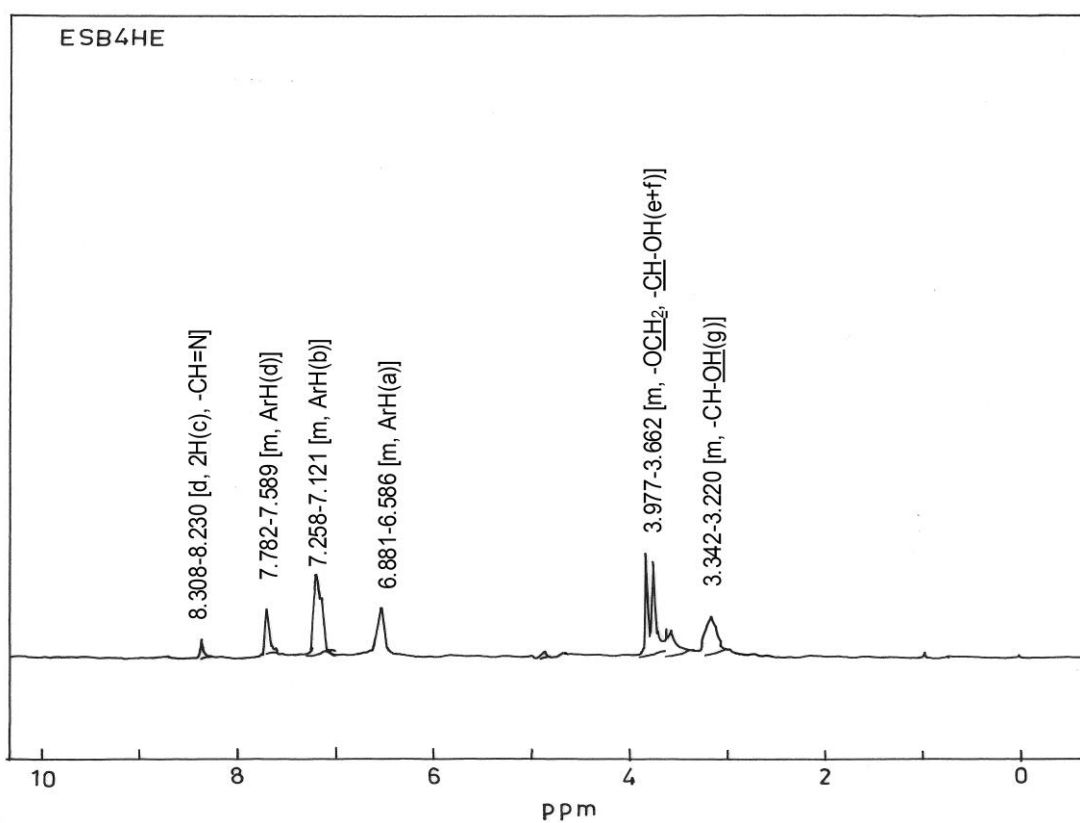
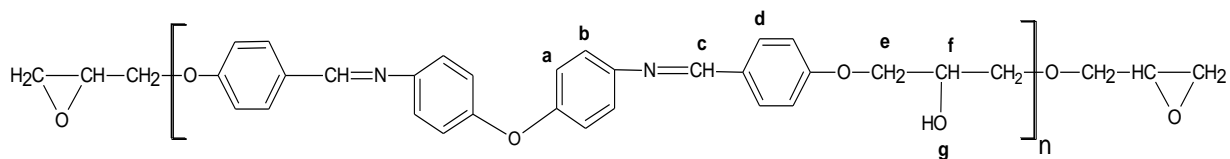


Fig. 3.38: NMR (400MHZ) spectrum of epoxy (ESB4HE) in DMSO-d<sub>6</sub>

### <sup>1</sup>HNMR spectral analysis of bisbenzoxazines

<sup>1</sup>HNMR spectra of BSB4HCy, BSB4HM, BSB4HE and BSB4HS are presented in Figs. 3.39 to 3.42, respectively. Chemical shifts (ppm) and multiplicity of different types of bisbenzoxazine protons are assigned in corresponding spectrum itself. Residual chloroform is appeared at about 7.25 ppm and overlapped with aromatic protons.

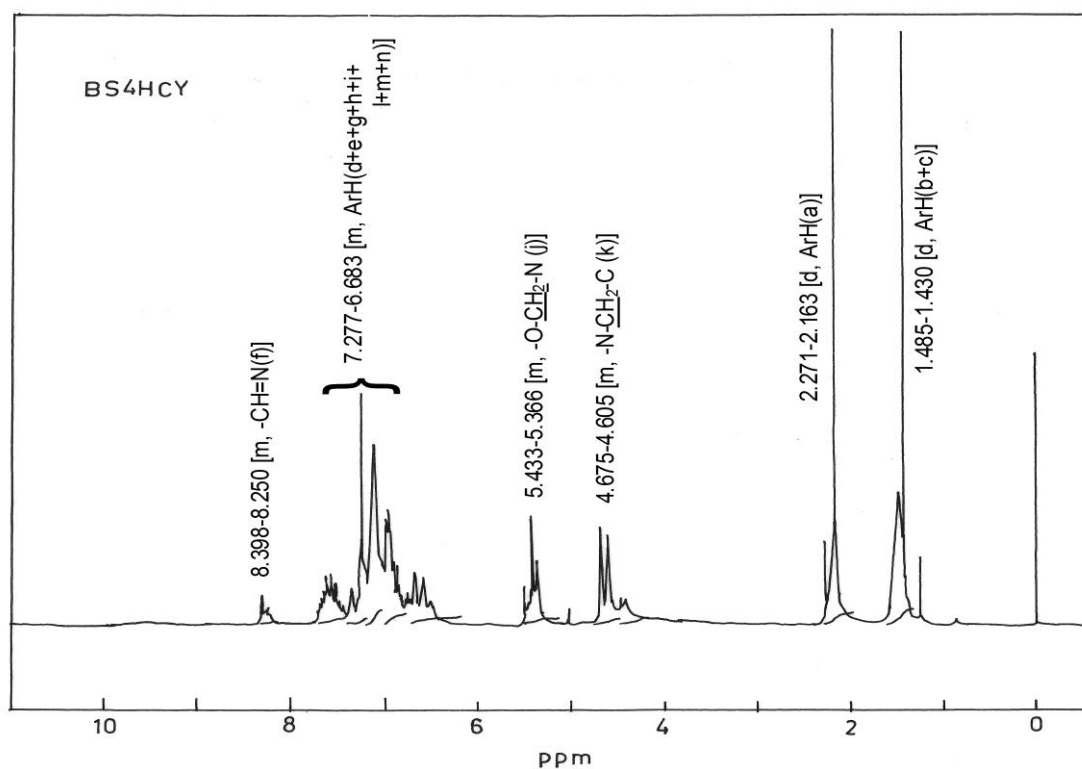
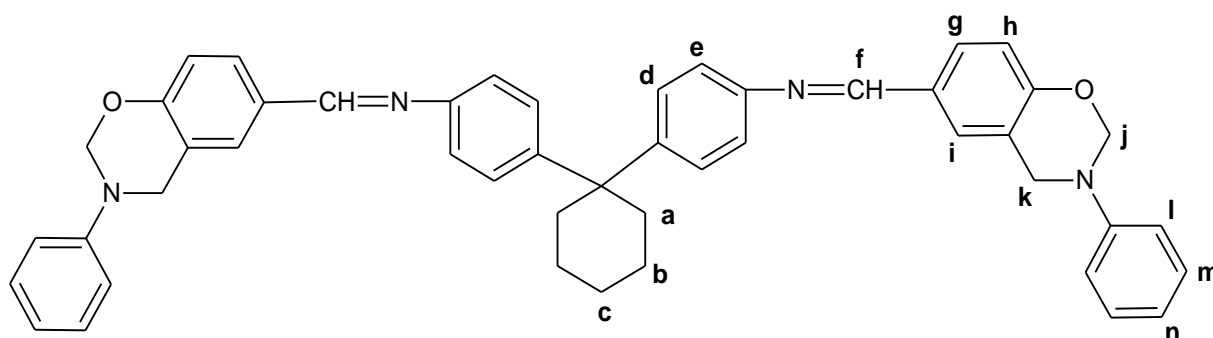


Fig. 3.39: NMR (400MHZ) spectrum of bisbenzoxazine (BSB4HCy) in CDCl<sub>3</sub>

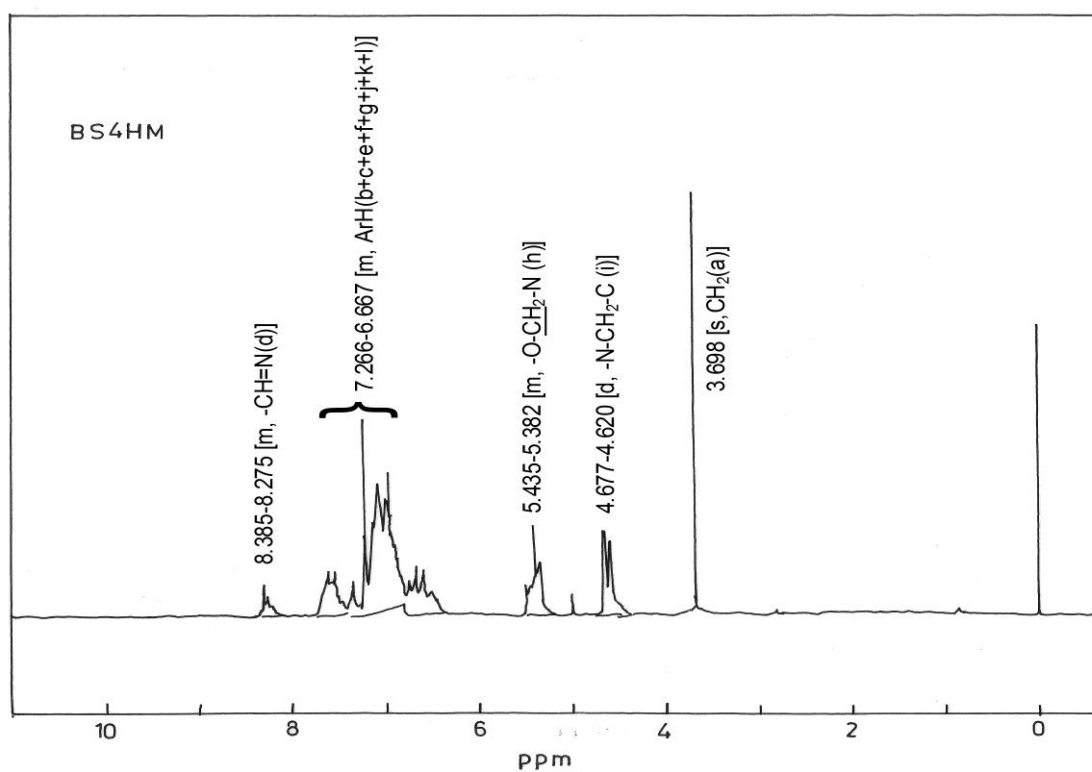
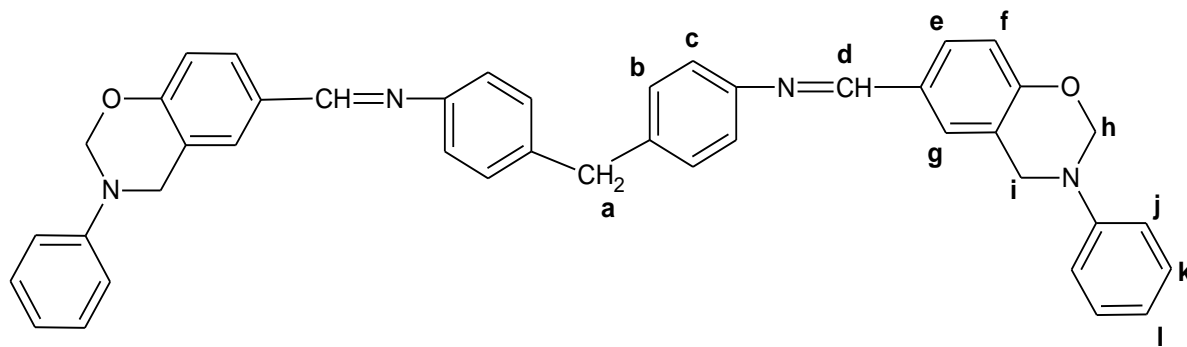


Fig. 3.40: NMR (400MHZ) spectrum of bisbenzoxazine (BSB4HM) in CDCl<sub>3</sub>

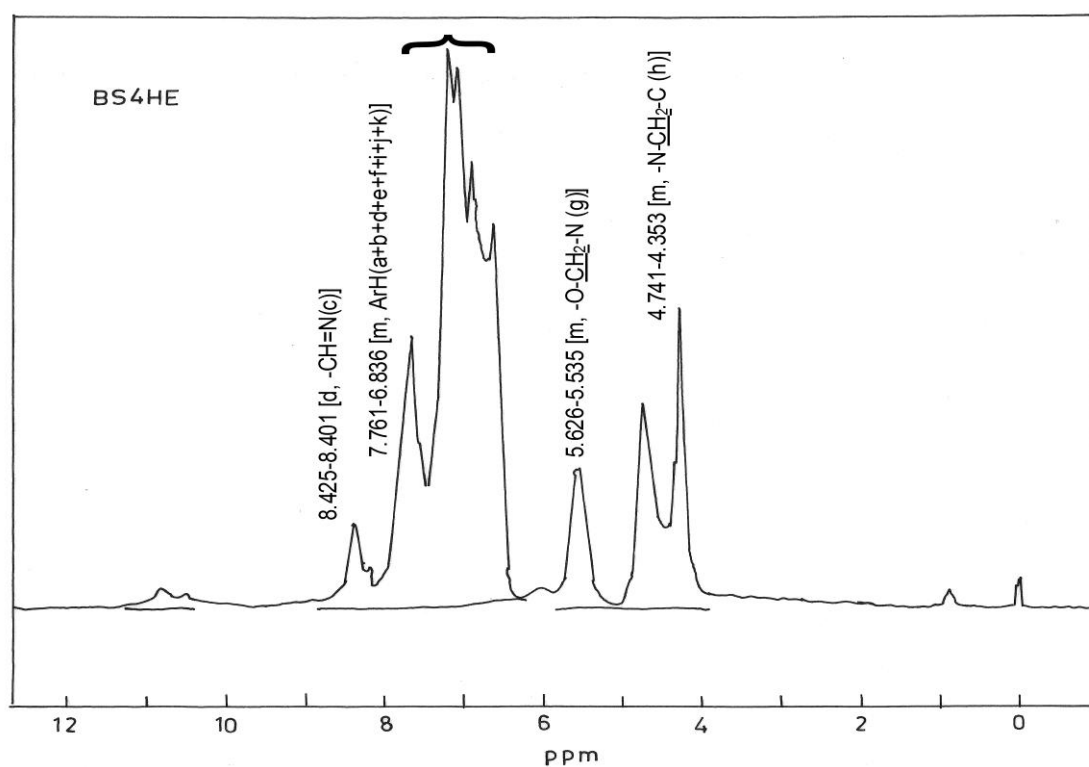
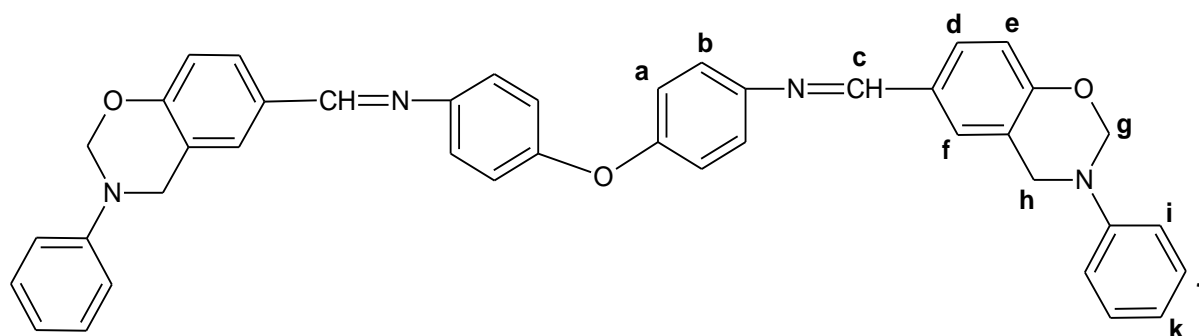


Fig. 3.41: NMR (400MHz) spectrum of bisbenzoxazine (BSB4HE) in DMSO-d<sub>6</sub>

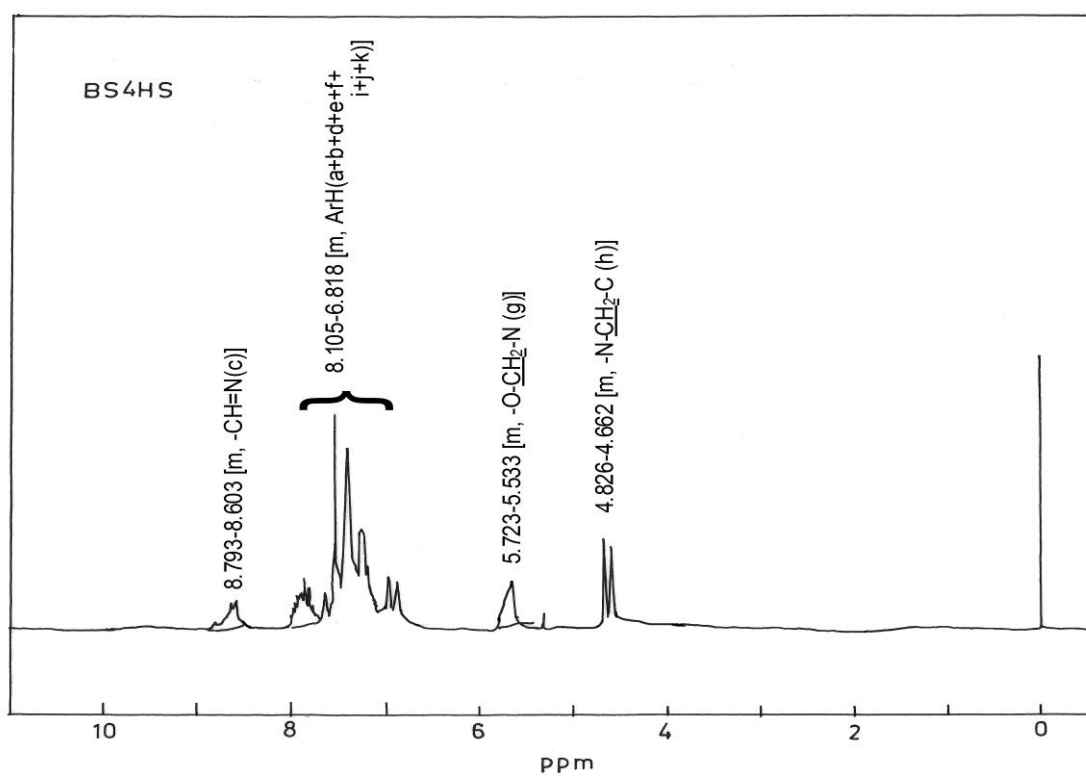
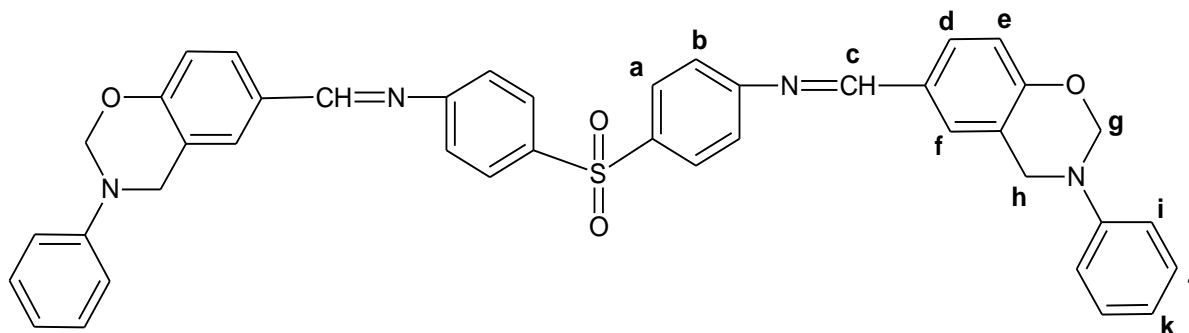


Fig. 3.42: NMR (400MHZ) spectrum of bisbenzoxazine (BSB4HS) in CDCl<sub>3</sub>

### $^1\text{H}$ NMR spectral analysis of polySchiff bases

$^1\text{H}$ NMR spectra of polySchiff bases: SB4HCy-DCDPS, SB4HM-DCDPS, SB4HE-DCDPS and SB4HS-DCDPS are presented in Figs. 3.43 to 3.46, respectively. Chemical shifts (ppm) and multiplicities of different types of polySchiff bases are assigned in corresponding spectrum itself.

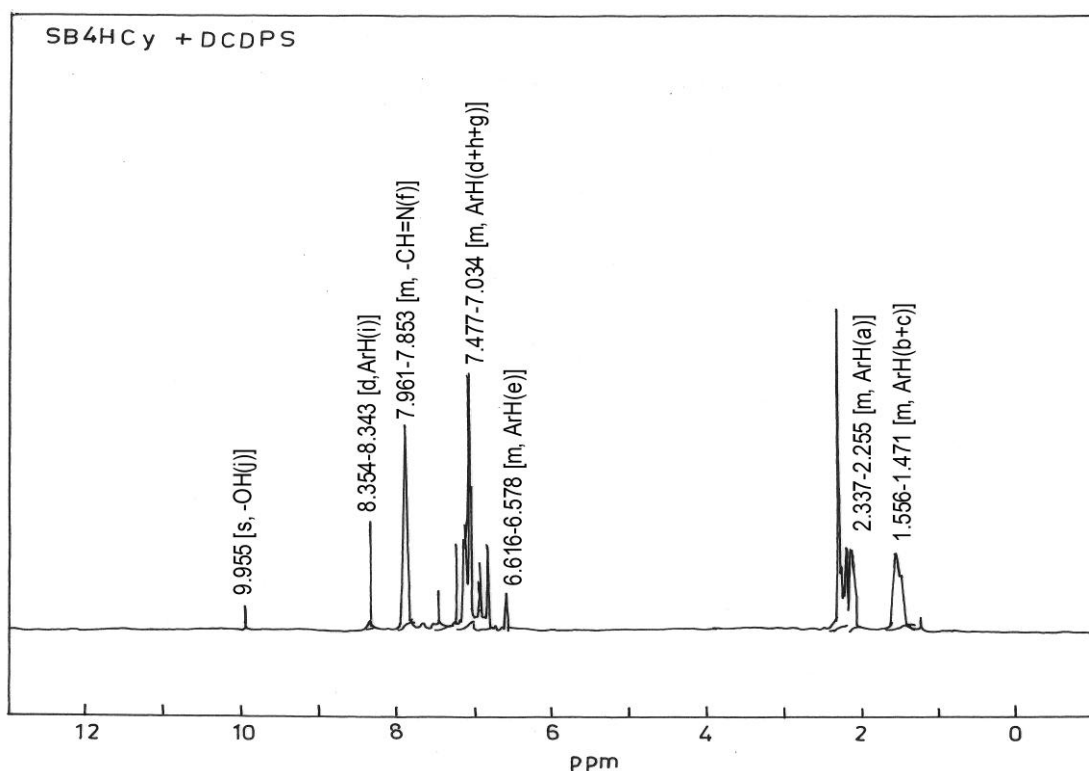
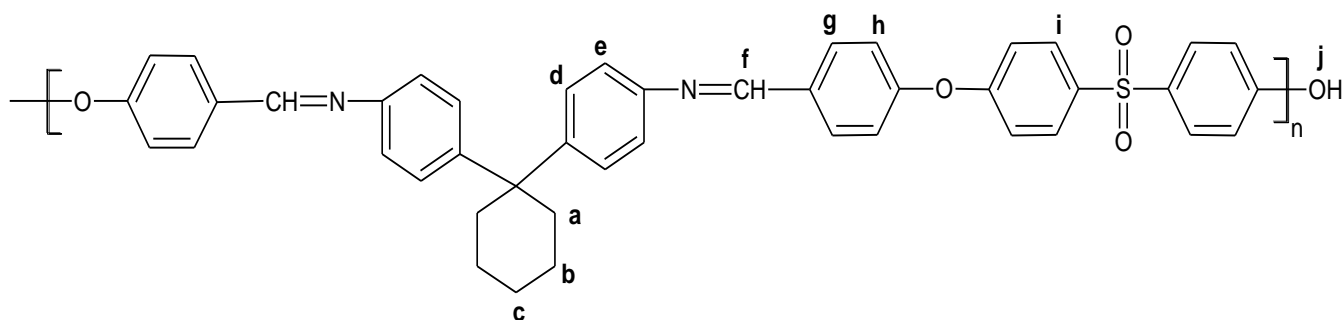


Fig. 3.43: NMR (400MHZ) spectrum of PolySchiff bases(SB4HCy-DCDPS) in DMSO-d<sub>6</sub>



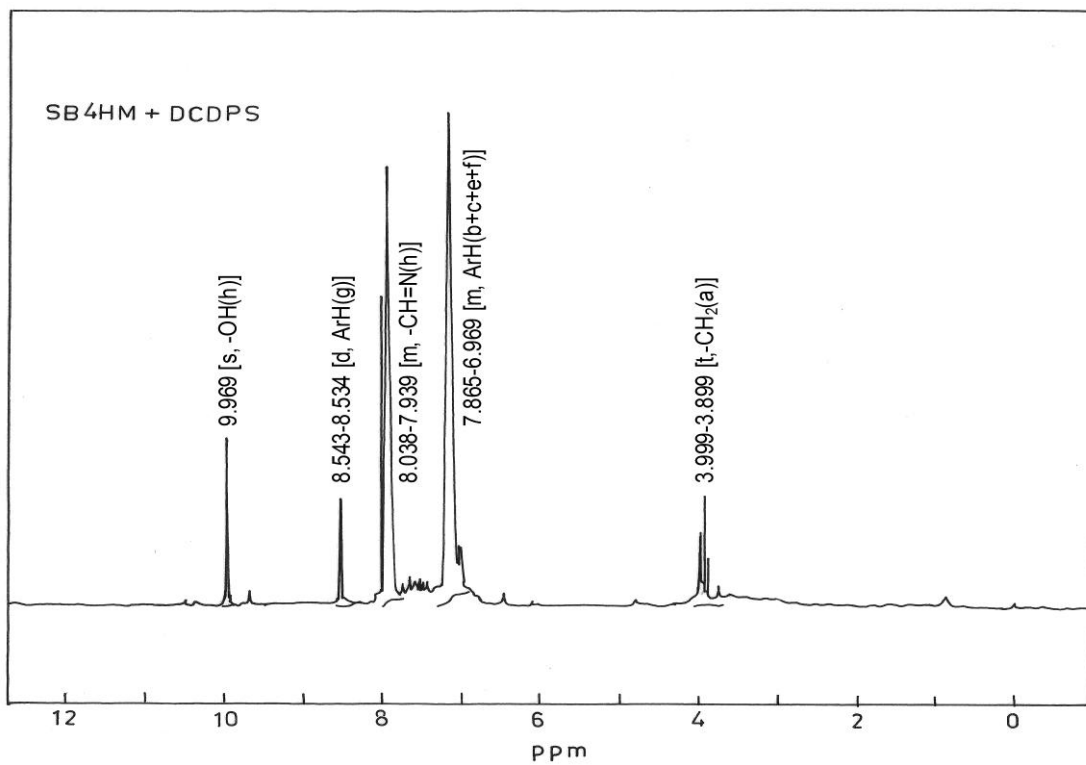
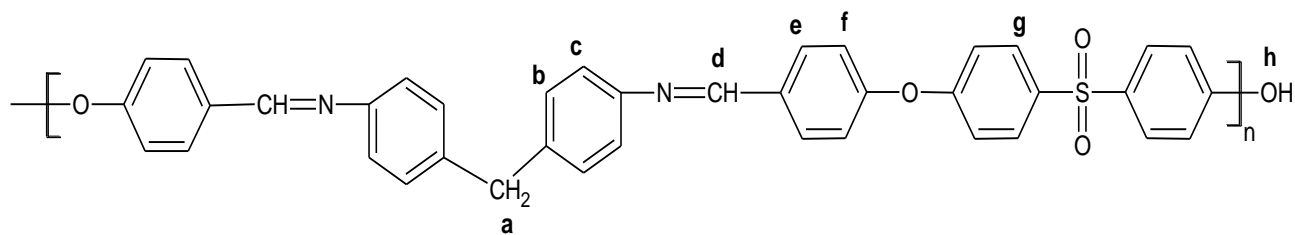
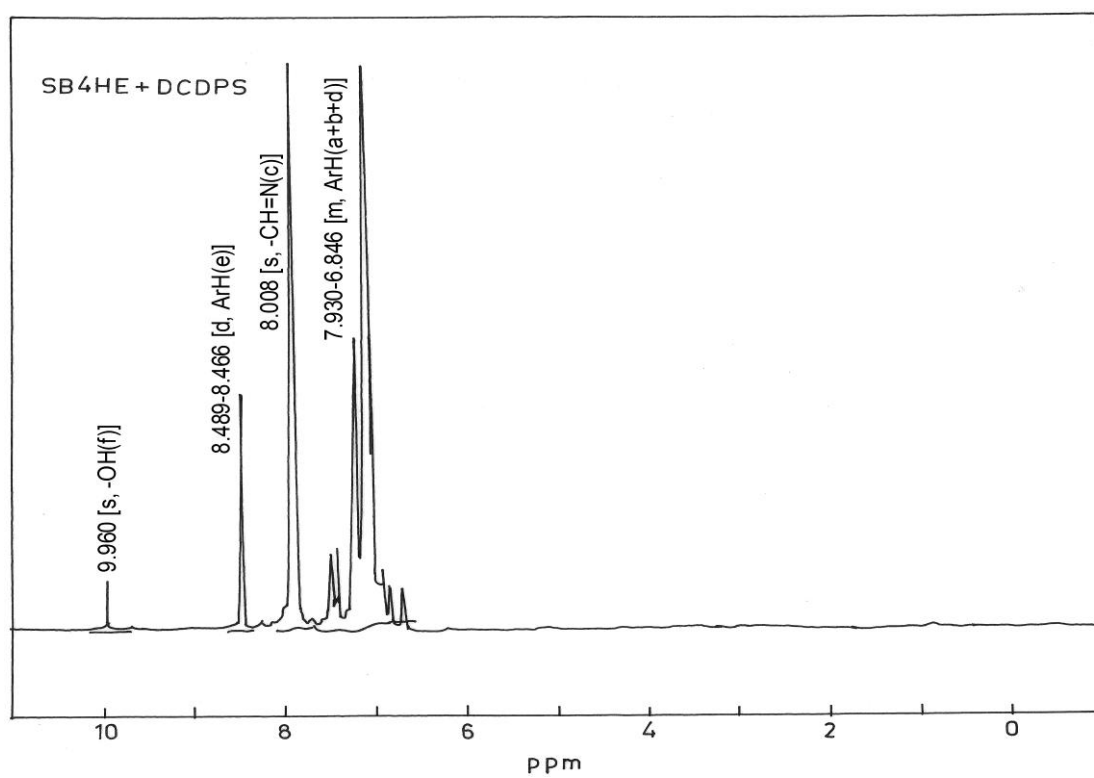
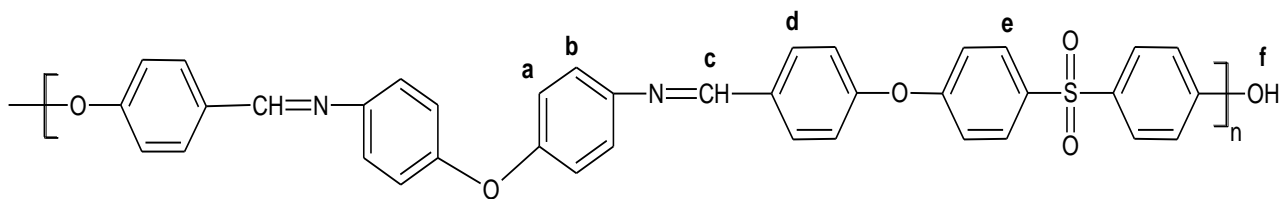
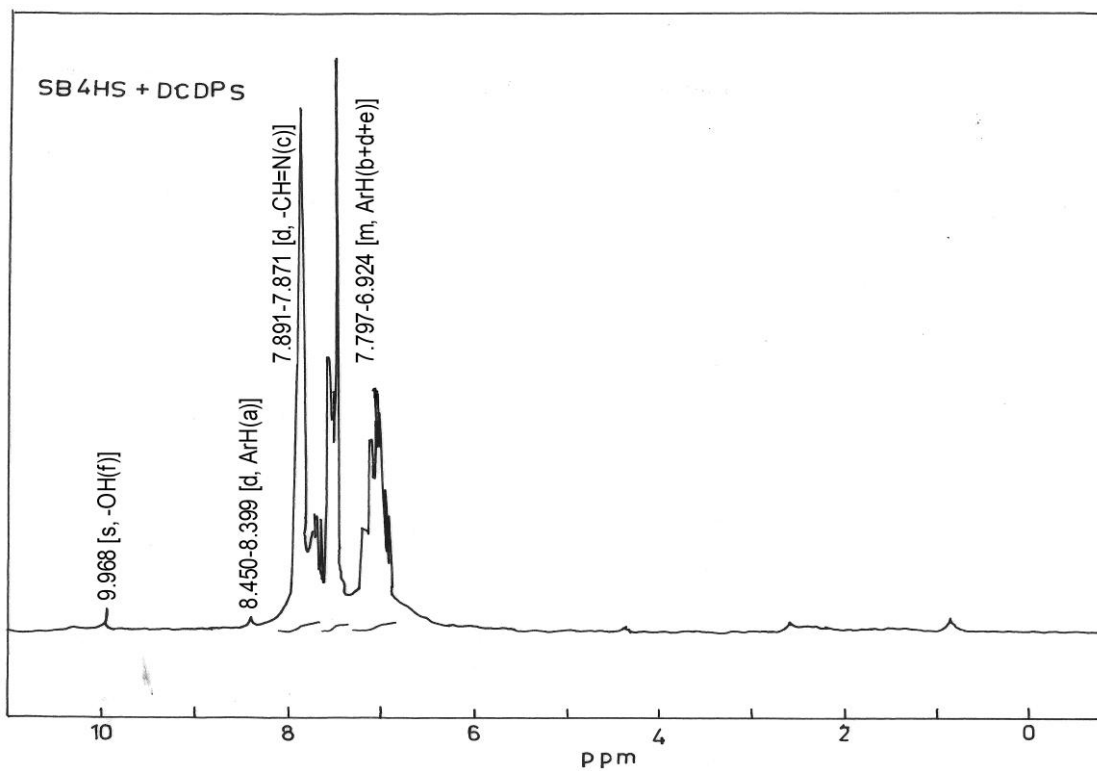
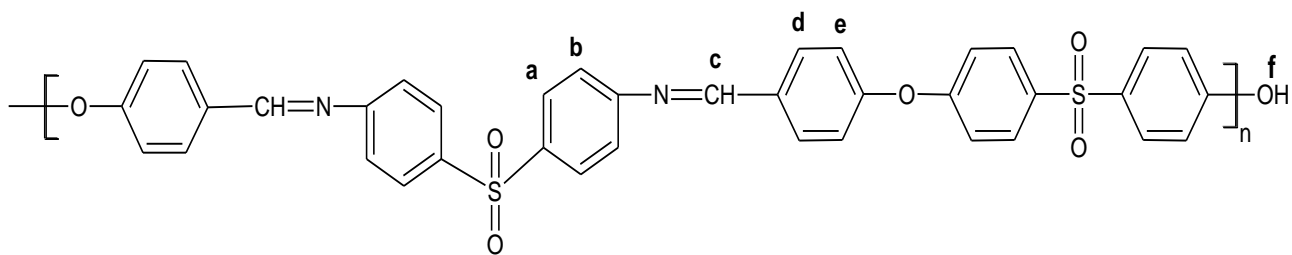


Fig. 3.44: NMR (400MHZ) spectrum of polySchiff base (SB4HM-DCDPS) in DMSO-d<sub>6</sub>



**Fig. 3.45: NMR (400MHz) spectrum of polySchiff base (SB4HE-DCDPS) in DMSO-d<sub>6</sub>**



**Fig. 3.46: NMR (400MHZ) spectrum of polySchiff base (SB4HS-DCDPS) in DMSO-d<sub>6</sub>**

### Section-III: Thermal analysis

Synthetic polymers are highly useful in the rapidly developing fields such as space exploration, terrestrial transportation, modern communications, energy saving, environmental protection, public health, microbiology, medicine, etc. A major driving force for the growth and interest in the studies of thermally stable polymers is attributed to their extensive applications in aeronautics and in supersonic appliances. Considerable research work has been undertaken [1] on the thermal stability of polymers to derive the polymers, which may be useful for high temperature applications.

Data on thermal characteristics are important tool for evaluating product performance as well as processability of polymeric materials. Thermal properties like specific heat and thermal conductivity are the determining factors in selection of processing parameters as well as designing the machines and tools for shaping of plastics. The data are also useful in screening the materials for specific applications.

On practical side, thermal analysis of polymers not only explains the behavior of polymers under conditions of high temperatures but also helps in selecting the right kind of material for the specific uses where high temperatures are encountered. It also suggests the design and synthesis of new materials for specific requirements in polymer technology such as high temperature resistant synthetic and natural fibers, transportation industries, electrical and electronic instruments, appliances, etc.

Kinetic study of thermal decomposition of epoxy resins containing flame retardant components was reported by Wang and Shi [2].

Hyperbranched polyphosphate ester (HPPE) and phenolic melamine (PM) were blended in different ratios with a commercial epoxy resin to obtain a series of flame retardant resins. The thermal decomposition mechanism of cured ester was studied by thermogravimetric analysis and in situ Fourier-transform infrared spectroscopy. The degradation behaviors of epoxy resins

- 
1. R. T. Conley, "Thermal stability of polymers", Marcell Dekker, New York, 1973.
  2. Q. Wang and W. Shi, "Kinetics study of thermal decomposition of epoxy resins containing flame retardant components", *Polym. Deg. and Stab.*, 91, 1747-1754, 2006.

containing various flame retardant components were found to be greatly changed.

Laza et al. [3] have studied the dynamic-mechanical properties of different mixtures formed by an epoxy resin (DGEBA type) and a phenolic resin (resole type) cured by triethylene tetramine and/or p-toluene sulphonic acid at different concentrations by means of dynamic mechanical thermal analysis (DMTA). All samples were cured by pressing at 90°C during 6h. The mechanical studies were performed between -100 to 300 °C at a heating rate of 2°C/min.

Thermal degradation and decomposition products of electronic boards containing BFRs have been studied by the Barontini et al. [4]. They have investigated the thermal degradation behavior of electronic boards manufactured using tetrabromobispheno-A and diglycidyl ether of bisphenol-A epoxy resins. Qualitative and quantitative information was obtained on the products formed in the thermal degradation process, and the bromine distribution in the different product fractions was determined. The more important decomposition products included hydrogen bromide, phenol, polybrominated phenols, and polybrominated bisphenol-A species.

Wang et al. [5] have reported the cure study of addition-cure-type and condensation-addition-type phenolic resins by the incorporation of propargyl and methylol groups on to novolac backbone, a series of addition-curable phenolic resins and condensation-addition dual-cure type phenolic resins (novolac modified by propargyl groups referred as PN, and novolac modified by propargyl and methylol groups simultaneously referred as MPN) were synthesized.

- 
3. J. M. Laza, J. L. Vilas, M. T. Garay, M. Rodríguez and L. M. León, "Dynamic mechanical properties of epoxy-phenolic mixtures", *J. Polym. Sci., Part B: Polym. Physics*, 43, 1548-1557, 2005.
  4. F. Barontini, K. Marsanich, L. Petarca and V. Cozzani, "Thermal degradation and decomposition products of electronic boards containing BFRs", *Ind. and Eng. Chem. Res.*, 44, 4186-4193, 2005.

The processing characteristics, thermal cure and catalytic cure behavior for both resins were investigated mainly by means of viscosity measurements and non-isothermal differential scanning calorimetry (DSC). The effect of propargyl and methylol content of PN and MPN, the molecular weight and the configuration of the parent novolac, on the processing and cure behavior was studied in details. Processing parameters and curing kinetic parameters were obtained. Both resins exhibit excellent processing properties. Thermal cure of PN resins possessed one cure mechanism and that of MPN resins possessed two cure mechanisms according to DSC analysis. The dual-cure-type mechanism made MPN resins superior to PN resins in terms of a mild and controllable cure process. Compared with thermal cure, catalytic cure of PN resins showed lower initiation temperature and cure temperature by about 60 °C. These novel resins have a bright prospect of application as matrix for thermal-structural composite materials.

Nair et al. [6] have reported the thermal characteristics of addition-cure phenolic resins. The thermal and pyrolysis characteristics of four different types of addition-cure phenolic resins were compared as a function of their structure. Whereas the propargyl ether resins and phenyl azo functional phenolics underwent easy curing, the phenyl ethynyl and maleimide-functional required higher thermal activation to achieve cure. All addition-cure phenolics exhibited improved thermal stability and char-yielding properties in comparison to conventional phenolic resole resin. The maleimide-functional resins exhibited lowest thermal stability and those crosslinked via ethynyl phenyl azo groups were the most thermally stable systems. Propargylated novolac and phenyl ethynyl functional phenolics showed intermediate thermal stability. The maximum char yield was also given by ethynyl phenyl azo system. Non-isothermal kinetic analysis of the degradation reaction implied that all the

- 
5. M. Wang, L. Wei and T. Zhao, "Cure study of addition-cure-type and condensation-addition type phenolic resins", *Eur. Polym. J.*, 41, 903-917, 2005.
  6. C. P. Reghunadhan Nair, R. L. Bindu and K. N. Ninan, "Thermal characteristics of addition-cure phenolic resins", *Poly. Deg. and Stab.*, 73, 251-263, 2001.

polymers undergo degradation in at least two steps, except in the case of ethynyl phenyl azo resin, which showed apparent single step degradation.

### **Effect of various operating parameters**

#### **1. Atmosphere**

The atmosphere associated with any thermal analysis, which is composed of gases that are introduced from outside and those are evolved from the samples. The presence or absence of such gases may have strong influence on the results. These gases may react with the sample or with each other and change the reaction mechanism or product composition. Inert atmosphere and vacuum will influence the decomposition processes as well. In vacuum the primary decomposition of gases will tend to be pumped away from the sample before the molecules collide with the surface and undergo secondary reactions. When these molecules collide with inert gas molecules, they may undergo homogeneous reactions or may be reflected back to the sample surface and react there.

#### **2. Container geometry**

The container geometry influences the gaseous environment and heat transfer to the samples. Even with a flowing gaseous atmosphere, a deep narrow container will limit the contact between the sample surface and gas, whereas a shallow, broad container will promote the contact.

#### **3. Container material**

It is reasonable to expect that in some cases the container material will react with material being tested or some of the products.

#### **4. Sample size**

Two major effects are associated with the sample size, namely surface and bulk effects. In carrying out degradation studies, it is customary to reduce film thickness or particle size until the rate of the decomposition becomes independent of size.

#### **5. Rate of heating**

In the case where only kinetic considerations are significant, an increase in rate of temperature rise will cause the process to be displayed to a higher temperature because they will be at the lower temperature for a shorter length of time. The rate of change of the measured parameter will also be greater for faster heating.

### **Differential scanning calorimetry (DSC) and differential thermal analysis (DTA)**

Physical transformation [7] such as glass transition, cold crystallization and crystallization from melts, crystalline disorientation, and melting can be studied by differential scanning calorimetry (DSC) and differential thermal analysis (DTA). Glass transition involves the motion of short segments in the amorphous region and is related to the brittleness of the polymer.

Crystallization from the melt is of great practical importance. A number of properties of polymers like melting range, heat of fusion and melting point depression, degree of crystallinity, random copolymer structure and stereo regularity and identification of composition of a mixture may be studied through melting. DSC is a method where by the energy necessary to establish a zero temperature difference between a substance and a reference material is recorded as a function of temperature or time. The energy input to the sample is compensated by an increased energy input to the sample in order to maintain a zero temperature difference because this energy input is precisely equivalent in magnitude to the energy absorbed during the transition in direct calorimetric measurement. The combination of programmed and isothermal techniques has been used for characterizing unresolved multistep reactions in polymers [8].

DSC provides useful informations about crystallinity, stability of crystallites, glass transition temperature, cross linking, kinetic parameters such as the activation energy, the kinetic order, frequency factor, entropy change and heat of polymerization.

### **Thermo Gravimetric Analysis (TGA)**

Thermogravimetry is a useful analytical technique for recording weight loss of a test sample as a function of the temperature or time, which may be useful for understanding the chemical nature of the polymer. Thus, the weight of a substance in an environment heated or cooled at a controlled rate is recorded as a function of time or temperature. There are three types of thermogravimetry namely

1. Static or isothermal thermogravimetry,
2. Quasistatic thermogravimetry and
3. Dynamic thermogravimetry



Most of the studies of polymers are generally carried out with dynamic thermogravimetry. Normally sample starts losing weight at a very slow rate up to a particular temperature and thereafter, the rate of loss becomes large over narrow range of temperature. After this temperature the loss in weight levels off. TGA curves are characteristic for given polymers because of unique sequence of physico-chemical reactions, which occur over definite temperature ranges and at the rates that are function of the polymer structures.

The change in weight is a result of the rupture and/or formation of various physical and chemical bonds at elevated temperatures that lead to the evaluation of volatile products in the formation of heavier reaction products. Pyrolysis of many polymers yields TG curves, which follow relatively simple sigmoidal curves. In such a case weight of sample decreases slowly as reaction begins and then decreases rapidly over a comparatively narrow range of temperature and finally levels off as the reaction gets completed. The shape of the curve depends on the kinetic parameters: reaction order ( $n$ ), frequency factor ( $A$ ) and activation energy ( $E_a$ ). The values of these parameters have been shown to be of major importance to elucidate the mechanism in polymer degradation [9, 10].

Reich and Levi [11] have described several temperature characteristics for qualitative assessment of relative thermal stability of polymers:

1. Initial decomposition temperature ( $T_0$ )
  2. Temperature of 10% weight loss ( $T_{10}$ )
  3. Temperature of maximum rate of decomposition ( $T_{max}$ )
- 
7. E. Heisenberg; Cellulose Chemie, 12,159; Chem. Abstr., 25, 59, 823, 1931.
  8. A. A. Duswalt, "The practice of obtaining kinetic data by differential scanning calorimetry", Thermochemica Acta, 8(1-2), 57-68, 1974.
  9. D. W. Levi, L. Reich and H. T. Lee," Degradation of polymers by thermal gravimetric techniques", Polym. Engg. Sci., 5, 135-141, 1965.
  10. H. L. Friedman, U. S. Dept. Com., Office. Tech. 24 pp, 1959; Chem. Abstr., 55, 26, 511, 1961.
  11. L. Reich and D. W. Levi, Macromol. Rev. Eds. Peterlin Goodman Willey Interscience, New York, 173, 1968.

4. Half volatilization temperature (Ts)
5. Differential decomposition temperature
6. Integral procedural decomposition temperature (IPDT)

For the estimation of kinetic parameters from TG traces, several so called exact methods have been proposed. All these methods involve the two assumptions that thermal and diffusion barriers are negligible and that Arrhenius equation is valid. Since small quantities of materials are employed in TG studies, thermal and diffusion barriers would be negligible. Since the shape of any TG curve is dependent on the nature of apparatus and the way in which it is used. Most kinetic treatments are based on relationship of the type.

$$\frac{dC}{dt} = k f(C) \quad \dots 3.1$$

Where C = Degree of conversion, t = time; k=rate constant, and f (C) = temperature independent function of C

The constant k is generally assumed to have the Arrhenius form

$$k = A e^{-Ea/RT} \quad \dots 3.2$$

C is defined as the conversion with respect to initial material

$$C = 1 - \frac{W}{W_o} \quad \dots 3.3$$

where  $W_o$ = Initial weight of the material and W= weight of the material at any time.

The residual weight fraction is given by

$$\frac{W}{W_o} = (1-C)$$

and the rate of conversion is given by

$$\frac{dC}{dt} = - \left( \frac{1}{W_o} \right) \frac{dW}{dt} \quad \dots 3.4$$

For homogeneous kinetics, the conversion would be assumed to have the form

$$f(C) = (1-C)^n \quad \dots 3.5$$

Where n = order of the reaction

Upon substituting Eqns. 3.2 and 3.5 into Eqn. 3.1

$$\frac{dC}{dt} = A e^{-E_a/RT} (1-C)^n$$

OR

$$\frac{dC}{dT} = \left(\frac{A}{\beta}\right) (e^{-E_a/RT}) (1-C)^n \quad \dots 3.6$$

Where  $\beta$  = Rate of heating

Methods of single heating rate

### 1. Freeman-Carroll [12] and Anderson-Freeman methods [13]

Freeman-Carroll has developed the following relation to analyze TGA data at single heating rate:

$$\frac{\Delta \ln(dC/dt)}{\Delta \ln(1-C)} = n - \frac{E_a}{R} \left[ \frac{\Delta(1/T)}{\Delta \ln(1-C)} \right] \quad \dots 3.7$$

A plot of L.H.S. against  $\Delta(1/T) / \Delta \ln(1-C)$  would yield a straight line with slope equal to  $-\frac{E_a}{R}$  and the intercept equal to  $n$ . Using Eqn. 3.7

Anderson-Freeman derived the Eqn. 3.8

$$\Delta \ln\left(\frac{dC}{dt}\right) = n \Delta \ln(1-C) - \frac{E_a}{R} \Delta\left(\frac{1}{T}\right) \quad \dots 3.8$$

According to Eqn. (3.8), the plot of  $\Delta \ln(dC/dt)$  against  $\Delta \ln(1-C)$  for equal interval of  $\Delta(1/T)$  would be a straight line with slope equal to  $n$  and the intercept equal to  $-E/R \Delta(1/T)$ .

- 
12. E. S. Freeman and B. Carroll, "The application of thermoanalytical techniques to reaction kinetics: the thermogravimetric evaluation of the kinetics of the decomposition of calcium oxalate monohydrate", *J. Phys. Chem.*, 62, 394-397, 1958.
  13. D. A. Anderson and E. S. Freeman, "The kinetics of the thermal degradation of polystyrene and polyethylene" *J. Polym. Sci.*, 54, 253-260, 1961.

## 2. Sharp-Wentworth method [14]

For a first order process ( $n=1$ ), Sharp-Wentworth derived the following relation to analyze TGA data.

$$\log \left[ \frac{dC/dt}{1-C} \right] = \log (A / \beta) - \frac{E_a}{2.303R} \frac{1}{T} \quad \dots\dots 3.9$$

Where  $C$  = fraction of polymer decomposed at temperature  $T$ ,  $\beta$  = rate of heating,  $A$  = Frequency factor and  $E_a$  = the activation energy of the process. The plot of  $\log [(dC/dt)/(1-C)]$  against  $1/T$  would be a straight line with slope equal to  $-(E_a/2.303 R)$  and the intercept equal to  $\log (A/\beta)$ .

## 3. Chatterjee method [15]

Chatterjee has developed the following relation for the determination of  $n$  from TG curves based on weight units.

$$n = \frac{\log \left( \frac{dW}{dt} \right)_1 - \log \left( \frac{dW}{dt} \right)_2}{\log W_1 - \log W_2} \quad \dots 3.10$$

Where  $W_1$  and  $W_2$  are the sample weights.

## 12. Horowitz -Metzger method

The value of  $E_a$  can be determined from a single TG curve according to Horowitz – Metzger method

$$\ln \left[ \ln(1-C)^{-1} \right] = \frac{E_a}{RT_s^2} \theta \quad \dots 3.11$$

Where,  $C$  = fraction of the compound decomposed at time  $t$ ,  $E_a$  = activation energy,  $T_s$  = Temperature at which the rate of decomposition is maximum and  $\theta = T - T_s$

The frequency factor  $A$  and entropy change  $\Delta S$  can be determined respectively according to Eqns. 4.12 and 4.13.

$$\ln E - \ln (RT_s^2) = \ln A - \ln \beta - \frac{E}{RT_s^2} \quad \dots 3.12$$

14. J. H. Sharp and S. A. Wentworth, "Kinetic analysis of thermo gravimetric data", *Anal. Chem.*, 41, 2060-2062, 1969.

15. P. K. Chatterjee, "Application of thermo gravimetric techniques to reaction kinetics", *J. Polym. Sci.*, A-3, 4253-4262, 1965.

$$A = \frac{k_b T}{h} e^{\Delta S / R} \quad \dots 3.13$$

Where  $k_b$  is Boltzmann constant

## Experimental

TG and DSC thermograms of epoxy resins [ESB4HCy, ESB4HM and ESB4HE], cured epoxy resins [ECyP-5, ECyP-10 and ECyP-15; EMP-5, EMP-10 and EMP-15; and EEP-5, EEP-10 and EEP-15], bisbenzoxazines [BSB4HCy, BSB4HM, BSB4HE and BSB4HS] and polySchiff bases [TDADPCy, TDADPM, TDADPE and TDADPS] were scanned on a Perkin Elmer TGA (Model Pyris-1) and Shimadzu DSC60 at the heating rate of 10°C/min in nitrogen atmosphere.

## Results and Discussion

### Thermal study of cured and uncured epoxy resins

DSC thermograms of uncured epoxy resins at the heating rate of 10 °C /min in nitrogen atmosphere are shown in Figs. 3.47 to 3.49. DSC transition(s) of each sample is/are summarized in Table 3.16. Exothermic transitions at 100° and 280.5°C for ESB4HCy are due to some physical change and decomposition, respectively. Physical change and degradation are confirmed respectively by no weight loss at 100°C and weight loss at about 281°C in its TG curve (Fig. 3.50).

In case of ESB4HM, endothermic transitions at 104.3 °C and 191.5 °C are due to some physical change and confirmed by no weight loss in its TG thermogram (Fig.3.50) over those temperatures. Endothermic transition at 76.3°C and exothermic transition at 240.8°C for ESB4HE are due to some physical changes.

ESB4HCy, ESB4HM and ESB4HE are thermally stable up to about 227°, 264° and 275 °C, respectively. ESB4HCy and ESB4HM followed two-step decomposition, while ESB4HE followed single step decomposition. Observed thermal stability order is ESB4HE > ESB4HM > ESB4HCy.

Initial decomposition temperature( $T_o$ ), decomposition range, temperature of maximum weight loss ( $T_{max}$ ), % weight loss involved and % residue left at 500°C are summarized in Table 3.16.

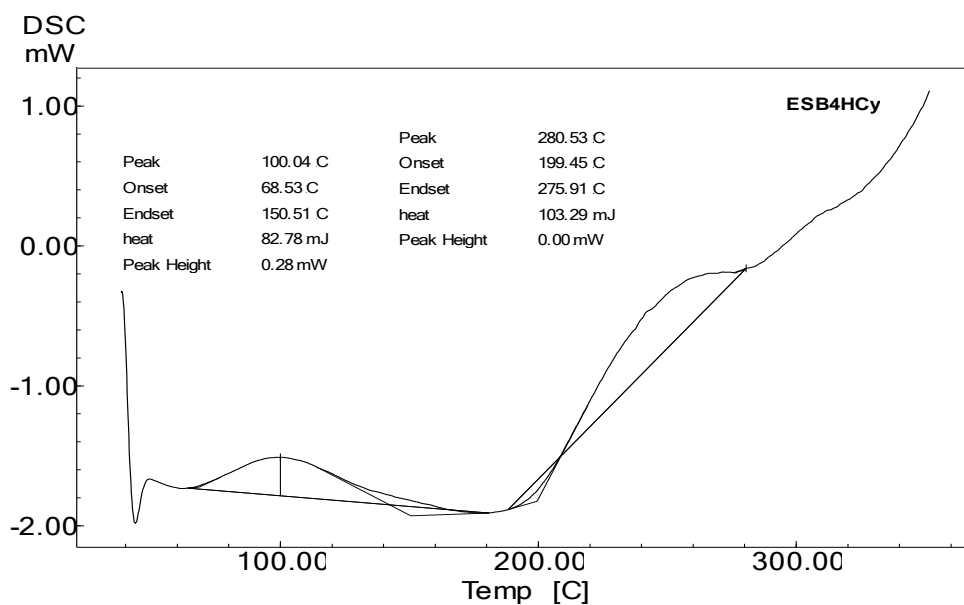


Fig. 3.47: DSC thermogram of ESB4HCy at the heating rate of 10°C/min in an N<sub>2</sub> atmosphere.

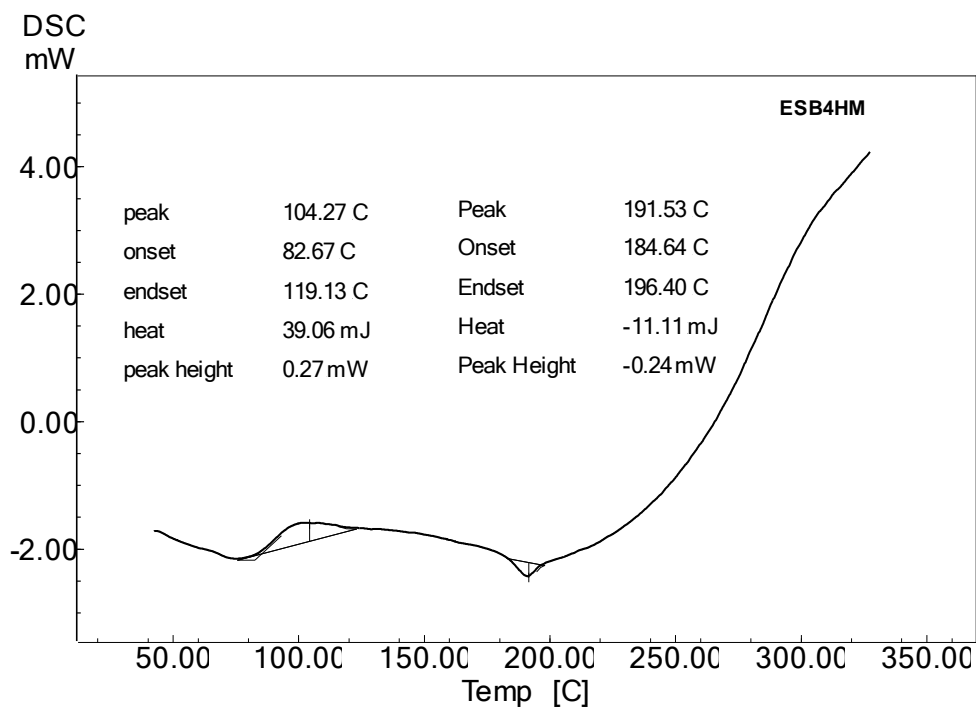


Fig. 3.48: DSC thermogram of ESB4HM at the heating rate of 10°C/min in an N<sub>2</sub> atmosphere.

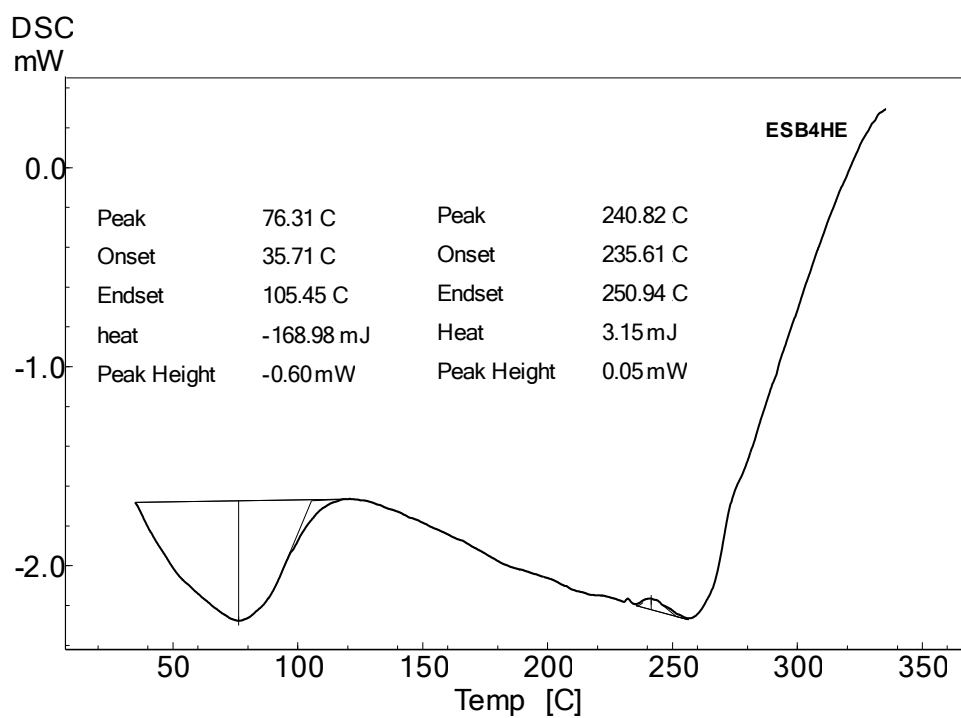


Fig. 3.49: DSC thermogram of ESB4HE at the heating rate of 10°C/min in an N<sub>2</sub> atmosphere.

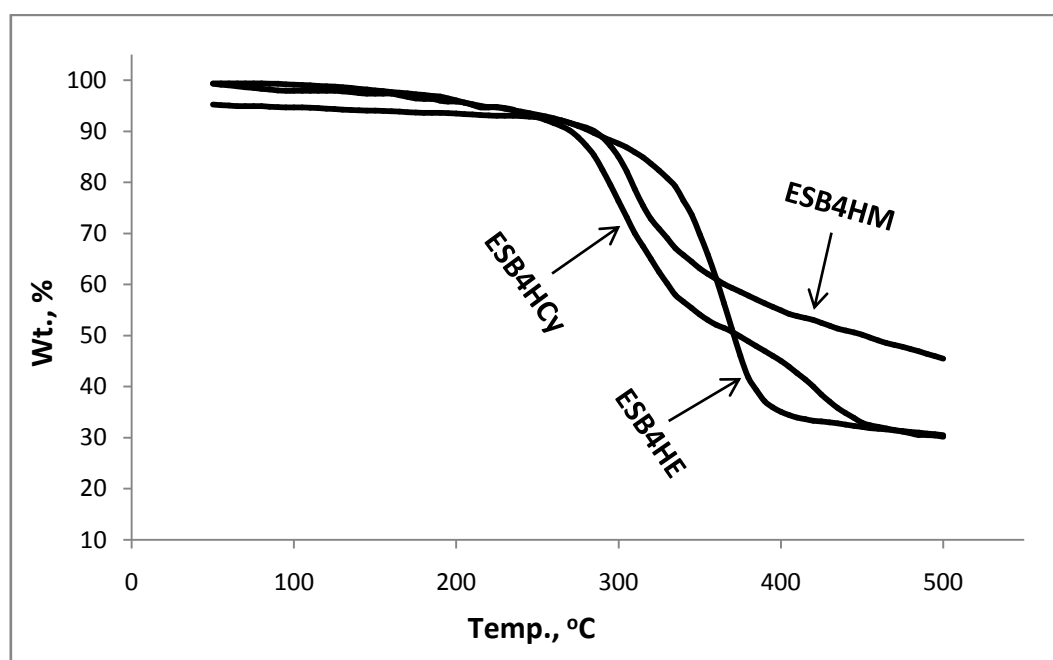


Fig. 3.50: TG thermograms of ESB4HCy, ESB4HM and ESB4HE at the heating rate of 10°C/min in an N<sub>2</sub> atmosphere

Table 3.16: DSC and TGA data of uncured epoxy resins.

Parameter	Epoxy		
	ESB4HCy	ESB4HM	ESB4HE
DSC Transition Temp., °C	100.0 (Exo.)	104.3 (Endo.)	76.3 (Endo.)
	280.5 (Exo.)	191.5 (Endo.)	240.8 (Exo.)
T <sub>0</sub> , °C	227	264	275
	390	398	
Decomposition range, °C	227-332	264-398	275-413
	390-460	398-563	
T <sub>max</sub> , °C	300.50	311.7	363.8
	425.00	502.1	
% Wt.loss	35.5	37	57.3
	15	14.7	
% Residue at 500°C	30.2	31.6 (800°C)	30.5
E, kJ mol <sup>-1</sup>	98.1	340.9	120.6
	265.2	73.2	
n	0.55	4.93	0.59
	1.45	1.01	
A, s <sup>-1</sup>	5.12 x 10 <sup>6</sup>	5.59 x 10 <sup>28</sup>	4.59 x 10 <sup>7</sup>
	7.61 x 10 <sup>17</sup>	208	
ΔS* JK <sup>-1</sup> mol <sup>-1</sup>	-121.9	299.8	-104.6
	90.3	-208.5	
R <sup>2</sup>	0.964	0.997	0.936
	0.956	0.993	



Observed order of weight loss involved in decomposition reaction is ESB4HE > ESB4HM > ESB4HCy. Similar order is observed for  $T_{\max}$ . The % residue left is almost same.

Associated kinetic parameters namely  $n$ ,  $E_a$ ,  $A$  and  $\Delta S^*$  were determined according to Eqns. 3.8, 3.12 and 3.13; Anderson-Freeman plots are shown in Figs. 3.51 to 3.53. Least square values along with regression coefficients ( $R^2$ ) are summarized in Table 3.16.

From Table 3.16, it is observed that ESB4HCy and ESB4HE followed either fractional or integral order degradation kinetics. In case of ESB4HM, first step followed complex order and second step followed first order kinetics. From  $E_a$  values rigidity order of the resins is ESB4HCy > ESB4HE > ESB4HM. In accordance to Arrhenius equation, higher is the value of  $E_a$  higher is the value of  $A$ . Large and positive values of  $\Delta S^*$  suggested that transition state is in less orderly state than individual resin molecules and vice versa.

Ether and azomethine linkages in the resin molecules are weak linkages. Selective degradation occurs from these weak points and form free radicals. These radicals further recombine to form new product(s), which degrade at elevated temperatures. Degradation of polymers undergoes a variety of reactions such as cross linking, branching, rearrangement, etc.

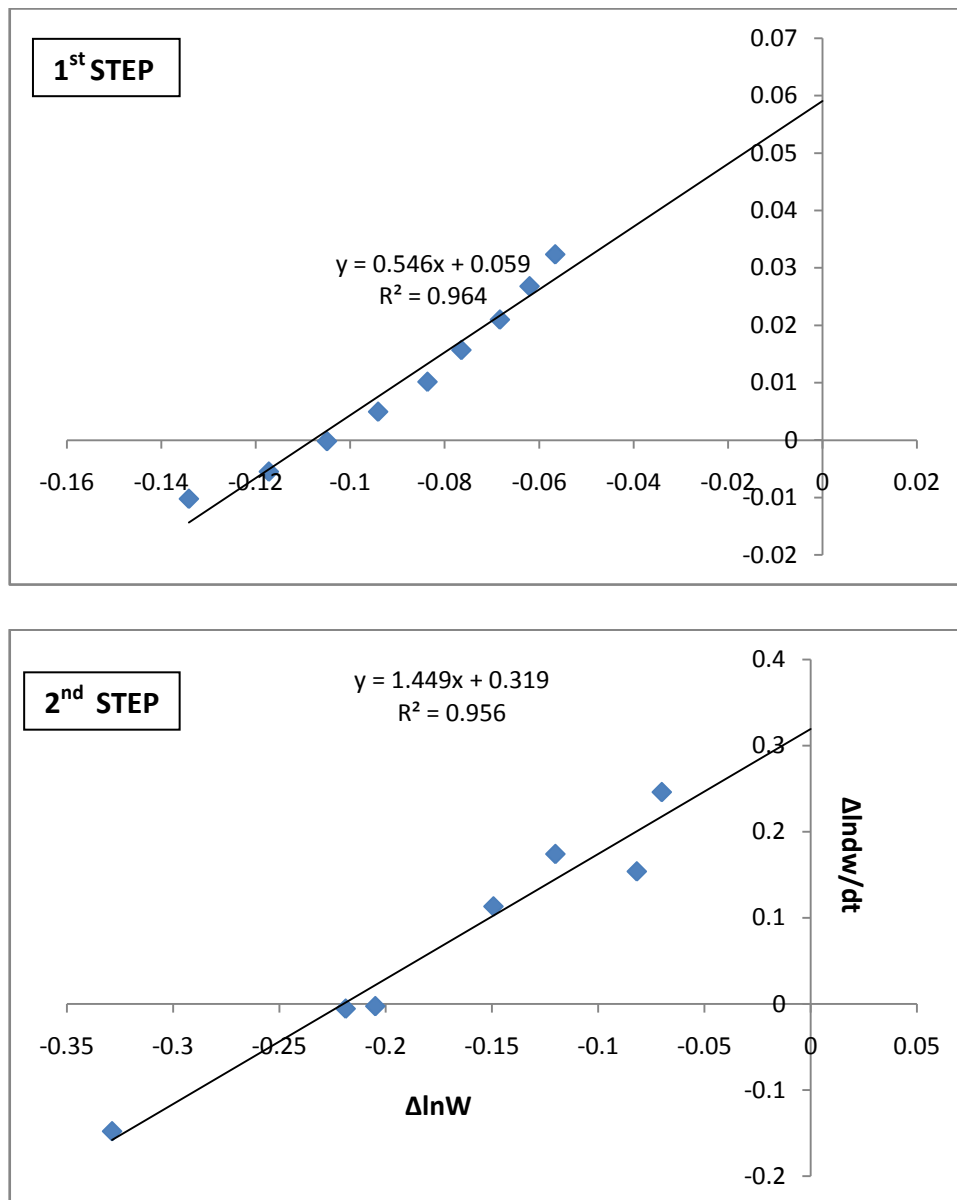


Fig. 3.51: The Anderson-Freeman plots for ESB4HCy

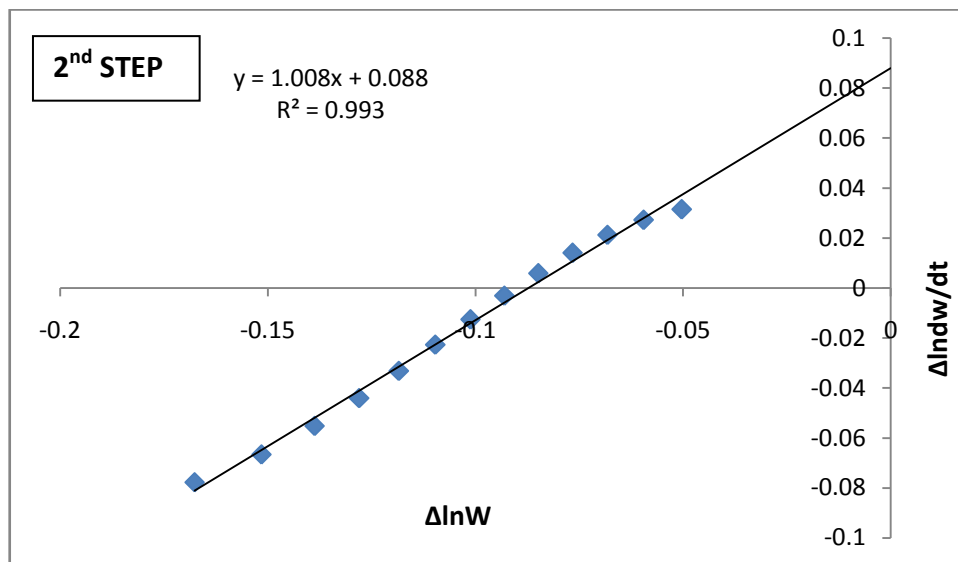
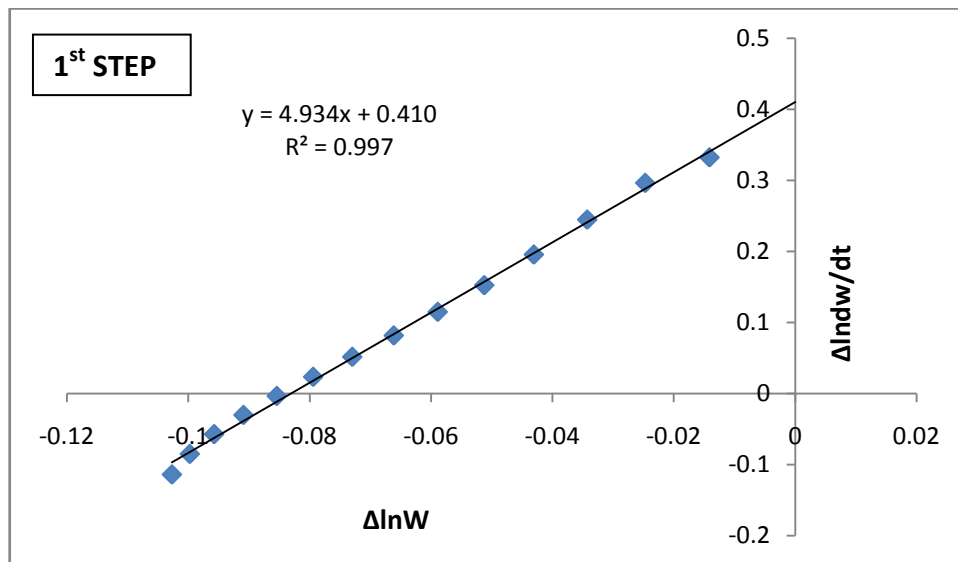


Fig. 3.52: The Anderson-Freeman plots for ESB4HM

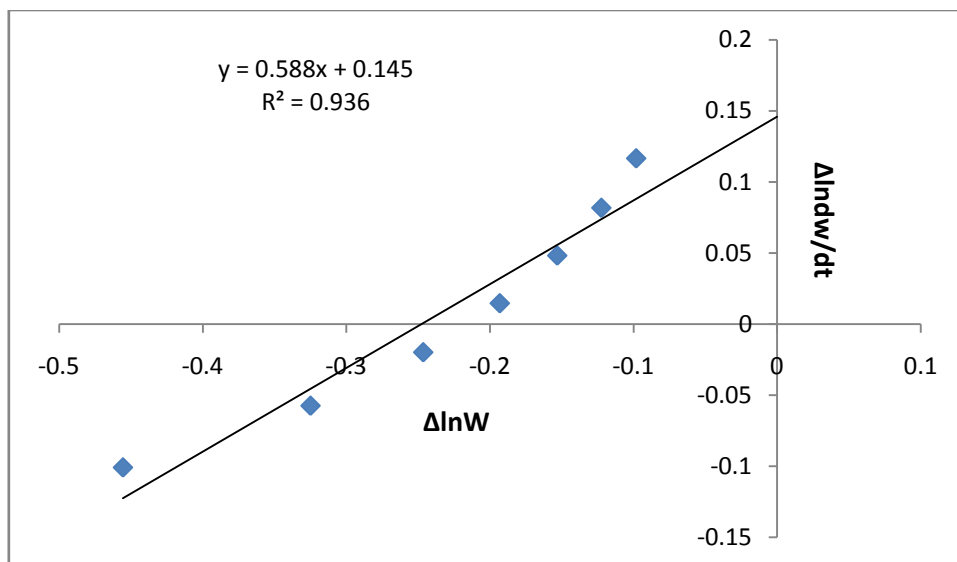


Fig. 3.53: The Anderson-Freeman plot for ESB4HE

### Cured epoxy resins

TG thermograms of cured epoxy resins are presented in Figs. 3.54 to 3.56.  $T_o$ , decomposition range,  $T_{max}$ , %weight loss and % residue left at 500°C for each of cured resins are summarized in Tables 3.17 to 3.19, respectively for ECyP-5 to ECyP-15, EMP-5 to EMP-15, EEP-5 to EEP-15. Least square associated kinetic parameters were derived according to Eqns. 3.8, 3.12 and 3.13 and also summarized in Tables 3.17 to 3.19. Freeman-Anderson plots are shown in Figs. 3.57-3.58. From Fig. 3.54 and Table 3.17, it is observed that ECyP-5 followed single step decomposition, while ECyP-10 and ECyP-15 followed three steps decomposition. Order of degradation is almost first order but E and A values for ECyP-10 are much higher than that of ECyP-5. Similarly % residue is also large. Increasing amount of phthalic anhydride, led to decrease in considerable thermal stability and  $T_{max}$ , which are probably due to increasing weak ester linkages.

From Fig. 3.55, it is observed that EMP-5 to EMP-15 followed apparently two steps decomposition. The % decomposition is very small. To decreased with increasing amount of phthalic anhydride.  $T_{max}$  has also increased up to 10% of hardener concentration. % weight loss for EMP-10 (~38%) is considerably greater than EMP-5 and EMP-15 (~24-27%). The % residue left at 500°C is practically same (~56-60%). Anderson-Freeman plots are shown in Figs. 3.59-3.61. All these samples followed fractional order degradation kinetics (0.4-2.5). E and A both increasing with PA concentration confirming increasing rigidity of the cured product and hence cross linking density. Increasing concentration of crosslinking density led to decrease in thermal stability due to weak ester linkages.

EEP-5 to EEP-15 (Fig.3.56) also followed apparently two step decomposition and weight loss for first step is considerably small. Practically no effect of PA concentration on thermal stability is observed  $T_{max}$  for EEP-15 (348°C) is somewhat higher than EEP-5 (329°C) and EEP-10 (326°C). The % residue at 500°C is almost same (61-63%) EEP-10 (n=4) followed complex order kinetics, while EEP-5 (n=1.8) and EEP-15 (n=1.3) followed second and first order kinetics. Anderson-Freeman plots are shown in Fig. 3.62 to 3.64. E and A values for EEP-10 are higher than EEP-5 and EEP-15.

Upon curing with phthalic anhydride thermal stability of ESB4HCy resin has lowered, and it is slightly improved in case of ESB4HM and ESB4HE. Ester and ether linkages are weak points in the cured products. Ester linkages are thermally less stable than ether linkages and preferentially decomposition starts from ester linkages with evolution of carbon dioxide.

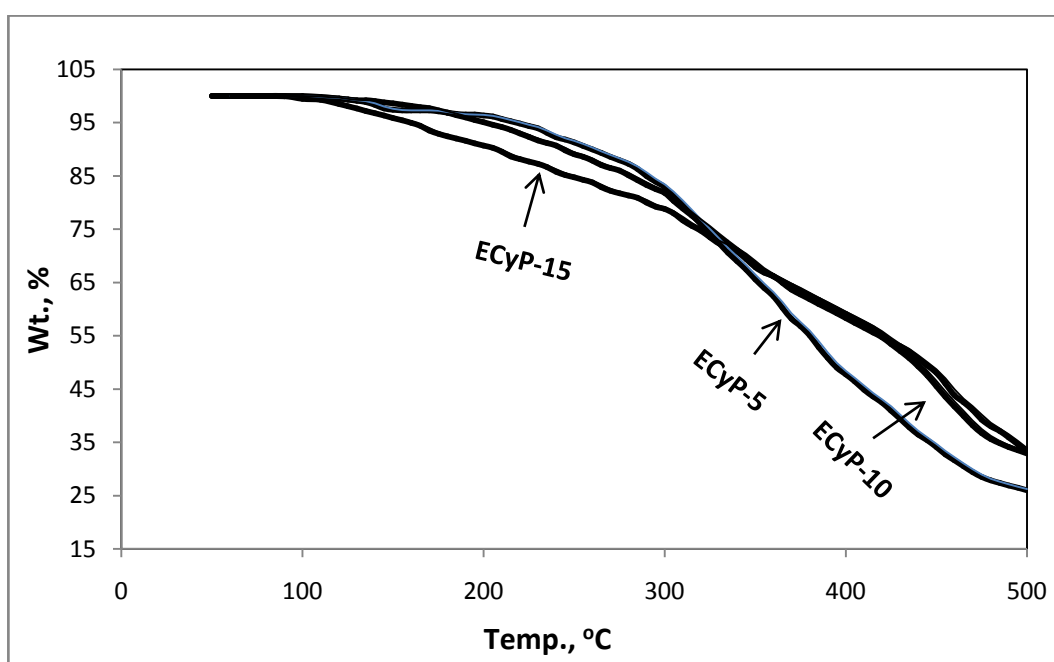


Fig. 3.54: TG thermograms of ECyP-5, ECyP-10 and ECyP-15 at the heating rate of  $10^{\circ}\text{C}/\text{min}$  in an  $\text{N}_2$  atmosphere

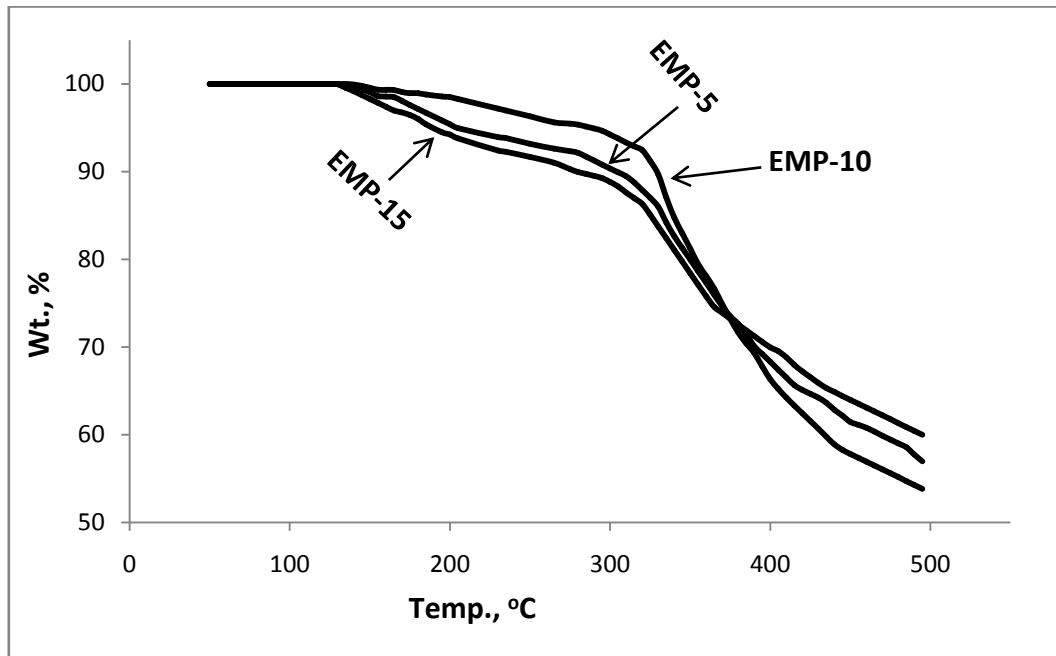


Fig. 3.55: TG thermograms of EMP-5, EMP-10 and EMP-15 at the heating rate of 10<sup>0</sup>C/min in an N<sub>2</sub> atmosphere

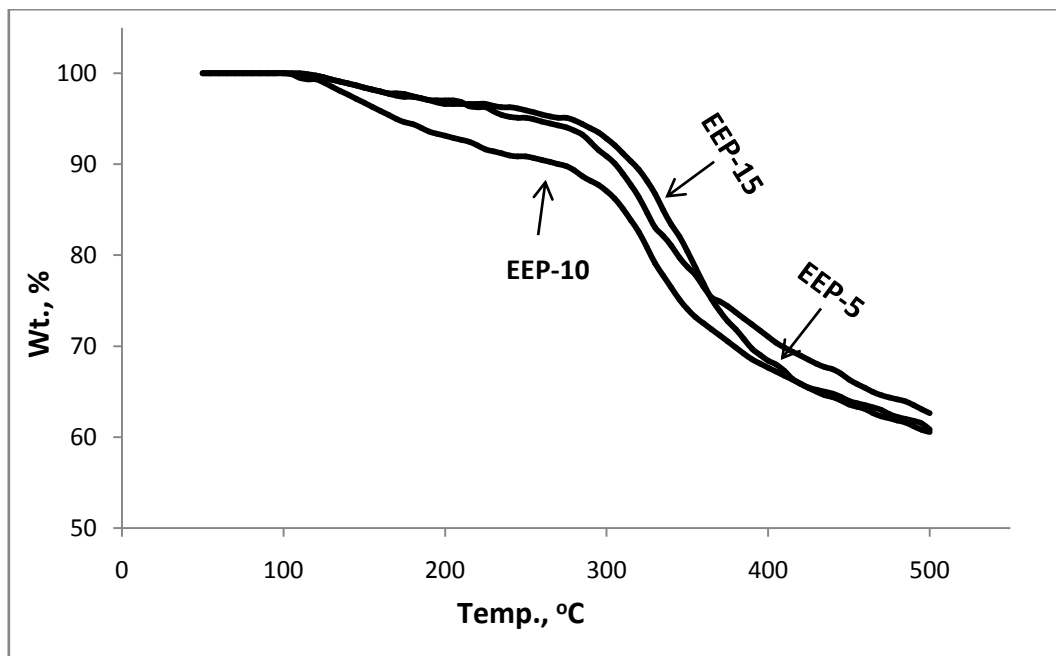


Fig. 3.56: TG thermograms of EEP-5, EEP-10 and EEP-15 at the heating rate of 10<sup>0</sup>C/min in an N<sub>2</sub> atmosphere

Table 3.17: TGA data of cured epoxy resins ESB4HCy

Parameter	Cured of epoxy resin	
	ECyP-5	ECyP-10
$T_0$ , °C	179	150
		291
		429
Decomposition range, °C	179-488	150-291
		291-429
		429-488
$T_{max}$ , °C	359	220.7
		331.1
		451.5
% Wt. loss	69.8	15.5
		30.7
		18.0
% Residue at 500°C	26	32.9
E, kJ mol <sup>-1</sup>	34.9	226.1
		61.5
		163.0
n	1.0	1.34
		1.03
		1.02
A, s <sup>-1</sup>	1.3	1.55 x 10 <sup>22</sup>
		7.04 x 10 <sup>2</sup>
		3.5 x 10 <sup>9</sup>
$\Delta S^*$ JK <sup>-1</sup> mol <sup>-1</sup>	-248.8	175.7
		-196.3
		-69.7
R <sup>2</sup>	0.979	0.971
		0.989
		0.969

Table 3.18: TGA data of cured epoxy resins ESB4HM

Parameter	Cured of epoxy resin		
	EMP-5	EMP-10	EMP-15
$T_0, ^\circ\text{C}$	293	276	293
Decomposition range, $^\circ\text{C}$	293-406	276-451	293-450
$T_{\text{max}}, ^\circ\text{C}$	355.8	363.8	340.4
% Wt.loss	23.8	37.8	26.5
% Residue at $500^\circ\text{C}$	56.3	53.4	59.6
$E, \text{kJ mol}^{-1}$	85.6	151.3	324.3
$n$	1.56	2.51	0.37
$A, \text{s}^{-1}$	$5.62 \times 10^4$	$1.92 \times 10^{10}$	$7 \times 10^{25}$
$\Delta S^* \text{ JK}^{-1} \text{ mol}^{-1}$	-160.2	-54.4	243.9
$R^2$	0.983	0.985	0.981

Table 3.19: TGA data of cured epoxy resin ESB4HE

Parameter	Cured epoxy resin		
	EEP-5	EEP-10	EEP-15
$T_0, ^\circ\text{C}$	267	276	267
Decomposition range, $^\circ\text{C}$	267-415	276-415	484
$T_{\text{max}}, ^\circ\text{C}$	329.3	325.7	348.0
% Wt.loss	25	23.4	33.2
% Residue at $500^\circ\text{C}$	62.6	60.6	60.8
$E, \text{kJ mol}^{-1}$	101.4	255.2	106.4
$n$	1.84	4.03	1.27
$A, \text{s}^{-1}$	$3.5 \times 10^6$	$2.63 \times 10^{20}$	$4.9 \times 10^6$
$\Delta S^* \text{ JK}^{-1} \text{ mol}^{-1}$	-125.5	140.2	-122.9
$R^2$	0.994	0.994	0.965



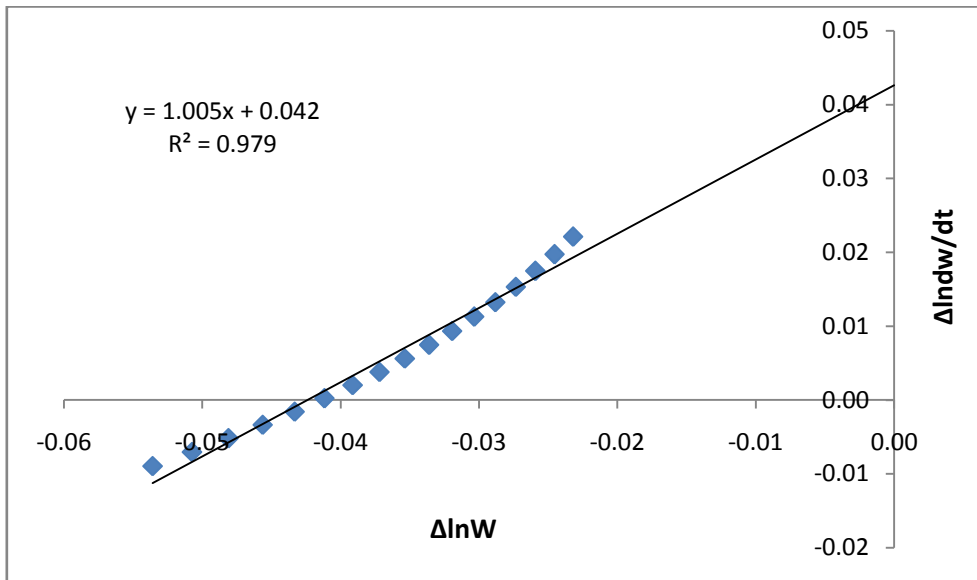
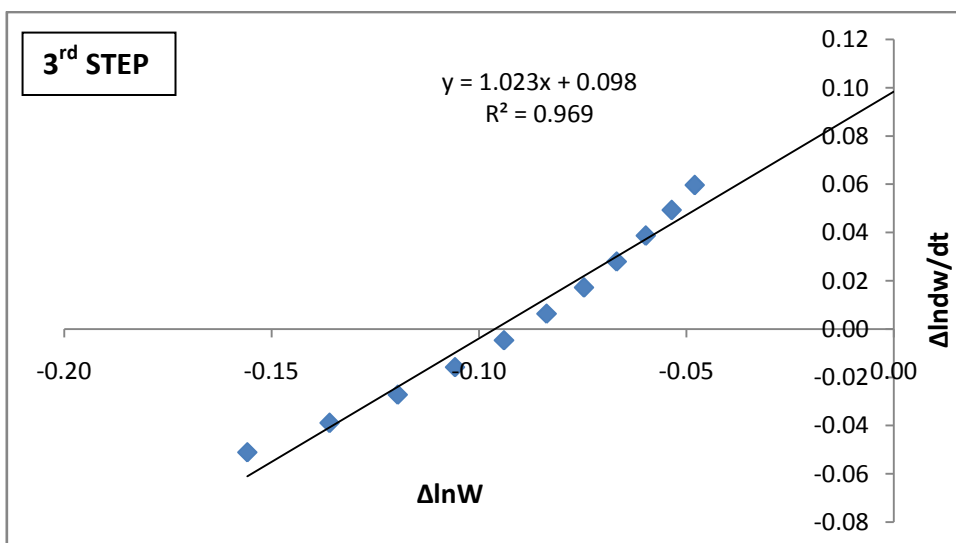
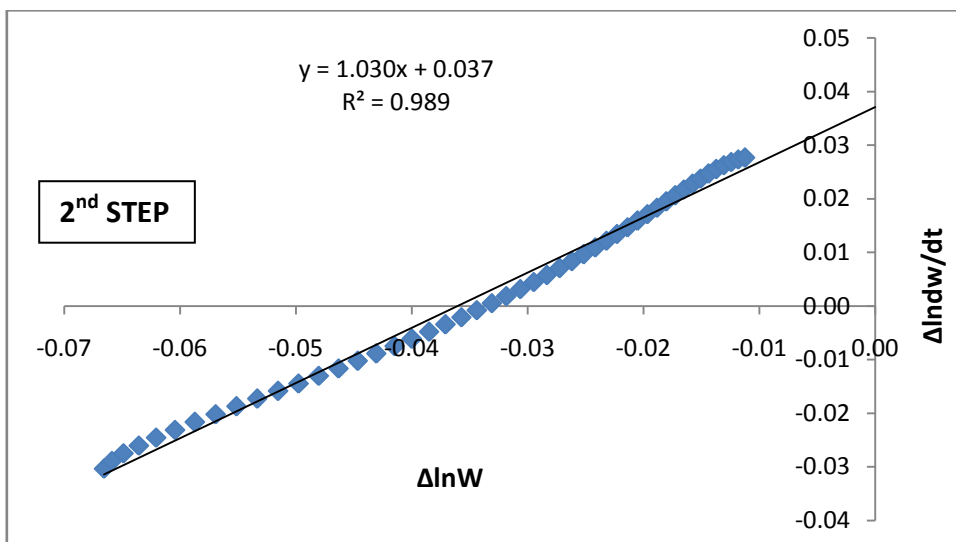
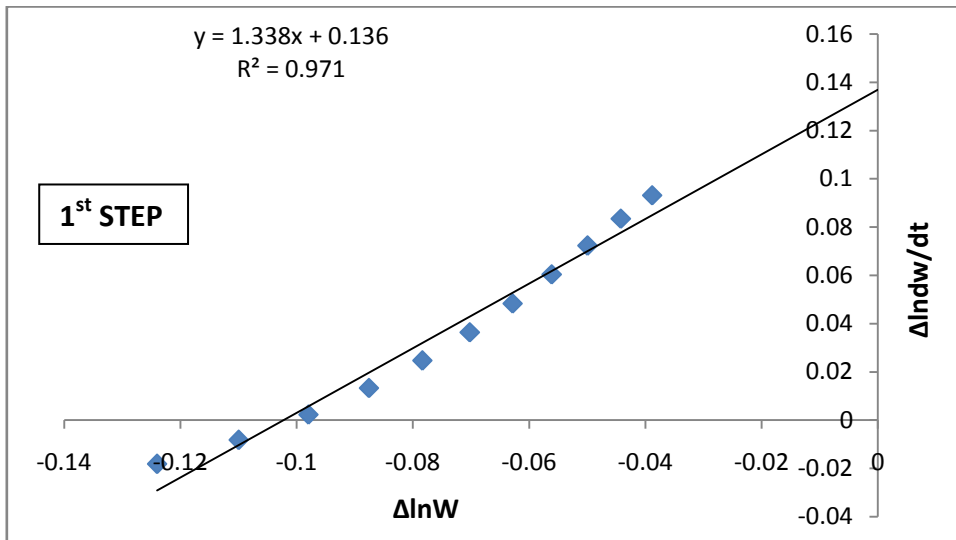
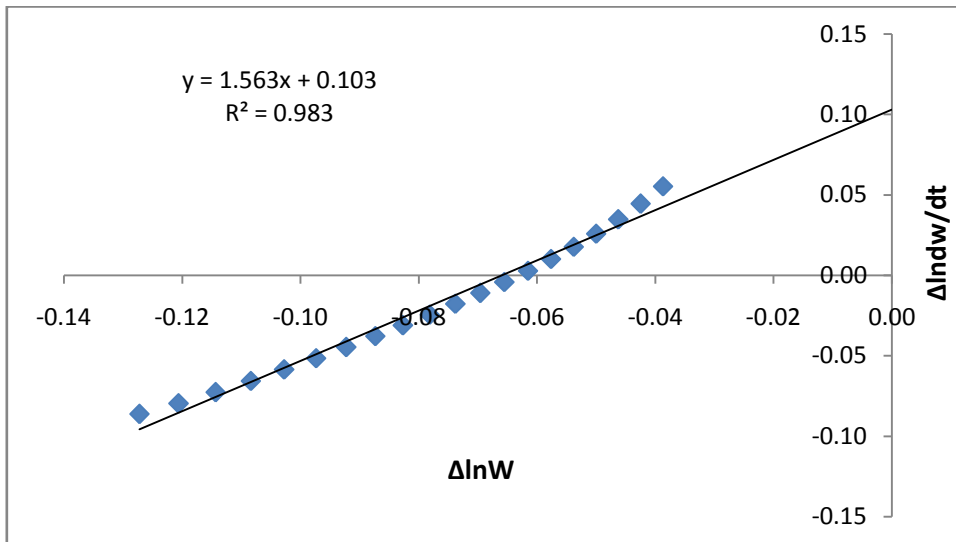


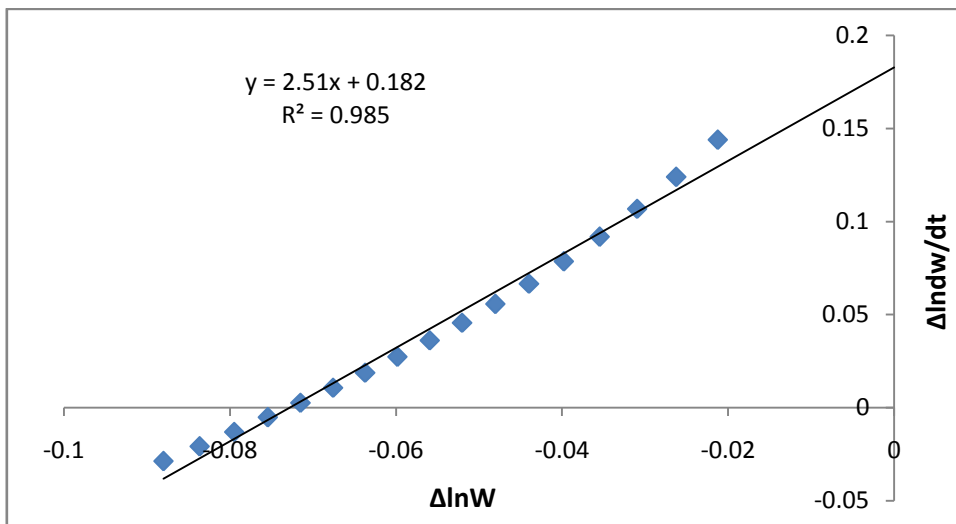
Fig. 3.57: The Anderson-Freeman plot for ECyP-5



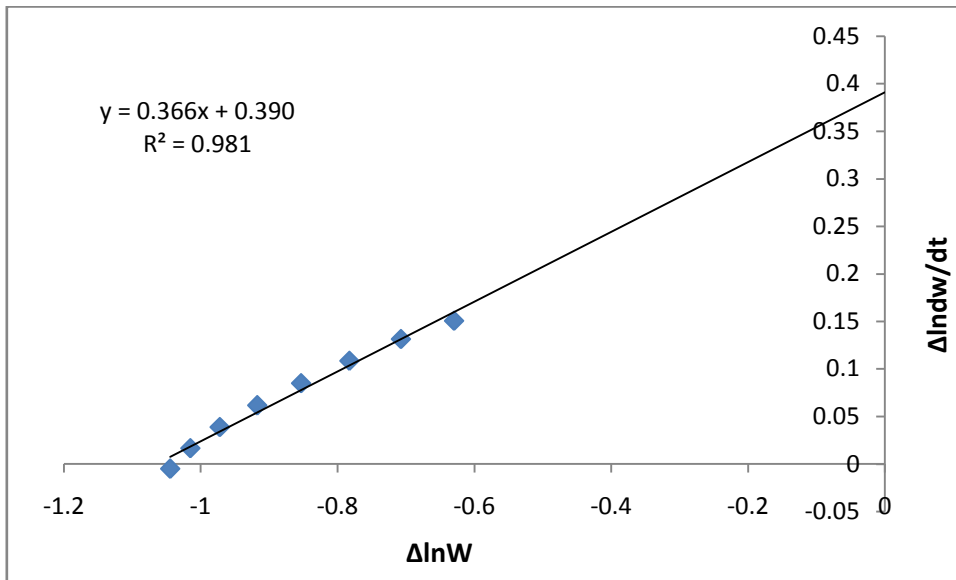
Figs. 3.58: The Anderson-Freeman plots for ECyP-10



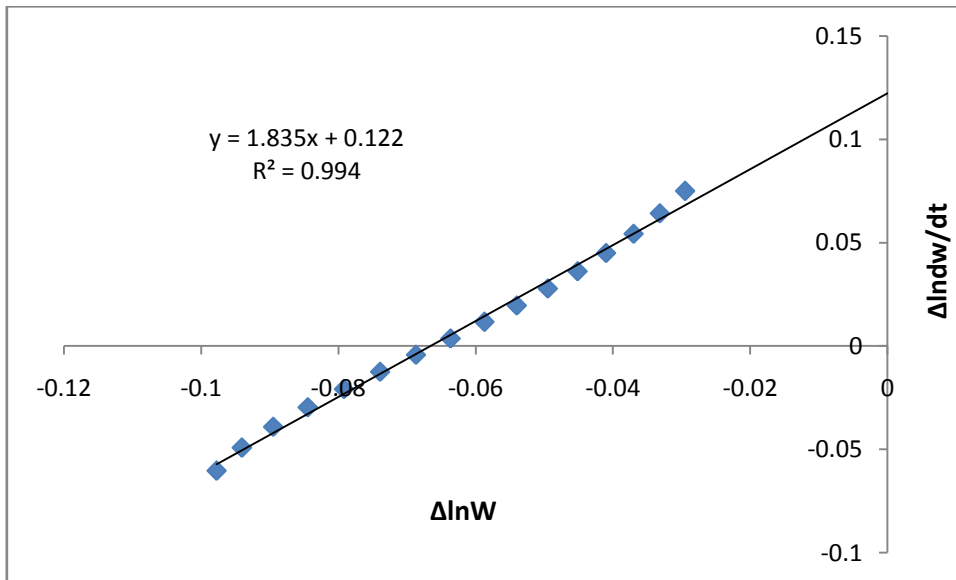
Figs. 3.59: The Anderson-Freeman plot for EMP-5



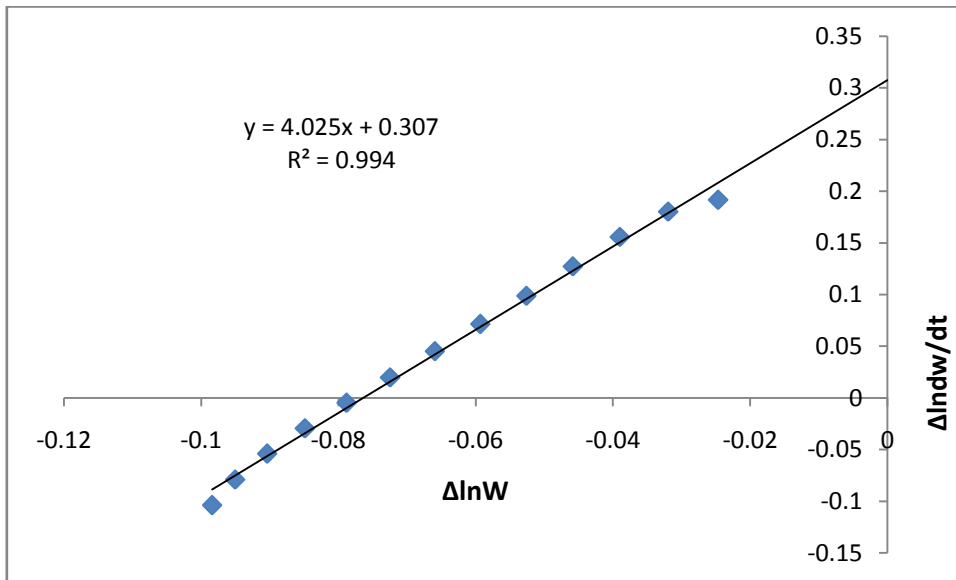
Figs. 3.60: The Anderson-Freeman plot for EMP-10



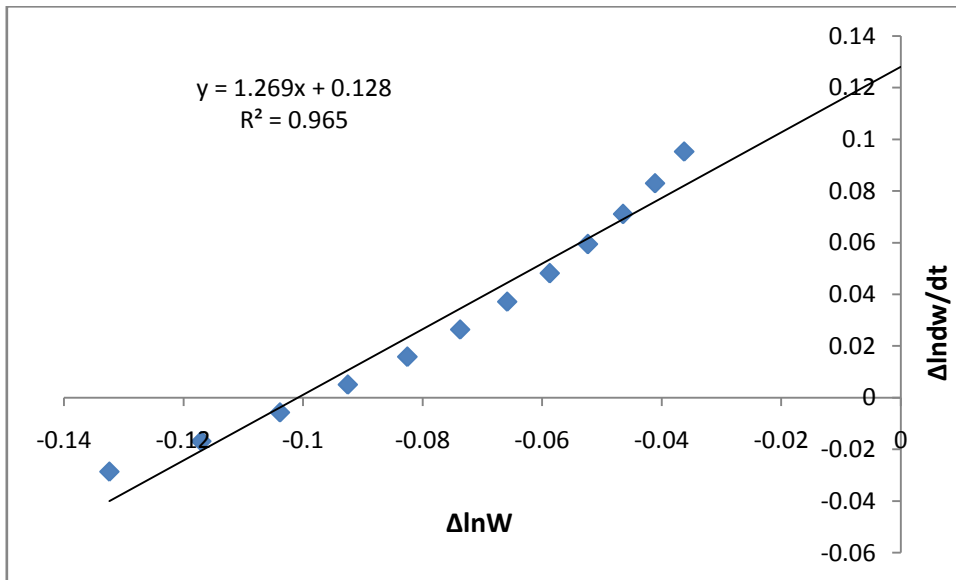
Figs. 3.61: The Anderson-Freeman plot for EMP-15



Figs. 3.62: The Anderson-Freeman plot for EEP-5



Figs. 3.63: The Anderson-Freeman plot for EEP-10



Figs. 3.64: The Anderson-Freeman plot for EEP-15

### Bisbenzoxazines

DSC thermograms of bisbenzoxazines (BSB4HCy, BSB4HM, BSB4HE, BSB4HS) at 10°C/min heating rate in an N<sub>2</sub> atmosphere are presented in Figs. 3.65 to 3.68. DSC transitions are summarized in Table 3.20. Endothermic transition at 81.7°C (BSB4HCy), 79.6°C (BSB4HM), 80.6°C (BSB4HE) and 95.7°C (BSB4HS) is due to melting transition for each of bisbenzoxazine. Endothermic transitions at 137.2°C and 142.5°C for BSB4HCy are due to some physical change, which are further confirmed by no weight loss over those temperature in TG thermogram (Fig.3.69). Exothermic transition at 221.7°C (BSB4HCy), 213.1°C (BSB4HM), 213.7°C (BSB4HE) and 183.3°C (BSB4HS) is due to ring opening polymerization of each of bisbenzoxazine and it is proved by no weight loss over that temperature in corresponding TG thermogram (Fig. 3.69).

From Fig. 3.69, it is observed that bisbenzoxazines are thermally stable up to about 305 °C (BSB4HCy), 352 °C (BSB4HM), 425 °C (BSB4HE) and 257 °C (BSB4HS) and followed apparently two step decomposition.  $T_0$ , decomposition range,  $T_{max}$ , % weight loss and % residue left are summarized in Table 3.20.

Associated kinetic parameters were determined according to Eqns. 3.8, 3.12 and 3.13. Anderson-Freeman plots for each of these resins are shown in Figs. 3.70 to 3.72. The least square kinetic parameters along with regression coefficients are summarized in Table 3.20 from which it is observed that degradation reactions followed fractional order kinetics. Large magnitudes of  $E$  and  $A$  indicated rigid nature of crosslinked products formation via ring opening polymerization of bisbenzoxazines. Large and negative magnitude of  $\Delta S^*$  confirmed that transition state is much in orderly state than individual bisbenzoxazine molecules, while positive magnitudes indicated less orderly state transition state. Ether and amine linkages are weak points in the crosslinked resins and preferentially decomposition starts from such weak point with formation of free radicals, which further undergo recombination and degrade at higher temperature. Relatively high amount of % residue left above 500°C indicated formation of highly thermal stable crosslined materials.

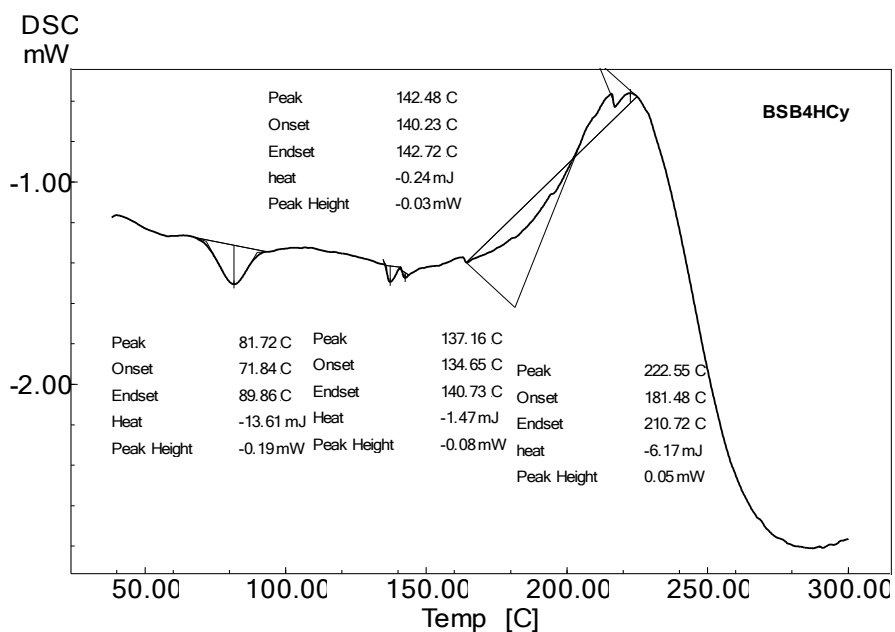


Fig. 3.65: DSC thermogram of BSB4HCy at the heating rate of 10°C/min in an N<sub>2</sub> atmosphere.

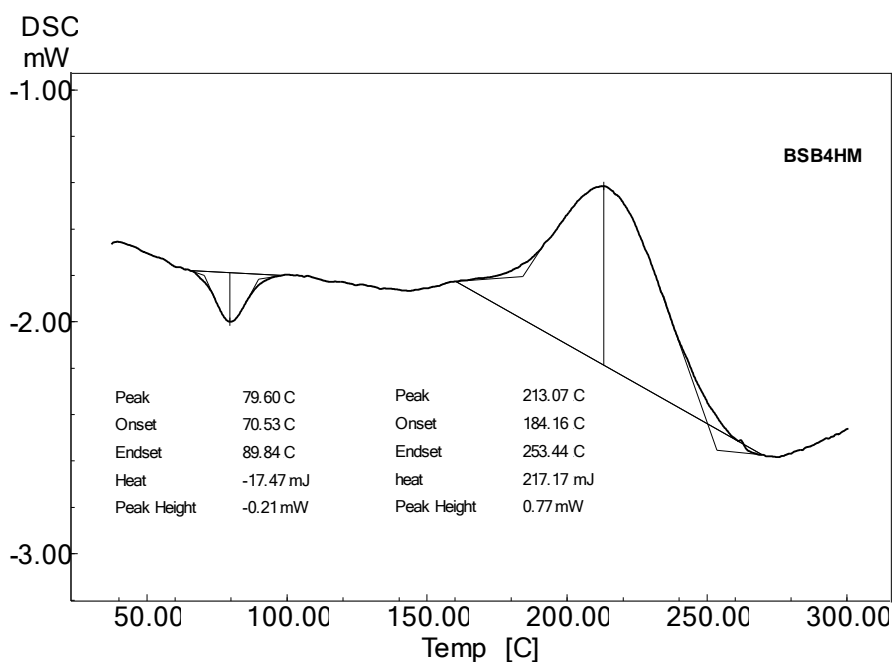


Fig. 3.66: DSC thermogram of BSB4HM at the heating rate of 10°C/min in an N<sub>2</sub> atmosphere.

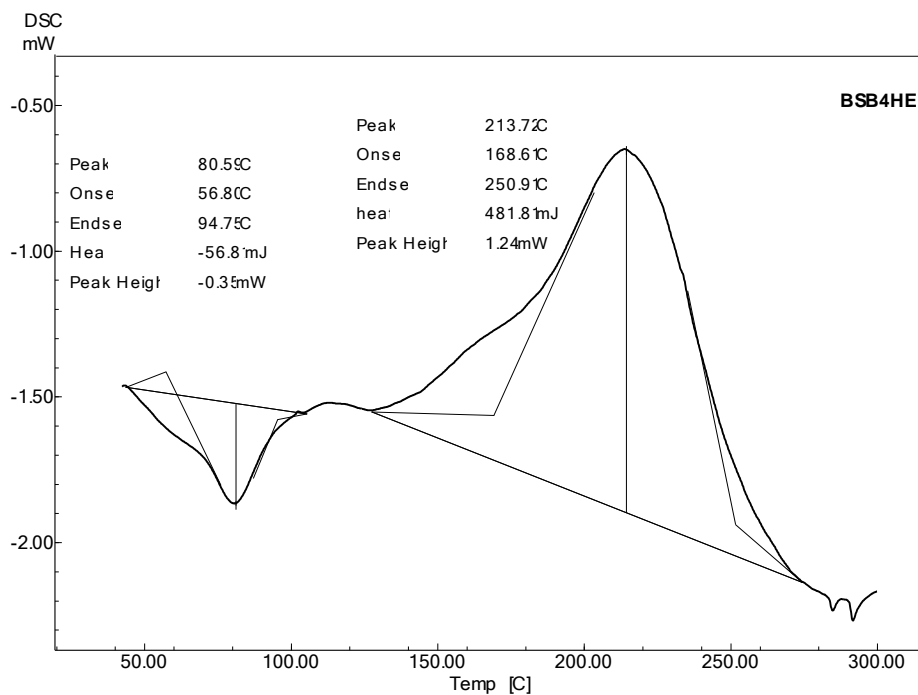


Fig. 3.67: DSC thermogram of BSB4HE at the heating rate of 10°C/min in an N<sub>2</sub> atmosphere.

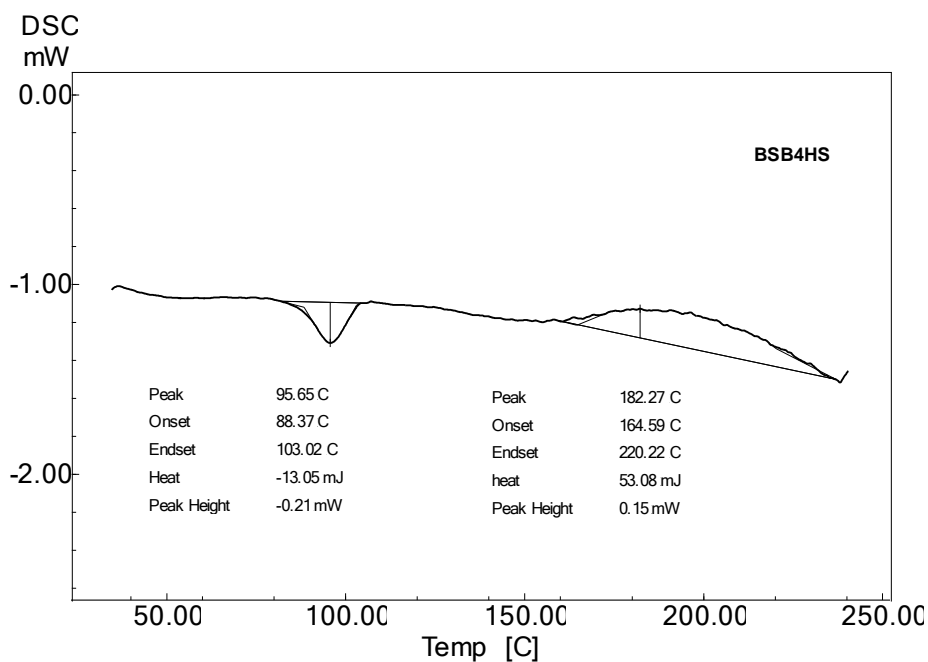


Fig. 3.68: DSC thermogram of BSB4HS at the heating rate of 10°C/min in an N<sub>2</sub> atmosphere.



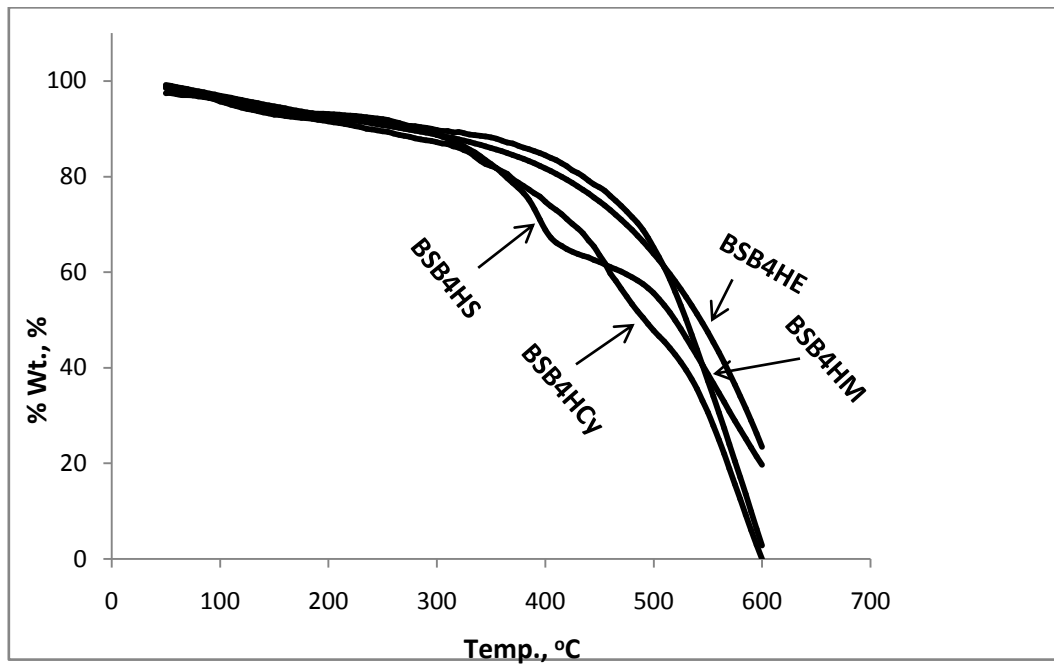
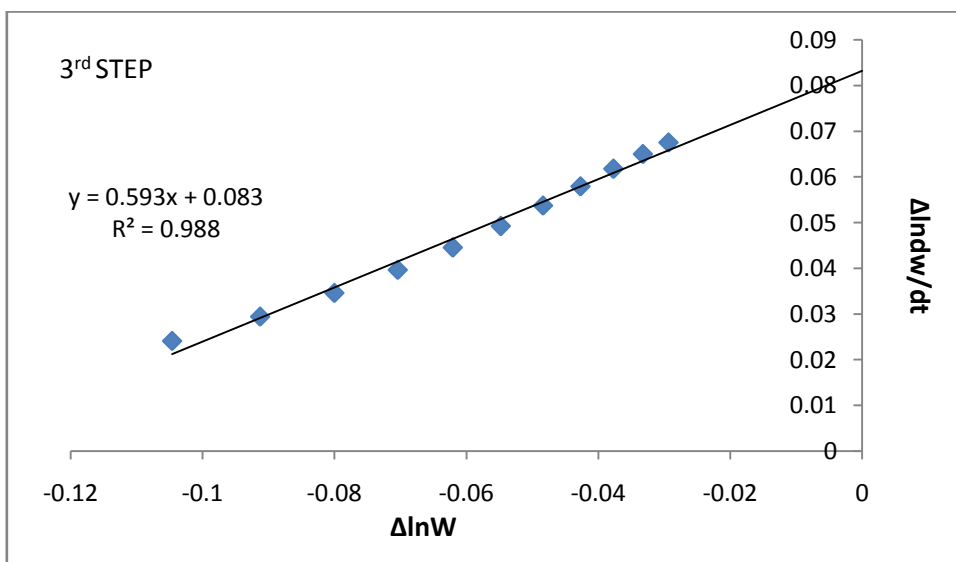
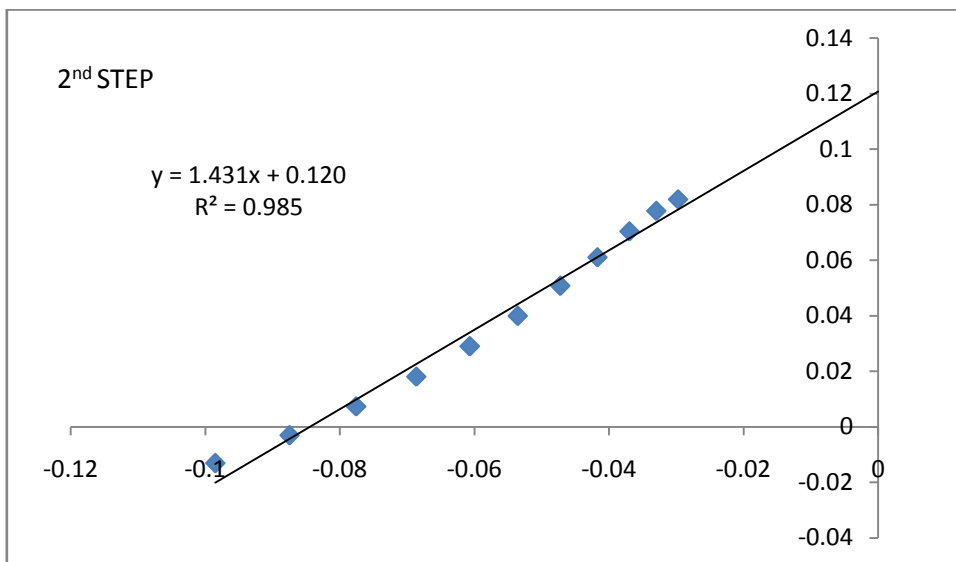
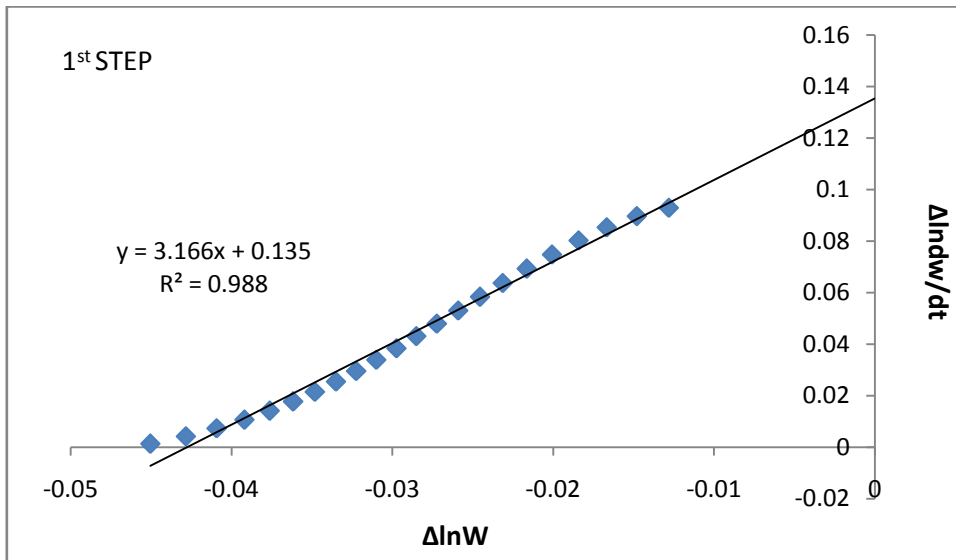


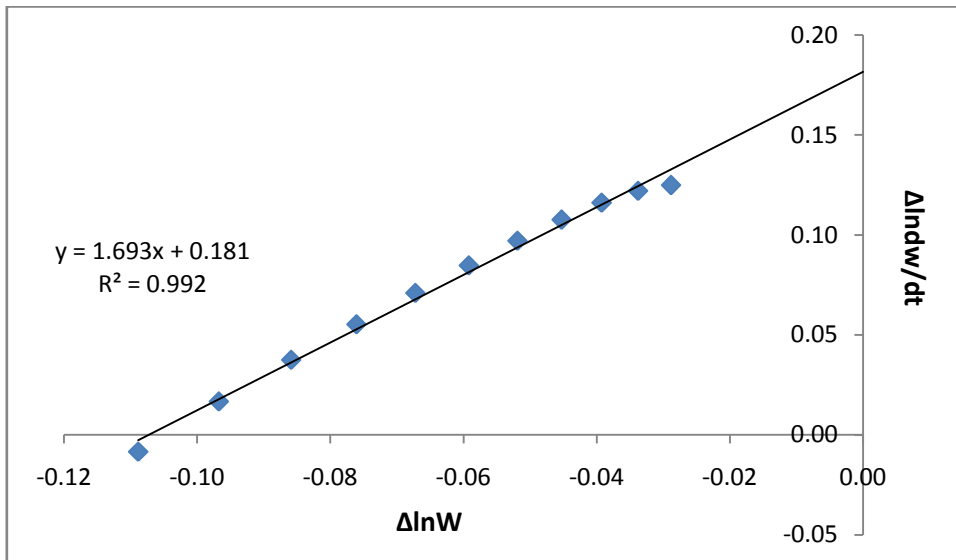
Fig. 3.69: TG thermograms of BSB4HCy, BSB4HM, BSB4HE and BSB4HS at the heating rate of 10 °C/min in an N<sub>2</sub> atmosphere

Table 3.20: DSC and TGA data of bisbenzoxazines

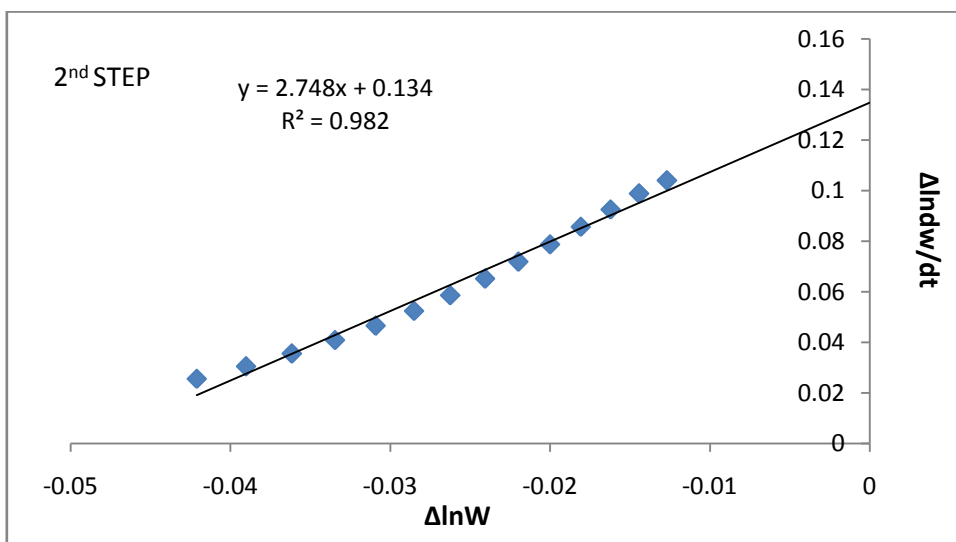
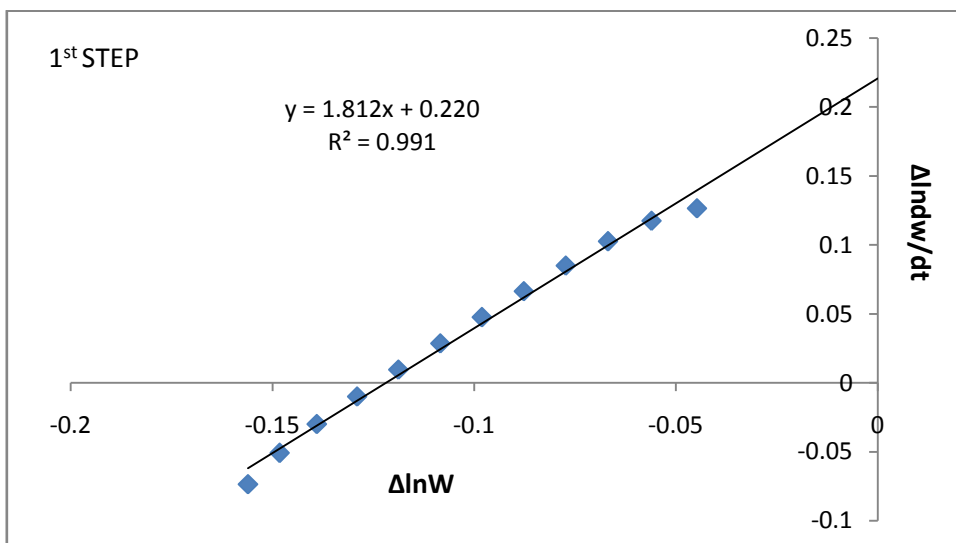
Parameter	Bisbenzoxazine			
	BSB4HCy	BSB4HM	BSB4HE	BSB4HS
DSC Transition Temp., °C	81.7 (Endo.) 137.2 (Endo.) 142.5 (Endo.) 221.7 (Exo.)	79.6 (Endo.) 213.1 (Exo.)	80.6(Endo.) 213.7(Exo.)	95.7(Endo.) 183.3(Exo.)
T <sub>0</sub> , °C	305 425 505	352	425	257 495
Decomposition range, °C	305-390 425-490 505-600	352-600	425-600	257-423 495-600
T <sub>max</sub> , °C	351.81 459.45 577.91	539.86	-	393.52 549.9
% Wt.loss	10.4 19.6 46.6	85.2	55.2	27.2 37.1
% Residue at 600°C	0	2.84	23.46	19.68
E, kJ mol <sup>-1</sup>	224.5 199.5 138.0	150.48	-	365.82 222.82
n	3.2 1.4 0.56	1.7	-	1.8 2.8
A, s <sup>-1</sup>	5.77 X 10 <sup>16</sup> 1.26 X 10 <sup>12</sup> 1.13 X 10 <sup>6</sup>	2.13 X 10 <sup>7</sup>	-	7.58 X 10 <sup>26</sup> 9.12 X 10 <sup>11</sup>
ΔS* JK <sup>-1</sup> mol <sup>-1</sup>	69.78 -20.76 -137.77	-112.98	-	262.99 -24.39
R <sup>2</sup>	0.988 0.985 0.988	0.992	-	0.991 0.982



Figs. 3.70: The Anderson-Freeman plots for BSB4HCy



Figs. 3.71: The Anderson-Freeman plot for BSB4HM



Figs. 3.72: The Anderson-Freeman plots for BSB4HS

### PolySchiff bases

DSC and TG thermograms of TDADPCy, TDADPM, TDADPE and TDADPS at the heating rate of 10°C/min and in an N<sub>2</sub> atmosphere are presented in Figs. 3.73-3.77. Endothermic transition at 54.9°C for TDADPCy and 71.2°C and 123.1°C for TDADPM; and exothermic transition at 66.8°C for TDADPE and 91.9°C for TDADPS is due to some physical/chemical change, which is confirmed by no weight loss in corresponding TG curve at that temperature.

From Fig. 3.77 it is observed that polySchiff bases followed single step decomposition. T<sub>o</sub>, decomposition range, T<sub>max</sub>, % weight loss and % residue above 500°C are summarized in Table 3.21. Thermal stability order is TDADPE > TDADPS > TDADPCy > TDADPM. PolySchiff bases left 35-45% residue at 500°C.

Associated kinetic parameters were derived according to Eqns. 3.8, 3.12 and 3.13. Anderson-Freeman plots for polySchiff bases are shown in Figs. 3.78 to 3.81. The least square kinetic parameters along with regression coefficients are presented in Table 3.21 from which it is observed that polySchiff bases followed either integral or fractional order degradation kinetics. From the magnitudes of E and A, rigidity order of polySchiff bases is TDADPS > TDADPCy > TDADPE > TDADPM. Large and negative magnitude of  $\Delta S^*$  signified highly orderly state of transition state and vice versa. Selective degradation occurs from weak linkages (azomethine, ether, sulfone) in polySchiff base molecule and formation of free radicals result, which may further undergo a variety of reactions and degrade at higher temperature. High % residue (35-45%) above 500°C indicated formation of highly thermally stable crosslinked products. Thus, polySchiff bases possess good thermal stability but their main bottleneck is their solubility.

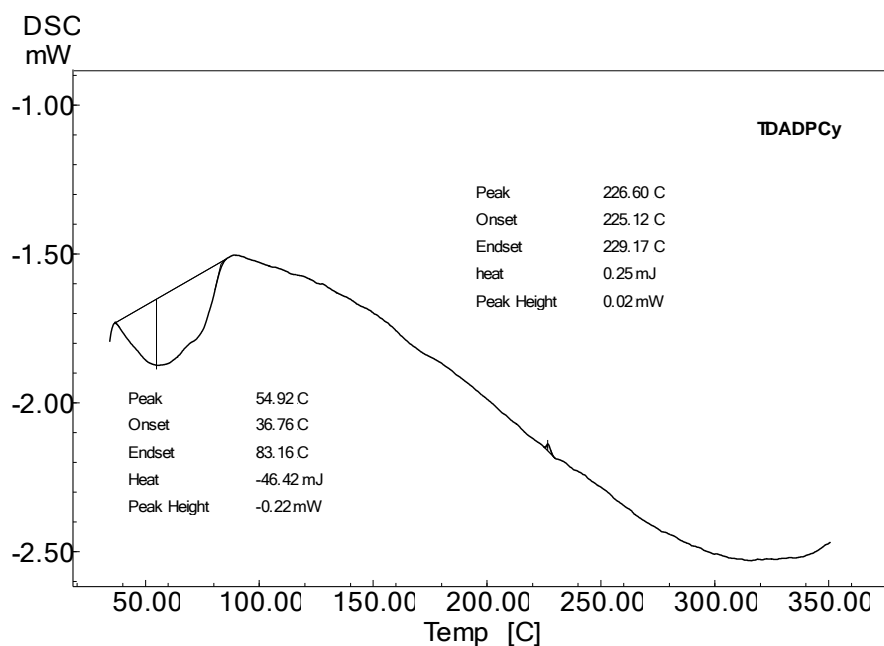


Fig. 3.73: DSC thermogram of TDADPCy at the heating rate of 10°C/min in an N<sub>2</sub> atmosphere.

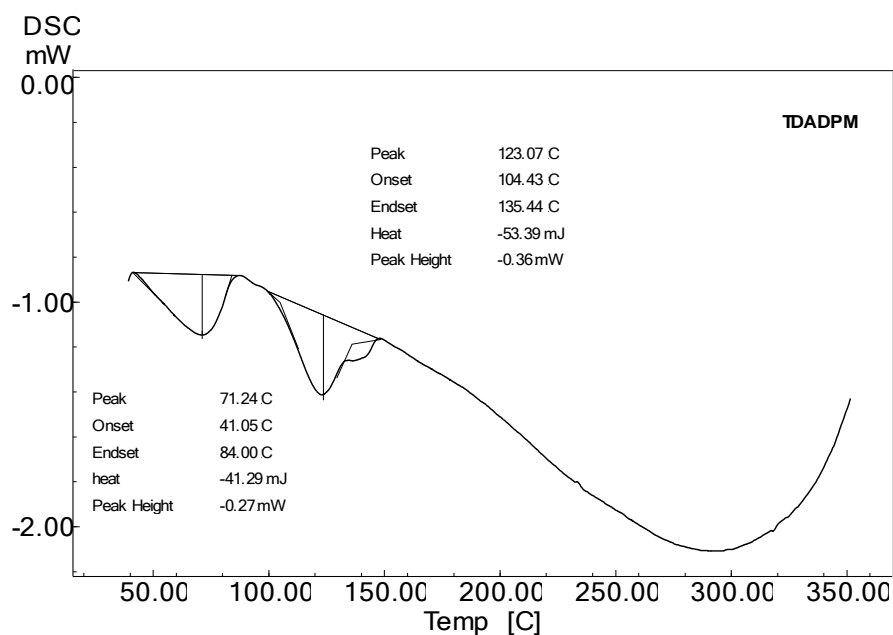


Fig. 3.74: DSC thermogram of TDADPM at the heating rate of 10°C/min in an N<sub>2</sub> atmosphere.

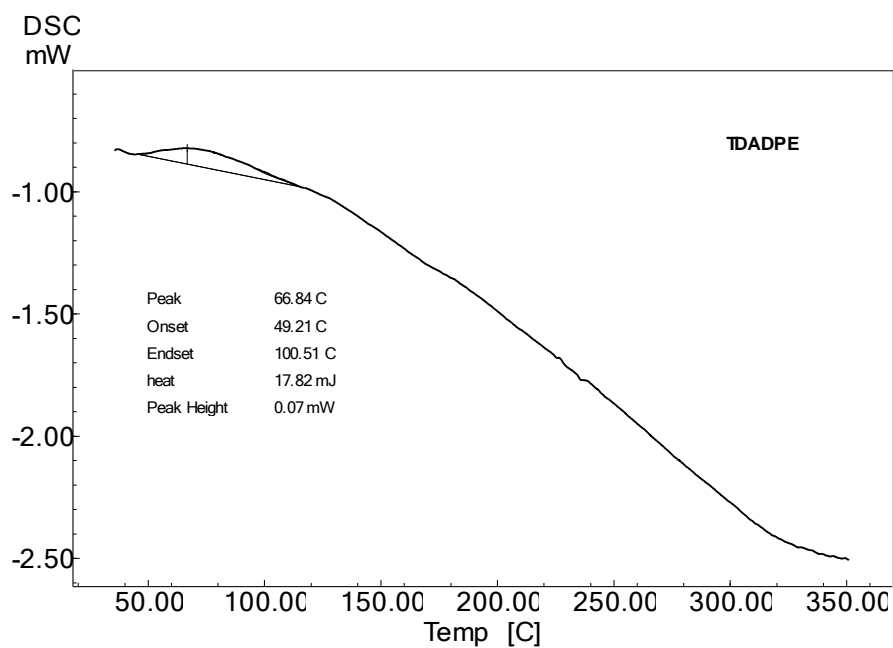


Fig. 3.75: DSC thermogram of TDADPE at the heating rate of 10°C/min in an N<sub>2</sub> atmosphere.

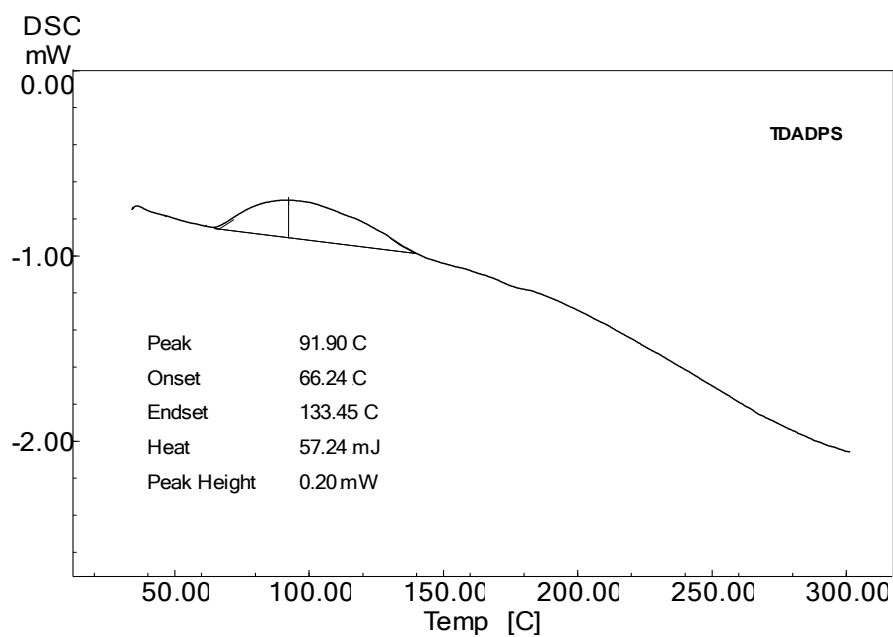


Fig. 3.76: DSC thermogram of TDADPS at the heating rate of 10°C/min in an N<sub>2</sub> atmosphere.

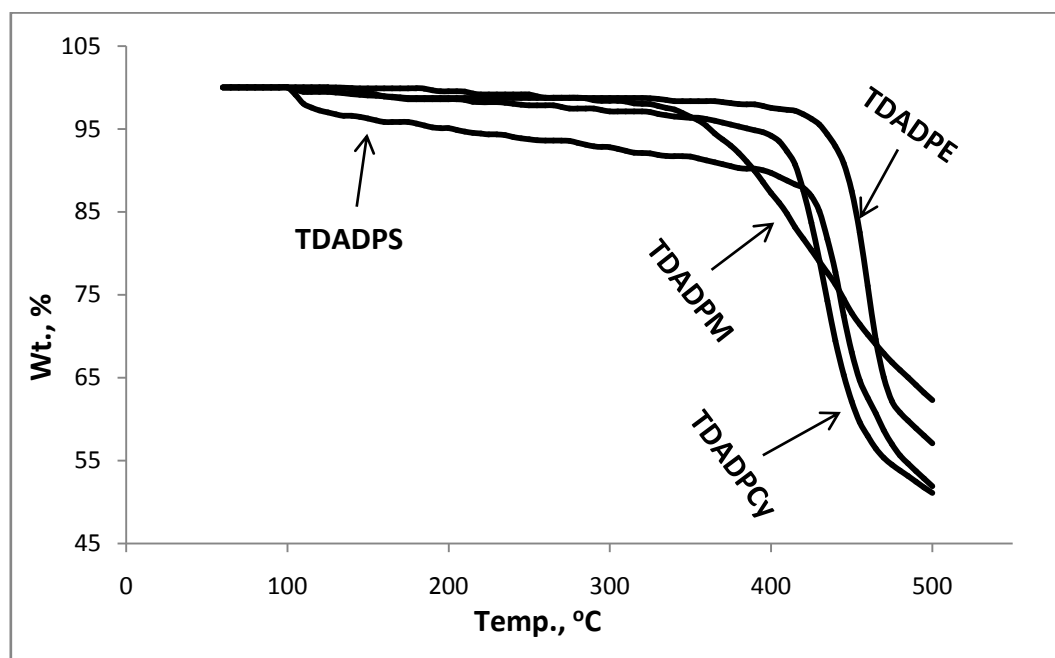
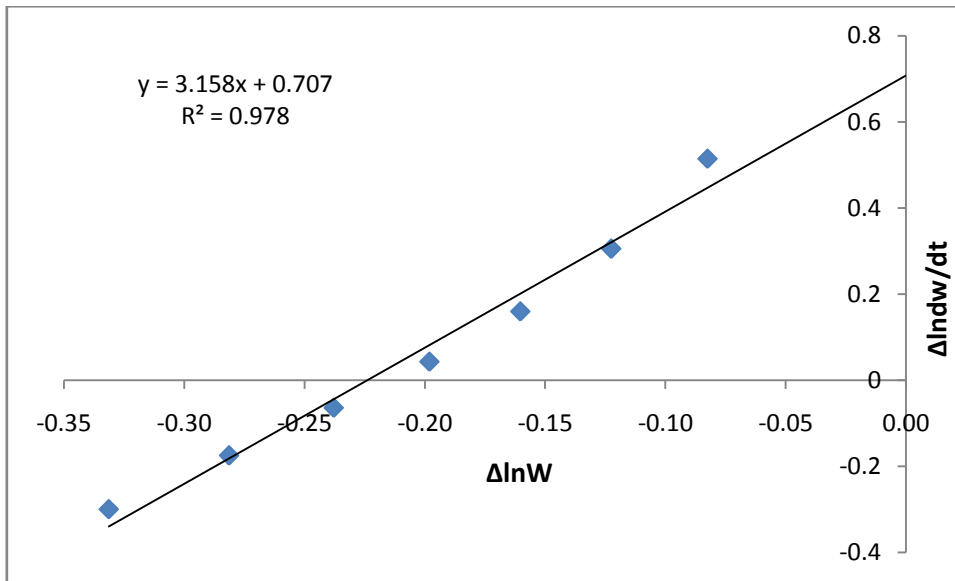


Fig. 3.77: TG thermograms of TDADPCy, TDADPM, TDADPE and TDADPS at the heating rate of 10<sup>0</sup>C/min in an N<sub>2</sub> atmosphere

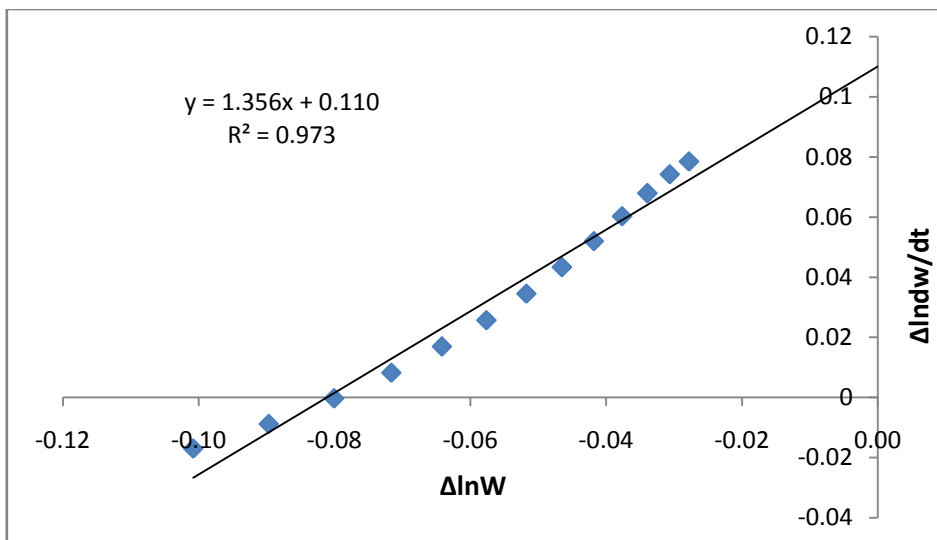
Table 3.21: DSC and TGA data of polySchiff bases

Parameter	PolySchiff bases			
	TDADPCy	TDADPM	TDADPE	TDADPS
DSC Transition Temp., °C	54.9(Endo.)	71.2(Endo.) 123.1(Endo.)	66.8(Exo.)	91.9(Exo.)
T <sub>0</sub> , °C	335	272	363	347
Decomposition range, °C	335-490	272-490	363-490	347-490
T <sub>max</sub> , °C	436.1	421.3	456.8	446.3
% Wt.loss	45	35	39	38
% Residue at 500°C	51.1	63.3	57.1	51.9
E, kJ mol <sup>-1</sup>	319.3	91.45	161.3	587.8
n	1.9	1.4	0.7	3.2
A, s <sup>-1</sup>	4.16 x 10 <sup>21</sup>	2.88 x 10 <sup>4</sup>	2.12 x 10 <sup>9</sup>	1.08 x 10 <sup>41</sup>
ΔS* JK <sup>-1</sup> mol <sup>-1</sup>	161.8	-166.6	-73.8	533.4
R <sup>2</sup>	0.981	0.973	0.953	0.978

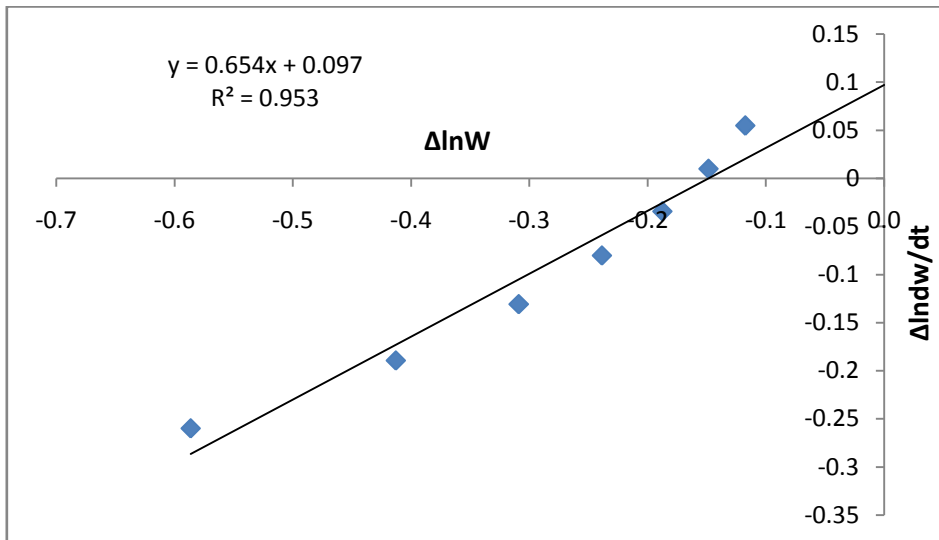




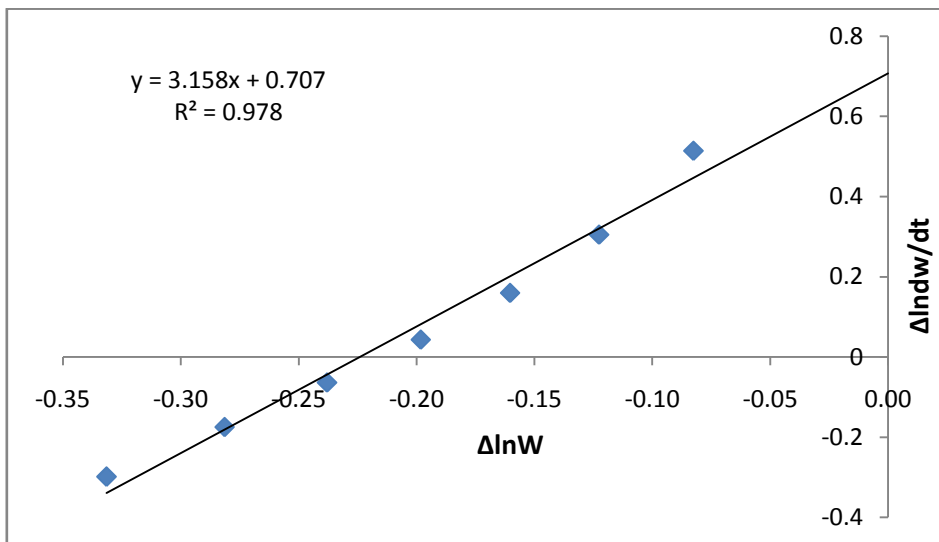
Figs. 3.78: The Anderson-Freeman plot for TDADPCy



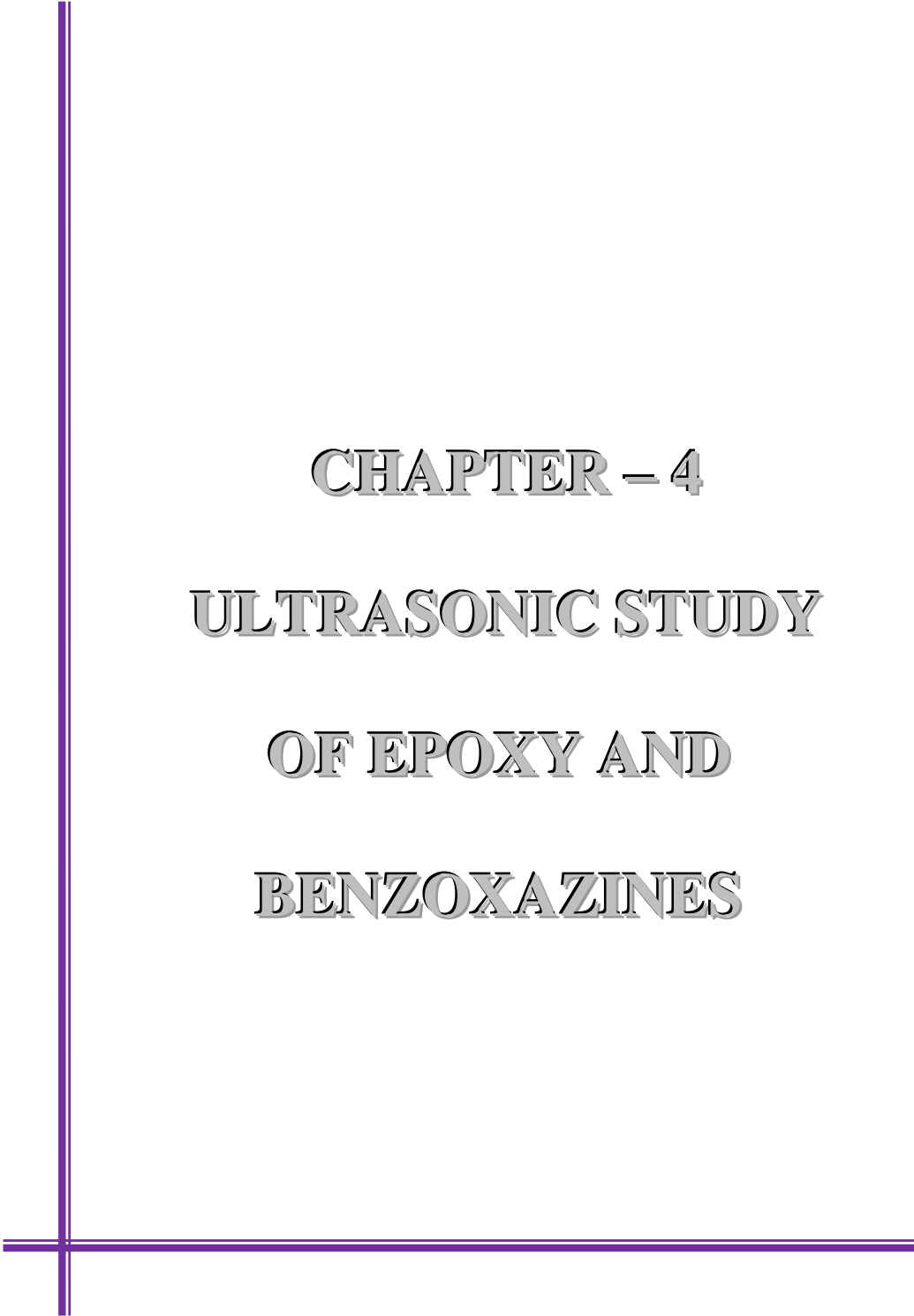
Figs. 3.79: The Anderson-Freeman plot for TDADPM



Figs. 3.80: The Anderson-Freeman plot for TDADPE



Figs. 3.81: The Anderson-Freeman plot for TDADPS



**CHAPTER – 4**

**ULTRASONIC STUDY**

**OF EPOXY AND**

**BENZOXAZINES**

## CHAPTER 4: ULTRASONIC STUDY OF EPOXY AND BISBENZOXAZINES

This chapter describes the density, viscosity and ultrasonic speed measurements of epoxy resin (ESB4HCy) solutions in THF and bisbenzoxazine (BSB4HCy, BSB4HM, BSB4HE and BSB4HS) solutions in 1,4 dioxane at 303, 308 and 313 K. Various acoustical parameters of these solutions are determined and discussed in light of effect of structure, concentration and nature of solvent.

Ultrasonic technology is now a days employed in a wide range of applications such as medicine, biology, industry, material science, agriculture, oceanography, dentistry, consumer industry, sonochemistry research, etc. due to its non-destructive nature [1-6].

It is most useful in investigating various organic liquids, polymers and aqueous and non-aqueous electrolyte solutions. It provides a wealth of information about molecular interactions, the nature and strength of interactions. It offers a rapid nondestructive method for characterizing materials. The extensive uses of polymers in technology have promoted ultrasonic studies to understand the structures of polymers and furnish knowledge on solvophilic or solvophobic nature of polymers [7-9].

1. G. L. Gooberman, "Ultrasonics, theory and applications", The English Universities Press Ltd., London, EC4 1968.
2. P. Resa, L. Elvira and F. M. Espinosa, "Concentration control in alcoholic fermentation processes from ultrasonic velocity measurements", *Food Research International*, 37, 587–594, 2004
3. W. Bell and R. A. Pethrik, "Ultrasonic investigations of linear and star shaped polybutadiene polymers in solutions of cyclohexane, hexane and ethylbenzene", *Polymer*. 23, 369-378, 1982.
4. Benedito, Antonio Mulet, J. Velasco, J. Jose and M. Carmen Dobarganes, "Ultrasonic assessment of oil quality during frying", *Agric. Food Chem.* 50, 4531-4536, 2002.
5. G. Chandrasekhar, P. Venkatesu and M. V. P. Rao, "Excess molar volumes and speed of sound of ethyl acetate and butyl acetate with 2-alkoxyethanols at 308.15 K", *J. Chem. Eng. Data*, 45, 590-597, 2000.

Applications in materials science include the determination of some properties of solids such as compressibility, specific heat ratios, elasticity, etc [10].

Ultrasound has also proved to be very useful for both soldering and welding. It is reported to improve the quality of homogenized milk. With the tracking of submarines, oceanographic applications include mapping of the sea bottom, discovering sunken ships and searching for schools of fish. Ultrasonic testing and evaluation techniques are widely used for obtaining information about micro structural and mechanical properties of metals and found wide applications in medical and biological fields [11-13].

Further, cleaning is the most common type of application of ultrasonic, which includes the removal of grease, dirt, rust and paint from metal, ceramic glass and crystal surfaces. Another area where ultrasonic is now-a-days being used, is to obtain the information about microstructures [14, 15].

- 
6. T. J. Mason, Editor., *Sonochemistry: "The uses of ultrasounds in Chemistry"*, Royal Soc. of Chem., 1990.
  7. M. Taghi Zafarani-Moattar and N. Kheyrabi. "Volumetric, ultrasonic, and transport properties of an aqueous solution of polyethylene glycol monomethyl ether at different temperatures", *J. Chem. Eng. Data*, 55, 3976–3982, 2010.
  8. N. M. Mehta, F. D. Karia and P. H. Parsania. "Effect of temperature on ultrasonic velocity and thermodynamic parameters of bisphenol-C-formaldehyde-acrylate resin solutions", *Fluid Phase Equilibria*, 262, 61-68, 2007.
  9. J. F. Rajasekaran, R. Balakrishnan and V. Arumugam, "Internal pressure-free volume relationship for rubber solutions", *J. Pure Appl. Ultrason.*, 19, 76-85, 1997.
  10. K. S. Suslick and G. J. Price, "Applications of ultrasound to materials chemistry" *Annu. Rev. Mater. Sci.*, 29, 295-326, 1999.
  11. Cunshan Zhou and Haile Ma, "Ultrasonic degradation of polysaccharide from a red algae (*Porphyra yezoensis*)" *J. Agric. Food Chem.* 54, 2223-2228, 2006.

Sound velocity measurements on condensation polymers and organic compounds in protic or aprotic solvents are carried out by Parsania et al. [16-35] and investigated the influence of solvent, concentration, temperature and the nature of the substituents on the structure of polymers and molecular interactions in the solutions under investigations.

12. J. J. Gilman, B. J. Cunningham and A. C. Holt, "Method for monitoring the mechanical state of a material", *Mater. Sci. and Engg.*, 39 A, 125-133, 1990.
13. J. Jaykumar, P. Palanichamy and R. Baldev. "Detection of hard intermetallics in  $\beta$ -quenched and thermally aged Zircaloy-2 using ultrasonic measurements", *J. Nuc. Mater.*, 255, 243-249, 1998.
14. H. Walaszek, H. P. Lieurade, C. Peyrac, J. Hoblos, and J. Rivenez, "Potentialities of ultrasonics for evaluating residual stresses: Influence of microstructure", *J. Pressure Vessel Technol.*, 124(3), 349-353, 2002.
15. J. D. Pandey, Y. Akhtar and A. K. Sharma, *Ind. J. Chem. Soc.*, 37,1094-1098, 1998.
16. M. M. Kamani and P. H. Parsania, "Ultrasonic velocity studies of chloroform and dichloroethane solutions of cardo polysulfone of 1,1'-bis(3-methyl-4-hydroxyphenyl)-cyclohexane and 4,4'-difluoro diphenyl sulphone" *J. Pure and Appl. Ultrason.*, 18, 46-54, 1996.
17. M. M. Kamani and P. H. Parsania, "Ultrasonic studies of chloroform-dioxane binary solutions of polysulfonate of 1,1'-bis(3-methyl-4-hydroxyphenyl) cyclohexane with toluene-2,4-disulfonyl chloride", *J. Polym. Mater.* 13, 191-194, 1996.
18. R. Shah and P. H. Parsania, "Acoustic properties of poly(4,4'-cyclohexylidene-2,2'-dimethyldiphenylene -3,3'- benzophenone disulfonates) in chlorinated and aprotic solvents at 30°C", *Euro. Polym. J.*, 33(8), 1245-1250, 1997.
19. K. M. Rajkotia and P. H. Parsania, "Studies on acoustical properties of poly (4,4'-cyclopentylidene diphenylene-2,4-disulfonate) in different solvents at 30°C", *Eur. Polym. J.*, 33, 1005-1010, 1997.
20. A. R. Shah and P. H. Parsania, "Acoustic properties of poly (4,4'-cyclohexylidene-R,R'-diphenylene-3,3'-benzophenone disulfonates) at

- 30°C”, *Eur. Polym. J.*, 33(8), 1245-1250, 1997.
21. M. M. Kamani and P. H. Parsania “Ultrasonic studies of solutions of polysulfonate of 1,1'-bis (3-methyl-4-hydroxyphenyl) cyclohexane and toluene-2,4-disulfonyl chloride”, *J. Pure and Appl. Ultrason.*, 19, 89-93, 1997.
  22. M. R. Sanariya and P. H. Parsania, “Studies on sound velocity and acoustical parameters of epoxy resins based on bisphenol-C”, *J. Pure and Appl. Ultrason.*, 22, 54-59, 2000.
  23. F. D. Karia and P. H. Parsania, “Ultrasonic velocity studies and allied parameters of poly (4, 4'-cyclohexylidene-R, R'-diphenylene diphenyl methane-4,4'-disulfonate) solutions at 30°C”, *Eur. Polym. J.*, 36, 519-524, 2000.
  24. D. R. Godhani, Y. V. Patel and P. H. Parsania, “Ultrasonic velocity and acoustical parameters of poly (4,4'-diphenyl phthalide diphenyl methane-4, 4'-disulfonate)-DMF solutions at 30, 35 and 40 °C” *J. Pure and Appl. Ultrason.*, 23, 58-62, 2001.
  25. D. R. Godhani and P. H. Parsania, “Studies on acoustical properties of poly (4, 4'-diphenylphthalide-diphenyl-4, 4'disulfonate) at 30°C”, *J. Ind. Chem. Soc.*, 79, 620-623, 2002.
  26. Y. V. Patel, D. R. Bhadja and P. H. Parsania “Ultrasonic study of poly (R, R', 4, 4'-cyclohexylidene diphenylene phosphorochloridate)-DMF solutions at different temperatures”, *J. Pure and Appl. Ultrason.*, 24, 47-53, 2002.
  27. D. R. Godhani, V. M. Kagathara and P. H. Parsania, “Investigation of molecular interactions in polysulfonates of phenolphthalein with 4, 4'-diphenylether/3,3'-benzophenone sulfonyl chloride solutions at different temperatures”, *J. Polym. Mater.*, 19, 343-348, 2002.
  28. Y. V. Patel and P. H. Parsania, “Ultrasonic velocity study of poly(R,R',4,4'-cyclohexylidene diphenylene diphenylether-4,4'-disulfonate solutions at 30, 35 and 40 °C”, *Eur. Polym. J.*, 38(10), 1971-1977, 2002.
  29. V. M. Kagathara and P. H. Parsania, “Studies on ultrasonic velocity and acoustical parameters of bromo epoxy resins of bisphenol-C solutions at different temperatures “, *Europ. Polym. J.*, 38(3), 607-610, 2002.

**Materials and methods**

Solvents used in the present investigation tetra hydro furan (THF) and 1, 4-dioxan (DO) used in the present study were of laboratory grade and purified according to literature methods [36]. Ultrasonic speed, density and velocity measurements of pure solvents: THF and 1,4-dioxane and epoxy resin (ESB4HCy) and bisbenzoxazines (BSB4HCy, BSB4HM, BSB4HE and BSB4HS) solutions (0.5, 1.0, 1.5 and 2.0 wt %) were carried out at 303, 308 and 313 K, by using F-80 Ultrasonic Interferometer (2 MHz) (Mittal Enterprises, New Delhi), specific gravity bottle and Ubbelohde suspended level viscometer. Ultrasonic speed (U), density ( $\rho$ ) and viscosity ( $\eta$ ) measurements were accurate to  $\pm 0.2\%$ ,  $\pm 0.1 \text{ kgm}^{-3}$  and  $\pm 0.1\%$ , respectively

30. B. G. Manwar, S. H. Kavthia and P. H. Parsania, "Ultrasonic velocity study of poly (R, R', 4, 4'-cyclohexylidene diphenylene toluene-2, 4-disulfonates) solutions at 30, 35 and 40°C", J. Pure and Appl. Ultrason., 26, 49-57, 2004.
31. R. R. Amrutia and P. H. Parsania, "Ultrasonic velocity and acoustical parameters of poly (4, 4'-cyclohexylidene diphenyloxy-4, 4'-diphenylene-sulfone) solutions at different temperatures", J. Sci. & Ind. Res., 65, 905-911, 2006.
32. B. J. Gangani and P. H. Parsania, "Density, viscosity and ultrasonic velocity studies of cardo group containing symmetric double Schiff bases solutions at 303, 308 and 313 K", J. Ind. Chem. Soc., 86(9), 942-949, 2009.
33. B. D. Bhuva and P. H. Parsania, "Effect of temperature and solvents on ultrasonic velocity and allied acoustical parameters of epoxy oleate of 9, 9'-bis (4-hydroxy phenyl) anthrone-10 solutions", J. Sol. Chem., In Press.
34. B. D. Bhuva and P. H. Parsania, "Synthesis, speed of ultrasound and associated acoustical parameters of epoxy acrylate of 9, 9'-bis (4-hydroxy phenyl) anthrone-10 solutions", J. Appl. Polym. Sci., In Press.
35. B. D. Bhuva and P. H. Parsania, "Effect of temperature and solvents on speed of ultrasound and allied acoustical parameters of epoxy ricinol of 9, 9'-bis (4-hydroxy phenyl) anthrone-10 solutions", J. Ind. Chem. So., In Press.



### Density measurements

Densities of pure solvents and solutions were measured by means of specific gravity bottle at  $308 \pm 0.1$  K by determining the weights of distilled water, solvents and solutions. The density ( $\rho$ ) was calculated according to Eqn. 4.1 with an accuracy of  $\pm 0.1 \text{ kgm}^{-3}$ .

$$\rho = \frac{\text{Wt.ofsolvent/solution}}{\text{Wt.ofwater}} \quad \dots 4.1$$

### Viscosity measurements

The method for determining the dynamic viscosity or coefficient of viscosity of liquids relies on Stoke's law.

In present investigation, suspended level viscometer developed by Ubbelohde was used. The viscometer was washed with chromic acid, distilled water, acetone and then dried at  $50^\circ\text{C}$  in an oven. Viscometer was suspended in a thermostat at  $308 \pm 0.1$  K and measured quantity of the distilled water / solvent / solution was placed into the viscometer reservoir by means of a pipette and thermally equilibrated for about 10 min. The efflux time of liquid between two marks was measured by means of digital stopwatch with an accuracy of  $\pm 0.01$  sec. Three replicate measurements on each liquid were made and the arithmetic mean was considered for the purpose of calculations.

Using the flow times ( $t$ ) and known viscosity of standard (water) sample, the viscosities of solvents and solutions were determined according to Eqn. 4.2 :

$$\frac{\eta_1}{\eta_2} = \frac{t_1\rho_1}{t_2\rho_2} \quad \dots 4.2$$

Where  $\eta_1$ ,  $\rho_1$ ,  $t_1$  and  $\eta_2$ ,  $\rho_2$ ,  $t_2$  are the viscosities, densities and flow times of standard and unknown samples, respectively.

---

36. E. S. Proskaur and A. Weisberger, "Techniques of organic solvents", New York. 1955.

### Sound velocity measurements

Ultrasonic interferometer (F-80) (Mittal Enterprises, New Delhi) was used in the present investigation. The working of interferometer was tested by measuring the sound velocity of pure solvents: Tetrahydrofuran (THF), 1, 4-dioxane (DO) and comparing the results with literature data.

The measuring cell (2 MHz) with quartz crystal was filled with the solvent/solution and then micrometer with reflector plate was fixed. The circulation of water from the thermostat (at 303, 308 and 313 K) was started and the experimental liquid in the cell is allowed to thermally equilibrate. The high frequency generator was switched on and the micrometer was rotated very slowly so as to obtain a maximum or minimum of the anode current. A number of maximum readings of anode current ( $n$ ) were counted. The total distance ( $d$ ) travelled by the micrometer for  $n=10$  were recorded. The wave length ( $\lambda$ ) was determined according to Eqn. 4. 3:

$$\lambda = \frac{2d}{n} \quad \dots 4.3$$

The ultrasonic speed ( $U$ ) of solvents and solutions were calculated from the wave length ( $\lambda$ ) and frequency ( $F$ ) according to Eqn. 4.4:

$$U = \lambda.F \quad \dots 4.4$$

### Theoretical equations for acoustical parameters

#### 1. Adiabatic compressibility

Adiabatic compressibility ( $\kappa_a$ ) can be evaluated according to Newton and Laplace:

$$\kappa_a = \frac{1}{U^2 \rho} \quad \dots 4.5$$

#### 2. Specific acoustical impedance

$$Z = U\rho \quad \dots 4.6$$

#### 3. Rao's molar sound function

Rao's molar sound function ( $R$ ) can be evaluated by employing a method suggested by Bagchi et. al [37]

$$R = \frac{M}{\rho} U^{1/3} \quad \dots 4.7$$

The apparent molecular weight (M) of the solution can be calculated according to Eqn. 4.8:

$$M = M_1W_1 + M_2W_2 \quad \dots 4.8$$

Where  $W_1$ ,  $M_1$  and  $W_2$ ,  $M_2$  are weight fractions and molecular weights of the solvent and solute, respectively.

#### 4. Van der Waal s constant

Van der Waals constant (b) [38] can be calculated according to Eqn.4.9

$$b = \frac{M}{\rho} \left[ 1 - \left[ \frac{RT}{MU^2} \right] \left[ \sqrt{1 + \frac{MU^2}{3RT}} - 1 \right] \right] \quad \dots 4.9$$

Where R (8.314 JK<sup>-1</sup> mol<sup>-1</sup>) is the gas constant and T (K) is the absolute temperature.

#### 5. Internal pressure

Internal pressure ( $\pi$ ) can be evaluated according to Suryanarayana and Kuppuswamy [39]:

$$\pi = b' RT \left( \frac{K\eta}{U} \right)^{1/2} \frac{\rho^{2/3}}{M^{7/6}} \quad \dots 4.10$$

Where R=8.3143 JK<sup>-1</sup> mol<sup>-1</sup> is the gas constant and b'=2, is the packing factor and K=4.28 X 10<sup>9</sup> is a constant. The internal pressure ( $\pi$ ) depends on temperature, density, ultrasonic speed and specific heat at a constant pressure.

#### 6. Classical absorption coefficient

The classical absorption coefficient ( $\alpha/f^2$ )<sub>cl</sub> has its origin in the viscosity of the medium and it is proposed by Subrahmanyam et. al [40]:

- 
37. S. Bagchi, S. K. Nema and R. P. Singh. "Ultrasonic and viscometric investigation of ISRO polyol in various solvents and its compatibility with polypropylene glycol", Eur. Polym. J., 22 (10) 851, 1989.
  38. P. Vigoureux, 'Ultrasonic', Chapman and Hall, London, 1952.
  39. C.V.Suryanarayana and J.Kuppuswamy, Indian J. Acoust Soc., 9(1), 4, 1954.
  40. T. V. S. Subrahmanyam, A. Viswanadhasharma and K. Subbarao, Indian J. Acoust. Soc. 7(1), 1, 1979.

$$\left(\frac{\alpha}{f^2}\right)_{cl} = \frac{8\pi^2\eta}{3U^3\rho} \quad \dots 4.11$$

### 7. Viscous relaxation time

The resistance offered by viscous force in the flow of sound wave appears as a classical absorption associated with it

is the viscous relaxation time ( $\tau$ ):

$$\tau = \frac{4\eta}{3\rho U^2} \quad \dots 4.12$$

### 8. Solvation number

The solvation number (Sn) can be evaluated according to Passynsky [41] method. The number of grams of solvent connected in the apparent solvation of 1 g of solute assuming that the solvent molecules participating in the solvation are effectively incompressible due to strong localized electronic fields, is expressed as:

$$n = \left[ 1 - \frac{\kappa_a(100 - X)}{\kappa_{a1}X} \right] \quad \dots 4.13$$

Where X is the number of grams of solute in 100 g of the solution.

The solvation number (Sn) can be expressed as:

$$Sn = \frac{M_2}{M_1 \left( 1 - \frac{\kappa_a}{\kappa_{a1}} \right) \left( \frac{100 - X}{X} \right)} \quad \dots 4.14$$

Where  $M_1$  and  $M_2$  are the molecular weights of solvent and solutes, respectively.

### 9. Apparent molar volume

Apparent molar volume [42] can be calculated according to Eqn.4.15:

$$\phi_{V2} = \frac{M}{\rho_1} \left[ 1 - \frac{(100)}{C} (\rho - \rho_1) \right] \quad \dots 4.15$$

Where, M is the repeat unit of epoxy resins and  $\rho_1$  and  $\rho$  are the densities of solvent and solution, respectively.

## 10. Apparent molar compressibility

Apparent molar compressibility [43] can be calculated according to Eqn. 4.16:

$$\phi\kappa_a = M_2\kappa_{a1} \left[ \frac{100}{C} \left( \frac{\kappa_a}{\kappa_{a1}} - \frac{\rho}{\rho_1} \right) + \frac{1}{\rho_1} \right] \quad \dots 4.16$$

Where C is the concentration in dl/g and  $\kappa_{a1}$  and  $\kappa_a$  are the adiabatic compressibility of solvent and solutions, respectively.

## 11. Free volume

Free volume [44] can be calculated according to Eqn. 4.17:

$$V_f = \left[ \frac{MU}{K\eta} \right]^{3/2} \quad \dots 4.17$$

## 12. Inter molecular free path length

Inter molecular free path length ( $L_f$ ) can be evaluated according to Eqn. 4.18, as proposed by Jacobson [45]:

$$L_f = K.(\kappa_s)^{1/2} \quad \dots 4.18$$

where  $\kappa_a = (93.875 + 0.375T) \times 10^{-8}$  is Jacobson's constant and temperature dependent.

In order to understand the effect of concentration, temperature, nature of solvents and nature of substituents of solute, various acoustical parameters were determined by using the experimental data on  $\rho$ ,  $\eta$  and U of solutions at 303, 308 and 313 K according to above mentioned standard relations. The concentration dependence acoustical parameters provide a valuable information about strength of molecular interactions occurring in the solutions. Various acoustical parameters were fitted with concentration according to least square method to ascertain concentration dependences of molecular interactions occurring in solutions and hence solvophilic or solvophobic nature of compounds under investigation.

---

41. Z. Passynsky, Acta Phys. Chem. USSR, 22, 317, 1943.

42. P. R. Chowdhury, Ind. J. Chem., 7, 692, 1969.

## Results and Discussion

### Ultrasonic study of epoxy resin

The  $\rho$ ,  $\eta$  and  $U$  data of THF and ESB4HCy solutions at three different temperatures are presented in Table-4.1 from which it is observed that  $\rho$  decreased linearly with concentration ( $C$ ) and temperature ( $T$ ), while  $\eta$  and  $U$  both increased linearly with  $C$  and decreased with  $T$ . The decrease of  $\rho$  with  $C$  is due to solvation of the resin. Because of solvation both apparent molecular mass and volume change. In present case apparent molecular volume is predominant over apparent molecular mass and hence lowering in  $\rho$  with  $C$ . These data (Figs. 4.1-4.3) are correlated with  $C$  and  $T$  and least square equations along with regression coefficients ( $R^2$ ) are summarized in Table-4.2, from which excellent correlation is observed ( $R^2=0.992-0.999$ ). The variation of  $\eta$  and  $U$  are considerably more than that of  $\rho$  due to specific molecular interactions (association, deassociation, unfolding, expansion, etc). Molecular interactions are governed by the forces acting amongst solvent and solute molecules and hence intermolecular motion is affected accordingly [46, 47]. Attractive forces result into molecular association (solvation), i.e. modification of the structure of the resin. Thus,  $\rho$ ,  $\eta$  and  $U$  are affected by

- 
43. C. V. Surayanarayana and J. Kuppusami, *J. Acoust. Soc. India*, 4, 75, 1976.
  44. S. Das, R. P. Singh and S. Maiti, "Ultrasonic velocities and Rao formulism in solution of polyesterimides", *Polym-Bull.*, 2, 403-409, 1980.
  45. B. Jacobson, *Nature*, 173, 772, 1954.
  46. W. Bell and R. A. Pethrik, "Ultrasonic investigations of linear and star shaped polyutadiene polymers in solutions of cuclohexane, hexane and ethylbenzene", *Polymer*, 23, 369-378, 1982.
  47. H. J. Mueller, J. Lauterjung, F. R. Schilling, C. Lathe and G. Nover, "Symmetric and asymmetric interferometric method for ultrasonic compressional and shear wave velocity measurements in piston-cylinder and multi-anvil high-pressure apparatus", *Eur. J. of Mineralogy*, 14, 581-585, 2002.

molecular interactions; Van der Waals, H-bonding, dipolar and London type forces between solvent and solute molecules; which result into the aggregation of solvent molecules around solute molecules as result of structural modification. Thus, nature of solvent and resin play an important role in determining transport and other properties.

**Table-4.1: The density ( $\rho$ ), viscosity ( $\eta$ ), ultrasonic speed (U) and standard deviation (s) data of epoxy resin ESB4HCy in THF at 303, 308 and 313 K.**

Conc., %	Density $\rho$ , kg/m <sup>3</sup>	Viscosity $\eta$ , mPa.s	Ave. Dist. d, mm	Wave length $\lambda$ , mm	U, ms <sup>-1</sup> (F=2MHz)	Std. devi., mm ( $\pm$ )
303 K						
0	883.3	0.496	3.082	0.6164	1232.8	0.0021
0.5	892.2	0.517	3.093	0.6186	1237.2	0.0084
1.0	891.6	0.532	3.101	0.6202	1240.4	0.0083
1.5	890.4	0.549	3.110	0.6220	1244.0	0.0047
2.0	889.3	0.567	3.119	0.6238	1247.6	0.0066
308 K						
0	881.3	0.442	3.064	0.6128	1225.6	0.0048
0.5	890.1	0.477	3.075	0.6150	1230.0	0.0044
1.0	889.2	0.490	3.080	0.6160	1232.0	0.0033
1.5	888.0	0.502	3.093	0.6186	1237.2	0.0053
2.0	887.1	0.520	3.104	0.6208	1241.6	0.0037
313 K						
0	875.5	0.396	3.031	0.6062	1212.4	0.0023
0.5	889.3	0.443	3.040	0.6080	1216.0	0.0029
1.0	887.8	0.454	3.047	0.6094	1218.8	0.0023
1.5	886.5	0.466	3.052	0.6104	1220.8	0.0020
2.0	885.7	0.477	3.060	0.6120	1224.0	0.0017



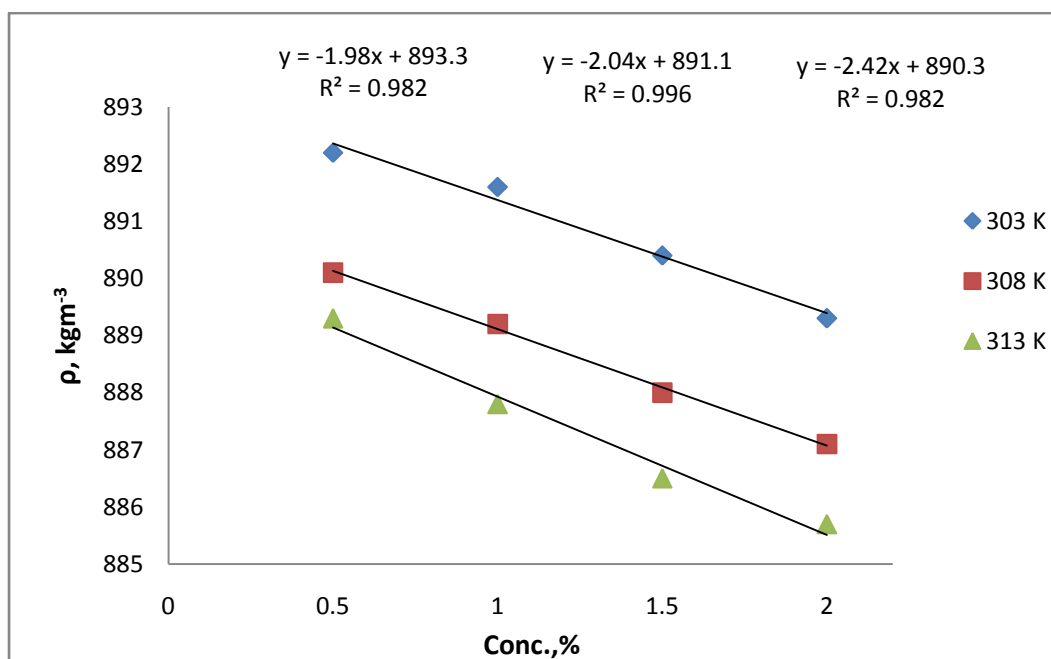


Fig. 4.1: The plots of density ( $\rho$ ) against concentration (%) of ESB4HCy in THF at 303, 308 and 313 K.

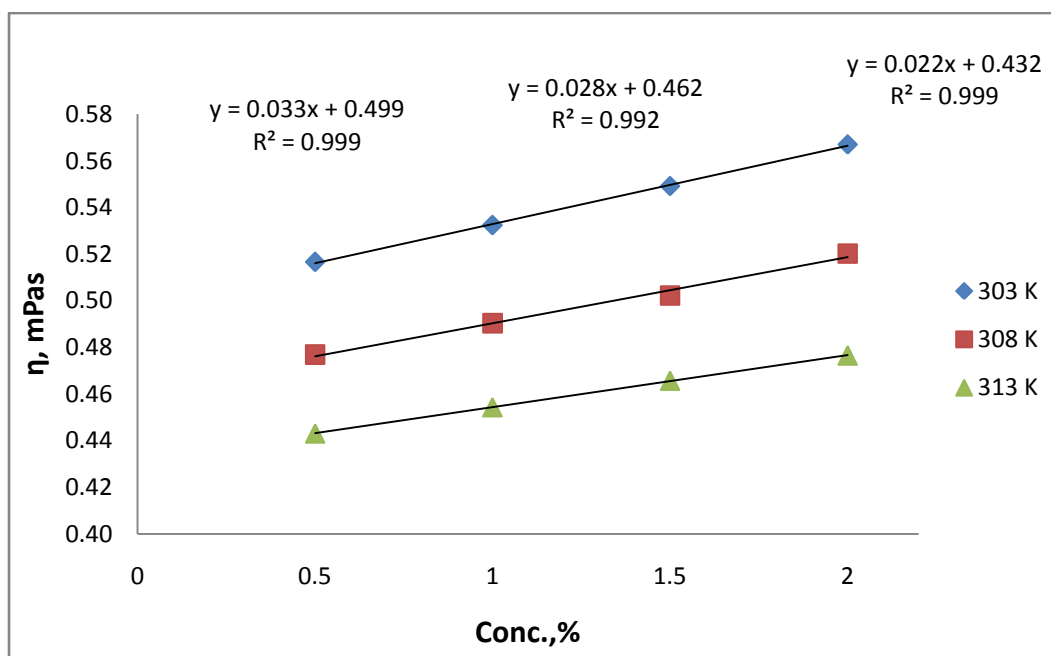
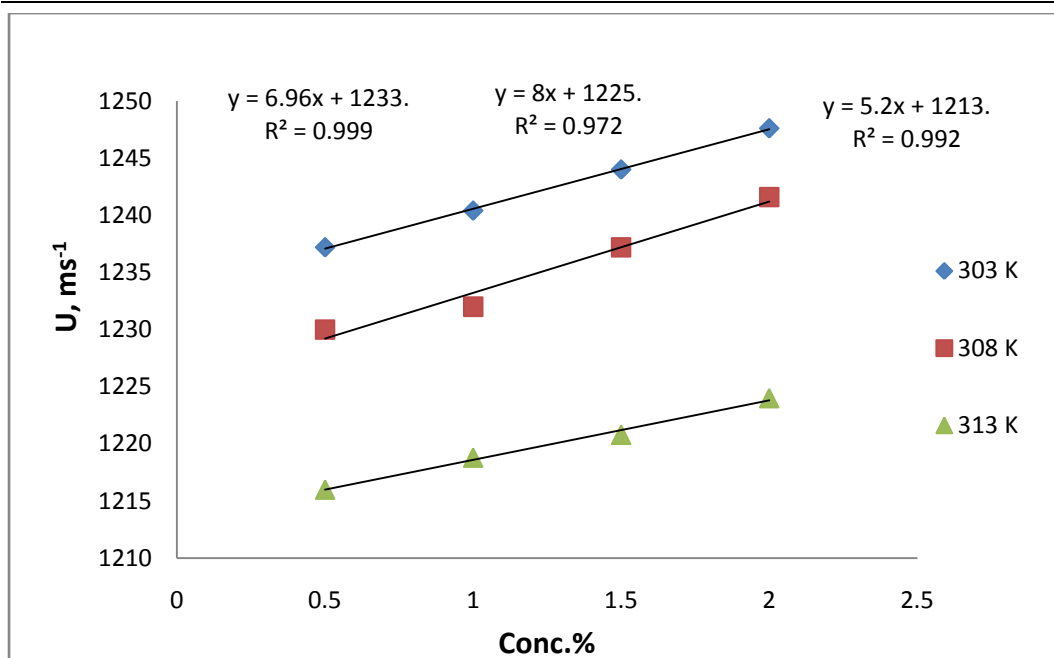


Fig. 4.2: The plots of viscosity ( $\eta$ ) against concentration (%) of ESB4HCy in THF at 303, 308 and 313 K.



**Fig. 4.3:** The plots of sound velocity (U) against concentration (%) of ESB4HCy in THF at 303, 308 and 313 K.

**Table-4.2: The correlation equations and regression coefficients of epoxy resin ESB4HCy in THF at 303, 308 and 313 K.**

Parameter	Correlation equation and regression coefficient, R <sup>2</sup>		
	303 K	308 K	313 K
$\rho$ , kgm <sup>-3</sup>	-1.98 C + 893.3 R <sup>2</sup> = 0.982	-2.04 C + 891.1 R <sup>2</sup> = 0.996	-2.42 C + 890.3 R <sup>2</sup> = 0.982
$\eta$ , mPa.s	0.033 C + 0.499 R <sup>2</sup> = 0.999	0.028 C + 0.462 R <sup>2</sup> = 0.992	0.022 C + 0.432 R <sup>2</sup> = 0.999
U, ms <sup>-1</sup>	6.96 C + 1233. R <sup>2</sup> = 0.999	8 C + 1225. R <sup>2</sup> = 0.972	5.2 C + 1213. R <sup>2</sup> = 0.992
Z, 10 <sup>6</sup> kg.m <sup>-2</sup> .s <sup>-1</sup>	0.003 C + 1.102 R <sup>2</sup> = 0.998	0.002 C <sup>2</sup> - 0.000 C + 1.094, R <sup>2</sup> = 0.985	0.001 C <sup>2</sup> - 0.001 C + 1.081, R <sup>2</sup> = 0.943
$\kappa_a$ , 10 <sup>-10</sup> Pa <sup>-1</sup>	-0.043 C + 7.628 R <sup>2</sup> = 0.973	-0.078 C + 7.474 R <sup>2</sup> = 0.963	-0.065 C + 7.355 R <sup>2</sup> = 1
L <sub>f</sub> , 10 <sup>-11</sup> m	-0.016 C + 5.782 R <sup>2</sup> = 0.973	-0.030 C + 5.724 R <sup>2</sup> = 0.963	-0.025 C + 5.678 R <sup>2</sup> = 1
R, 10 <sup>-4</sup> m <sup>10/3</sup> .s <sup>-1/3</sup> .mol <sup>-1</sup>	5.425 C + 10.50 R <sup>2</sup> = 1	5.437 C + 10.53 R <sup>2</sup> = 1	5.414 C + 10.53 R <sup>2</sup> = 1
b, 10 <sup>-5</sup> m <sup>3</sup>	5.018 C + 9.7 R <sup>2</sup> = 1	4.997 C + 9.697 R <sup>2</sup> = 1	4.972 C + 9.673 R <sup>2</sup> = 1
$\pi$ , 10 <sup>8</sup> Pa	-0.685 C + 2.869 R <sup>2</sup> = 0.977	-0.665 C + 2.761 R <sup>2</sup> = 0.977	-0.670 C + 2.765 R <sup>2</sup> = 0.977
V <sub>f</sub> , 10 <sup>-7</sup> m <sup>3</sup>	3.332 C + 4.250 R <sup>2</sup> = 0.999	2.935 C + 3.941 R <sup>2</sup> = 0.999	2.542 C + 3.568 R <sup>2</sup> = 1
$\tau$ , 10 <sup>-13</sup> s	0.278 C + 4.899 R <sup>2</sup> = 0.999	0.226 C + 4.607 R <sup>2</sup> = 0.99	0.198 C + 4.395 R <sup>2</sup> = 0.998
( $\alpha/f^2$ ) <sub>cl</sub> 10 <sup>-15</sup> , s <sup>2</sup> m <sup>-1</sup>	0.395 C + 7.835 R <sup>2</sup> = 0.999	0.310 C + 7.418 R <sup>2</sup> = 0.985	0.288 C + 7.144 R <sup>2</sup> = 0.997

Various acoustical parameters ( $Z$ ,  $\kappa_a$ ,  $L_f$ ,  $R$ ,  $b$ ,  $\pi$ ,  $V_f$ ,  $\tau$  and  $(\alpha/f^2)_{cl}$ ) of ESB4HCy solutions are correlated with  $C$  and  $T$  (Figs. 4.4-4.12), and the least square equations and  $R^2$  are summarized in Table 4.2. Polynomial regression analysis carried out wherever nonlinear behavior is observed.  $Z$  (except at 308 and 313 K),  $R$ ,  $b$ ,  $V_f$ ,  $\tau$  and  $(\alpha/f^2)_{cl}$  increased linearly with  $C$ , and decreased with  $T$  except  $R$ ,  $b$  and  $V_f$ . Practically no temperature effect is observed on  $R$  and  $b$ .  $V_f$  increased with  $T$  due to increase of free path length.  $\kappa_a$ ,  $L_f$ , and  $\pi$  decreased linearly with  $C$  and increased linearly with  $T$ . A fairly good to excellent correlation between said parameters and  $C$  is observed. Linear or nonlinear increase or decrease of above mentioned parameters suggested the existence of strong molecular interactions in the resin solutions. Increasing temperature has two opposite effects namely structure formation (intermolecular association) and structure destruction formed previously. The structure forming tendency is primarily due to solvent-solute interactions, while destruction of structure formed previously is due to thermal fluctuations. When thermal energy is greater than that of interaction energy, it causes destruction of structure formed previously.

Strong molecular interactions are further supported by positive values of  $S_n$  (Fig.4.13). Nonlinear increase of  $S_n$  with  $C$  and  $T$  confirmed existence of strong solvent-solute and solute-solute interactions in the solutions. Decrease of  $S_n$  above 1 % concentration at 313 K is due to powerful solute-solute interactions over solvent-solvent interactions. Dipole-dipole interactions of the opposite type favor structure formation while, of the some type favor structure breaking tendency. Azomethine, hydroxyl and ether groups ESB4HCy are polar groups besides other alkyl and aromatic groups, which may interact with THF molecules under set of experimental conditions (concentration, temperature, pressure, etc). Thus, studied parameters provided solvophilic nature of the resin. Knowledge of interactions in the solutions is useful in resin processing.

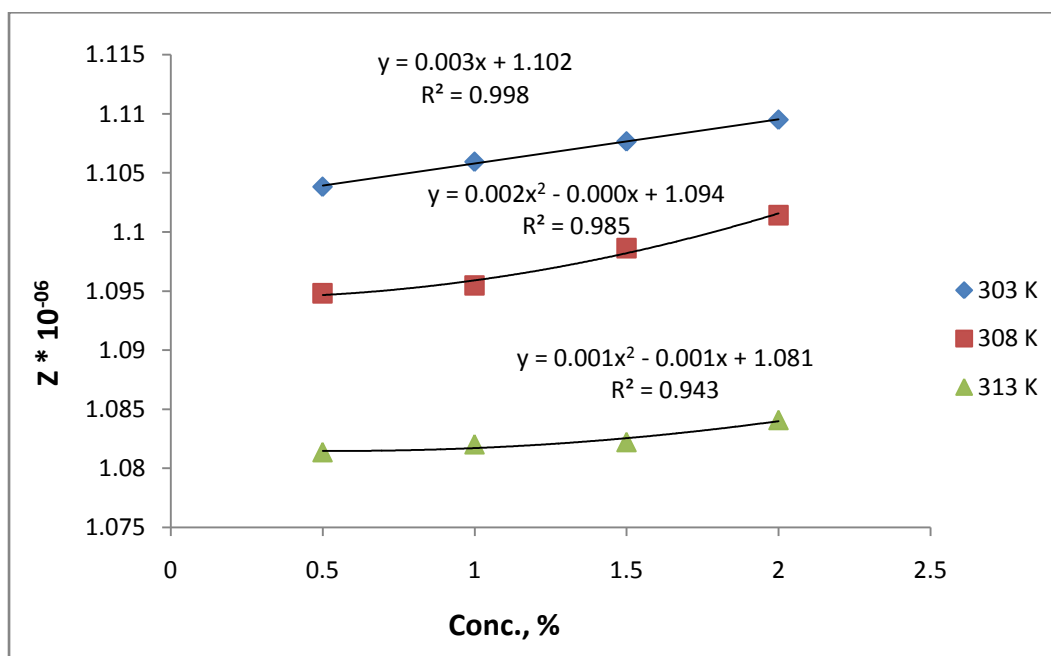


Fig. 4.4: The plots of specific acoustical impedance ( $Z$ ) against concentration (%) of ESB4HCy in THF at 303, 308 and 313 K.

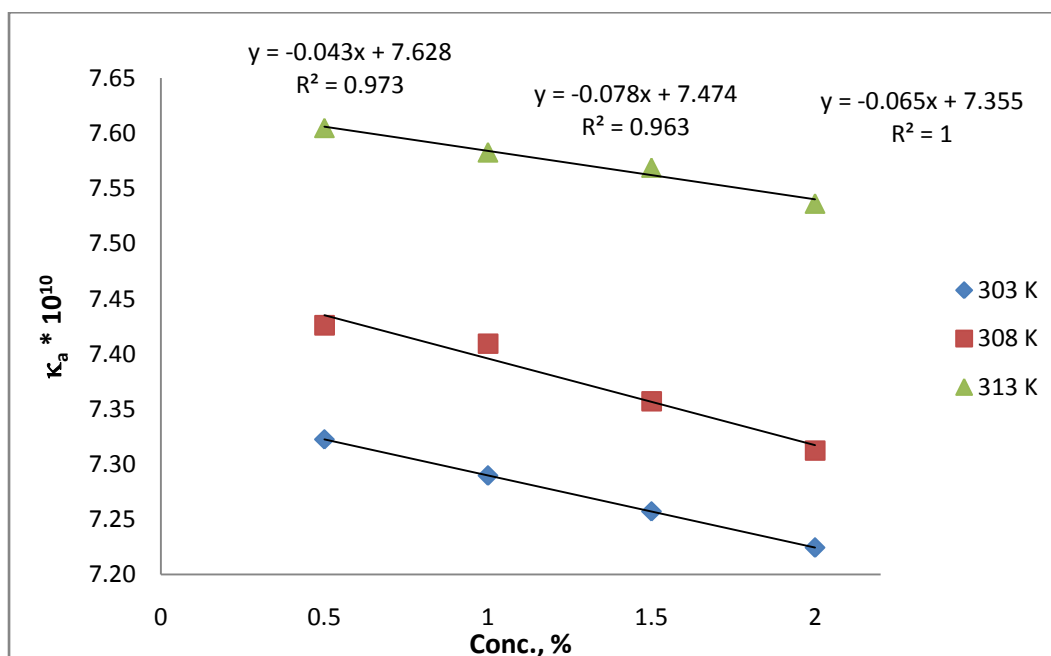


Fig. 4.5: The plots of adiabatic compressibility ( $\kappa_a$ ) against concentration (%) of ESB4HCy in THF at 303, 308 and 313 K.

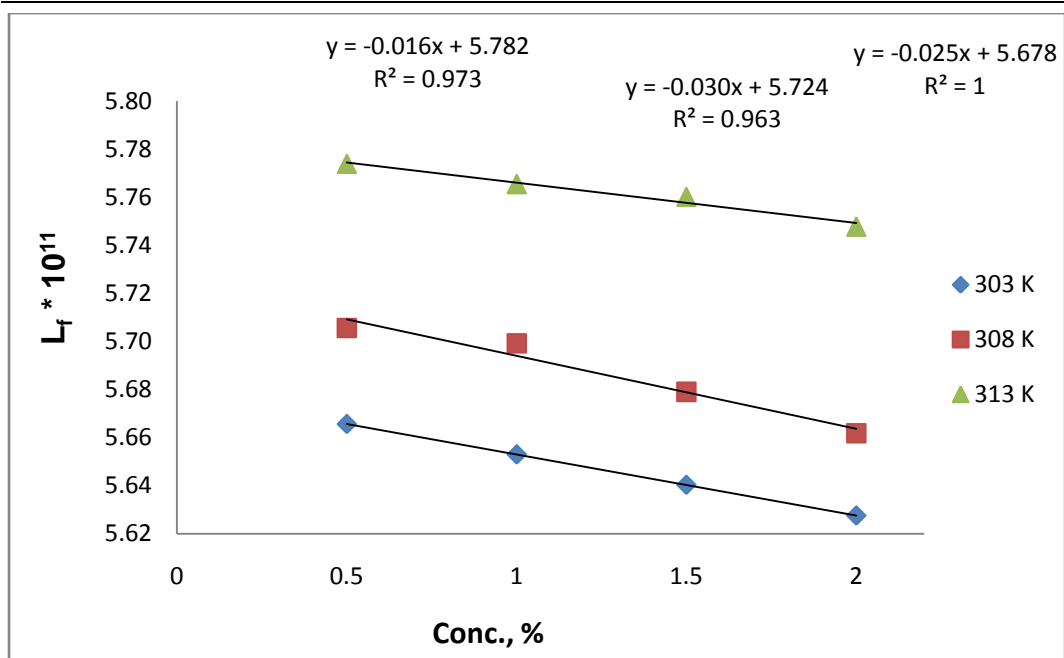


Fig. 4.6: The plots of inter molecular free path length ( $L_f$ ) against concentration (%) of ESB4HCy in THF at 303, 308 and 313 K.

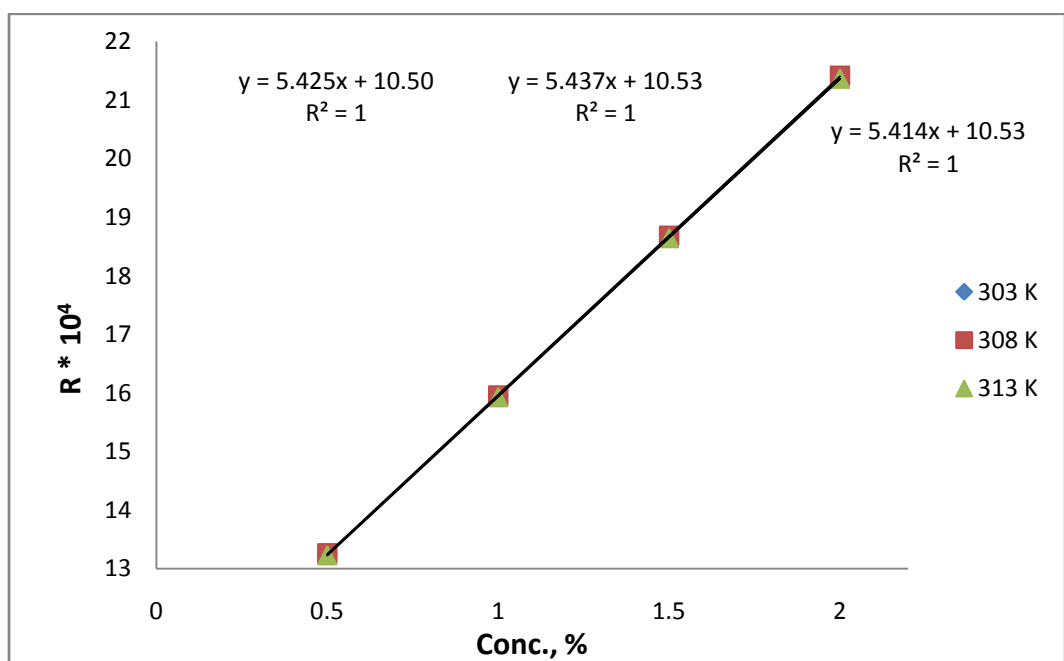


Fig. 4.7: The plots of Rao's molar sound function (R) against concentration (%) of ESB4HCy in THF at 303, 308 and 313 K.

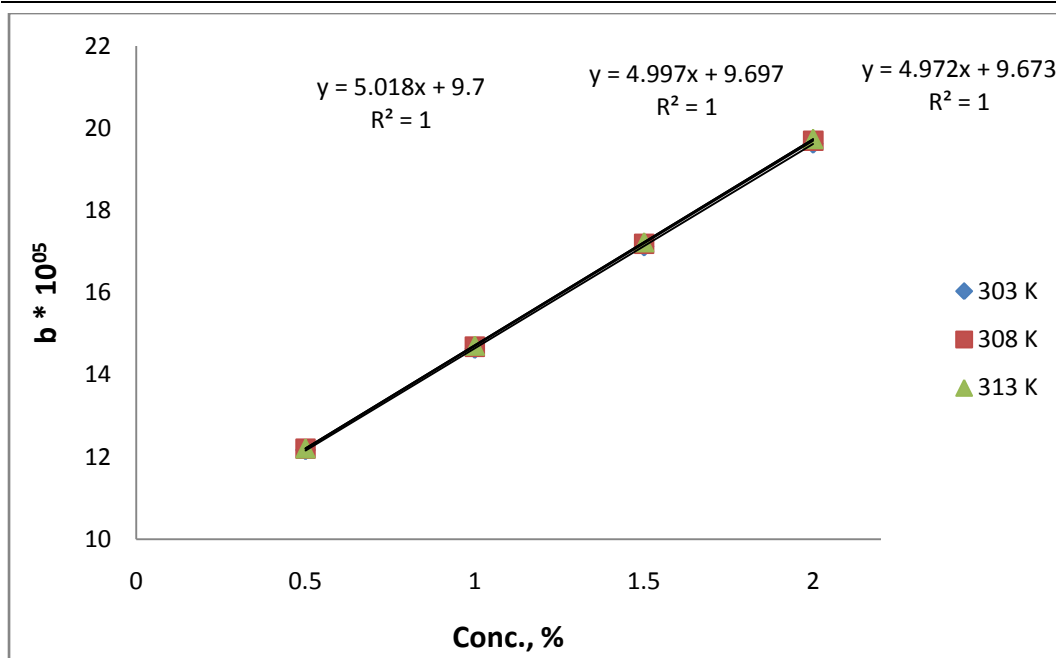


Fig. 4.8: The plots of Van der Waals constant ( $b$ ) against concentration (%) of ESB4HCy in THF at 303, 308 and 313 K.

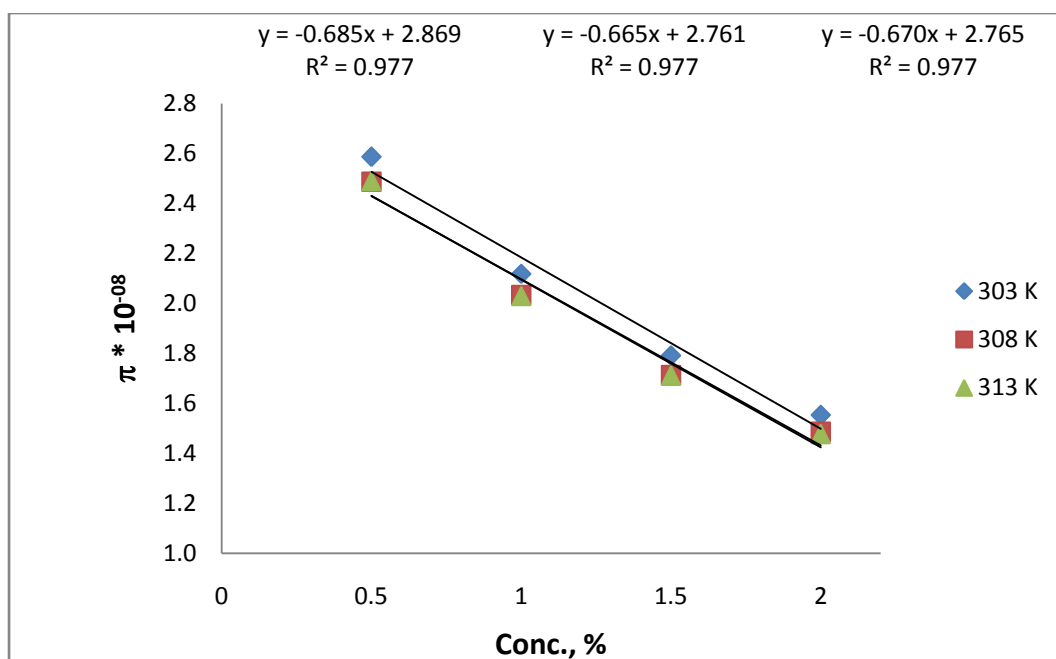


Fig. 4.9: The plots of internal pressure against concentration (%) of ESB4HCy in THF at 303, 308 and 313 K.

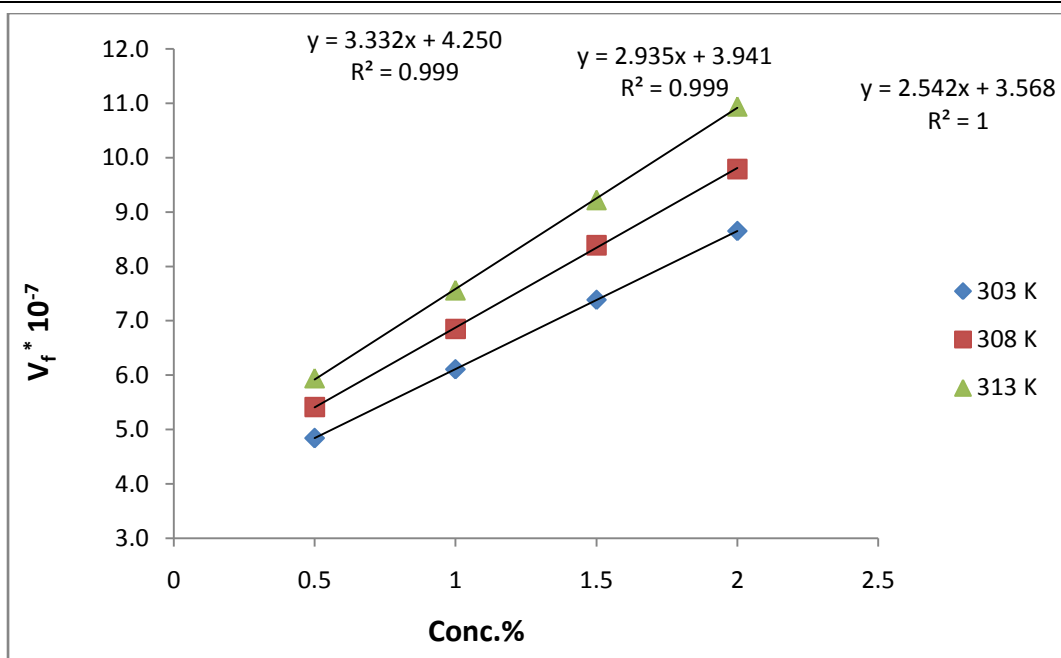


Fig. 4.10: The plots of free volume ( $V_f$ ) against concentration (%) of ESB4HCy in THF at 303, 308 and 313 K.

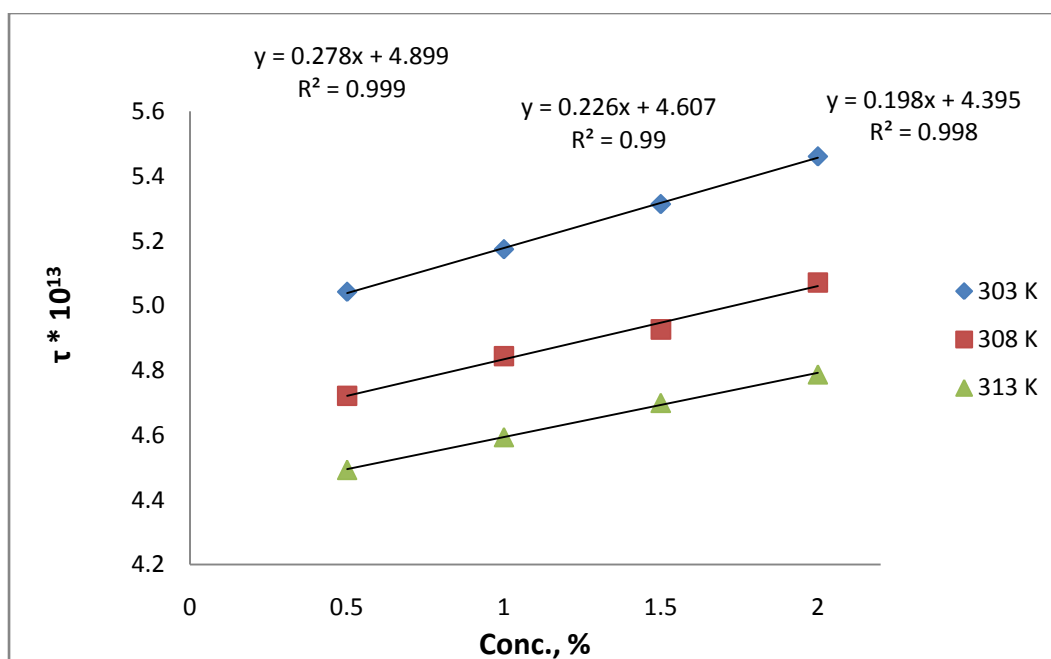


Fig. 4.11: The plots of viscous relaxation time ( $\tau$ ) against concentration (%) of ESB4HCy in THF at 303, 308 and 313 K.



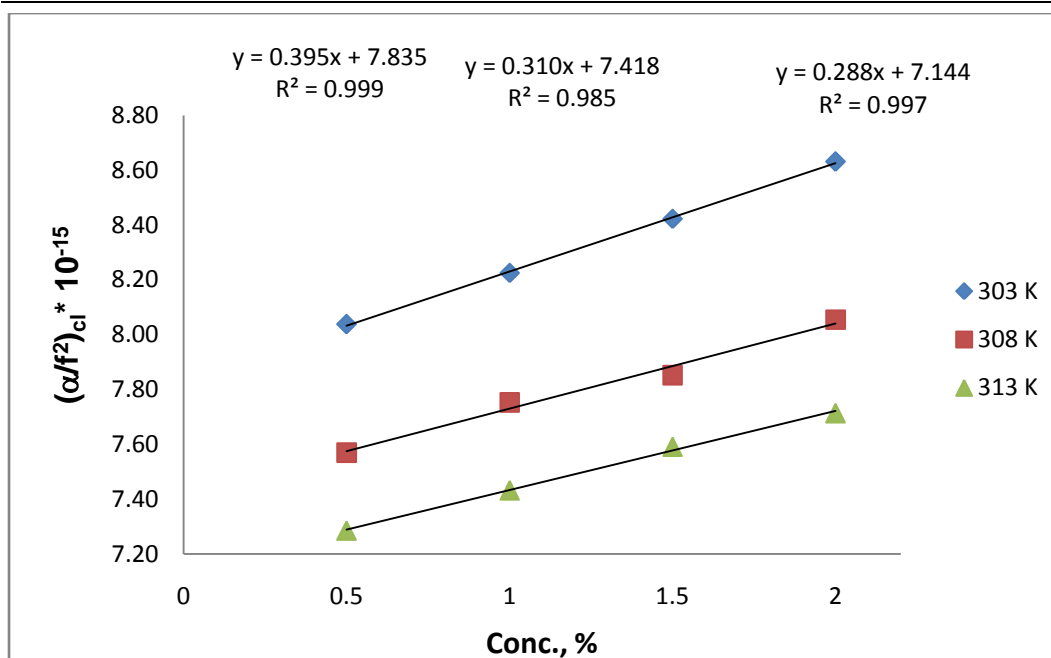


Fig. 4.12: The plots of classical absorption co-efficient (CAC) against concentration (%) of ESB4HCy in THF at 303, 308 and 313 K.

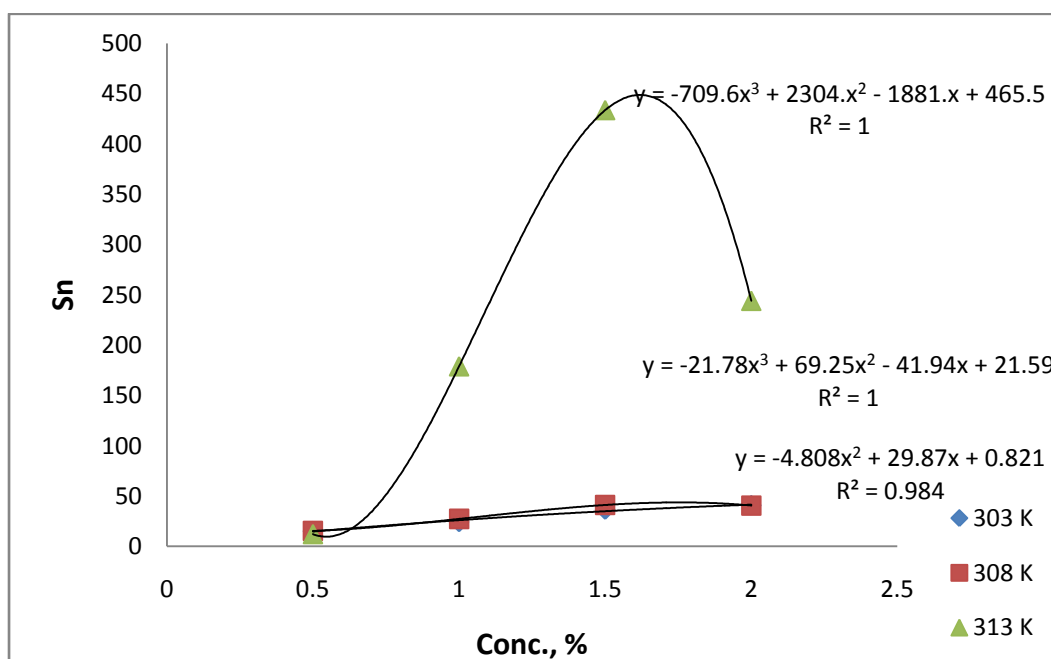


Fig. 4.13: The plots of solvation number (Sn) against concentration (%) of ESB4HCy in THF at 303, 308 and 313 K.

High frequency (> 1MHz, usually low intensity) waves are useful in providing information on relaxation phenomena such as segmental motion, conformational analysis, vibrational-translational energy interchange and polymer-solvent interactions, whereas low frequency waves provide information on both polymerization and depolymerization.

When a low intensity wave one without cavitation is passed through a liquid, there is attenuation,  $\alpha$ , of the wave due to viscous and thermal losses

$$\frac{\alpha}{f^2} = \frac{2\pi^2}{\rho U^3} \left\{ \frac{4\eta_s}{3} + \frac{(\gamma-1)K}{C_p} \right\} \quad \dots 4.19$$

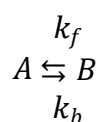
Where  $f$  = frequency,  $K$  = thermal conductivity,  $\gamma = C_p/C_v$ ,  $C_p$  = molar heat capacity at constant pressure,  $\eta_s$  and  $\rho$  are viscosity and density of the medium and  $U$  = ultrasonic speed. For a given liquid at temperature  $T$ , all the parameters on the right hand side should be constant making  $\alpha/f^2$  constant no matter what the frequency.

The total energy of a given system is not restricted solely to translational energy but is the sum of many components. For liquids conformational and structural energies must be taken into account. The coupling of the translational energy with other forms of energies leads to the absorption of sound in excess of that deduced by Eqn. 4.19 and no constancy of  $\alpha/f^2$  with increasing frequency.

The time lag between the excitation and deexcitation process is observed as an acoustic relaxation. This relaxation process is observed as either an increase in velocity with frequency or a decrease in the  $\alpha/f^2$  with frequency.

The dependence of attenuation with temperature allows determination of  $\Delta G$ ,  $\Delta H$ ,  $\Delta V$  and  $\Delta S$  associated with various conformational changes. There will be a perturbation of the equilibrium on the passage of an ultrasonic wave.

It is possible to obtain information on the rate constants for forward ( $k_f$ ) and backward ( $k_b$ ) reactions, the free energy barrier  $\Delta G_b^*$  and the free energy difference  $\Delta G$ .



Assuming unimolecular reaction in ideal solution, relaxation frequency  $f_r$  can be correlated with the rate constants.

$$f_r = \frac{1}{2\pi\tau} = \frac{k_f + k_b}{2\pi} \quad \dots 4.20$$

Where  $\tau$  = relaxation time of the equilibrium.

For any reaction the rate constant  $k$  can be expressed in terms of the free energy of activation  $\Delta G^*$ .

$$\begin{aligned} f_r &= \frac{k_B T}{h} e^{-\frac{\Delta G_f^*}{RT}} \\ &= \frac{k_B T}{2\pi h} \left[ e^{-\frac{\Delta G_f^*}{RT}} + e^{-\frac{\Delta G_b^*}{RT}} \right] \quad \dots 4.21 \end{aligned}$$

Where  $k_B$  = Boltzmann constant and  $h$  = Planck's constant.

Assuming that equilibrium lies well to the left then

$$\Delta G_f^* \gg \Delta G_b^* \text{ such that}$$

$$f_r = \frac{k_B T}{2\pi h} e^{-\frac{\Delta G_b^*}{RT}} \quad \dots 4.22$$

Since

$$\Delta G = \Delta H - T\Delta S \quad \dots 4.23$$

$$f_r = \frac{k_B T}{2\pi h} \left( e^{-\frac{\Delta S_b^*}{RT}} \right) \left( e^{-\frac{\Delta H_b^*}{RT}} \right) \quad \dots 4.24$$

$$\ln \frac{f_r}{T} = \ln \frac{k_B}{2\pi h} + \frac{\Delta S_b^*}{RT} - \frac{\Delta H_b^*}{RT} \quad \dots 4.25$$

From the plot of  $\ln f_r/T$  against  $1/T$ ,  $\Delta H_b^*$  and  $\Delta S_b^*$  can be determined.

In the present case,  $\Delta G_b^*$  was determined for a given concentration and temperature; and correlated with  $C$  and  $T$ . The deduced  $\Delta G_b^*$  values at different concentrations and temperatures are summarized in Table 4.3 along with least square equations and  $R^2$  values. From Table-4.3, it is clear that  $\Delta G^*$  remained practically constant with  $C$  but is decreased with  $T$ . Negligible concentration effect on  $\Delta G_b^*$  is observed but temperature effect is considerable. The values of  $\Delta S_b^*$  and  $\Delta H_b^*$  are determined according to Eqn. 4.25 and also summarized in Table-4.3.

Table 4.3. :  $\Delta G^*$ ,  $\Delta H$  and  $\Delta S$  data of ESB4HCy

Conc., %	$\Delta G^*$ , kJ mol <sup>-1</sup>			$\Delta H$ , kJ mol <sup>-1</sup>	$\Delta S$ , J K <sup>-1</sup> mol <sup>-1</sup>
	303 K	308 K	313 K		
0.5	2.96	2.84	2.76	6.56	12.04
1	3.02	2.90	2.81	6.83	12.70
1.5	3.09	2.95	2.87	7.08	13.28
2	3.16	3.02	2.92	7.77	15.36
Average	3.06	2.93	2.84		

$$\Delta G^* = 133.8 C + 2892, R^2 = 0.999 \text{ at } 303 \text{ K}$$

$$\Delta G^* = 118.5 C + 2781, R^2 = 0.991 \text{ at } 308 \text{ K}$$

$$\Delta G^* = 111.3 C + 2703, R^2 = 0.998 \text{ at } 313 \text{ K}$$

**Ultrasonic study of bisbenzoxazine BSB4HCy**

The  $\rho$ ,  $\eta$  and  $U$  data of 1, 4-dioxane and BSB4HCy solutions at three different temperatures are summarized in Table-4.4 and observed that practically  $\rho$  remained constant with  $C$  but decreased minimum with  $T$ . The  $\rho$  and  $U$  both increased considerably with  $C$  and decreased with  $T$  (Fig. 4.14-4.16) due to specific solvent-solute interactions as discussed in previous section. The least square equations along with  $R^2$  values of these data are summarized in Table-4.5 from which it is clear that observed correlation is fairly good between a particular parameter with  $C$  and  $T$ .

Various acoustical parameters were determined according to standard equations and correlated with  $C$  and  $T$  (Fig. 4.17-4.26). The least square equations along with  $R^2$  values are reported in Table-4.5 from which it is clear that good to excellent correlation between a given parameter with  $C$  and  $T$  is observed. Polynomial regression is carried out whenever nonlinear behavior is observed due to specific interactions.

Linear increase of  $Z$  (except at 308 K),  $R$  and  $b$  (practically no temperature effect),  $V_f$ ,  $\tau$  and  $(\alpha / f^2)_{cl}$  (except 308 and 313 K) and decrease with  $T$ ; and linear decrease of  $\kappa_a$  and  $L_f$  (except 308 and 313 K) and  $\pi$  with  $C$  and increase with  $T$  supported existence of strong molecular interactions in solutions and structure forming tendency of BSB4HCy and is further supported by positive values of  $S_n$ . Nonlinear behavior of  $S_n$  with  $C$  suggested presence of solvent-solute and solute-solute interactions in the solutions. An interaction increased with both  $C$  and  $T$ . Solute-solute interactions is powerful over solvent-solute interactions above 1 % concentration.

Various activation parameters namely  $\Delta G^*$ ,  $\Delta H^*$  and  $\Delta S_b^*$  are determined according to Eqns. 4.25 at various concentrations and temperatures and presented in Table-4.6. Practically concentration effect on various activation parameters is negligible but temperature effect is considerable, i.e. thermodynamic parameters decreased with  $T$ .

**Table-4.4: The density ( $\rho$ ), viscosity ( $\eta$ ), ultrasonic speed (U) and standard deviation (s) data of bisbenzoxazine BSB4HCy in 1,4 dioxane at 303, 308 and 313 K.**

Conc., %	Density $\rho$ , kg/m <sup>3</sup>	Viscosity $\eta$ , mPa.s	Ave. Dist. D, mm	Wave length $\lambda$ , mm	U ms <sup>-1</sup> (F=2MHz)	Std. devi., mm ( $\pm$ )
303 K						
0	1029.6	1.109	3.281	0.6562	1312.4	0.0016
0.5	1029.6	1.135	3.300	0.6600	1320.0	0.0020
1.0	1029.5	1.161	3.320	0.6640	1328.0	0.0033
1.5	1029.4	1.184	3.335	0.6670	1334.0	0.0015
2.0	1029.3	1.215	3.361	0.6722	1344.4	0.0013
308 K						
0	1028.8	1.008	3.235	0.6470	1294.0	0.0025
0.5	1028.7	1.047	3.256	0.6512	1302.4	0.0016
1.0	1028.6	1.059	3.282	0.6564	1312.8	0.0026
1.5	1028.6	1.080	3.296	0.6592	1318.4	0.0030
2.0	1028.4	1.113	3.305	0.6610	1322.0	0.0029
313 K						
0	1028.1	0.915	3.181	0.6362	1272.4	0.0037
0.5	1028.0	0.929	3.205	0.6410	1282.0	0.0014
1.0	1027.9	0.971	3.209	0.6418	1283.6	0.0029
1.5	1027.8	0.986	3.217	0.6434	1286.8	0.0031
2.0	1027.6	1.014	3.227	0.6454	1290.8	0.0020

**Table-4.5: The correlation equations and regression coefficients of bisbenzoxazine BSB4HCy in 1,4 dioxane at 303,308 and 313 K.**

Parameter	Correlation equation and regression coefficient, R <sup>2</sup>		
	303 K	308 K	313 K
$\rho$ , kgm <sup>-3</sup>	-0.2 C + 1029. R <sup>2</sup> = 1	-0.19 C + 1028. R <sup>2</sup> = 0.983	-0.243 C + 1028. R <sup>2</sup> = 0.998
$\eta$ , mPa.s	0.052 C + 1.108 R <sup>2</sup> = 0.996	0.043 C + 1.020 R <sup>2</sup> = 0.953	0.053 C + 0.907 R <sup>2</sup> = 0.966
U, ms <sup>-1</sup>	15.84 C + 1311. R <sup>2</sup> = 0.989	12.88 C + 1297. R <sup>2</sup> = 0.945	5.92 C + 1278. R <sup>2</sup> = 0.967
Z, 10 <sup>6</sup> kg.m <sup>-2</sup> .s <sup>-1</sup>	0.016 C + 1.350 R <sup>2</sup> = 0.988	-0.007 C <sup>2</sup> + 0.030 C + 1.326 R <sup>2</sup> = 0.998	0.005 C + 1.314 R <sup>2</sup> = 0.963
$\kappa_a$ , 10 <sup>-10</sup> Pa <sup>-1</sup>	-0.052 C + 5.951 R <sup>2</sup> = 0.966	0.060 C <sup>2</sup> - 0.260 C + 5.844 R <sup>2</sup> = 0.998	-0.129 C + 5.640 R <sup>2</sup> = 0.99
L <sub>f</sub> , 10 <sup>-11</sup> m	-0.022 C + 5.107 R <sup>2</sup> = 0.966	0.026 C <sup>2</sup> - 0.114 C + 5.062 R <sup>2</sup> = 0.998	-0.057 C + 4.973 R <sup>2</sup> = 0.989
R, 10 <sup>-4</sup> m <sup>10/3</sup> .s <sup>-1/3</sup> .mol <sup>-1</sup>	4.075 C + 9.288 R <sup>2</sup> = 1	4.121 C + 9.322 R <sup>2</sup> = 1	4.144 C + 9.342 R <sup>2</sup> = 1
b, 10 <sup>-5</sup> m <sup>3</sup>	3.701 C + 8.431 R <sup>2</sup> = 1	3.697 C + 8.429 R <sup>2</sup> = 1	3.692 C + 8.422 R <sup>2</sup> = 1
$\pi$ , 10 <sup>8</sup> Pa	-1.058 C + 4.660 R <sup>2</sup> = 0.981	-1.025 C + 4.494 R <sup>2</sup> = 0.976	-0.982 C + 4.416 R <sup>2</sup> = 0.985
V <sub>f</sub> , 10 <sup>-7</sup> m <sup>3</sup>	0.94 C + 1.538 R <sup>2</sup> = 0.998	0.900 C + 1.302 R <sup>2</sup> = 0.999	0.802 C + 1.165 R <sup>2</sup> = 0.999
$\tau$ , 10 <sup>-13</sup> s	0.181 C + 8.347 R <sup>2</sup> = 1	0.242 C <sup>2</sup> - 0.434 C + 8.159 R <sup>2</sup> = 1	-0.135 C <sup>2</sup> + 0.693 C + 7.037 R <sup>2</sup> = 0.968
( $\alpha/f^2$ ) <sub>cl</sub> 10 <sup>-14</sup> , s <sup>2</sup> m <sup>-1</sup>	0.118 C + 12.54 R <sup>2</sup> = 0.979	0.424 C <sup>2</sup> - 0.924 C + 12.47 R <sup>2</sup> = 0.999	-0.232 C <sup>2</sup> + 1.071 C + 10.82 R <sup>2</sup> = 0.960

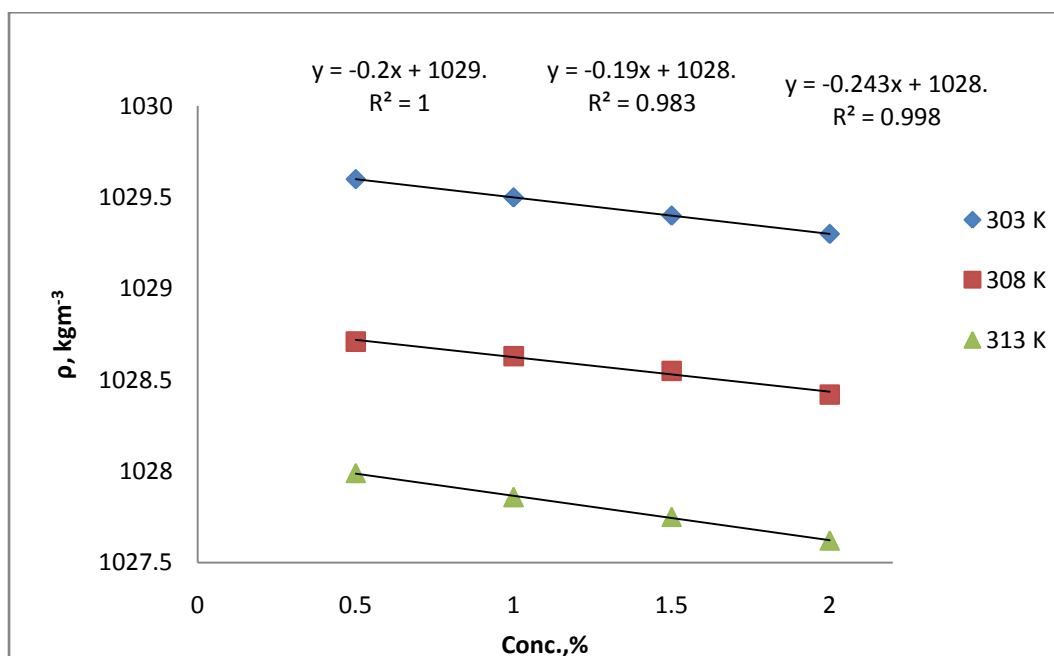


Fig. 4.14: The plots of density ( $\rho$ ) against concentration (%) of BSB4HCy in 1,4 dioxane at 303, 308 and 313 K.

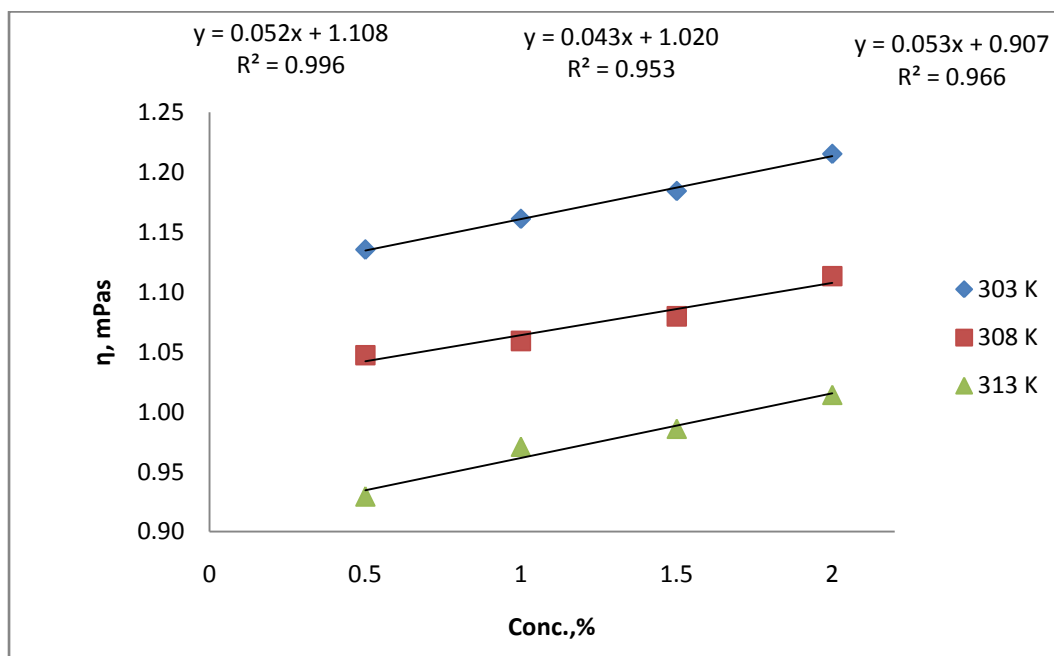


Fig. 4.15: The plots of viscosity ( $\eta$ ) against concentration (%) of BSB4HCy in 1,4 dioxane at 303, 308 and 313 K.



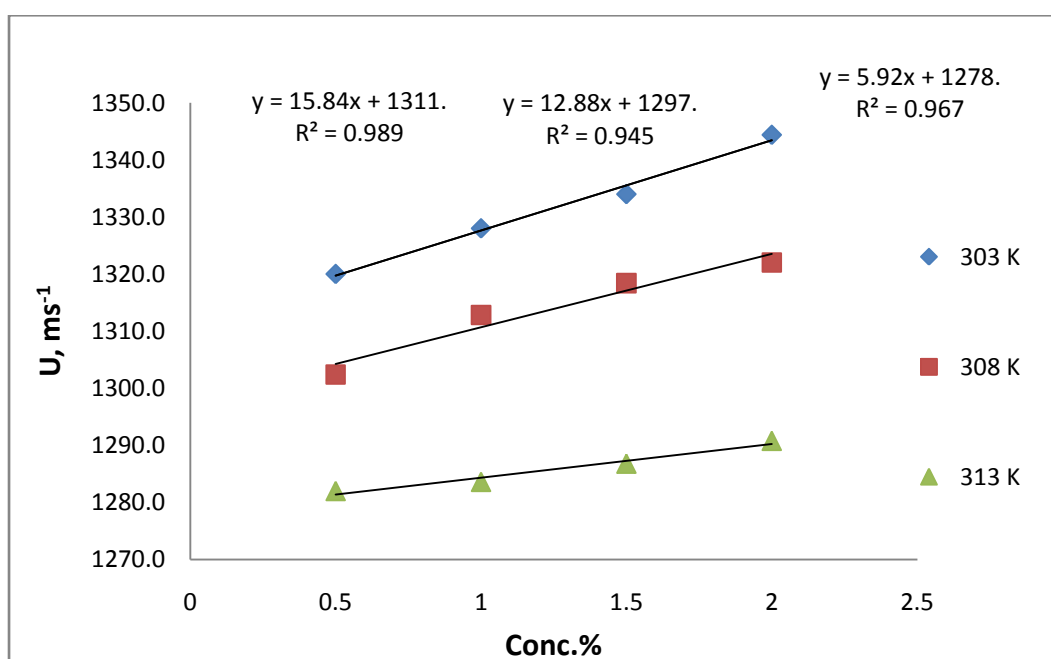


Fig. 4.16: The plots of sound velocity ( $U$ ) against concentration (%) of BSB4HCy in 1,4 dioxane at 303, 308 and 313 K.

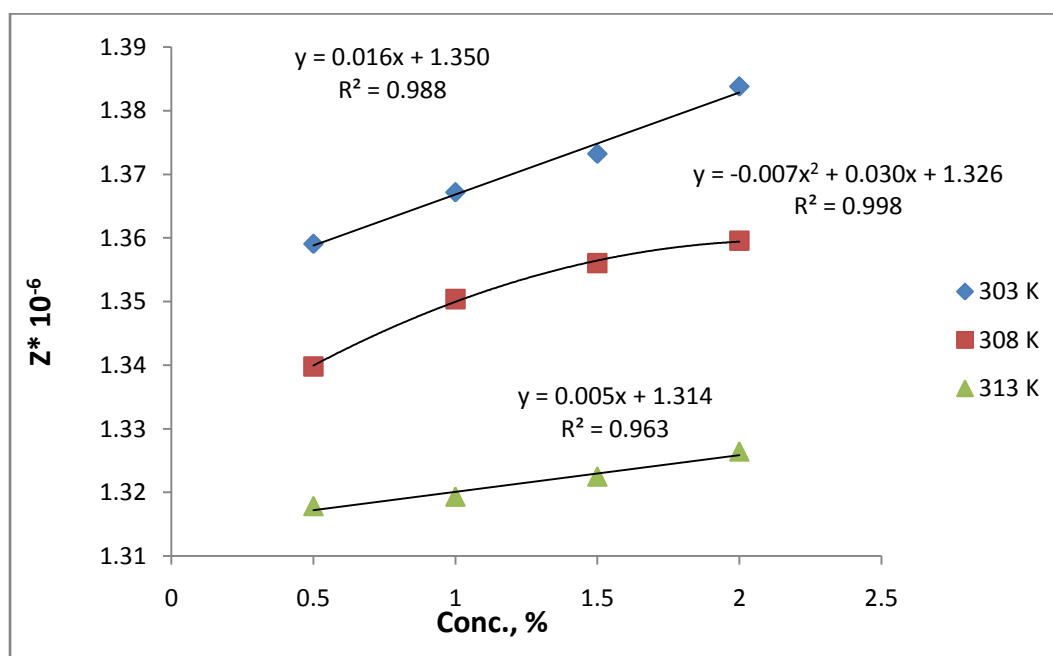


Fig. 4.17: The plots of specific acoustical impedance ( $Z$ ) against concentration (%) of BSB4HCy in 1,4 dioxane at 303, 308 and 313 K.

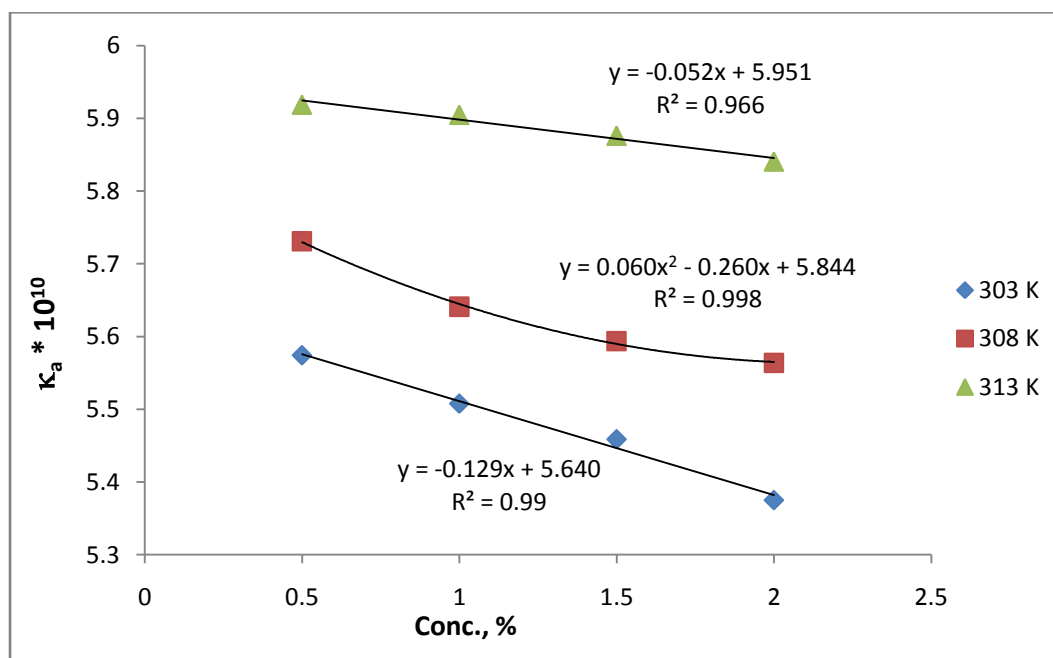


Fig. 4.18: The plots of adiabatic compressibility ( $\kappa_a$ ) against concentration (%) of BSB4HCy in 1,4 dioxane at 303, 308 and 313 K.

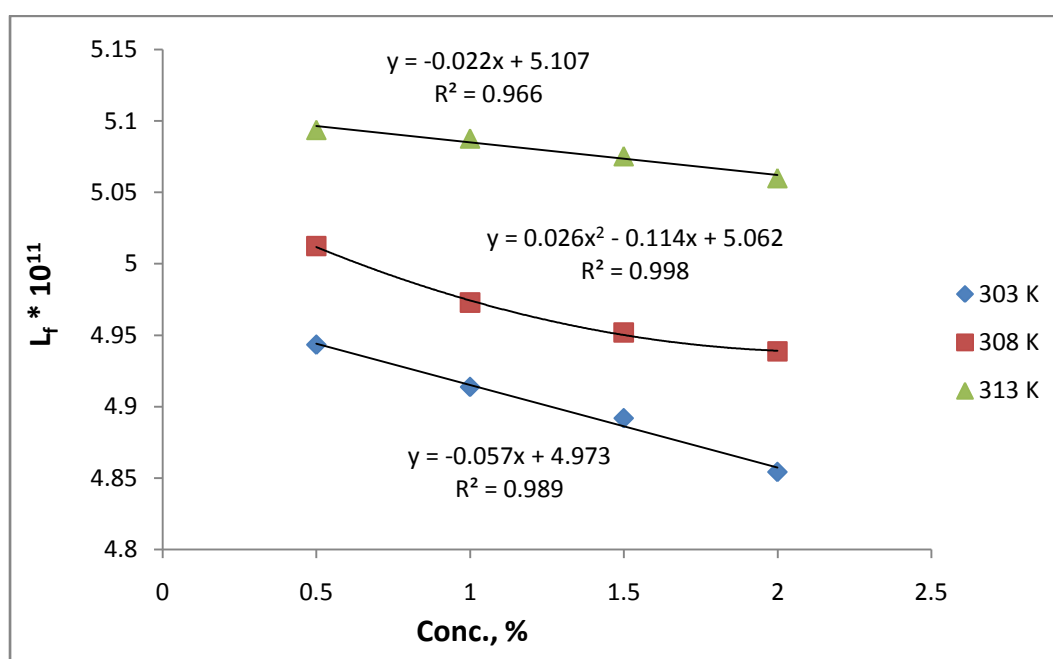


Fig. 4.19: The plots of inter molecular free path length ( $L_f$ ) against concentration (%) of BSB4HCy in 1,4 dioxane at 303, 308 and 313 K.

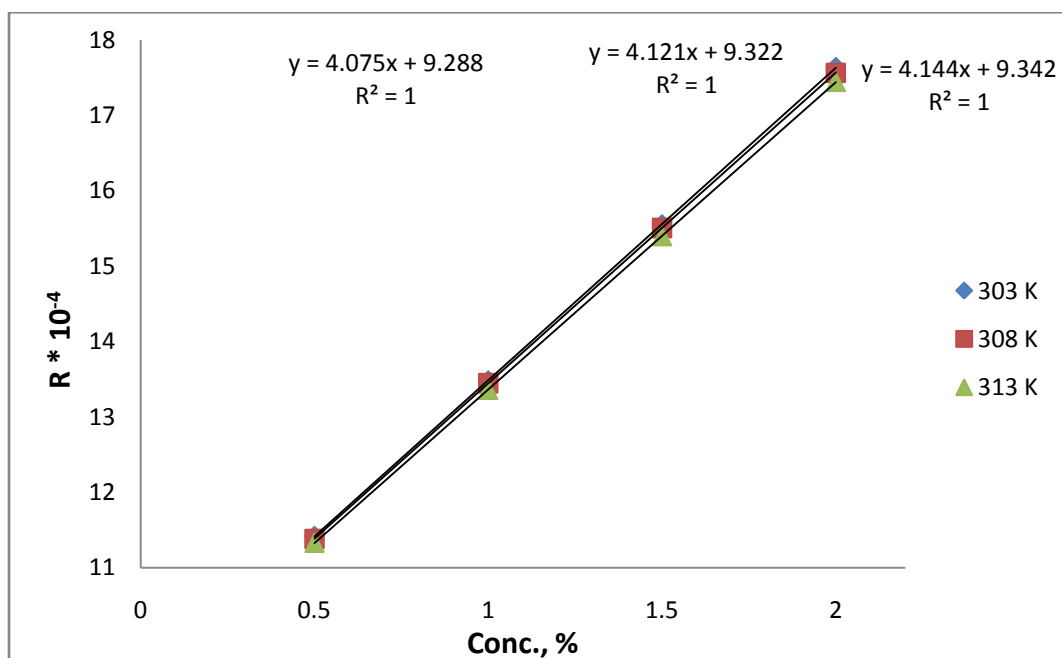


Fig. 4.20: The plots of Rao's molar sound function (R) against concentration (%) of BSB4HCy in 1,4 dioxane at 303, 308 and 313 K.

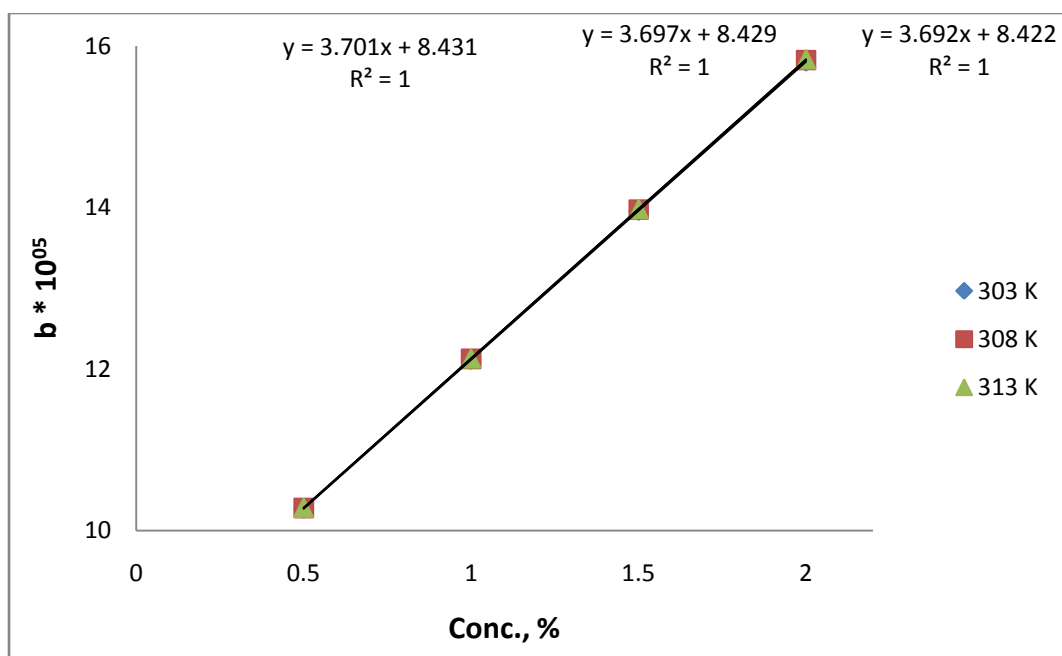


Fig. 4.21: The plots of Van der Waals constant (b) against concentration (%) of BSB4HCy in 1,4 dioxane at 303, 308 and 313 K.

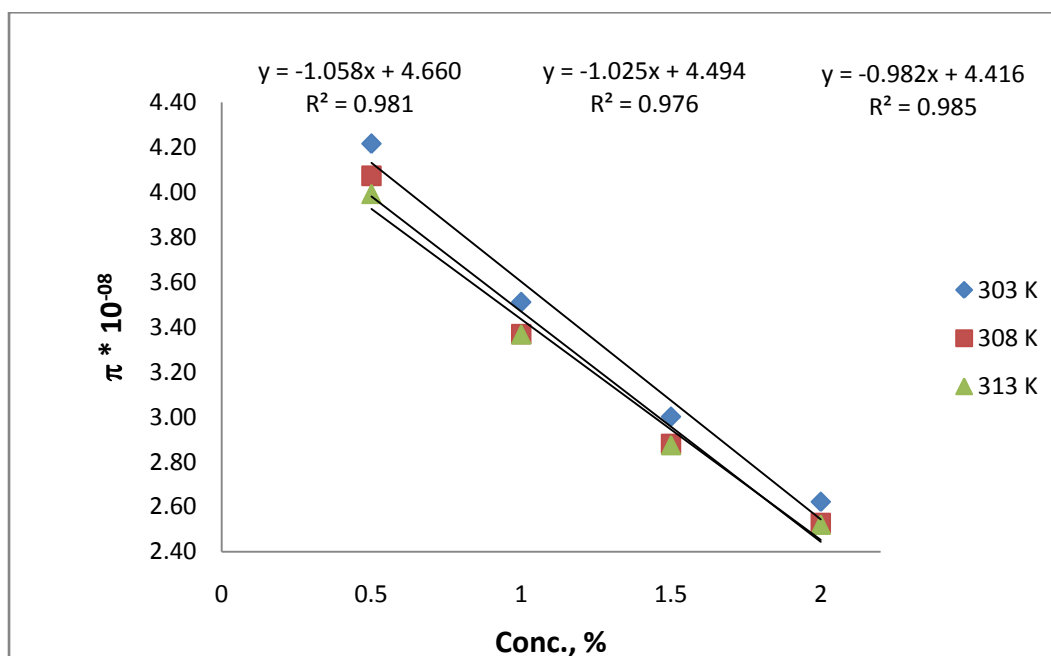


Fig. 4.22: The plots of internal pressure against concentration (%) of BSB4HCy in 1,4 dioxane at 303, 308 and 313 K.

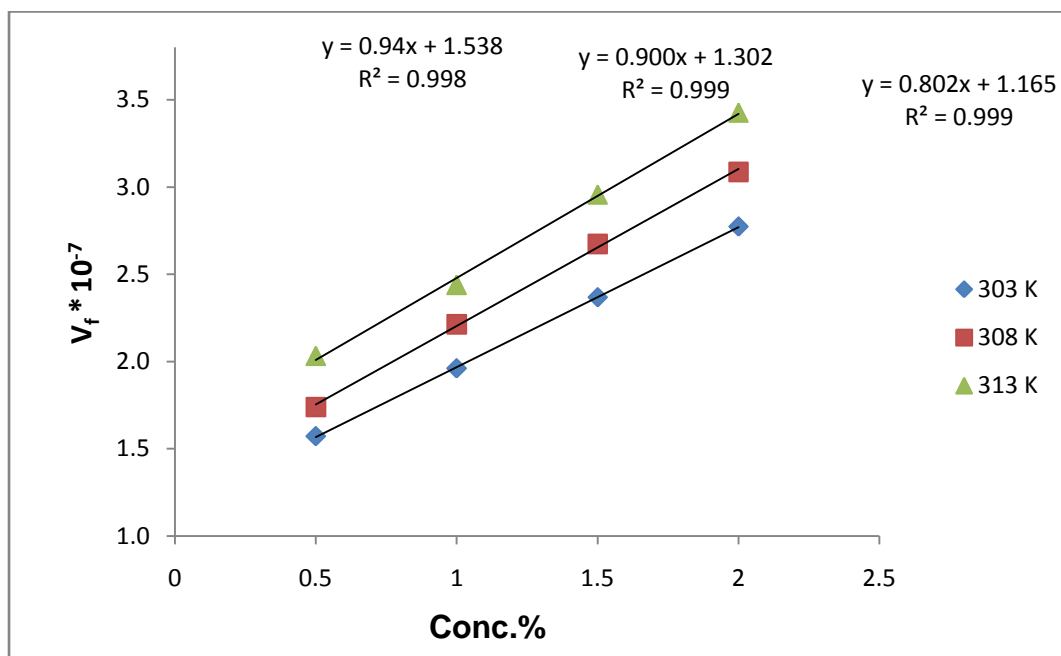


Fig. 4.23: The plots of free volume ( $V_f$ ) against concentration (%) of BSB4HCy in 1,4 dioxane at 303, 308 and 313 K.

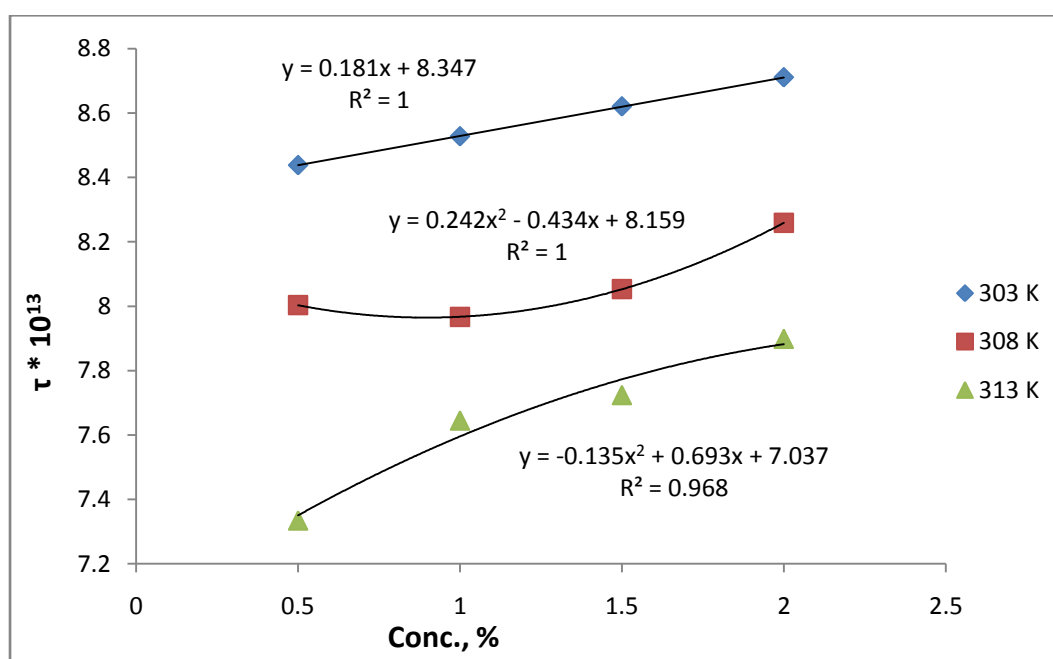


Fig. 4.24: The plots of viscous relaxation time ( $\tau$ ) against concentration (%) of BSB4HCy in 1,4 dioxane at 303, 308 and 313 K.

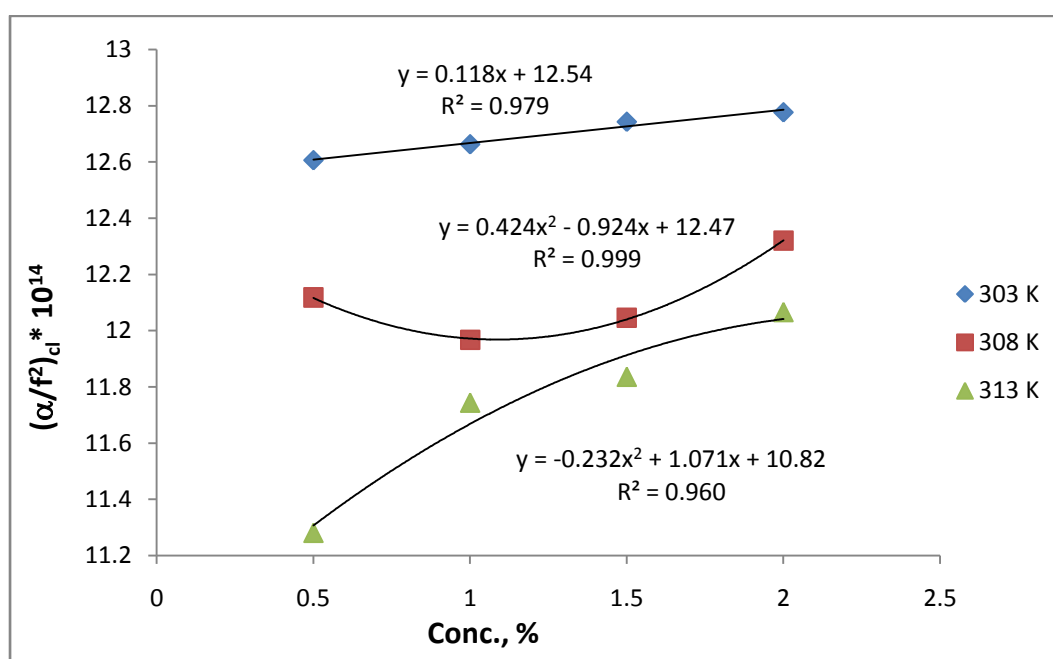
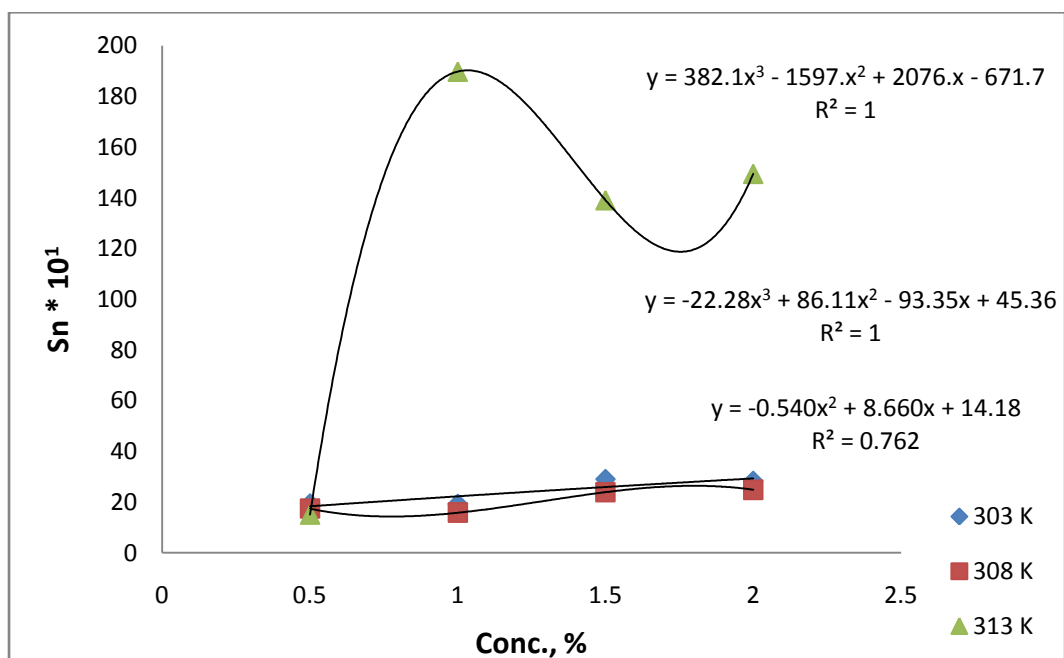


Fig. 4.25: The plots of classical absorption co-efficient (CAC) against concentration (%) of BSB4HCy in 1,4 dioxane at 303, 308 and 313 K.



**Fig. 4.26: The plots of solvation number (Sn) against concentration (%) of BSB4HCy in 1,4 dioxane at 303, 308 and 313 K.**

**Table 4.6:  $\Delta G^*$  data of BSB4HCy**

Conc., %	$\Delta G^*$ , kJ mol <sup>-1</sup>			$\Delta H$ , kJ mol <sup>-1</sup>	$\Delta S$ , J K <sup>-1</sup> mol <sup>-1</sup>
	303 K	308 K	313 K		
<b>0.5</b>	4.33	4.19	4.03	8.48	14.03
<b>1</b>	4.36	4.18	4.14	6.07	6.05
<b>1.5</b>	4.38	4.21	4.17	6.11	6.05
<b>2</b>	4.41	4.27	4.23	5.15	2.81
<b>Average</b>	4.37	4.21	4.14		

$$\Delta G^* = 54.34 C + 4300, R^2 = 1 \text{ at } 303 \text{ K}$$

$$\Delta G^* = 92.23 C + 4082, R^2 = 0.949 \text{ at } 308 \text{ K}$$

$$\Delta G^* = 121.1 C + 3990, R^2 = 0.936 \text{ at } 313 \text{ K}$$

### Ultrasonic study of bisbenzoxazine BSB4HM

The  $\rho$ ,  $\eta$  and  $U$  data of 1, 4-dioxane and BSB4HM solutions at three different temperatures are reported in Table-4.7. Similar behavior is observed as in BSB4HM due to specific molecular interactions. These data are correlated with  $C$  and  $T$  (Figs. 4.27-4.29). The least square equations along with  $R^2$  values of these data are summarized in Table-4.8 from which it is clear that a fairly good to excellent correlation is observed between a particular parameter with  $C$  and  $T$ .

Various acoustical parameters were determined using  $\rho$ ,  $\eta$  and  $U$  data are correlated with  $C$  and  $T$  (Figs. 4.30-4.39). The least square equations along with  $R^2$  values are summarized in Table-4.9 from which it is clear that a good to excellent correlation is observed with a particular parameter with  $C$  and  $T$ . Linear increase of  $Z$ ,  $R$  and  $b$  (practically no temperature effect),  $V_f$ ,  $\tau$  and  $(\alpha/f^2)_{cl}$  (nonlinear at 308 and 313 K) with  $C$  and decrease with  $T$ ; and linear decrease of  $\kappa_a$  and  $L_f$  and  $\pi$  with  $C$  and increase with  $T$  furnished information about presence of strong molecular interactions in the solutions and structure forming tendency of BSB4HM and is further confirmed by positive values of  $S_n$ . Nonlinear increase of  $S_n$  with  $C$  and  $T$  confirmed further presence of both solvent-solute and solute-solute interactions in the solutions.

Various activation parameters namely  $\Delta G_b^*$ ,  $\Delta H_b^*$  and  $\Delta S_b^*$  are determined according to Eqns. 4.25 at various concentrations and temperatures using  $\tau$  data. These data are reported in Table-4.9 from which it is clear that  $\Delta G_b^*$  remained practically constant with  $C$  but it decreased a little with  $T$ .



**Table-4.7: The density ( $\rho$ ), viscosity ( $\eta$ ), ultrasonic speed (U) and standard deviation (s) data of bisbenzoxazine BSB4HM in 1,4 dioxane at 303, 308 and 313 K.**

Conc., %	Density $\rho$ , kg/m <sup>3</sup>	Viscosity $\eta$ , mPa.s	Ave. Dist. d, mm	Wave length $\lambda$ , mm	U ms <sup>-1</sup> (F=2MHz)	Std. devi., mm ( $\pm$ )
303 K						
0	1029.6	1.109	3.281	0.6562	1312.4	0.0016
0.5	1029.9	1.131	3.310	0.6620	1324.0	0.0016
1.0	1029.7	1.148	3.323	0.6646	1329.2	0.0026
1.5	1029.6	1.170	3.336	0.6672	1334.4	0.0012
2.0	1029.5	1.185	3.348	0.6696	1339.2	0.0021
308 K						
0	1028.8	1.008	3.235	0.6470	1294.0	0.0025
0.5	1028.6	1.031	3.298	0.6596	1319.2	0.0019
1.0	1028.6	1.047	3.317	0.6634	1326.8	0.0025
1.5	1028.5	1.073	3.326	0.6652	1330.4	0.0012
2.0	1028.4	1.094	3.236	0.6672	1334.4	0.0021
313 K						
0	1028.1	0.915	3.181	0.6362	1272.4	0.0037
0.5	1027.8	0.930	3.202	0.6404	1280.8	0.0026
1.0	1027.7	0.949	3.226	0.6452	1290.4	0.0012
1.5	1027.6	0.969	3.239	0.6478	1295.6	0.0026
2.0	1027.4	1.008	3.252	0.6504	1300.8	0.0022

**Table-4.8: The correlation equations and regression coefficients of bisbenzoxazine BSB4HM in 1,4 dioxane at 303, 308 and 313 K.**

Parameter	Correlation equation and regression coefficient, R <sup>2</sup>		
	303 K	308 K	313 K
$\rho$ , kgm <sup>-3</sup>	-0.22 C + 1030 R <sup>2</sup> = 0.998	-0.091 C <sup>2</sup> + 0.051 C + 1028. R <sup>2</sup> = 0.956	-0.242 C + 1027. R <sup>2</sup> = 0.953
$\eta$ , mPa.s	0.036 C + 1.112 R <sup>2</sup> = 0.995	0.042 C + 1.007 R <sup>2</sup> = 0.991	0.051 C + 0.9 R <sup>2</sup> = 0.965
U, ms <sup>-1</sup>	9.84 C + 1315. R <sup>2</sup> = 0.966	10.16 C + 1319 R <sup>2</sup> = 0.999	13.04 C + 1275. R <sup>2</sup> = 0.973
Z, 10 <sup>6</sup> kg.m <sup>-2</sup> .s <sup>-1</sup>	0.010 C + 1.358 R <sup>2</sup> = 0.999	0.009 C + 1.353 R <sup>2</sup> = 0.963	0.013 C + 1.311 R <sup>2</sup> = 0.970
$\kappa_a$ , 10 <sup>-10</sup> Pa <sup>-1</sup>	-0.116 C + 5.976 R <sup>2</sup> = 0.969	-0.081 C + 5.617 R <sup>2</sup> = 0.963	-0.082 C + 5.579 R <sup>2</sup> = 0.999
L <sub>f</sub> , 10 <sup>-11</sup> m	-0.050 C + 5.119 R <sup>2</sup> = 0.970	-0.036 C + 4.962 R <sup>2</sup> = 0.964	-0.036 C + 4.945 R <sup>2</sup> = 0.999
R, 10 <sup>-4</sup> m <sup>10/3</sup> .s <sup>-1/3</sup> .mol <sup>-1</sup>	4.108 C + 9.275 R <sup>2</sup> = 1	4.124 C + 9.368 R <sup>2</sup> = 1	4.122 C + 9.364 R <sup>2</sup> = 1
b, 10 <sup>-5</sup> m <sup>3</sup>	3.704 C + 8.432 R <sup>2</sup> = 1	3.697 C + 8.431 R <sup>2</sup> = 1	3.690 C + 8.421 R <sup>2</sup> = 1
$\pi$ , 10 <sup>8</sup> Pa	-1.066 C + 4.650 R <sup>2</sup> = 0.981	-1.008 C + 4.434 R <sup>2</sup> = 0.979	-0.991 C + 4.403 R <sup>2</sup> = 0.977
V <sub>f</sub> , 10 <sup>-7</sup> m <sup>3</sup>	0.986 C + 1.551 R <sup>2</sup> = 0.998	0.928 C + 1.352 R <sup>2</sup> = 0.999	0.849 C + 1.154 R <sup>2</sup> = 0.999
$\tau$ , 10 <sup>-13</sup> s	0.139 C + 8.282 R <sup>2</sup> = 0.985	0.08 C <sup>2</sup> + 0.000 C + 7.652 R <sup>2</sup> = 0.973	0.205 C <sup>2</sup> - 0.267 C + 7.439 R <sup>2</sup> = 0.997
( $\alpha/f^2$ ) <sub>cl</sub> 10 <sup>-14</sup> , s <sup>2</sup> m <sup>-1</sup>	0.111 C + 12.38 R <sup>2</sup> = 0.955	0.149 C <sup>2</sup> - 0.160 C + 11.51 R <sup>2</sup> = 0.937	0.35 C <sup>2</sup> - 0.614 C + 11.54 R <sup>2</sup> = 0.998

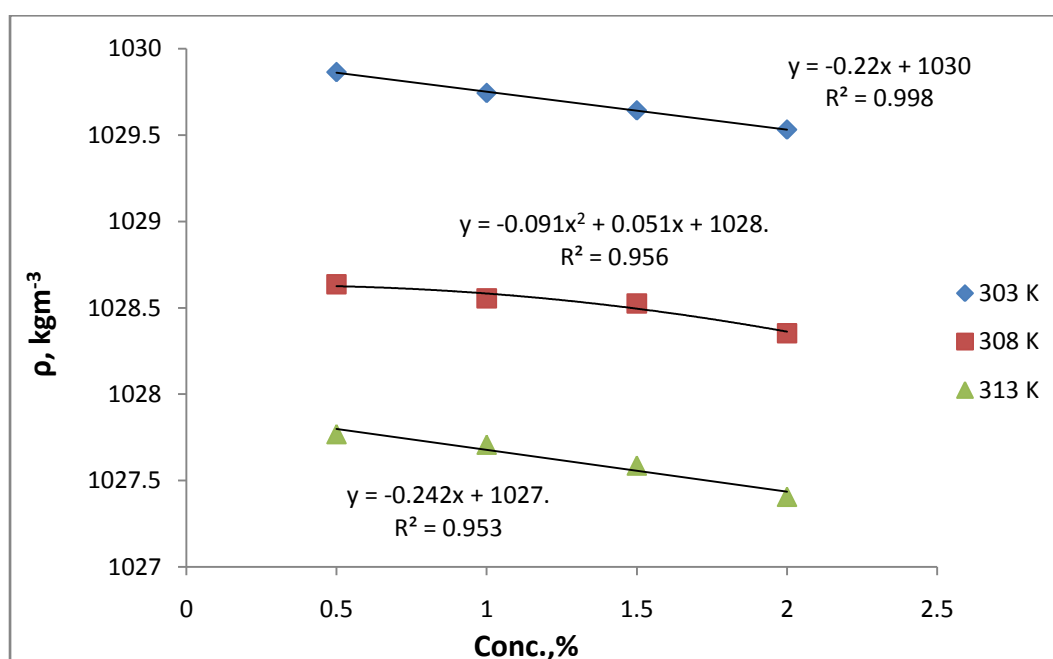


Fig. 4.27: The plots of density ( $\rho$ ) against concentration (%) of BSB4HM in 1,4 dioxane at 303, 308 and 313 K.

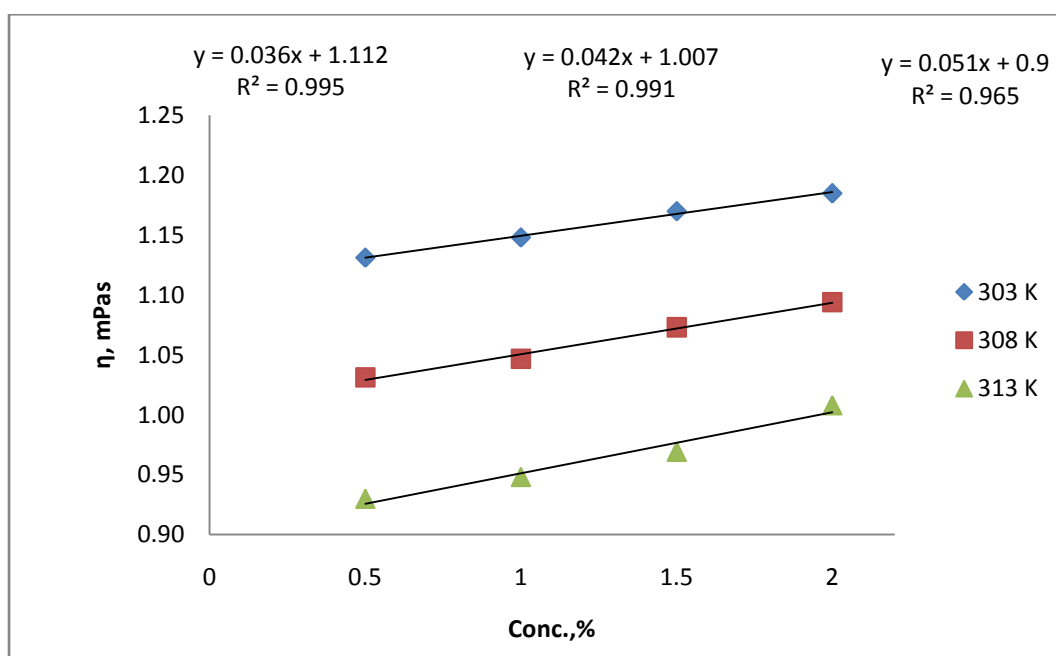


Fig. 4.28: The plots of viscosity ( $\eta$ ) against concentration (%) of BSB4HM in 1,4 dioxane at 303, 308 and 313 K.

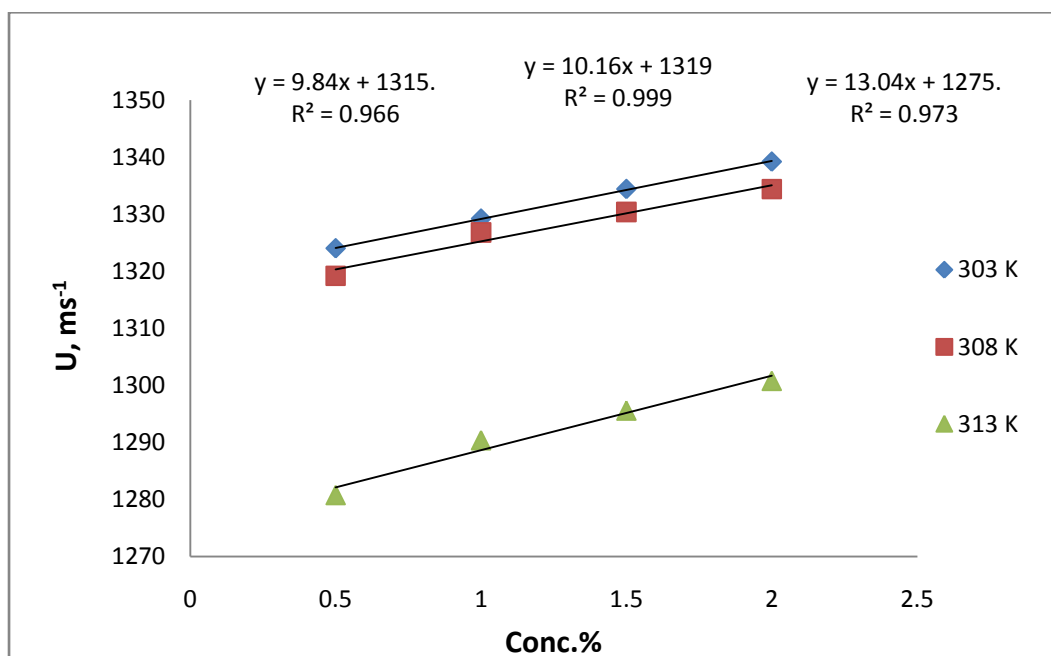


Fig. 4.29: The plots of sound velocity ( $U$ ) against concentration (%) of ESB4HM in 1,4 dioxane at 303, 308 and 313 K.

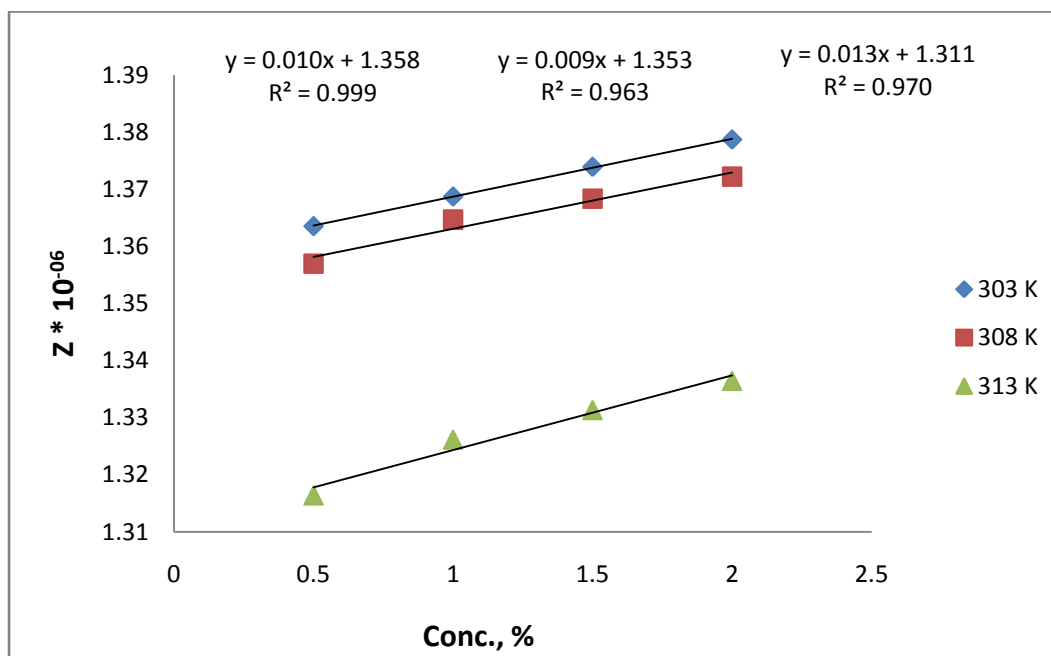


Fig. 4.30: The plots of specific acoustical impedance ( $Z$ ) against concentration (%) of BSB4HM in 1,4 dioxane at 303, 308 and 313 K.

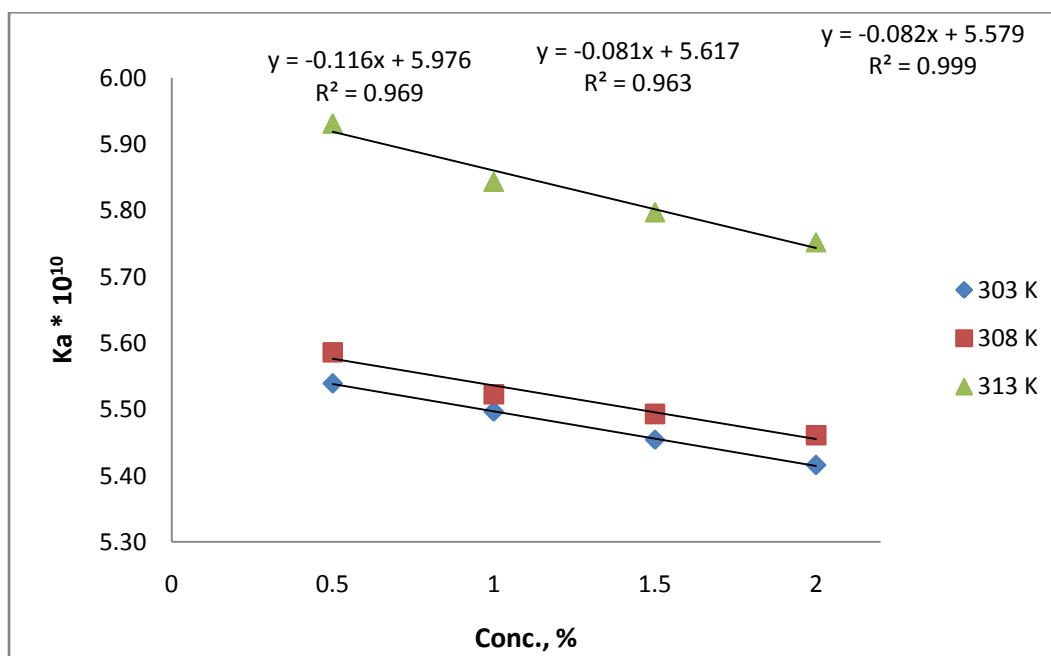


Fig. 4.31: The plots of adiabatic compressibility ( $\kappa_a$ ) against concentration (%) of BSB4HM in 1,4 dioxane at 303, 308 and 313 K.

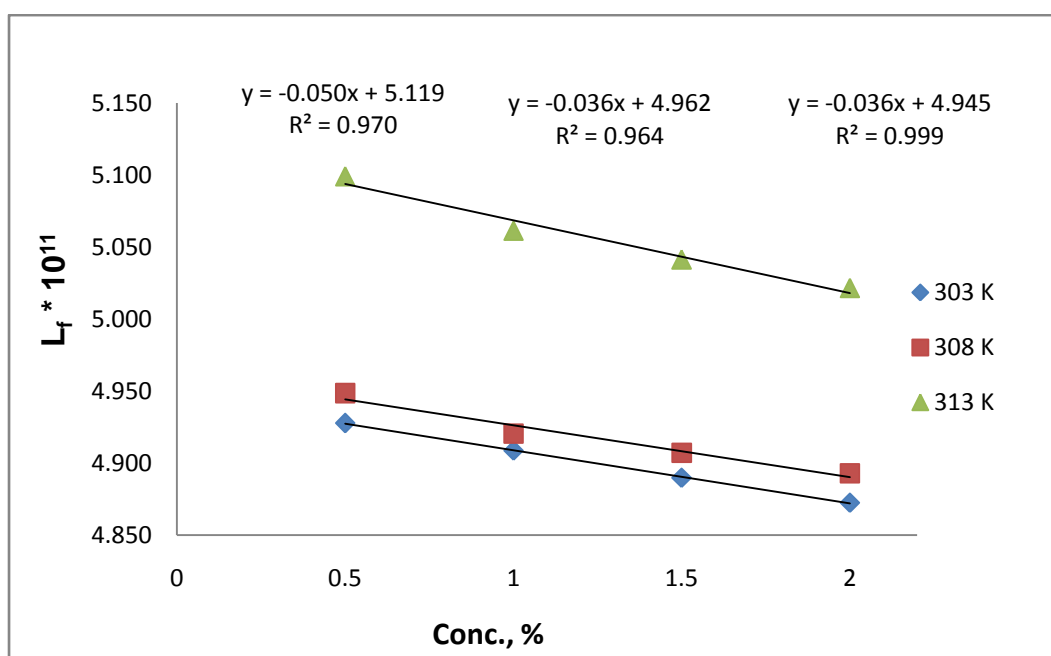


Fig. 4.32: The plots of inter molecular free path length ( $L_f$ ) against concentration (%) of BSB4HM in 1,4 dioxane at 303, 308 and 313 K.

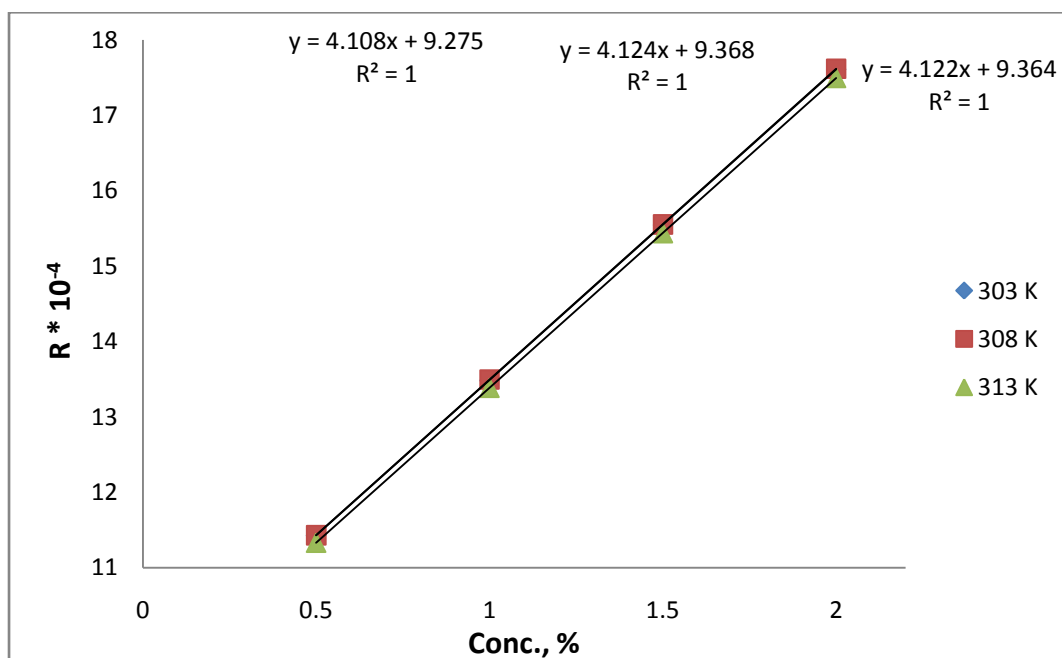


Fig. 4.33: The plots of Rao's molar sound function ( $R$ ) against concentration (%) of BSB4HM in 1,4 dioxane at 303, 308 and 313 K.

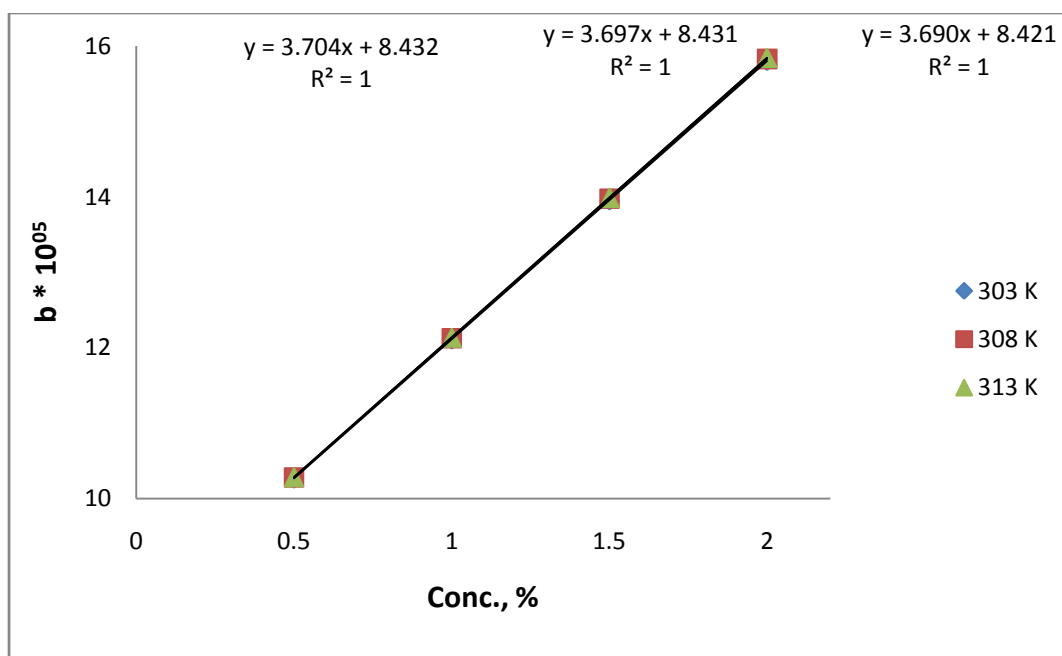


Fig. 4.34: The plots of Van der Waals constant ( $b$ ) against concentration (%) of BSB4HM in 1,4 dioxane at 303, 308 and 313 K.

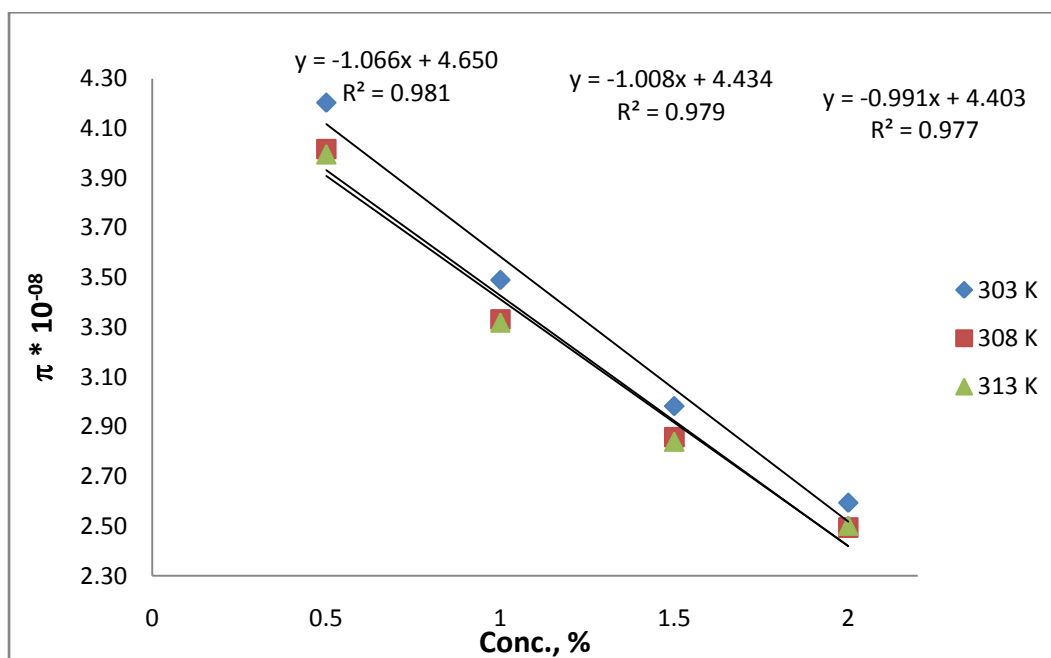


Fig. 4.35: The plots of internal pressure against concentration (%) of BSB4HM in 1,4 dioxane at 303, 308 and 313 K.

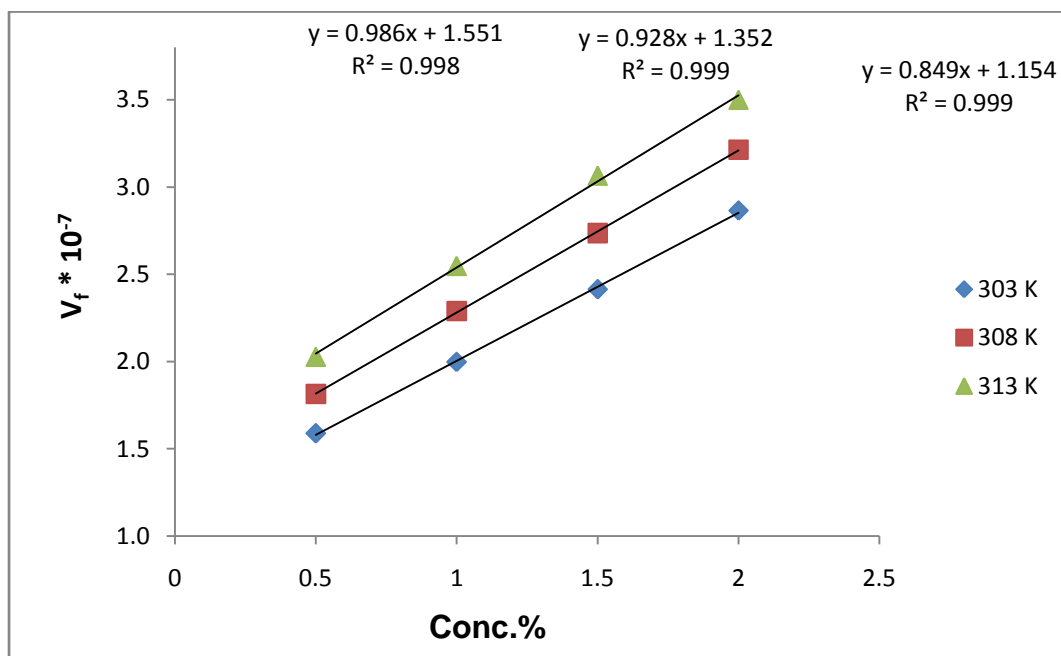


Fig. 4.36: The plots of free volume ( $V_f$ ) against concentration (%) of BSB4HM in 1,4 dioxane at 303, 308 and 313 K.

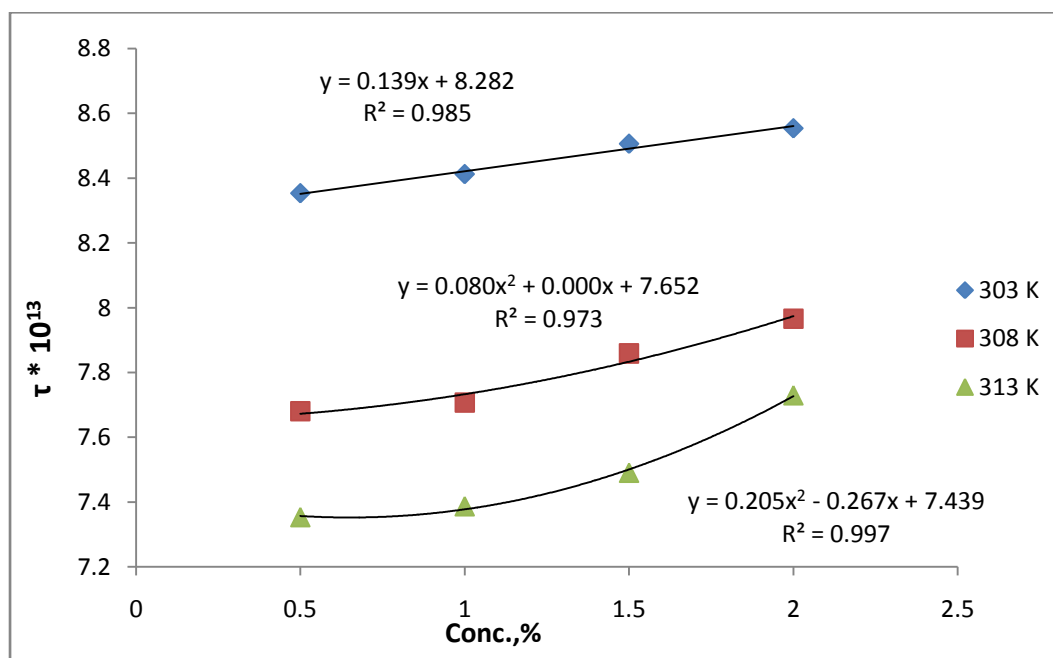


Fig. 4.37: The plots of viscous relaxation time ( $\tau$ ) against concentration (%) of BSB4HM in 1,4 dioxane at 303, 308 and 313 K.

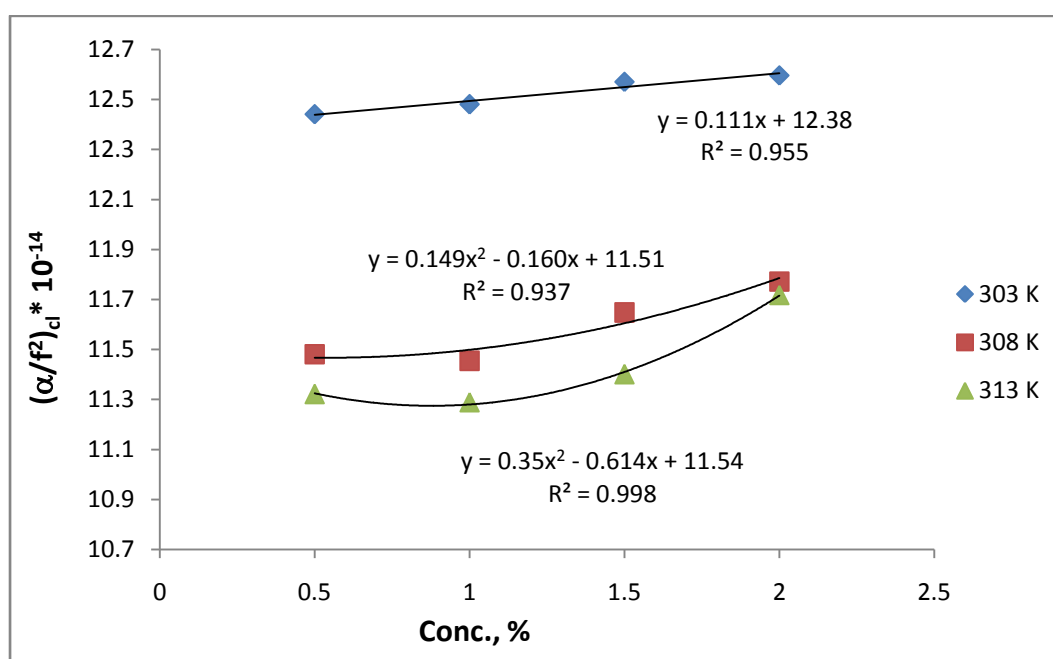
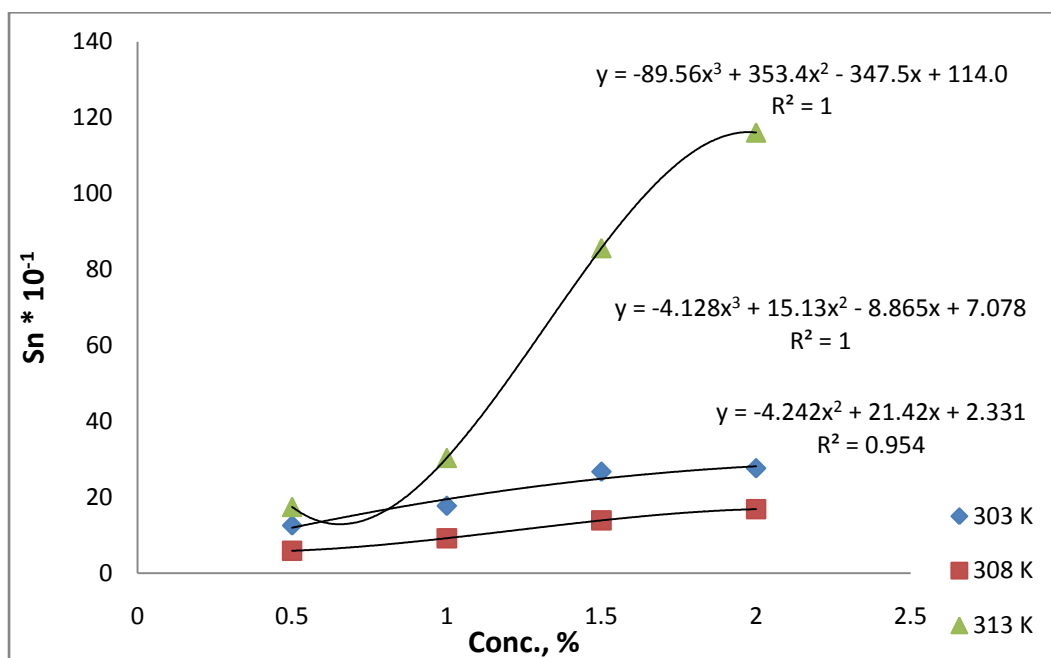


Fig. 4.38: The plots of classical absorption co-efficient (CAC) against concentration (%) of BSB4HM in 1,4 dioxane at 303, 308 and 313 K.





**Fig. 4.39:** The plots of solvation number (Sn) against concentration (%) of BSB4HM in 1,4 dioxane at 303, 308 and 313 K.

Table-4.9:  $\Delta G^*$  data of BSB4HM

Conc.	$\Delta G^*$ , kJ mol <sup>-1</sup>			$\Delta H$ , kJ mol <sup>-1</sup>	$\Delta S$ , J K <sup>-1</sup> mol <sup>-1</sup>
	303 K	308 K	313 K		
<b>0.5</b>	4.23	4.09	4.04	8.25	13.20
<b>1</b>	4.25	4.10	4.05	7.13	9.54
<b>1.5</b>	4.28	4.15	4.09	7.69	11.21
<b>2</b>	4.29	4.18	4.17	7.23	9.63
<b>Average</b>	4.26	4.13	4.09		

$$\Delta G^* = 41.59 C + 4211, R^2 = 0.985 \text{ at } 303 \text{ K}$$

$$\Delta G^* = 65.95 C + 4044, R^2 = 0.944 \text{ at } 308 \text{ K}$$

$$\Delta G^* = 118.1 C + 3926, R^2 = 0.952 \text{ at } 313 \text{ K}$$

### Ultrasonic study of bisbenzoxazine BSB4HE

The  $\rho$ ,  $\eta$  and  $U$  data of 1, 4-dioxane and BSB4HE solutions at different temperatures are presented in Table-4.10. Similar behavior is observed as in BSB4HCy and BSB4HM due to specific interactions occurring in the solutions. These data correlated with  $C$  and  $T$  (Fig.4.40-4.42). The least squares equations and  $R^2$  values are reported in Table-4.11 from which it is observed that excellent correlation is observed.

Various acoustical parameters are determined using  $\rho$ ,  $\eta$  and  $U$  data and correlated with  $C$  and  $T$  (Figs. 4.43-4.52). The least square equations along with  $R^2$  values are summarized in Table-4.11 from which it is clear that a good to excellent correlation is observed. Linear increase of  $Z$ ,  $R$  and  $b$  (practically no temperature effect),  $V_f$ ,  $\tau$  and  $(\alpha/f^2)_{cl}$  (nonlinear at 303 and 308 K) with  $C$  and decrease with  $T$ ; and  $\kappa_a$  and  $L_f$  (nonlinear at 313 K) and  $\pi$  with  $C$  and increase with  $T$  suggested existence of powerful molecular interactions and structure forming nature of BSB4HE and is further supported by positive values of  $S_n$ . Non linear increase of  $S_n$  with  $C$  and  $T$  suggested co-existence of solvent-solute and solute-solute interactions. The trend signified powerful solvent-solute interactions over solute-solute interactions.

The activation thermodynamic parameters namely  $\Delta G_b^*$ ,  $\Delta H_b^*$  and  $\Delta S_b^*$  are determined at various  $C$  and  $T$  according to Eqns. 4.25. The data are summarized in Table-4.12 from which it is clear that practically  $\Delta G_b^*$  remained constant with  $C$  but it is decreased a little with  $T$ .

**Table-4.10: The density ( $\rho$ ), viscosity ( $\eta$ ), ultrasonic speed (U) and standard deviation (S) data of bisbenzoxazine BSB4HE in 1,4 dioxane at 303, 308 and 313 K.**

Conc., %	Density $\rho$ , kg/m <sup>3</sup>	Viscosity $\eta$ , mPa.s	Ave. Dist. d, mm	Wave length $\lambda$ , mm	U ms <sup>-1</sup> (F=2MHz)	Std. devi., mm ( $\pm$ )
303 K						
0	1029.6	1.109	3.281	0.6562	1312.4	0.0016
0.5	1029.1	1.137	3.295	0.6590	1318.0	0.0010
1.0	1029.0	1.155	3.319	0.6638	1327.6	0.0020
1.5	1028.8	1.187	3.329	0.6658	1331.6	0.0016
2.0	1028.7	1.209	3.340	0.6680	1336.0	0.0021
308 K						
0	1028.8	1.008	3.235	0.6470	1294.0	0.0025
0.5	1029.0	1.036	3.263	0.6526	1305.2	0.0032
1.0	1028.9	1.055	3.280	0.6560	1312.0	0.0015
1.5	1028.7	1.078	3.291	0.6582	1316.4	0.0017
2.0	1028.6	1.103	3.305	0.6610	1322.0	0.0023
313 K						
0	1028.1	0.915	3.181	0.6362	1272.4	0.0037
0.5	1028.9	0.929	3.190	0.6380	1276.0	0.0027
1.0	1027.8	0.950	3.201	0.6402	1280.4	0.0020
1.5	1027.7	0.972	3.215	0.6430	1286.0	0.0024
2.0	1027.5	0.996	3.227	0.6454	1290.8	0.0021

**Table-4.11: The correlation equations and regression coefficients of bisbenzoxazine BSB4HE in 1,4 dioxane at 303, 308 and 313 K.**

Parameter	Correlation equation and regression coefficient, R <sup>2</sup>		
	303 K	308 K	313 K
$\rho$ , kgm <sup>-3</sup>	-0.256 C + 1029. R <sup>2</sup> = 0.999	-0.236 C + 1029. R <sup>2</sup> = 0.987	-0.246 C + 1029 R <sup>2</sup> = 0.993
$\eta$ , mPa.s	0.049 C + 1.110 R <sup>2</sup> = 0.988	0.044 C + 1.011 R <sup>2</sup> = 0.996	0.044 C + 0.906 R <sup>2</sup> = 0.998
U, ms <sup>-1</sup>	11.6 C + 1313. R <sup>2</sup> = 0.951	10.96 C + 1300. R <sup>2</sup> = 0.993	10 C + 1270. R <sup>2</sup> = 0.998
Z, 10 <sup>6</sup> kg.m <sup>-2</sup> .s <sup>-1</sup>	0.011 C + 1.352 R <sup>2</sup> = 0.948	0.011 C + 1.338 R <sup>2</sup> = 0.992	0.01 C + 1.307 R <sup>2</sup> = 0.998
$\kappa_a$ , 10 <sup>-10</sup> Pa <sup>-1</sup>	-0.090 C + 6.016 R <sup>2</sup> = 0.998	-0.092 C + 5.746 R <sup>2</sup> = 0.992	0.044 C <sup>2</sup> - 0.206 C + 5.683 R <sup>2</sup> = 0.989
L <sub>f</sub> , 10 <sup>-11</sup> m	-0.039 C + 5.135 R <sup>2</sup> = 0.998	-0.040 C + 5.019 R <sup>2</sup> = 0.992	0.019 C <sup>2</sup> - 0.091 C + 4.991 R <sup>2</sup> = 0.989
R, 10 <sup>-4</sup> m <sup>10/3</sup> .s <sup>-1/3</sup> .mol <sup>-1</sup>	4.082 C + 9.255 R <sup>2</sup> = 1	4.112 C + 9.33 R <sup>2</sup> = 1	4.132 C + 9.355 R <sup>2</sup> = 1
b, 10 <sup>-5</sup> m <sup>3</sup>	3.695 C + 8.423 R <sup>2</sup> = 1	3.696 C + 8.427 R <sup>2</sup> = 1	3.696 C + 8.426 R <sup>2</sup> = 1
$\pi$ , 10 <sup>8</sup> Pa	-1.059 C + 4.660 R <sup>2</sup> = 0.979	-1.015 C + 4.471 R <sup>2</sup> = 0.980	-0.999 C + 4.424 R <sup>2</sup> = 0.980
V <sub>f</sub> , 10 <sup>-7</sup> m <sup>3</sup>	1.001 C + 1.514 R <sup>2</sup> = 1	0.903 C + 1.321 R <sup>2</sup> = 1	0.8 C + 1.167 R <sup>2</sup> = 0.999
$\tau$ , 10 <sup>-13</sup> s	0.212 C + 8.339 R <sup>2</sup> = 0.909	0.205 C + 7.760 R <sup>2</sup> = 0.984	0.234 C + 7.275 R <sup>2</sup> = 0.997
( $a/f^2$ ) <sub>cl</sub> 10 <sup>-14</sup> , s <sup>2</sup> m <sup>-1</sup>	-0.587 C <sup>3</sup> + 2.393 C <sup>2</sup> - 2.725 C + 13.53 R <sup>2</sup> = 1	0.090 C <sup>2</sup> - 0.018 C + 11.88 R <sup>2</sup> = 0.991	0.269 C + 11.29 R <sup>2</sup> = 0.995

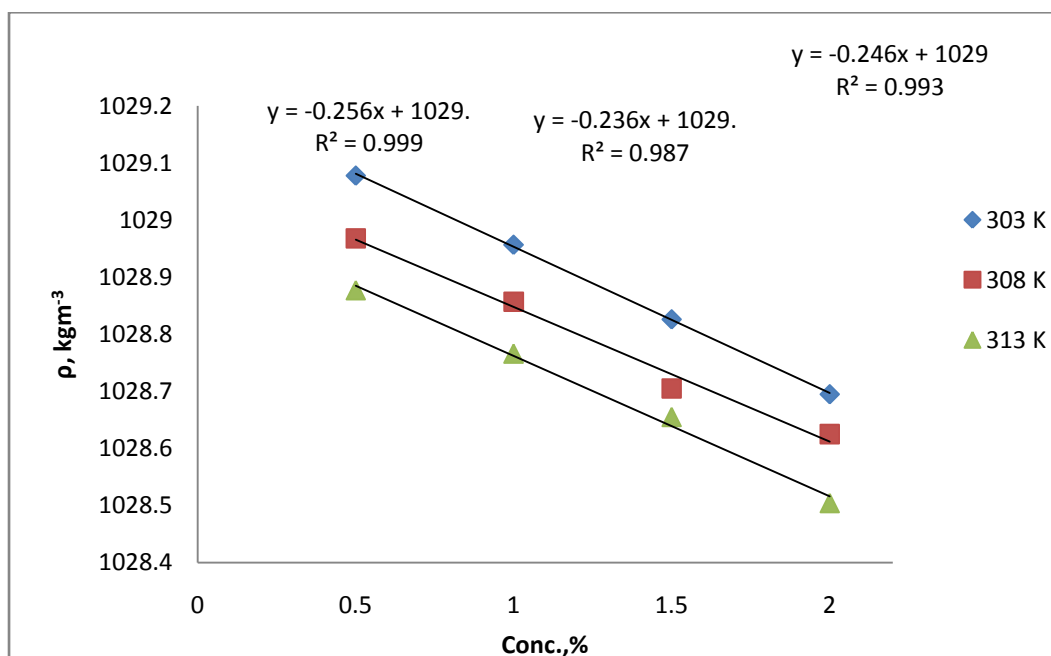


Fig. 4.40: The plots of density ( $\rho$ ) against concentration (%) of BSB4HE in 1,4 dioxane at 303, 308 and 313 K.

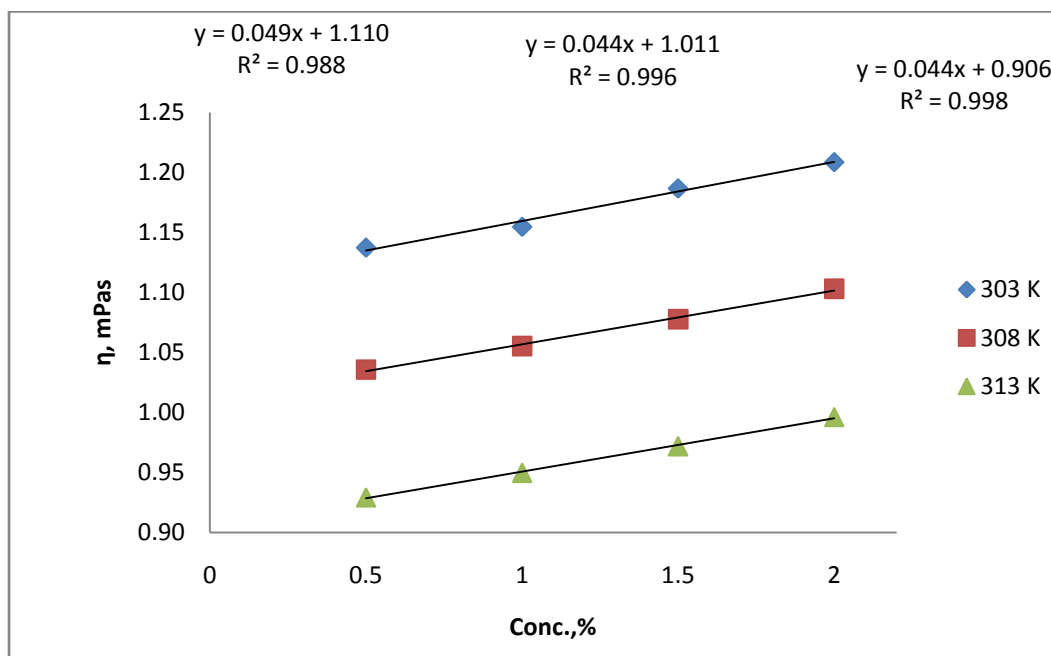


Fig. 4.41: The plots of viscosity ( $\eta$ ) against concentration (%) of BSB4HE in 1,4 dioxane at 303, 308 and 313 K.

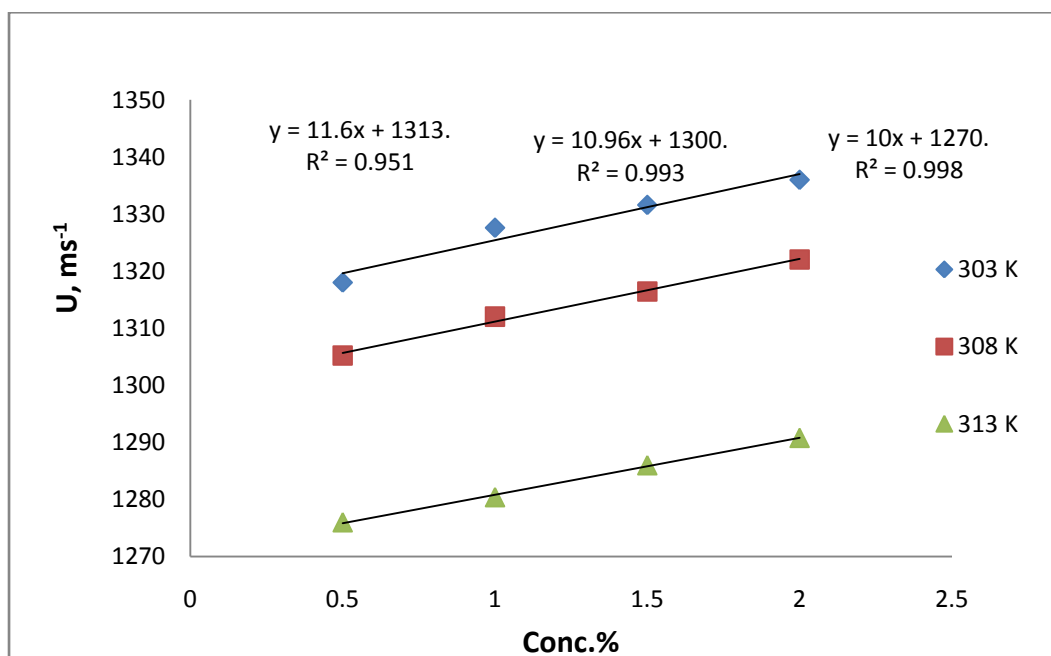


Fig. 4.42: The plots of sound velocity ( $U$ ) against concentration (%) of ESB4HE in 1,4 dioxane at 303, 308 and 313 K.

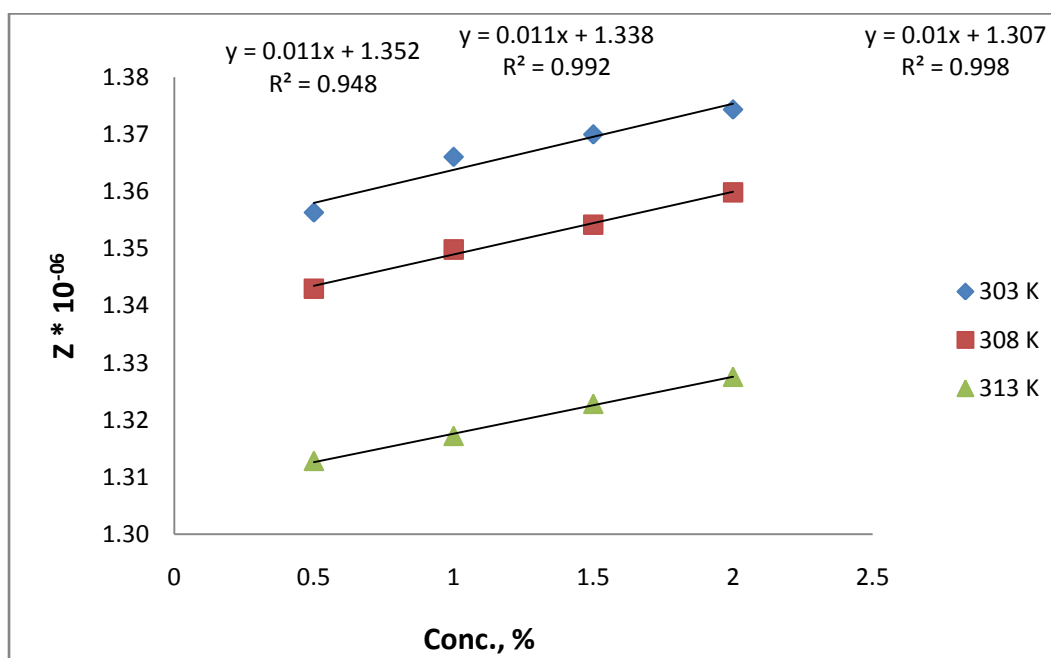


Fig. 4.43: The plots of specific acoustical impedance ( $Z$ ) against concentration (%) of BSB4HE in 1,4 dioxane at 303, 308 and 313 K.

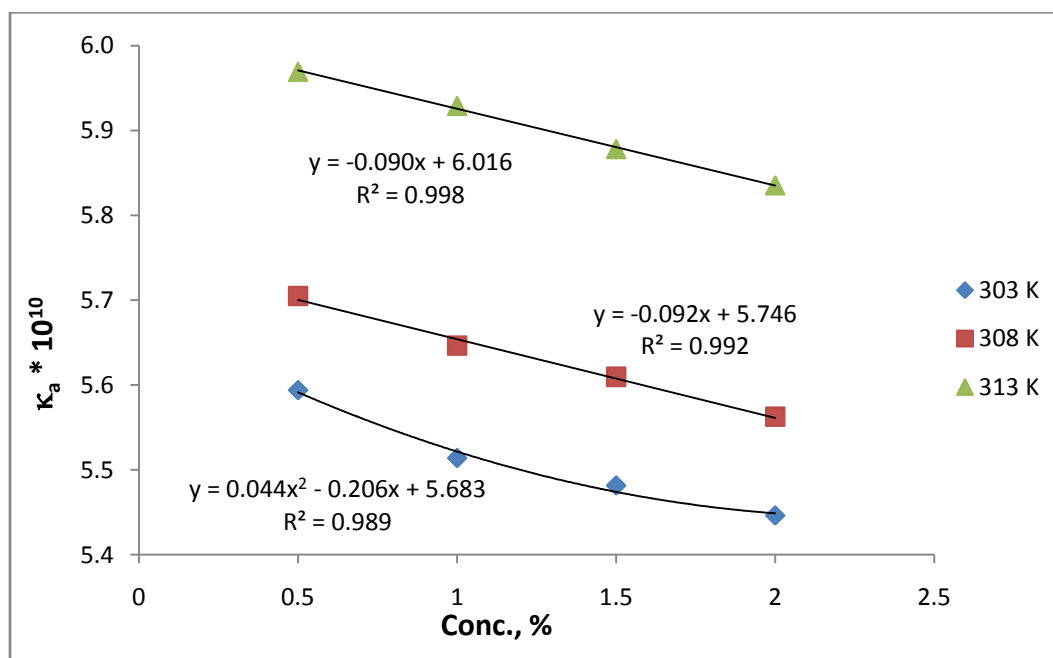


Fig. 4.44: The plots of adiabatic compressibility ( $\kappa_a$ ) against concentration (%) of BSB4HE in 1,4 dioxane at 303, 308 and 313 K.

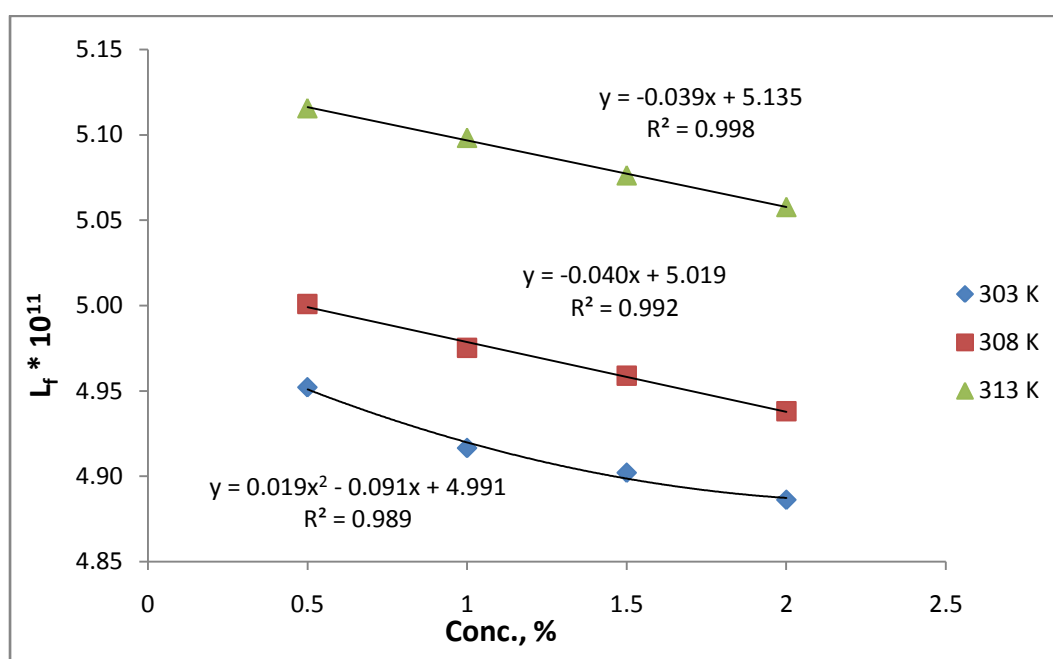


Fig. 4.45: The plots of inter molecular free path length ( $L_f$ ) against concentration (%) of BSB4HE in 1,4 dioxane at 303, 308 and 313 K.



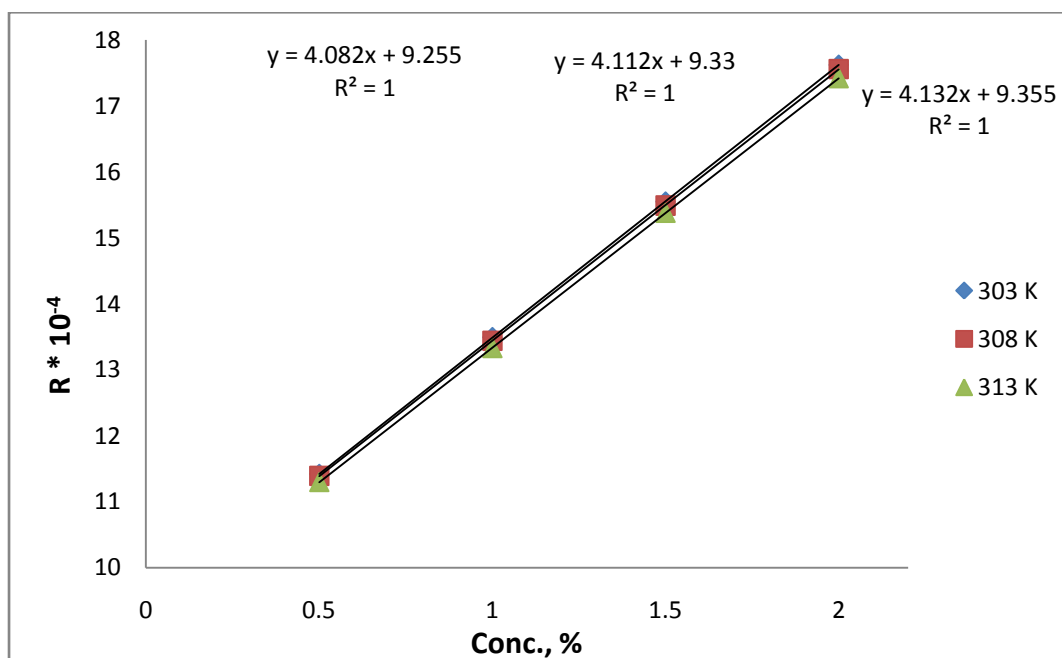


Fig. 4.46: The plots of Rao's molar sound function (R) against concentration (%) of BSB4HE in 1,4 dioxane at 303, 308 and 313 K.

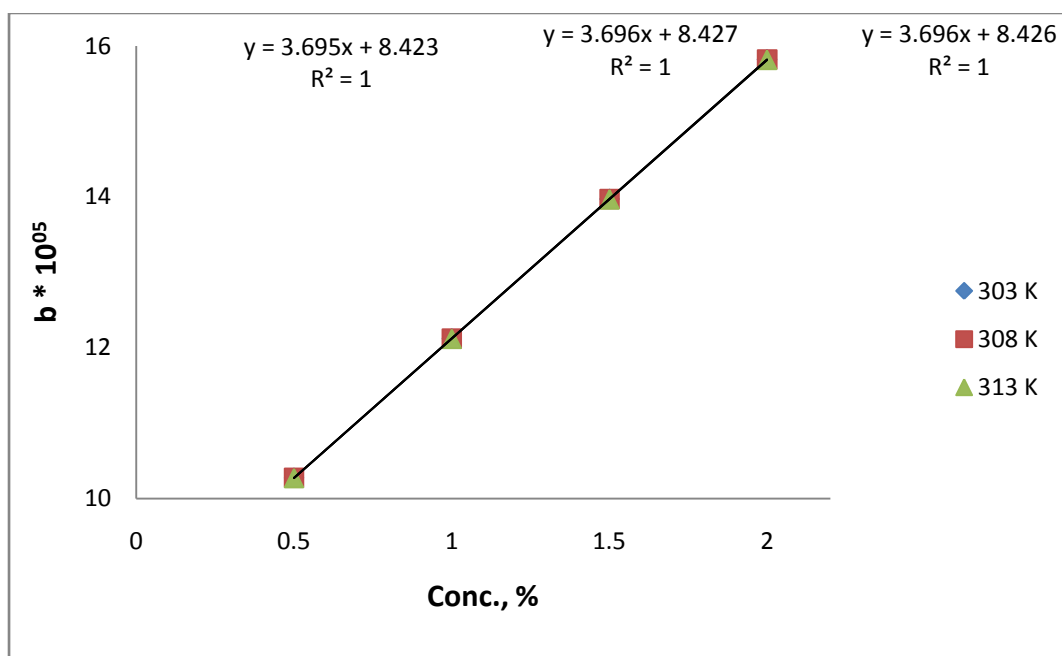


Fig. 4.47: The plots of Van der Waals constant (b) against concentration (%) of BSB4HE in 1,4 dioxane at 303, 308 and 313 K.

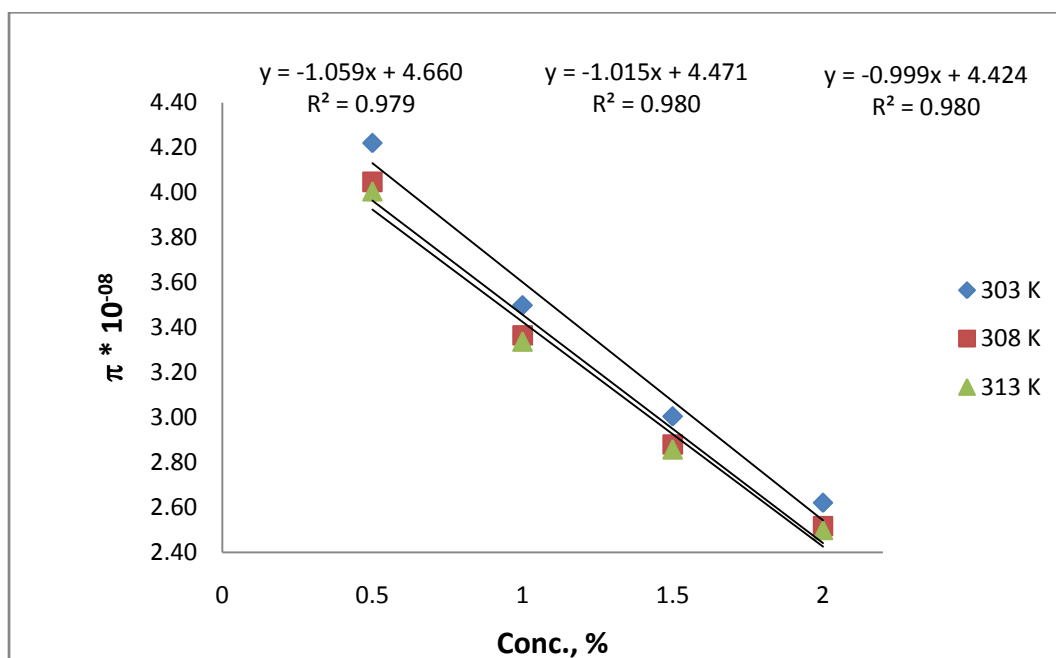


Fig. 4.48: The plots of internal pressure against concentration (%) of BSB4HE in 1,4 dioxane at 303, 308 and 313 K.

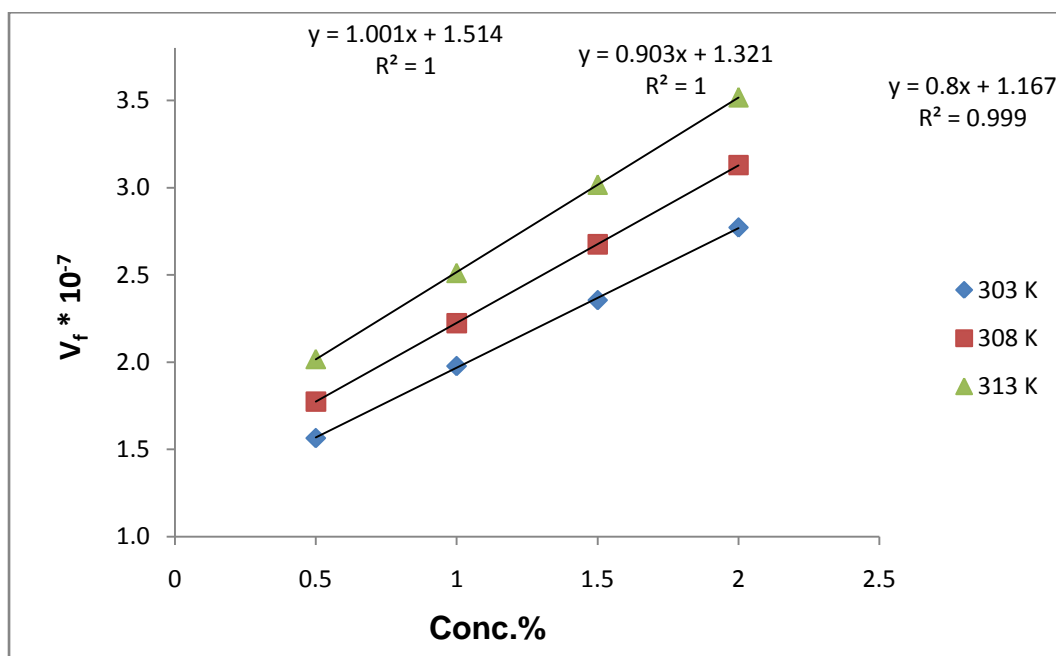


Fig. 4.49: The plots of free volume ( $V_f$ ) against concentration (%) of BSB4HE in 1,4 dioxane at 303, 308 and 313 K.

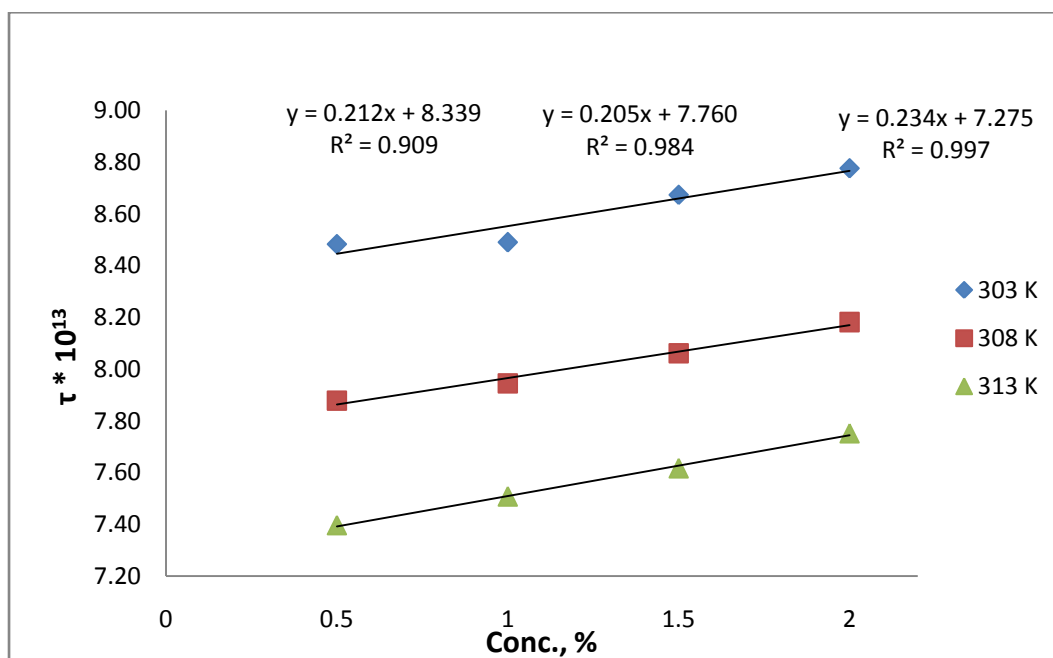


Fig. 4.50: The plots of viscous relaxation time ( $\tau$ ) against concentration (%) of BSB4HE in 1,4 dioxane at 303, 308 and 313 K.

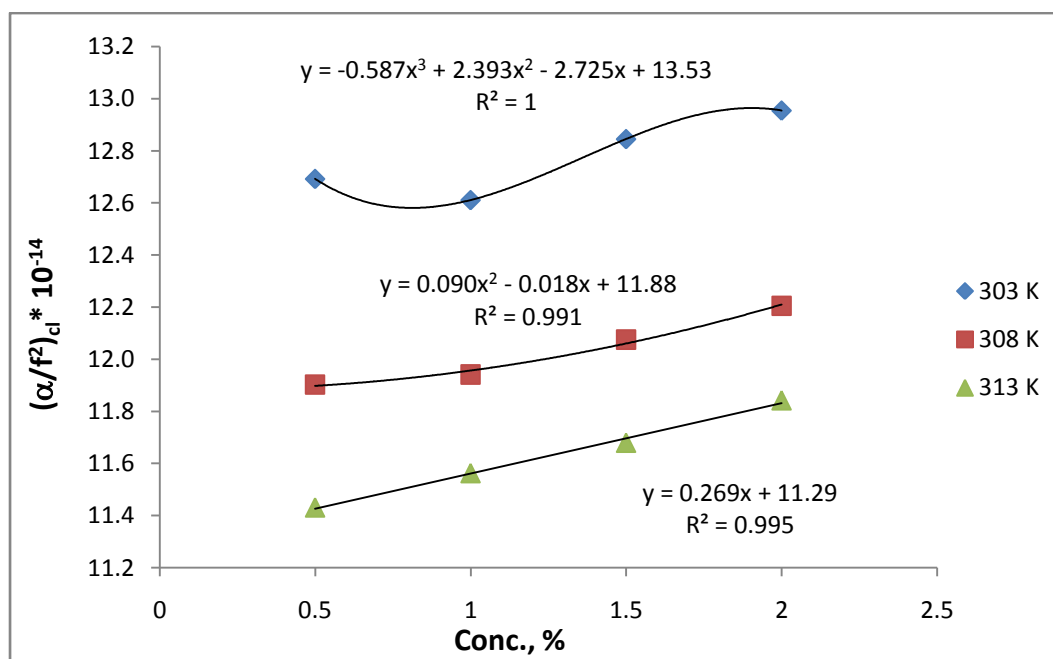
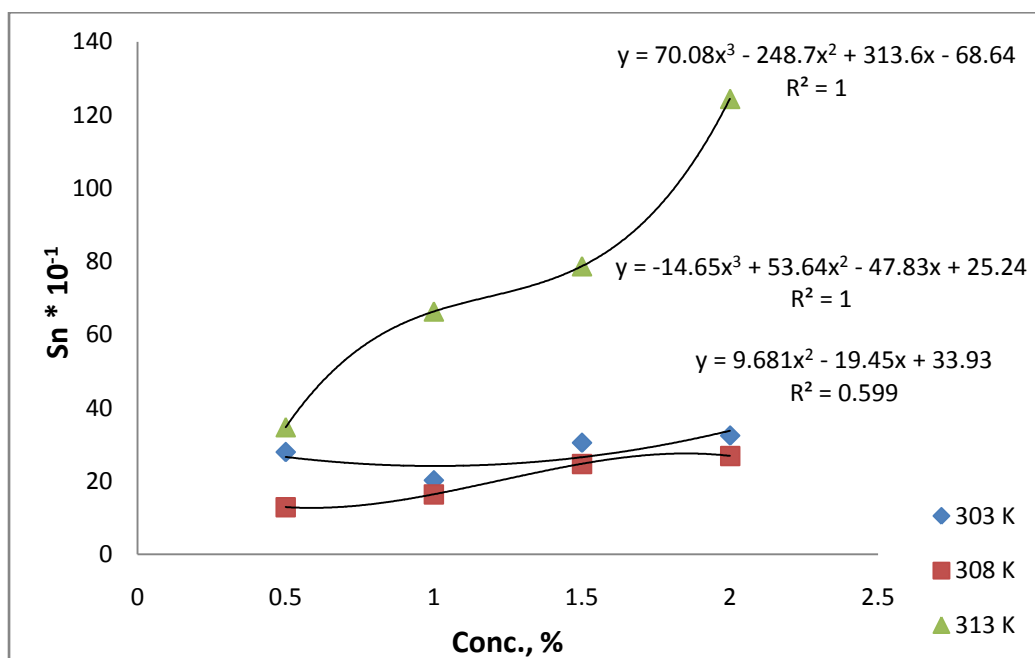


Fig. 4.51: The plots of classical absorption co-efficient (CAC) against concentration (%) of BSB4HE in 1,4 dioxane at 303, 308 and 313 K.



**Fig. 4.52:** The plots of solvation number (Sn) against concentration (%) of BSB4HE in 1,4 dioxane at 303, 308 and 313 K.

**Table-4.12. :  $\Delta G^*$  data of BSB4HE**

Conc.	$\Delta G^*$ , kJ mol <sup>-1</sup>			$\Delta H$ , kJ mol <sup>-1</sup>	$\Delta S$ , J K <sup>-1</sup> mol <sup>-1</sup>
	303 K	308 K	313 K		
<b>0.5</b>	4.27	4.15	4.06	8.25	13.20
<b>1</b>	4.27	4.17	4.09	7.13	9.54
<b>1.5</b>	4.33	4.21	4.13	7.69	11.21
<b>2</b>	4.36	4.25	4.18	7.23	9.63
<b>Average</b>	4.31	4.20	4.12		

$$\Delta G^* = 62.25x + 4229, R^2 = 0.909 \text{ at } 303 \text{ K}$$

$$\Delta G^* = 65.50x + 4114, R^2 = 0.985 \text{ at } 308 \text{ K}$$

$$\Delta G^* = 80.67x + 4013, R^2 = 0.998 \text{ at } 313 \text{ K}$$

### Ultrasonic study of bisbenzoxazine BSB4HS

The  $\rho$ ,  $\eta$  and  $U$  data of 1, 4-dioxane and BSB4HS solutions at different temperatures are reported in Table-4.13, similar behavior is observed as in BSB4HCy, BSB4HM and BSB4HE. The change in  $\rho$  and  $U$  with  $C$  and  $T$  are not as appreciable as  $\eta$  due to specific molecular interactions occurring in the solutions. These data are correlated with  $C$  and  $T$  (Figs. 4.53-4.55). The least square equations and regression coefficients are presented in Table-4.14 from which it is clear that excellent correlation exists between studied parameters and  $C$  at different temperatures.

Various acoustical parameters are derived from  $\rho$ ,  $\eta$  and  $U$  data and are correlated with  $C$  and  $T$  (Figs. 4.56-4.65). The least square equations and  $R^2$  values are presented in Table-4.14 from which it is observed that a fairly good to excellent correlation is observed. Linear increase of  $Z$ ,  $R$  and  $b$  (practically no temperature effect),  $V_f$ ,  $\tau$  and  $(\alpha / f^2)_{cl}$  (nonlinear) with  $C$  and decrease with  $T$ ; and linear decrease of  $\kappa_a$ ,  $L_f$  and  $\pi$  with  $C$  and increase with  $T$  provided information about presence of strong molecular interactions and solvophilic nature of BSB4HS and it is further confirmed by positive values of  $S_n$ . Nonlinear increase of  $S_n$  with  $C$  and  $T$  further confirmed coexistence of solvent-solute and solute-solute interactions in the solutions. The observed trend signified that solvent-solute interactions are strong over solute-solute interactions.

The activation thermodynamic parameters namely  $\Delta G_b^*$ ,  $\Delta H_b^*$  and  $\Delta S_b^*$  are derived according to Eqns. 4.25 using  $\tau$  data at different  $C$  and  $T$ . These data are presented in Table-4.15 from which it is observed that  $\Delta G_b^*$  remained practically constant and decreased a little with  $T$ .

Physical properties like density, viscosity, refractive index, intermolecular free path length, free volume, internal pressure, adiabatic compressibility, etc affect the ultrasonic speed in different organic solvents and solutions. Because of molecular interactions, the structure of the solute is modified and hence physical properties under consideration change accordingly. Linear or nonlinear increase of  $\rho$  and  $U$  with  $C$  gives information about increase of cohesive forces because of strong molecular interactions, while decrease of these parameters with  $T$  supports the decrease of cohesive

forces. The increase in temperature has two opposite effects namely structure formation (intermolecular association) and structure destruction formed previously. The structure forming tendency is primarily due to solvent-solute interactions, while destruction of structure formed previously is due to thermal fluctuations. When thermal energy is greater than that of interaction energy, it causes destruction of structure formed previously.

Variation of  $U$  in the solutions depends on intermolecular free path length. When ultrasonic waves are incident on the solution, the molecules get perturbed. Due to some elasticity of the medium, perturbed molecules regain their equilibrium positions. When a solute is added to a solvent, its molecules attract certain solvent molecules toward them. This phenomenon is known as a limiting compressibility. Generally  $\kappa_a$  and  $L_f$  decrease with increasing  $C$  and decrease with increasing  $T$ . The aggregation of solvent molecules around solute molecules supports strong solvent-solute interactions and consequently structural modification takes place. Relaxation process causes dispersion of  $U$  in the system. Molecular interactions such as solvent-solute interactions, quantum mechanical dispersive forces and dielectric forces cause either contraction or expansion of the liquids and solutions and hence change in transport properties. Molecular association affects both apparent molecular size and hence  $\rho$ ,  $\eta$  and  $U$  and other derived parameters vary with  $C$  and  $T$ . Thus, knowledge of ultrasonic speed and other derived parameters are very useful in understanding the structure and strength of the molecular interactions, in the solutions, which are very important in various industries.

**Table-4.13: The density ( $\rho$ ), viscosity ( $\eta$ ), ultrasonic speed (U) and standard deviation (S) data of bisbenzoxazine BSB4HS in 1,4 dioxane at 303, 308 and 313 K.**

Conc., %	Density $\rho$ , kg/m <sup>3</sup>	Viscosity $\eta$ , mPa.s	Ave. Dist. d, mm	Wave length $\lambda$ , mm	U ms <sup>-1</sup> (F=2MHz)	Std. devi., mm ( $\pm$ )
303 K						
0	1029.6	1.109	3.281	0.6562	1312.4	0.0016
0.5	1029.7	1.132	3.305	0.6610	1322.0	0.0036
1.0	1029.4	1.151	3.322	0.6644	1328.8	0.0027
1.5	1029.3	1.168	3.342	0.6684	1336.8	0.0020
2.0	1029.2	1.188	3.367	0.6734	1346.8	0.0019
308 K						
0	1028.8	1.008	3.235	0.6470	1294	0.0025
0.5	1028.6	1.024	3.272	0.6544	1308.8	0.0021
1.0	1028.5	1.040	3.296	0.6592	1318.4	0.0014
1.5	1028.3	1.064	3.325	0.6650	1330.0	0.0035
2.0	1028.2	1.076	3.339	0.6678	1335.6	0.0026
313 K						
0	1028.1	0.915	3.181	0.6362	1272.4	0.0037
0.5	1027.8	0.937	3.216	0.6432	1286.4	0.0040
1.0	1027.6	0.956	3.240	0.6480	1296.0	0.0025
1.5	1027.4	0.981	3.268	0.6536	1307.2	0.0020
2.0	1027.2	1.001	3.285	0.6570	1314.0	0.0036



**Table-4.14: The correlation equations and regression coefficients of bisbenzoxazine BSB4HS in 1,4 dioxane at 303, 308 and 313 K.**

Parameter	Correlation equation and regression coefficient, R <sup>2</sup>		
	303 K	308 K	313 K
$\rho$ , kgm <sup>-3</sup>	-0.312 C + 1029. R <sup>2</sup> = 0.980	-0.312 C + 1028. R <sup>2</sup> = 0.964	-0.379 C + 1028 R <sup>2</sup> = 0.990
$\eta$ , mPa.s	0.037 C + 1.113 R <sup>2</sup> = 0.999	0.036 C + 1.005 R <sup>2</sup> = 0.986	0.043 C + 0.913 R <sup>2</sup> = 0.997
U, ms <sup>-1</sup>	18.4 C + 1300. R <sup>2</sup> = 0.983	16.48 C + 1313 R <sup>2</sup> = 0.992	18.8 C + 1277. R <sup>2</sup> = 0.991
Z, 10 <sup>6</sup> kg.m <sup>-2</sup> .s <sup>-1</sup>	0.016 C + 1.352 R <sup>2</sup> = 0.991	0.018 C + 1.337 R <sup>2</sup> = 0.982	0.018 C + 1.313 R <sup>2</sup> = 0.991
$\kappa_a$ , 10 <sup>-10</sup> Pa <sup>-1</sup>	-0.164 C + 5.957 R <sup>2</sup> = 0.990	-0.153 C + 5.746 R <sup>2</sup> = 0.981	-0.133 C + 5.629 R <sup>2</sup> = 0.993
L <sub>f</sub> , 10 <sup>-11</sup> m	-0.071 C + 5.111 R <sup>2</sup> = 0.990	-0.067 C + 5.019 R <sup>2</sup> = 0.982	-0.059 C + 4.968 R <sup>2</sup> = 0.993
R, 10 <sup>-4</sup> m <sup>10/3</sup> .s <sup>-1/3</sup> .mol <sup>-1</sup>	4.142 C + 9.270 R <sup>2</sup> = 1	4.155 C + 9.319 R <sup>2</sup> = 1	4.151 C + 9.342 R <sup>2</sup> = 1
b, 10 <sup>-5</sup> m <sup>3</sup>	3.708 C + 8.431 R <sup>2</sup> = 1	3.701 C + 8.428 R <sup>2</sup> = 1	3.694 C + 8.421 R <sup>2</sup> = 1
$\pi$ , 10 <sup>8</sup> Pa	-1.073 C + 4.658 R <sup>2</sup> = 0.981	-1.024 C + 4.446 R <sup>2</sup> = 0.981	-1.008 C + 4.422 R <sup>2</sup> = 0.980
V <sub>f</sub> , 10 <sup>-7</sup> m <sup>3</sup>	1.045 C + 1.491 R <sup>2</sup> = 0.999	0.986 C + 1.309 R <sup>2</sup> = 0.999	0.864 C + 1.138 R <sup>2</sup> = 0.999
$\tau$ , 10 <sup>-13</sup> s	0.063 C + 8.363 R <sup>2</sup> = 0.931	0.056 C + 7.711 R <sup>2</sup> = 0.958	0.124 C + 7.270 R <sup>2</sup> = 0.986
( $\alpha/f^2$ ) <sub>cl</sub> 10 <sup>-14</sup> , s <sup>2</sup> m <sup>-1</sup>	-0.084 C <sup>2</sup> + 0.152 C + 12.45 R <sup>2</sup> = 0.996	0.056 C <sup>2</sup> - 0.219 C + 11.76 R <sup>2</sup> = 0.999	0.073 C <sup>2</sup> - 0.157 C + 11.31 R <sup>2</sup> = 0.967

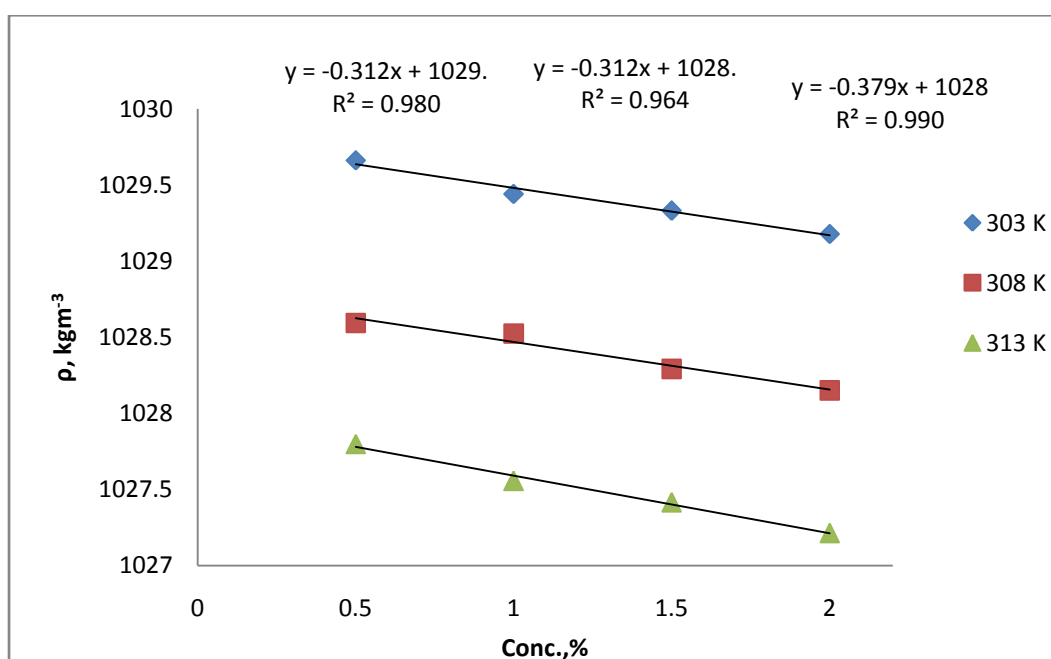


Fig. 4.53: The plots of density ( $\rho$ ) against concentration (%) of BSB4HS in 1,4 dioxane at 303, 308 and 313 K.

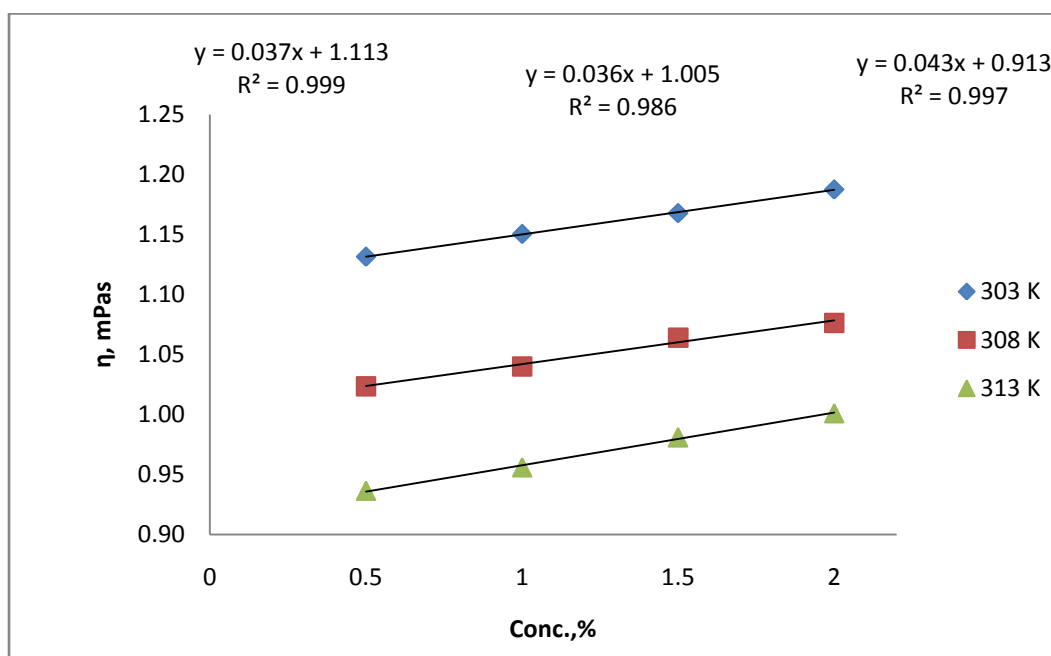


Fig. 4.54: The plots of viscosity ( $\eta$ ) against concentration (%) of BSB4HS in 1,4 dioxane at 303, 308 and 313 K.

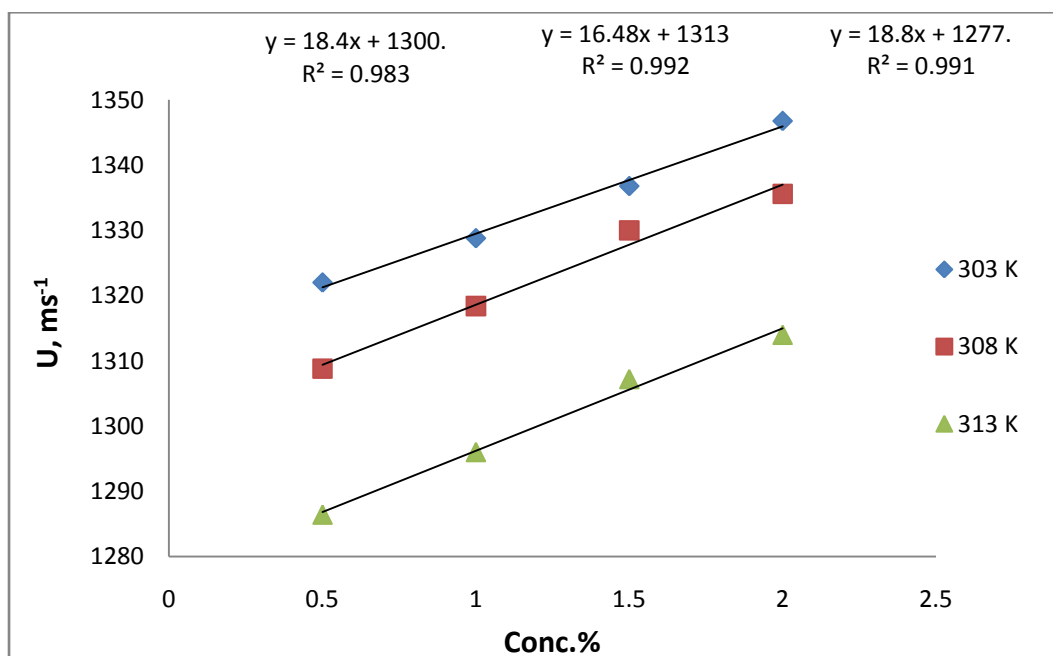


Fig. 4.55: The plots of sound velocity (U) against concentration (%) of ESB4HS in 1,4 dioxane at 303, 308 and 313 K.

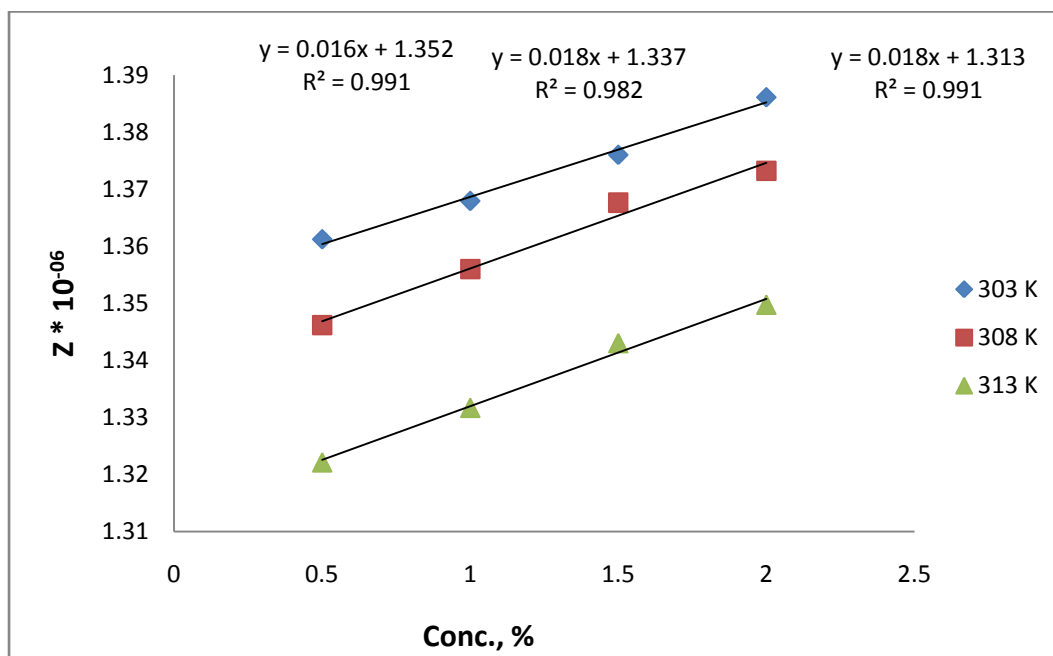


Fig. 4.56: The plots of specific acoustical impedance (Z) against concentration (%) of BSB4HS in 1,4 dioxane at 303, 308 and 313 K.

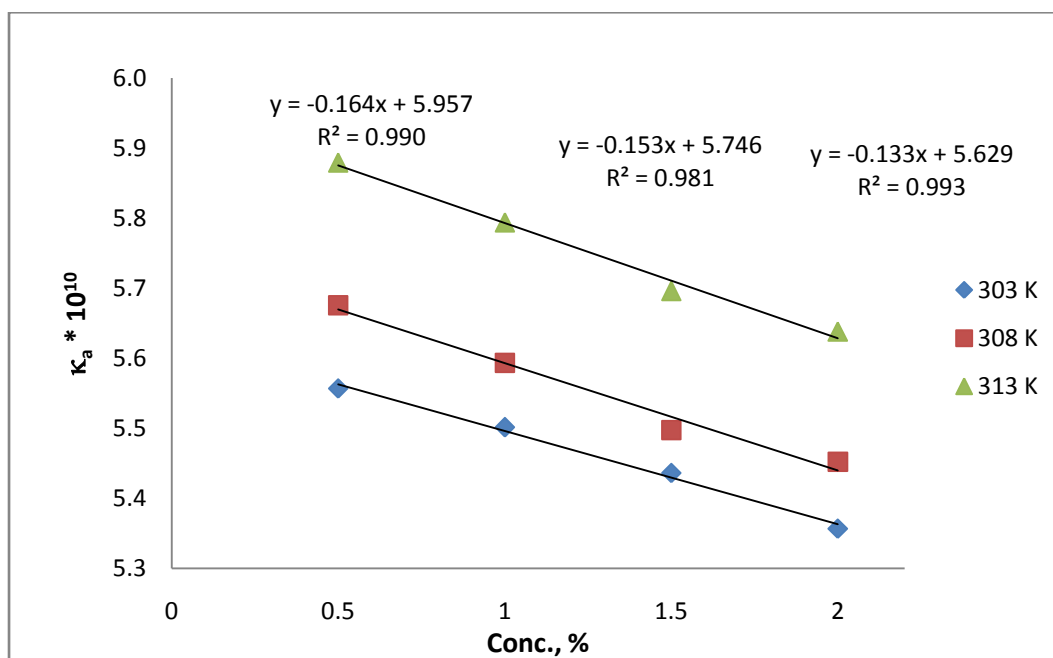


Fig. 4.57: The plots of adiabatic compressibility ( $\kappa_a$ ) against concentration (%) of BSB4HS in 1,4 dioxane at 303, 308 and 313 K.

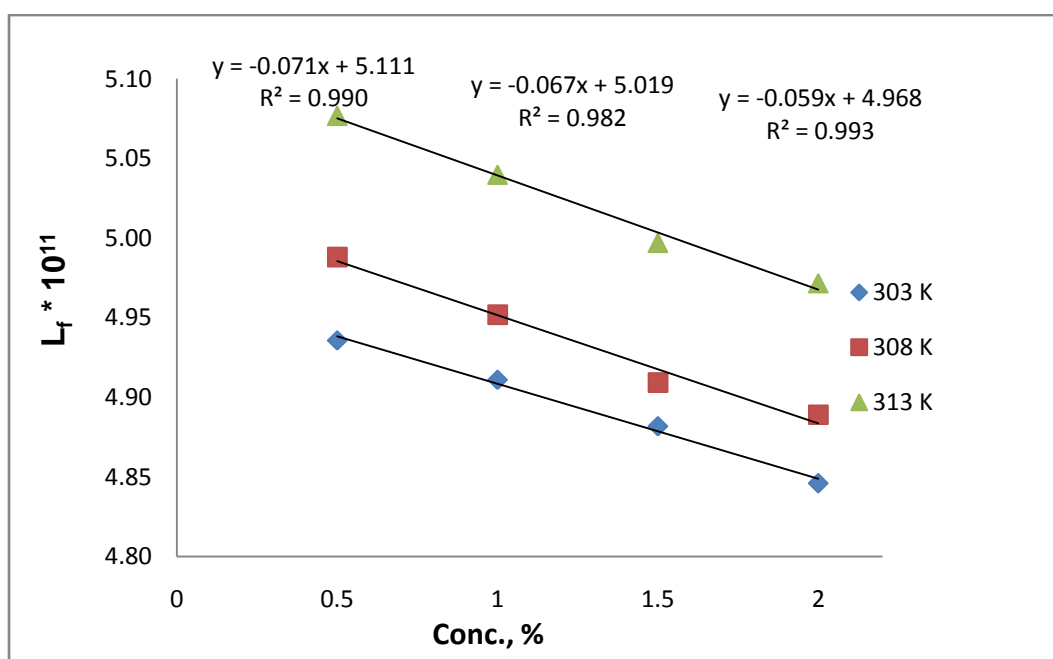


Fig. 4.58: The plots of inter molecular free path length ( $L_f$ ) against concentration (%) of BSB4HS in 1,4 dioxane at 303, 308 and 313 K.

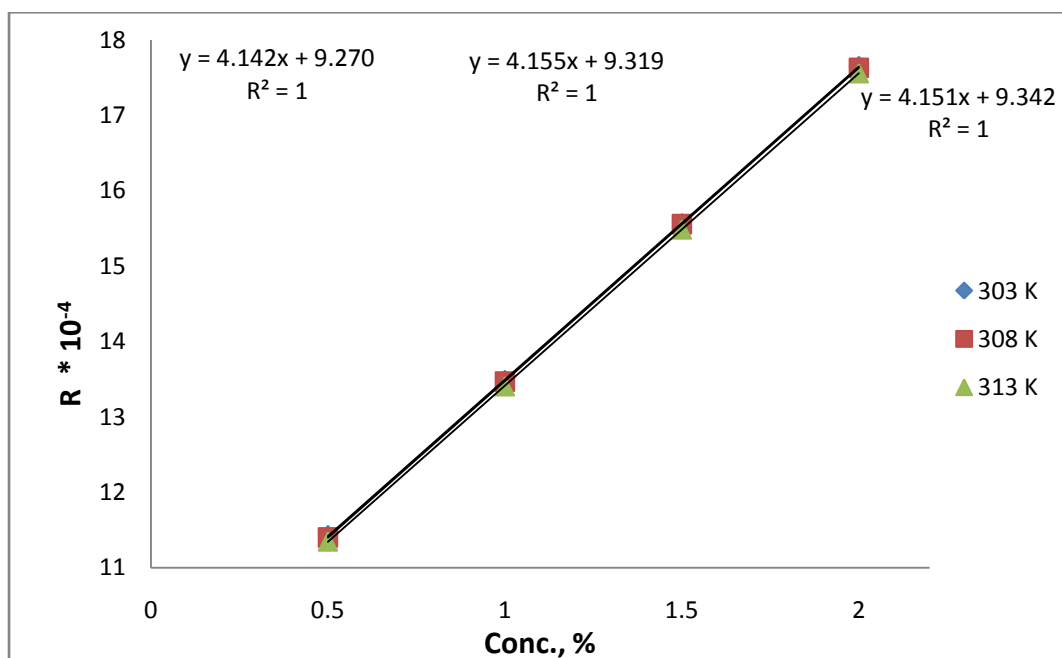


Fig. 4.59: The plots of Rao's molar sound function (R) against concentration (%) of BSB4HS in 1,4 dioxane at 303, 308 and 313 K.

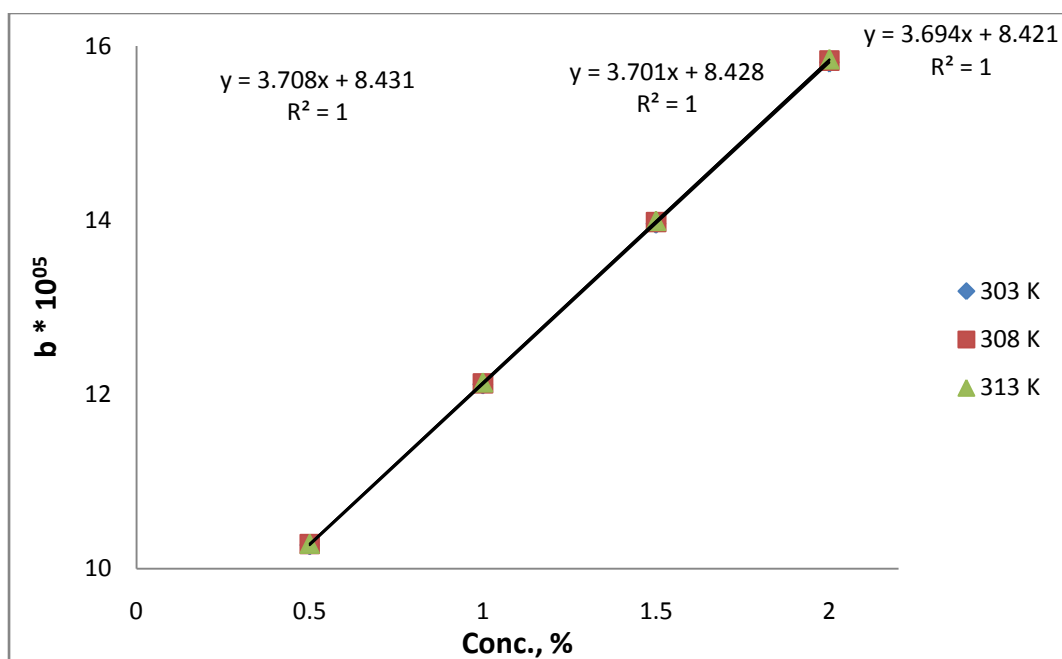


Fig. 4.60: The plots of Van der Waals constant (b) against concentration (%) of BSB4HS in 1,4 dioxane at 303, 308 and 313 K.

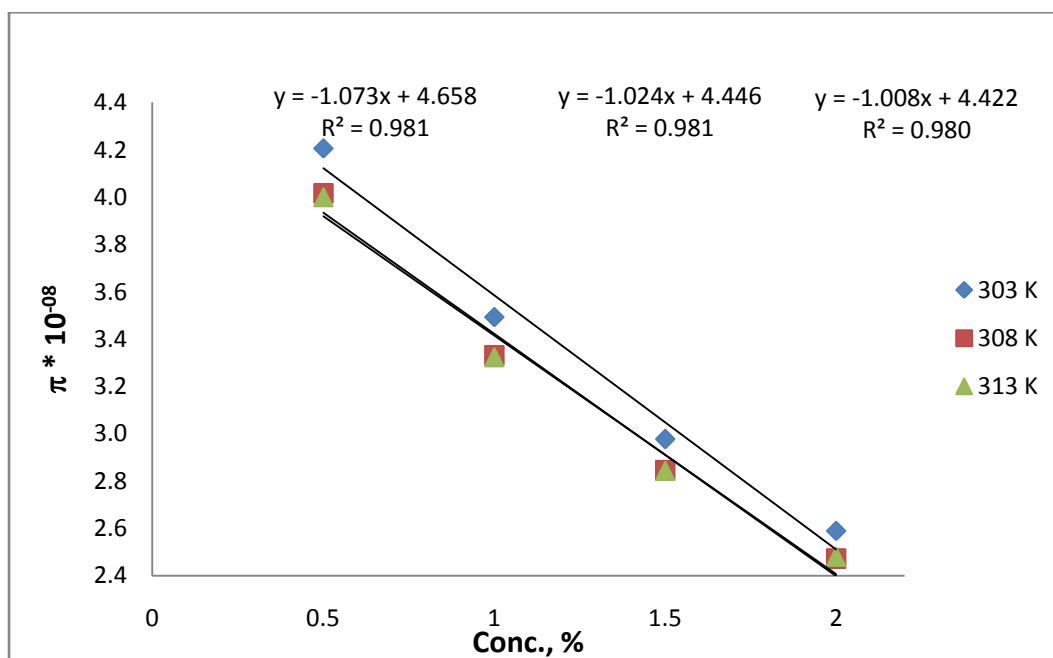


Fig. 4.61: The plots of internal pressure against concentration (%) of BSB4HS in 1,4 dioxane at 303, 308 and 313 K.

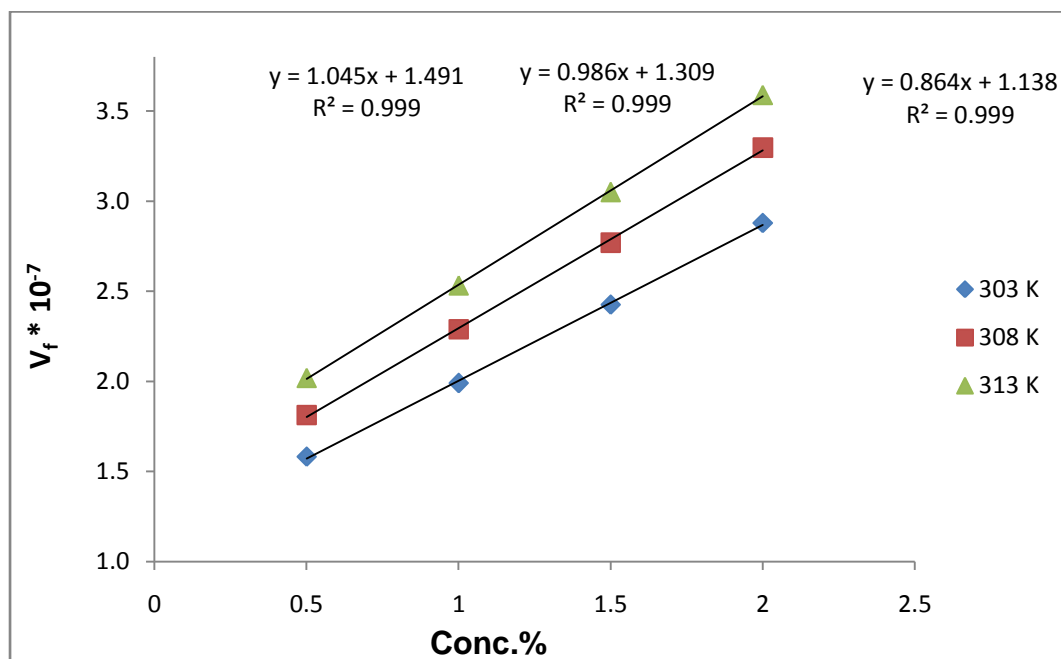


Fig. 4.62: The plots of free volume ( $V_f$ ) against concentration (%) of BSB4HS in 1,4 dioxane at 303, 308 and 313 K.

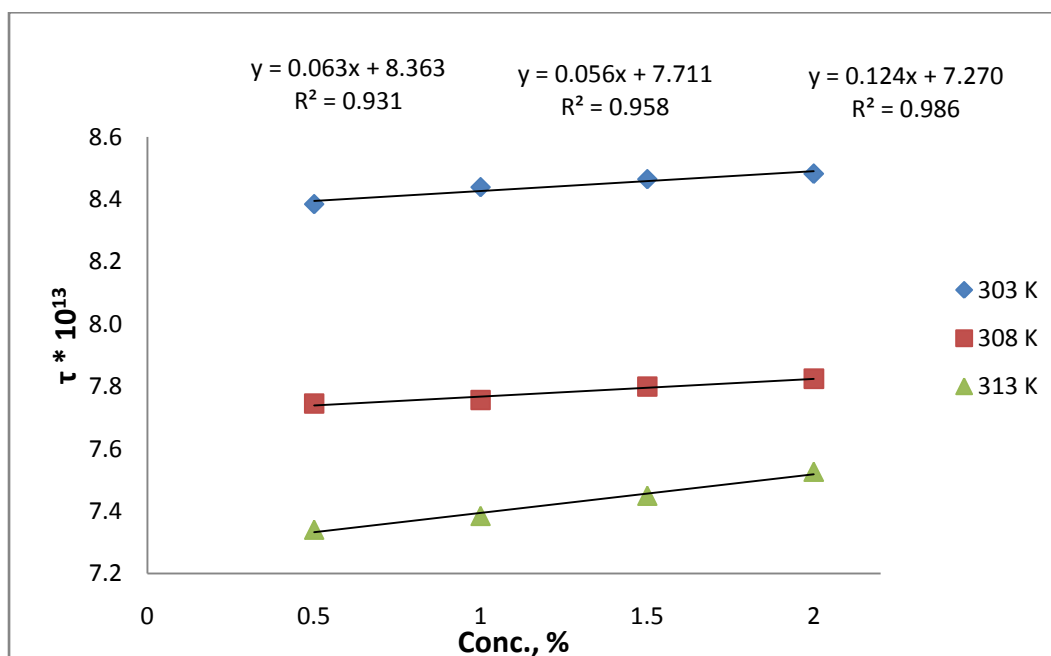


Fig. 4.63: The plots of viscous relaxation time ( $\tau$ ) against concentration (%) of BSB4HS in 1,4 dioxane at 303, 308 and 313 K.

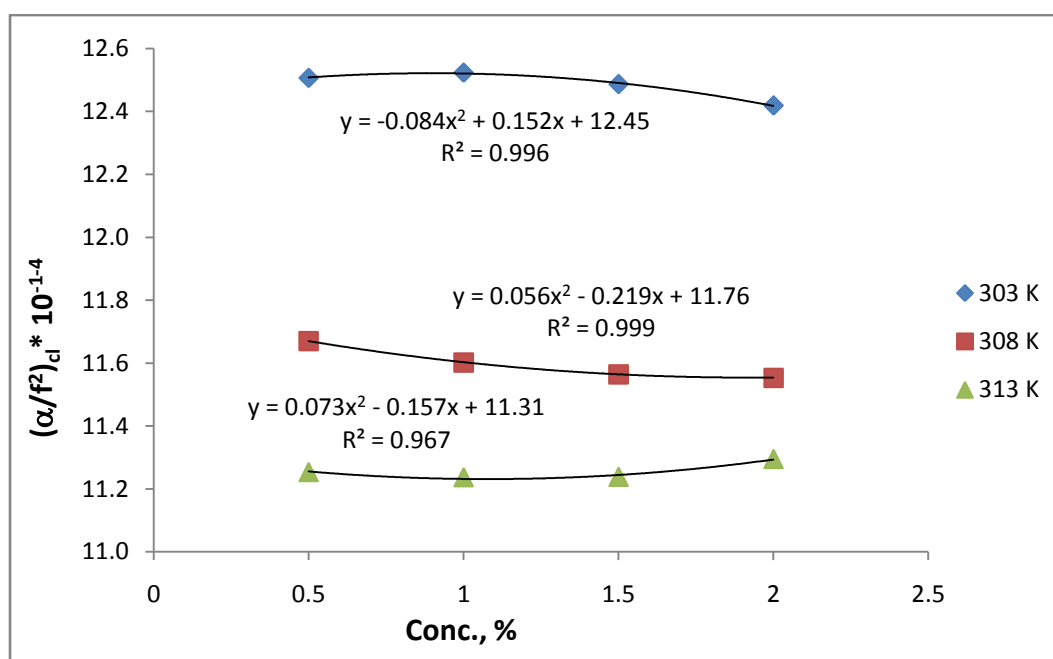


Fig. 4.64: The plots of classical absorption co-efficient (CAC) against concentration (%) of BSB4HS in 1,4 dioxane at 303, 308 and 313 K.

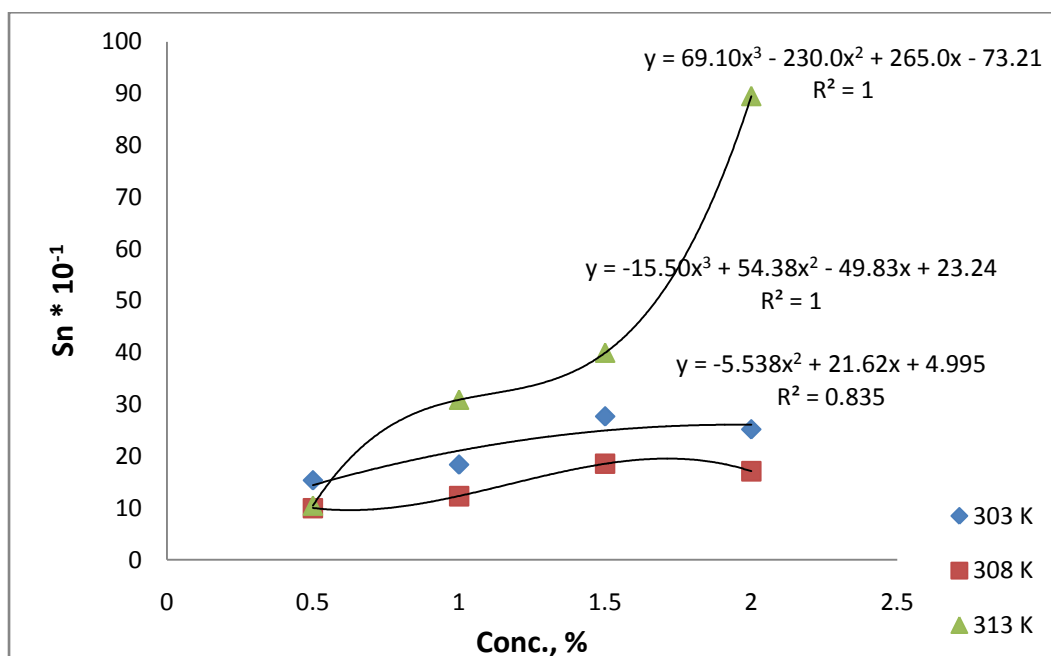


Fig. 4.65: The plots of solvation number ( $S_n$ ) against concentration (%) of BSB4HS in 1,4 dioxane at 303, 308 and 313 K.

Table-4.15:  $\Delta G^*$  data of BSB4HS

Conc.	$\Delta G^*$ , kJ mol $^{-1}$			$\Delta H$ , kJ mol $^{-1}$	$\Delta S$ , J K $^{-1}$ mol $^{-1}$
	303 K	308 K	313 K		
0.5	4.24	4.11	4.04	7.93	12.29
1	4.26	4.11	4.05	7.97	12.45
1.5	4.27	4.13	4.07	7.53	10.96
2	4.27	4.14	4.10	6.88	8.79
<b>Average</b>	4.26	4.12	4.07		

$$\Delta G^* = 19.02x + 4235, R^2 = 0.930$$

$$\Delta G^* = 18.56x + 4097, R^2 = 0.958$$

$$\Delta G^* = 43.48x + 4010, R^2 = 0.987$$





# CHAPTER – 5

## SUMMARY

## CHAPTER-5 SUMMARY

This chapter of the thesis deals with brief summary of the work incorporated in the thesis.

### CHAPTER-1

This chapter of the thesis describes up to date literature survey on synthesis, characterization and applications of diamines, symmetric double Schiff bases and their epoxy resins, bisbenzoxazines and polySchiff bases.

### CHAPTER-2

This chapter describes synthesis of 1-1' bis(4-aminophenyl) cyclohexane, symmetric double Schiff bases and their epoxy resins, bisbenzoxazines and polySchiff bases. Curing study of epoxy resins using varying amount of phthalic anhydride and ring opening polymerization of bisbenzoxazines is also included in this chapter.

### CHAPTER-3

This chapter describes the characterization of synthesized compounds by solubility, IR and <sup>1</sup>HNMR spectral techniques, DSC and TGA techniques at the heating rate of 10°C/min in an N<sub>2</sub> atmosphere. ESB4HE, ECyP-5, EMP-5, EMP-10, EMP-15, EEP-5, EEP-10, EEP-15, TDADPCy, TDADPM, TDADPE and TDADPS followed single step degradation, while ESB4HCy and ESB4HM followed two-step degradation and ECyP-10 followed three steps degradation. Associated kinetic parameters were determined according to Anderson-Freeman method and compared. PolySchiffbases (TDADPCy, TDADPM, TDADPE, and TDADPS) are thermally stable up to about 400°C. Epoxy resins (ESB4HCy, ESB4HE, ESB4HM) are thermally stable up to about 250°C, while all others (ECyP-5, ECyP-10, ECyP-15, EMP-5, EMP-10, EMP-15, EEP-5, EEP-10, EEP-15) are thermally stable up to between 200 to 250°C.

## CHAPTER-4

This chapter describes the acoustical properties of epoxy resin (ESB4HCy) and bisbenzoxazines (BSB4HCy, BSB4HM, BSB4HE and BSB4HS) solutions at 303, 308 and 313 K. Various acoustical parameters such as adiabatic compressibility ( $\kappa_a$ ), specific acoustical impedance (Z), Rao's molar sound function (R), Van der Waals constant (b), Internal pressure ( $\pi$ ), Classical absorption coefficient  $(\alpha/f^2)_{cl}$ , viscous relaxation time ( $\tau$ ), solvation number ( $S_n$ ), free volume ( $V_f$ ) and intermolecular free length ( $L_f$ ) were determined and discussed in light of effect of solvent, temperature, concentration and nature of the polymer.

The change in  $\rho$  and U with C and T are not as appreciable as  $\eta$  due to specific molecular interactions occurring in the solutions. Linear increase of Z, R and b (practically no temperature effect observed),  $V_f$ ,  $\tau$  and  $(\alpha/f^2)_{cl}$  (nonlinear) with C and decrease with T; and linear decrease of  $\kappa_a$ ,  $L_f$  and  $\pi$  with C and increase with T provided information about presence of strong molecular interactions occurring in the solutions and solvophilic nature of BSB4HS is confirmed by positive values of  $S_n$ . Nonlinear increase of  $S_n$  with C and T further confirmed coexistence of solvent-solute and solute-solute interactions in the solutions. The observed trend signified that solvent-solute interactions are strong over solute-solute interactions.

The activation thermodynamic parameters namely  $\Delta G_b^*$ ,  $\Delta H_b^*$  and  $\Delta S_b^*$  were derived by using  $\tau$  data at different C and T. It is observed that  $\Delta G_b^*$  remained practically constant and decreased a little with T.



# ACHIEVEMENTS

## **CONFERENCES/WORKSHOP/SEMINAR/SYMPOSIUM PARTICIPATED AND PAPERS PRESENTED**

1. International Conference on Recent Trends in Materials and Characterization, NIT Mangalore (February 14-15, 2010).
2. International Seminar on Recent Developments in Structure and Ligand Based Drug Design, Saurashtra University, Rajkot (December 23, 2009).
3. National Seminar on Emerging Trends in Polymer Science and Technology (Poly-2009), Saurashtra University, Rajkot (October 08-10, 2009).
4. Two Days National Workshop on Patents & IPR Related Updates, Saurashtra University, Rajkot (September 19-20, 2009).
5. National Conference on Spectroscopy & Stereochemistry, Saurashtra University, Rajkot (March 18-20, 2009).
6. National Workshop on Updates in Process & Medicinal Chemistry, Saurashtra University, Rajkot (March 3-4, 2009).
7. XXIII Carbohydrate Conference, Bhavnagar University, Bhavnagar (January 22-24, 2009).
8. National Seminar on Emerging Trends in Chemical Science Research, Sardar Patel University, V.V. Nagar (January 20-21, 2009)
9. Workshop on Applications of Thermal Analysis (WATA-08), M.S.University, Vadodara (October 6, 2008)
10. XXII Gujarat Science Congress, Bhavnagar University, Bhavnagar (March 9, 2008).
11. National Workshop on "Management & Use of Chemistry Databases & Patent Literature", Department of Chemistry, Saurashtra University, Rajkot (February 27-29, 2008).